DEVELOPMENT AND APPLICATION OF ELECTROANALYTICAL TECHNIQUES FOR BIOLOGICAL MATRICES

A thesis

Submitted for the Degree

of

Doctor of Philosophy in Chemistry

at the

University of Canterbury

by

Alisa D Roddick

1995

Acknowledgements

I wish to extend my sincere thanks to my supervisor Dr Alison Downard for her expert guidance, good humour, Spuddie stories and constructive comments during the writing of this thesis.

I would also like to thank Steve for his extensive help with computational aspects of my work and for proof reading this thesis. Thanks also to Kathryn for proof reading, Don for helpful discussions and fellow students, Jan, Maureen, Katherine and Brendon for providing a pleasant working environment.

I wish to acknowledge the proficient academic and technical staff of the University of Canterbury for their assistance over the years and to thank the Evans Fund for financial aid. I would also like to thank Professor A. M. Bond and La Trobe University for enabling me to carry out microelectrode studies.

Finally, my thanks to Gilly for her support, especially over the latter years of my studies, and to Dad, Vic and Paul for their encouragement.

Contents

CHAPTER SIX: *PARA*-PHENYLACETATE AND *PARA*-ALKYLBENZENE CMES AS DETECTORS IN FLOWING SOLUTIONS

Abstract

This thesis presents a study on the development and application of electrochemical techniques for analysis in biological fluids. Two main problems which occur when measurements are made directly in biological matrices were addressed. Firstly, interferences from other electroactive components and secondly, adsorption of high molecular weight organic species (such as proteins) onto the electrode surface.

Much of the work described utilised glassy carbon electrodes covalently modified by a diazonium salt coupling procedure. This method of modification produced stable electrode surfaces suitable for use in flowing streams and with organic solvents (such as those used in reversed phase-HPLC). The properties of the chemically modified electrodes (CMEs) could be varied by changing the *para* substituent of the aryl species grafted onto the electrode surface. Modification with *p*-phenylacetate and *p*-benzoate moieties generated CMEs which were negatively charged at physiological pH (7.4) and were selective for cationic analytes relative to anionic species. The suitability of these CMEs as probes for the measurement of the catecholamine neurotransmitter dopamine (DA) was investigated in detail. The CMEs exhibited fast response times to DA and good selectivity to DA over ascorbic acid making them suitable for DA measurements with fast timescale electrochemical techniques. Uncharged CMEs were also prepared using the diazonium salt procedure. The selectivity of *p*-alkylbenzene modified electrodes was investigated in batch and flow injection analysis conditions. The selective measurement of biologically important species (acetaminophen and chlorpromazine) over interferents (ascorbic acid and uric acid), was investigated. Chlorpromazine was able to be measured in the presence of uric acid using a retention-time based technique coupled with a *p*-phenylacetate/*p*-methylbenzene modified detector. The simultaneous determination of acetaminophen, ascorbic acid and uric acid was achieved at an array of modified detectors.

Covalently modified electrodes were used in protein adsorption studies. The extent of protein adsorption was evaluated by monitoring the electrochemical response of suitable probe analytes. Protein adsorption was influenced by monolayer modification. Anionic groups close to the electrode surface did not affect protein adsorption whilst hydrophobic groups increased protein adsorption. Charged groups which extended further into solution decreased protein adsorption. Protein adsorption was also examined at different carbon materials, electrochemically pretreated glassy carbon and CMEs prepared by methods other than diazonium salt modification. Glassy carbon was less prone to adsorption of high molecular weight foulants compared to other unmodified carbon electrodes. Some

assembly of anionic surfactant on basal plane graphite and incorporation of anionic surfactant in graphite epoxy decreased protein adsorption relative to unmodified electrodes. Electrodes coated with the polymer, cellulose acetate, decreased protein adsorption but gave poor reproducibility and suffered from time-dependent response.

Major symbols

STANDARD SUBSCRIPTS

a	anodic
c	cathodic
d	diffusion
dl	double layer
k	kinetic
l	limiting
m	modified
p	peak
u	unmodified

SYMBOLS

β	tunneling coefficient
C_o	bulk concentration
D	diffusion coefficient
E	potential of an electrode versus a reference
ΔE_p	difference in anodic and cathodic peak potentials in cyclic voltammetry
$E^{o'}$	formal potential of an electrode
$E_{p/2}$	potential where $i = i_{p/2}$ in linear sweep voltammetry
$E_{1/2}$	measured half-wave potential
$E_{1/4}$	potential where $i/i_d = 1/4$
$E_{3/4}$	potential where $i/i_d = 3/4$
ϕ_2	potential of the OHP with respect to bulk solution
ϕ_M	absolute electrostatic potential of the electrode
ϕ_S	absolute electrostatic potential of the bulk solution
Γ	surface excess at equilibrium
i	current
i_p^{BSA}	peak current in the presence of BSA
k^o	standard (intrinsic) heterogeneous rate constant
ν	scan rate
θ	fractional coverage of an interface
T_{10}	time for current of an FIA peak to decay to 10 % of the maximum value

T_{90}	time for current of an FIA peak to reach 90 % of the maximum value

ABBREVIATIONS

AA	ascorbic acid
acet	acetaminophen
ACN	acetonitrile
BPG	basal plane graphite
BSA	bovine serum albumin
CA	cellulose acetate
CC	chronocoulometry
cmc	critical micelle concentration
CMCT	1-cyclohexyl-3-(2-morpholino-ethyl)carbodiimide metho-*p*-toluenesulfonate (CMCT)
CME	chemically modified electrode
CP(E)	carbon paste (electrode)
CPZ	chlorpromazine
CTAB	hexadecyltrimethylammonium bromide
CV	cyclic voltammetry
DA	dopamine
DASA	1,2-dihydroxyanthraquinone-3-sulfonate
DDW	doubly distilled water
DMF	*N,N*-dimethylformamide
DP(V)	differential pulse (voltammetry)
DOPAC	3,4-dihydroxyphenylacetic acid
ECF	extracellular fluid
ECP	electrochemical pretreatment
EGO	electrochemical graphite-oxide
FCA	ferrocenemonocarboxylic acid
FcAm	N,N-dimethylaminomethylferrocene methiodide
FcOH	ferrocenemethanol
FCV	fast scan rate cyclic voltammetry
FIA	flow injection analysis
GC	glassy carbon
GE	graphite epoxy
HD(V)	hydrodynamic voltammogram
HOPG	highly ordered pyrolytic graphite
4-MC	4-methylcatechol

MeOH	methanol
NADH	nicotinamide adenine dinucleotide
NP(V)	normal pulse (voltammetry)
PB	phosphate buffer
PBS	phosphate buffered saline
Q	charge passed during electrolysis
PVP	poly(vinylpyridine)
RAM	random array microdisk
RP-HPLC	reversed phase high performance liquid chromatography
RSD	relative standard deviation
SAM	self-assembled monolayer
SCE	saturated calomel electrode
SDS	sodium dodecyl sulfate
$TBABF_4$	tetra-*n*-butylammonium fluoborate
UA	uric acid
XPS	X-ray photoelectron spectroscopy

Chapter One: Introduction

1.1 Electroanalytical Techniques

A wide range of species can be determined using electrochemical techniques. Applications range from environmental monitoring of metal ions, to chemical process control and determination of neurotransmitters in the living brain. High sensitivity, accuracy and precision can be achieved with comparatively low cost instrumentation[1]. Electrochemical methods are also suitable for analysis of small sample volumes and have the capacity for automation. They are applicable over a wide range of concentrations (approximately 10^{-3} - 10^{-10} M) depending on the technique used, and can provide information about sample speciation on the basis of complex lability[2]. Further, these techniques can be applied in numerous solvents and solvent mixtures, including highly resistive media. Electroanalytical methods are useful for analysis of clinical samples as many biological analytes are easily oxidised or reduced. The appropriate choice of electrochemical technique is dictated by the analytical problem, and a number of potential waveforms specifically tailored for given analyses have emerged. Some techniques which have been applied in clinical samples are discussed below.

Differential pulse voltammetry (DPV) is commonly used for the analysis of clinical samples[3]. It has high sensitivity, typically in the 10^{-7}– 10^{-8} M range, and the relatively symmetrical and narrow peak shaped response allows resolution of analytes providing they undergo electron transfer at sufficiently different potentials. Typical scan rates of 1-10 mV s^{-1}, however, make DPV inappropriate when high sample throughput or analysis of rapidly changing concentrations is required. The low detection limits achievable with this technique have led to its application to *in vivo* monitoring of drugs in body fluids[1,3] and neurotransmitters in brain extracellular fluid (ECF)[4]. Under optimised conditions i.e. with electrochemically pretreated (ECP) carbon fibres or carbon fibre electrodes coated with the perfluorosulfonated polymer, Nafion, basal levels of neurotransmitters (nM–μM concentrations) can be measured by DPV with adequate resolution[4]. Limitations arise from slow scan rates and concomitant depletion of analytes in the region of the electrode which necessitates a rest period of 60-120 s between scans.

Increased sensitivity and selectivity can be achieved by coupling a preconcentration step with a sensitive stripping technique such as DPV or square wave voltammetry. For example, analysis of trace metals is possible using anodic stripping techniques. Hanging mercury drop electrodes and thin mercury film electrodes (on glassy carbon) are the most practical, allowing measurement of approximately 20 amalgam-forming metals[1]. An

improvement in the response for some metals is possible using adsorptive stripping analysis which involves the formation and adsorptive accumulation of surface-active metal chelates. Adsorptive stripping voltammetric techniques have also been applied to trace analysis of compounds of biological importance[3].

Fast scan rate cyclic voltammetry (FCV) in which the scan rate (v) is >100 V s^{-1}, is an electrochemical technique originally developed for analysis of biological analytes in the neurophysical environment. It was first described in 1981 by Millar et al[5] and has become one of the most widely used electrochemical techniques for neurotransmitter measurement[4]. When used with bare or Nafion coated carbon fibre microelectrodes, subsecond temporal resolution can be obtained allowing rapid concentration changes to be monitored[6-14]. The reverse scan aids the identification of electroactive species and helps to maintain an unperturbed environment *in vivo*. It is generally recognised that FCV is not sufficiently sensitive to measure concentrations below micromolar levels[15].

Electrochemical detection following liquid chromatography (LCEC) is a powerful analytical technique[3]. The electrochemical detector possesses important features: high sensitivity, low dead volume, fast linear response, and low cost[16]. In its simplest form, resolution is achieved with the appropriate choice of column and the detector electrode is held at a constant potential which is suitable to oxidise or reduce analytes of interest. Conductive solvents such as those used in reversed-phase high performance liquid chromatography (RP-HPLC) are compatible with electrochemical detection allowing good potential control. In flow injection analysis (FIA) it is usual to determine only one species in a sample and selectivity is achieved via appropriate choice of reagents or separation scheme and electrode potential. Flow injection analysis is suitable for rapid assays of simple samples though more complex mixtures may be dealt with for example by using fast potential scanning techniques or chemically modified detector electrodes. Strategies which can be applied to allow analysis of multicomponent mixtures in FIA are discussed in more detail in Chapter Six.

In principle, voltammetric techniques are well suited to analysis of clinical samples, however, particular problems may arise as a result of the complex sample matrix. These include:

(1) Fouling of the working electrode surface by non-electroactive species. For example, an adsorbed layer may result in dramatically decreased sensitivity and retardation of analyte electron transfer kinetics.

(2) Interference from other electroactive components in the matrix which undergo redox processes at similar potentials. This causes a loss of selectivity for the target analyte because the signal will contain contributions from all species with similar redox potentials.

(3) Slow electron transfer kinetics of many important analytes at solid electrodes. Slow kinetics necessitates the application of large overpotentials which increases the likelihood of interference from other electroactive species.

(4) Interaction of the analyte with protein which leads to a perturbation of its electrochemical response. There may be a shift in redox potential, a decrease in diffusion rate or complete loss of response due to isolation of the electroactive analyte from the electrode surface. A poorly defined reactive fraction may result because the response arising from bound analyte depends on its lability and the particular analysis technique used.

These effects have necessitated the routine application of clean-up procedures to clinical samples prior to electrochemical measurements. The most common separation technique for the voltammetric determination of drugs in complex matrices is solvent extraction[1]. High selectivity can be obtained with appropriate choice of pH and organic solvent polarity. Another widely used pretreatment step involves the precipitation of proteins with inorganic salts or organic solvents[17]. Such sample pretreatments are not possible, of course, when making measurements *in vivo*.

It is desirable that strategies are developed which allow direct electrochemical analyses in biological samples without the need for prior clean-up procedures. Analytical procedures would thus be greatly simplified and analysis times decreased. Further, the ability to make measurements directly in biological fluids lends itself to the development of protocols for routine analyses in the doctor's surgery and for patient self-testing. One strategy to overcome problems which arise when using electrochemical techniques directly in biological fluids is to employ chemically modified electrodes.

1.2 Chemically Modified Electrodes (CMEs)

Chemical sensor design is an extensive and active field of research[18]. Chemically modified electrodes (CMEs) are electrodes at which chemical species have been deliberately immobilised to produce desirable properties[19,20]. Increased selectivity, sensitivity and antifouling properties may be achieved by applying an appropriate surface coating. Additionally, the rate of heterogeneous electron transfer at CMEs may be changed relative to the unmodified surface. Chemically modified electrodes can be classified into two main types, namely, chemical sensors and biosensors. Biosensors are a special group of CMEs which incorporate a biological element such as a substrate specific enzyme[1,21]. Chemical sensors, which as the name suggests, utilise chemical modifiers to achieve desirable properties, are more relevant to the work presented in this thesis.

1.2.1 Classification of CMEs according to preparation method

CMEs can be classified according to four general methods of preparation[20]: formation of a polymeric surface film; covalent attachment of a modifying layer; chemisorption, and integration of modifying agents into the electrode material itself. Often several of these features are present in a particular CME. Examples from each of these categories are described below. The examples selected are of particular relevance to the work in this thesis.

(i) Polymeric films. Application of polymer films is a widely used method of preparing CMEs[20]. Several procedures have been utilised to generate polymeric layers on electrode surfaces. For example, electropolymerization of monomers in solution[22-24] or by evaporative[25-27] or electrochemical precipitation[28] of a preformed polymer. The adherence of these films relies on chemisorption and/or their limited solubility in solution. The film itself may convey desired properties to the electrode or alternatively, electroactive species may be incorporated in the coating after preparation. Numerous types of polymeric films have been used for analysis in clinical samples; Nafion and cellulose acetate which are commonly applied coatings, are discussed here.

Nafion. The perfluorosulfonated membrane, Nafion, (the chemical structure of which is shown in Figure 1.1) may be drop-coated onto the electrode from an alcohol solution[29-31]. An alternative procedure has been developed to coat cylindrical carbon fibre electrodes[4,32]. This involves brief electrolysis (4 to 6 s) in a 5% Nafion solution at anodic potentials (typically > 3.0 V). Nafion shows good resistance to organic fouling, is permeable to cations (and small uncharged species such as hydrogen peroxide) and repels anions. Nafion films have been used for many applications in analysis of clinical samples. For example, very thin films have been applied to carbon fibre microelectrodes for measurement of catecholamines in the neurological environment where there is a large excess of ascorbic acid[4,29,32-34]. Discrimination is facilitated by a high selectivity for hydrophobic relative to hydrophilic cations[29]. Nafion coated mercury thin film electrodes (MTFE) have also allowed direct anodic stripping voltammetric measurement of trace metals in biological media[30, 31]. Some disadvantages of Nafion, however, are slow response times at thick films which result from low diffusion coefficients of analytes in the coating, memory effects due to the strong binding between cationic analytes and Nafion, and saturation of the negative sites when high concentrations of cations are present[29,35,36].

Figure 1.1: The chemical structure of Nafion

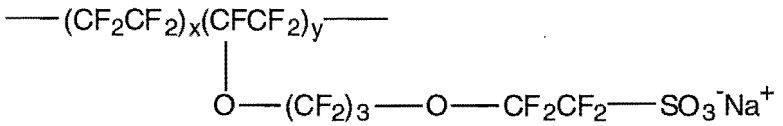

Cellulose Acetate. Cellulose acetate (CA) is a commonly used selectively permeable polymeric film. The usual preparation method for CA films is evaporative coating from organic solutions. In an early study, Sittampalam and Wilson showed that hydrogen peroxide could be measured at a CA coated Pt detector without interference from other electroactive plasma components[26]. This modification also conferred desirable anti-fouling properties by isolating the electrode from high molecular weight adsorbents. In later work the porosity of these coatings was increased by controlled base-hydrolysis which causes fragmentation of the polymer and the formation of pores in the coating[27]. Short hydrolysis times (for example < 30 minutes in 0.07 M KOH) gives a small pore size and low molecular weight cut-off for species able to diffuse to the electrode surface. Long hydrolysis times result in larger pores and higher molecular weight cut-offs. Selectivity of the films is found to be not merely a function of molecular weight, however, and factors such as analyte charge, shape and conformation appear to be important. For example, the permeability to chlorophenols is found to be high whilst ascorbic acid gives a small response at hydrolysed CA modified electrodes[27]. Loss of size selection occurs when hydrolysis times greater than 50 minutes (in 0.07 M KOH) are used. This is due to catastrophic loss of film integrity arising from increased hydrophilicity as the polymer is broken into smaller units (monoacetyl cellulose is water soluble).

To achieve permeation of higher molecular weight species into CA films, Kuhn et al[37] investigated an alternative means of casting the coatings. Phase-inversion membranes were made by applying a mixture of aqueous magnesium perchlorate (which acts as a pore-former), solvent (e.g. acetone) and CA onto the electrode surface. Film thickness and porosity were altered by systematic variation of pore-former, solvent and CA content. After application of the mixture to the electrode, a brief drying time followed (usually at constant humidity). During the drying time, solvent evaporates preferentially from the outer surface forming a less porous outer layer. After drying, the electrode was placed in a water bath at room temperature for 15 minutes to effect gelation. Finally, the CME was placed in ice-water where leaching occurred. Anisotropic films with porous inner regions and a less porous outer surfaces resulted, allowing rapid permeation of compounds up to molecular weight of 1500.

Mixed polymeric coatings. Further control of CME properties can be obtained using combinations of polymers. This has been achieved, for example, by copolymerisation of a monomer mixture[22] and by casting discrete layers onto the electrode surface[35, 38-41]. Nafion and CA are widely investigated components of mixed coatings. The size discrimination properties of CA and charge selectivity of Nafion have been combined with other polymers or together to achieve an extra dimension of selectivity. A bilayer Nafion/CA electrode was used by Wang and co-workers[35] to discriminate between catecholamines. Large catecholamines (norepinephrine and epinephrine) were excluded by CA but the smaller dopamine analyte was selectively partitioned into the underlying Nafion film. In a recent study Zhang et al[40] investigated the permeability of hydrogen peroxide and interferents acetaminophen and ascorbic acid at various CMEs. It was found that selectivity of hydrogen peroxide response was attainable at a comparatively thin film of mixed Nafion/CA whereas thick films of the individual polymers were required to achieve the same degree of selectivity.

(ii) Covalently bound modifications. A modifier can be covalently bound to the electrode by reaction with the surface. This method may be used to form an approximate monolayer coating of modifier[42,43] or to create a less dense scattering of modified sites which are available to act as precursors for attaching enzymes or polymeric films[19]. Attractive features of covalently modified CMEs include their stability under hydrodynamic conditions and greater tolerance to organic solutions, relative to polymeric coatings. Covalent bonds have been formed, for example, by reactions of surface metal-oxide moieties with organo-silanes and by amine couplings to derivatised functional groups on carbon electrodes[19]. Recently, covalent attachment to glassy carbon via amine radical cations[44] and diazonium radicals[42,43] have been described. Self-assembled monolayers (SAMs) such as those formed by alkanethiols at gold electrodes[45-49] are also included in this category[50].

Metal oxide reaction with organosilanes. Surface oxide groups of many metal or semi-metal electrodes (including RuO_2, Pt/PtO, Au/AuO, TiO_2, Si/SiO_2 and SnO_2) are reactive towards organosilanes and alkoxysilanes[19]. This is shown in Figure 1.2, for a SnO_2 electrode.

Figure 1.2: Covalent bond formation by reaction of surface metal-oxides with chlorosilanes[a]

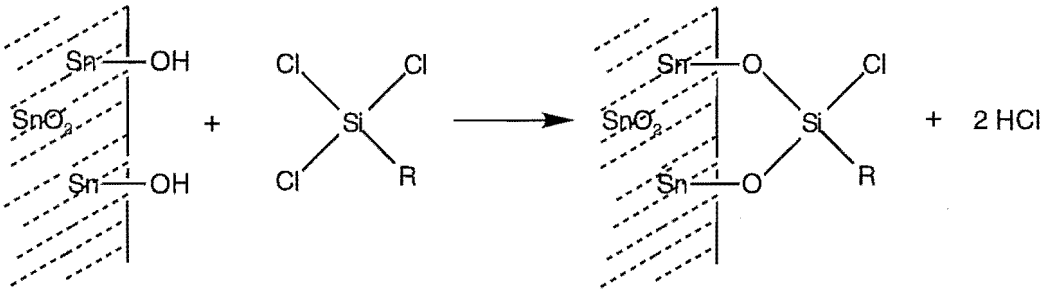

[a]R = organic substituent

When di– or trichloro silanes are used, the number of actual M–O–Si bonds formed is usually unknown. Evidence of "dangling" –Si–Cl groups has been obtained using spectroscopic techniques and it is thought that some lateral condensation reactions between neighbouring silanes occurs. The most useful organosilane modifiers have R– substituents that are either electroactive or chemically reactive coupling functionalities. Ferrocene derivatives, for example, have been attached to mediate electron transfer of other analytes and to provide a suitable environment in which the ferrocene heterogeneous electron transfer reactions themselves can be studied. Organosilanes with unsaturated R– substituents, for example R = $-(CH_2)_3COO(CH_3)C=CH_2$, can be used to anchor polymers to the electrode surface[19].

Reactions with functional groups on carbon surfaces. Freshly exposed edge plane carbon surfaces rapidly react with oxygen and water in the atmosphere to produce a variety of functional groups[19,51]. Carboxylic acid groups on carbon electrode surfaces, for example, can be used as precursors to further electrode modification. The quantity of these functional groups may be increased by abrasive polishing, heating at 400–500 °C in air, treatment with radio-frequency O_2 plasma and electrochemical oxidation of the surface[19,51]. These treatments however, tend to have detrimental effects on electrode performance as they increase background currents and may result in a decreased signal to noise ratio. Carboxylate moieties themselves are not sufficiently reactive to couple to amines but as shown in Figure 1.3 they can be activated by attachment of acid chloride, ester or diimide groups[19]. These methods of generating reactive carbon surfaces suffer some complications. For example, thionyl chloride adsorbs on carbon and often needs to be often removed by washing procedures. Exposure of the surface to water however, can cause hydrolytic loss of active surface groups. The acid chloride method can result in low coverages due to the greater reactivity of the solution acid chloride relative to the surface bound species. Formation of active groups via the DCC coupling procedure may be restricted as a result of steric factors[19].

Figure 1.3: Covalent bond formation by reactions with existing carbon functional groups

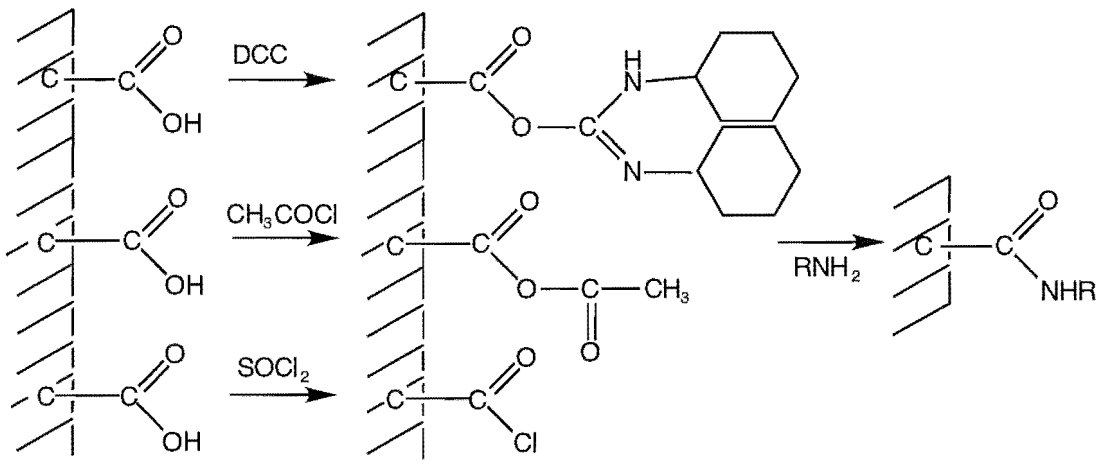

These modification procedures are most commonly used as a means of coupling electroactive amines to the electrode surface. Tetra(aminophenyl)porphyrins, for example, have been attached using the thionyl chloride reaction, to mediate electron transfer of halogenated phenyl alkanes[19]. The DCC method has been used to attach 3,4-dihydroxybenzylamine moieties which catalyse the reaction of the biologically important molecule, NADH[52].

Self-assembled monolayers (SAMs) of alkanethiols on gold. Self-assembly of a monolayer from a solution of reagent onto a surface is often a combination of two processes: i) the binding of a chemical functionality of the reagent to the surface and ii) microstructural organisation of the assembled monolayer which is driven by hydrophobic and van der Waals interactions between non-polar segments of the reagent[50]. Much interest in self assembled monolayers (SAMs) stems from their good microstructural definition. Self assembled monolayers of alkanethiols ($X(CH_2)_nSH$) on Au with X= CH_3, COOH and OH are the most thoroughly characterised. Polymethylene chains of these SAMs are densely packed and tilted at ca. 30° from the underlying surface[50] (as shown in Figure 1.4).

Figure 1.4: Covalent bond formation by reaction of alkanethiols with Au

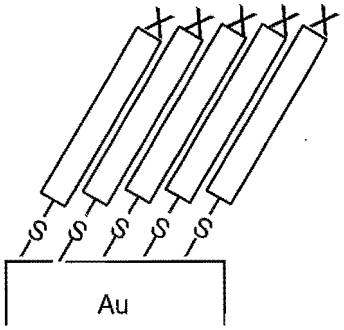

Self-assembled monolayers on Au have been most widely used to gain information about electron transfer reactions[46-48]. In these experiments, the SAM forms a thin (1–3 nm) blocking film which retards electron transfer rates and thus allows measurement of heterogeneous rate constants of redox couples with fast electrode kinetics. Preliminary applications of SAMs to clinical analysis have been reported by Malem and Mandler[45]. In this work, the responses of dopamine (DA) and ascorbic acid (AA) at a SAM of ω-mercaptocarboxylic acid on Au were investigated using CV. Selective permeability of DA relative to AA was observed at the monolayer, which is predominantly anionic at neutral pH. Monolayers constructed from modifiers of intermediate length (six methylene chain) were found to optimise selectivity whilst allowing adequate rates of electron transfer. Recently, it has been suggested that the observed permeability of the coatings used in the above study are attributable to defects in the assembled monolayer[49].

Reaction of carbon with diazonium salts. Covalent attachment of aromatic moieties onto carbon electrodes has been achieved by reducing an aromatic diazonium salt at a carbon electrode[42,43]. The mechanism of attachment, illustrated in Figure 1.5, is thought to involve a one electron reduction of the diazonium salt to form a radical species which then couples with the carbon surface. The *para* substituent may be varied and the density of surface groups controlled by changing the concentration of the diazonium salt and/or electrolysis time. This method of electrode modification has been utilised for much of the work described in this thesis. A more detailed description is given in the introduction to Chapter Three.

Figure 1.5: Covalent bond formation by a diazonium salt coupling procedure at carbon electrodes

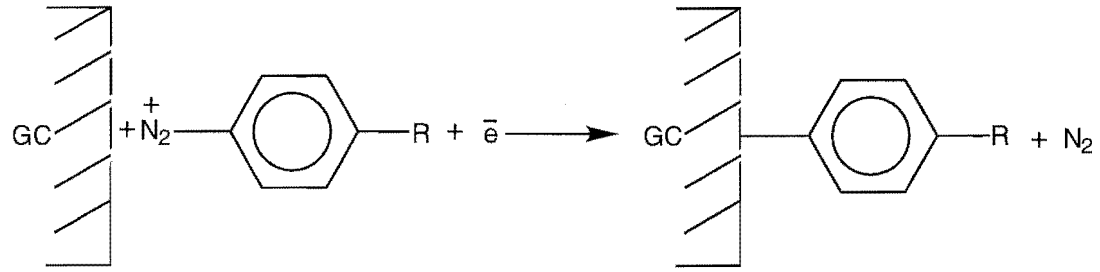

(iii) Chemisorption. Electrode modification by chemisorption is simple to achieve when the modifier exhibits strong irreversible adsorption to the electrode material. Adsorption of modifiers onto carbon surfaces can be generalised into three types of interaction, namely: adsorption of extended π-systems, interactions with charged groups, and hydrophobic interactions. As discussed below, pyrene, porphyrin and phthalocyanine compounds adsorb as a result of π-bond interactions, whilst phospholipids and other surfactants rely on electrostatic interactions with charged groups on the electrode surface, together with hydrophobic stabilisation.

Adsorption of pyrene derivatives. Pyrene derivatised catechol molecules were adsorbed to graphite electrodes by Jaegfeldt et al[53] to mediate electron transfer for the coenzyme nicotinamide adenine dinucleotide (NADH). NADH, which is an important biological redox transfer agent, requires high overpotentials for oxidation at bare carbon electrodes. Chemisorption of catechol mediators greatly lowered (from 410 to 150 mV) the overpotential for NADH oxidation. The chemical structures of NADH and the pyrene derivative are shown in Figure 1.6.

Figure 1.6: Molecular structures of a pyrene-catechol derivative and NADH

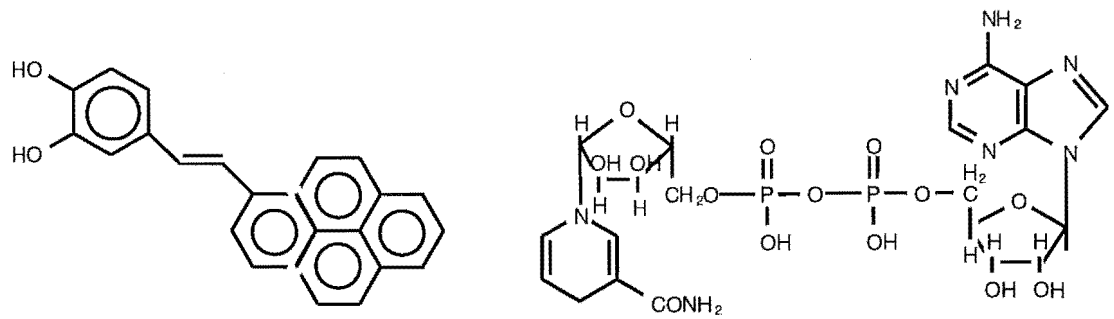

4-[2-(1-pyrenyl)vinyl]catechol

NADH

Adsorption of porphyrins and phthalocyanines. Highly aromatic porphyrin-metal complexes have been chemisorbed to carbon electrodes from solutions dissolved in concentrated sulfuric acid. These CMEs have found applications in mediated electron transfer. For example, electrocatalysis of important biological analytes NADH, hydrazine, acetaminophen, adrenaline, cysteine, penicillamine and oxalic acid, was reported by Wang and Golden[54] at electrodes modified with manganese(III)*meso*-tetra-phenylporphryins. Electrocatalytic activity was observed in quiescent solutions (using CV and DPV) and under flow injection analysis (FIA) conditions, indicating that adsorption was strong. Metallated phthalocyanine complexes have also been adsorbed to graphite electrodes (from either sulfuric acid or dilute aqueous solutions) to catalyse electrochemical reactions of biological analytes. Much of the early work in this field was performed by Zagal[55], who investigated the oxidations of cysteine and hydrazine at metal/phthalocyanine (M-Pc) and metal/tetrasulfonate phthalocyanine (M-TSP) modified electrodes. It was found that the electron transfer reactions of both analytes were catalysed at Co-Pc and Co-TSP modified electrodes. Further investigations of hydrazine oxidation revealed that Mn and Fe phthalocyanine complexes also resulted in electrocatalysis. The nuclei of porphyrin and phthalocyanine molecules are shown in Figure 1.7.

Figure 1.7: Molecular structure of the porphyrin and phthalocyanine nuclei

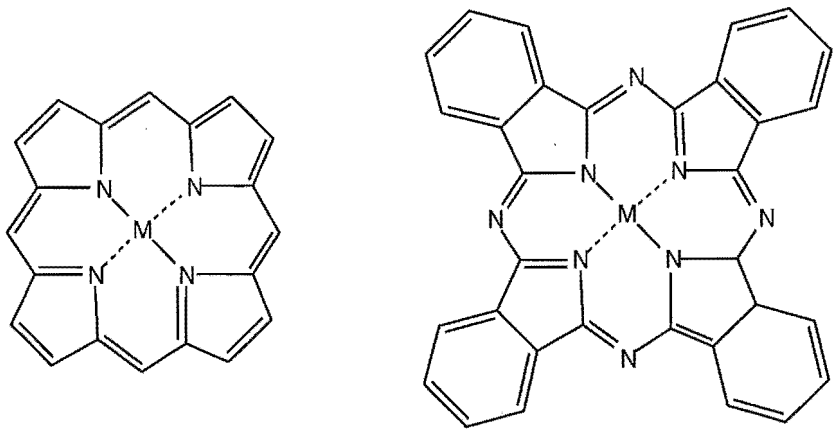

Porphryin Phthalocyanine

Phospholipid adsorption. Electrode coatings made by adsorption of phospholipids drop-coated from chloroform solutions onto GC have been reported[56-59]. Hydrophobic species preferentially partition into these biomembrane-like coatings allowing the measurement of therapeutic drugs, such as the antitumor agent marcellomycin[56] (shown in Figure 1.8) and ergot alkaloids[57], in the presence of biological interferents. An inherent problem with early examples of these coatings was their poor

mechanical stability[57]. The addition of cholesterol into the modifying matrix, however, improved the coating stability by interacting with the alkyl backbone of the phospholipid increasing the rigidity of the film and decreasing water penetration[58].

Figure 1.8: Molecular structure of the drug marcellomycin

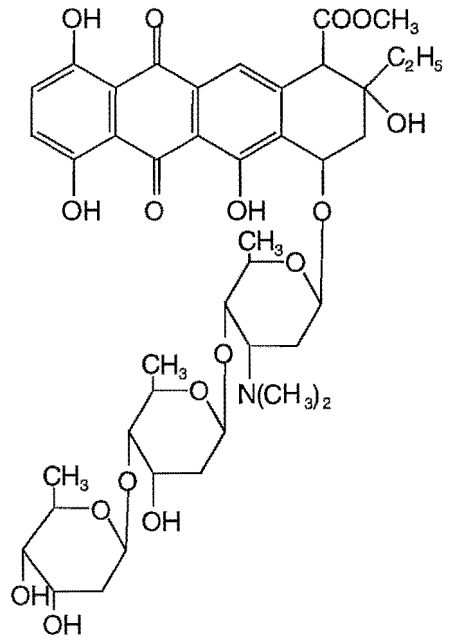

marcellomycin

Surfactant adsorption. Modification of various carbon surfaces by adsorption of charged surfactants has been investigated[60-62]. Assembly of anionic sodium dodecyl sulfate (SDS) and cationic hexadecyltrimethylammonium bromide (CTAB) at glassy carbon and rough pyrolytic graphite (RPG) at pH 7 was investigated by Brajter-Toth et al[61,62]. The electrochemical responses of catechol derivatives 3,4-dihydroxyphenylacetic acid (DOPAC) and DA were used to probe the structures of the modifying layers. It was found that both GC and RPG surfaces caused "head-on" orientations of the surfactant molecules at the electrode which resulted in the formation of hemimicelles. Further, the effect of adding surfactant on the response of the probe analyte depended on the relative strengths of probe-surface, surfactant-surface and surfactant-probe interactions. For example, the greatest enhancement in electrode kinetics at GC was observed for DOPAC (which is anionic at pH 7) in the presence of CTAB. In this situation the DOPAC–CTAB and CTAB–surface interactions dominate over the interaction of DOPAC with the GC surface, which is electrostatically disfavoured due to anionic sites.

(iv) Integrated systems. Integrated systems in which reagents are mixed into carbon paste and graphite epoxy materials, offer a simple method of modifying electrodes.

Modified carbon paste electrodes. Carbon paste electrodes (CPEs) were first reported in the late 1950s[63]. Since then, CPEs and modified CPEs have been used in numerous applications. Direct mixing of reagents with the carbon paste is now recognised to be a convenient way of modifying CPEs and a diverse range of chemicals have been immobilised by this method. These include lipids, surfactants, resins, silica, catalysts, complexing agents and biological entities. Sensors based on CPEs have recently been reviewed by Kalcher et al[64].

Modified CPEs have been applied to analyses in biological samples and a typical mode of operation involves preconcentration or complexation of the target analyte followed by stripping analysis[64]. For example, fatty acid modified CPEs have been used to preconcentrate phenothiazine drugs from diluted urine and serum samples giving detection limits of 5×10^{-8} M and 2×10^{-7} M respectively in each medium[65]. A CPE modified with the magnesium trisilicate, sepiolite, was used to determine traces of the drug bentazepam directly in urine[66]. This involved a 10 minute accumulation in diluted, buffered urine followed by analysis using DPV. Stearate modified carbon paste microelectrodes have also been applied to neurotransmitter analyses in vivo[67], however, it was later shown that anomalously high response to neurotransmitters occurred in these experiments because the modified CPEs were unstable in lipophilic environments[68].

Modified graphite epoxy electrodes. Graphite epoxy (GE) electrodes are made from epoxy bonded graphite resins. They can be cured at room temperature or heated to produce a very hard polishable surface. Various chemical modifiers including electrocatalysts[69], preconcentrating agents[69] and biological sensing elements[70] have been incorporated into GE material to produce robust CMEs. The utility of this method of modification was demonstrated by Wang et al[69]. In this work, graphite epoxy electrodes modified with a sulfonated polystyrene cation exchange resin were applied to the measurement of cupric ion. Currents arising from reduction of the preconcentrated metal ion were shown to be reproducible (after polishing of the CME), indicating the dispersion of modifier in the graphite epoxy material was homogeneous. When phthalocyanine catalysts were incorporated into GE, the overpotential for oxidation of biological analytes such as hydrazine and L-cysteine was lowered giving enhanced sensitivity to these analytes in flow injection analysis systems[69].

1.2.2 Classification of CMEs according to redox activity and electronic conductivity

Chemically modified electrodes can be further classified on the basis of their redox activity or inactivity and electronic conductivity or non-conductivity. Examples of some of these types of CMEs are mentioned in the above sections, and it is useful to summarise this information again.

Redox active CMEs. The electron transfer kinetics of biological analytes are often slow at carbon electrodes[71]. Hence, much research has been centred on the development of electrochemical sensors containing redox mediators which facilitate transfer of electrons between the electrode and biological analyte i.e. electrocatalysts. Mediated electron transfer involves the oxidation/reduction of the substrate by the electroactive mediator species. This is only possible when the redox potential of the mediator is sufficient to cause the redox reaction of the solution species. Many compounds have been utilised to mediate electron transfer[71]. Some of these have already been introduced and include organometallic species, such as ferrocenes, phthalocyanines, metallated phenanthroline[72] and metalloporphryins, and several organic mediators, including quinone, tetrathiafulvalene, phenazine and phenothiazine[71]. Redox active CMEs exist in several forms. Examples of CMEs at which electron mediators are adsorbed to the electrode surface are given in the previous section. In this case pyrene derivatives[53], phthalocyanines[55] and porphyrins[54] were used to mediate electron transfer of biological analytes such as NADH, cysteine and hydrazine. Redox active CMEs can also be constructed by incorporating mediators into electrode materials such as carbon paste and graphite epoxy as discussed above.

A popular method for immobilising redox mediators into CMEs is to use a polymer coating[20]. Two types of redox polymer may be distinguished, namely, those with covalently bound redox sites and those in which electron transfer mediators have been electrostatically incorporated[20]. The latter variety of redox polymer can be prepared by exchanging charge-compensating ions in a polymer such as Nafion or protonated poly(vinylpyridine) (PVP) with electroactive ones. For example, PVP with electrostatically immobilised ferricyanide has been applied to mediate the electron transfer between NADH and a carbon paste electrode[73]. In this case, NADH was the product of a yeast cell catalysed reaction with ethanol and thus the CME was used for ethanol determination.

Conducting polymers. Conducting polymers differ from redox polymers because electron transport occurs through the polymer via a delocalised band structure rather than a site to site hopping mechanism[19]. Reactions of species dissolved in the contacting solutions occurs at the polymer/solution interface and permeation into the polymer is not necessary for electron transfer. However, when pinholes or pores exist both

modes of electron transfer may be operating. Examples of commonly used conducting polymers include polypyrrole, polyaniline, polyacetylene and polyphenylenes[19]. The conductivity of several of these polymers can be altered by electrochemical oxidation or reduction of the film. Hence they may be converted to non-conducting and non-redox active polymers.

Non-redox active and non-conducting CMEs. Chemically modified electrodes which are non-electroactive and non-conducting have been used to select analytes on the basis of charge, hydrophilicity/hydrophobicity and size. Examples of size selective CMEs are those coated with cellulose acetate[26,27,37] and non-conductive polyaniline[24], polypyrrole[23,24] and polyphenol[24] films. Lipid modified GC[56-59] and carbon paste electrodes[64] represent CMEs which select analytes based on hydrophobic/hydrophilic interactions. Selectivity based on charge has been achieved, for example, using Nafion coated electrodes which are especially permeable to cationic neurotransmitters. Alternatively, poly(4-vinylpyridine) in its protonated form, is cationic and therefore selective for anions such as ascorbic and uric acids (relative to cationic catecholamines)[39].

1.2.3 Electron transfer at CMEs

Effect of electrode modification on electron transfer rates. Chemical modification of an electrode can affect the rate of electron transfer of analytes. The presence of a modifying monolayer or film can alter electron transfer rates by catalysing the reaction, increasing the distance of closest approach of the analyte, forcing electron transfer to proceed via a non-adiabatic mechanism (for an insulating coating) and by changing the electrical double layer.

As discussed earlier, electrode reactions are catalysed when their rates are enhanced in the presence of an agent without consumption of that agent. Electrocatalysis may also arise from the electrode itself. It is thought in this instance that catalysis results from configurations of atoms on the surface which are effective at promoting the desired conversion because they can form transitory bonds with the starting material and critical intermediates[50].

Electron transfer rates can be slowed by coating the surface with an ultra-thin (~0.8 nm) uncharged insulating film[49] which increases the distance of closest approach of the analyte. Coating electrodes with thicker, neutral insulating films (typically 1–3 nm) forces electron transfer to proceed at decreased rates by non-adiabatic (electron tunneling) processes[46]. The tunneling barrier coefficient, β, for a film can be calculated by observation of the current arising at different film thicknesses. The variation in the current is given by equation 1.1:

$$i = i_0 e^{-\beta d} \qquad (1.1)$$

where i_0 is the current measured at the bare electrode and d is the thickness of the monolayer film.

Reaction rates can be increased or decreased by changes in the electrical double layer at the electrode surface induced by electrode modification. A simplified diagram representing the potential profile across the double layer region is shown in Figure 1.9. There are two ways in which changes in the electrical double layer at the electrode are manifested: the ϕ_2–effect and by electrostatic interactions[49,74,75]. The ϕ_2–effect is important when specific adsorption of ions onto the electrode surface occurs or when a charged monolayer or ultra-thin neutral layer is applied to the electrode. The potential difference driving the electrode reaction changes from (ϕ_M - ϕ_S) to (ϕ_M - ϕ_S - ϕ_2). Hence, when an anionic layer is present at the electrode surface, the driving force for electron transfer of solution species increases for oxidation and decreases for reduction. The converse is true for a cationic coating, whilst a neutral adsorbent decreases the driving force for oxidation and reduction via resistive effects. Electrostatic interactions may be important because a charge at the electrode/solution interface will alter the concentration of charged species near the surface and hence affect the observed rate of electron transfer. The rate of electron transfer of positively charged electroactive analytes will be increased at negative surfaces, and that of anionic species will be decreased[75] (and *vice versa* for positively charged surface coatings).

Figure 1.9: Gouy-Chapman-Stern model for the potential (ϕ) profile across the electrical double layer

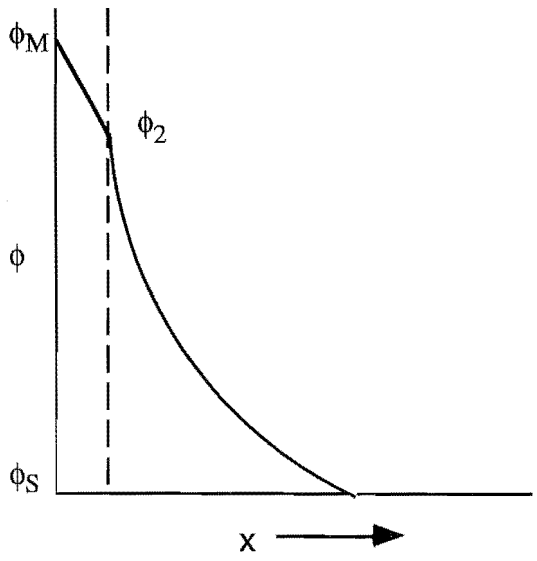

Mode of electron transfer. Coating an electrode surface can give rise to several modes of electron transfer depending on the characteristics of the modifying layer and electroactive species. Assuming the coating is homogeneous (and not itself electroactive), three modes of electron transfer can be distinguished. These are outlined in Figures 1.10, 1.11 and 1.12 below for the oxidation of A to A^+ + an electron, where M^- represents the counterion.

(i) Across-film electron transfer. As mentioned above, electron tunneling may occur when thin fully-insulating films are present at the electrode surface. This mechanism is the dominant mode of electron transfer at closely packed self-assembled monolayers of ω-hydroxythiols on Au[46,47].

Figure 1.10: Electron tunneling across a spacing layer

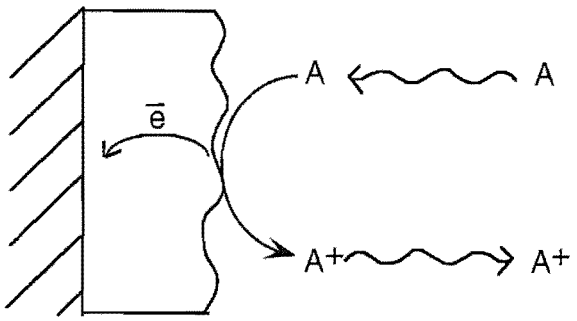

(ii) Diffusion through pinholes/channels. Electron transfer involves diffusion of electroactive species through solvent-filled pores or channels in the film with oxidation of species A at the electrode surface (see Figure 1.11). Electron transfer only occurs at areas where the channels communicate with the electrode surface, as the modified regions are assumed to completely block electron transfer reactions[76].

Figure 1.11: Diffusion through pinholes/channels

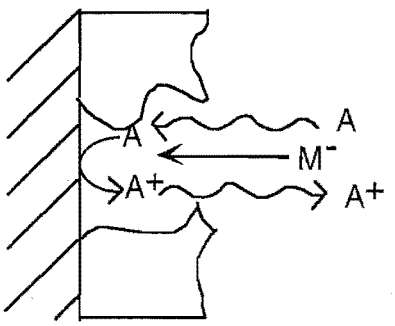

(iii) Membrane diffusion. This mode of reaction (illustrated in Figure 1.12) involves diffusion through the film material itself, characterised by a diffusion coefficient (D_m) which may not be the same as that in solution (D_s). Here, the species diffuse in a completely homogeneous phase. The permeability (P_m) of an analyte at a membrane coated electrode depends on its apparent diffusion coefficient (D_{app}) and the film thickness (δ_m)[23]. The apparent diffusion coefficient is a function of D_m and the partition coefficient (α). These relationships are shown in the equation (1.2) below.

$$P_m = D_{app}/\delta_m = \alpha D_m/\delta_m \qquad (1.2)$$

Figure 1.12: Membrane diffusion

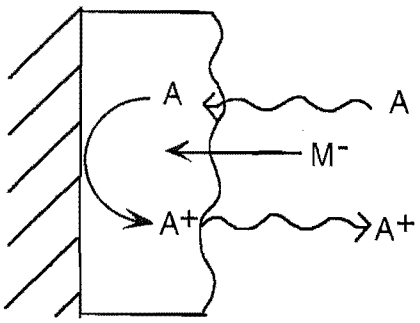

Often, at coated electrodes, more than one of the above modes of electron transfer may be operating. Further, when inhomogeneous electrode coatings are present, the size and spacing of modified and unmodified regions can affect the apparent rates of electron transfer. This is discussed below.

Manifestations on apparent rates of electron transfer. Apparent changes in electron transfer rates can be observed at partially blocked (or modified) electrode surfaces and the theory for this has been developed for CV techniques[77]. The apparent rate constant (k^o) at an electrode surface modified by adsorbed electroinactive species is a function of the fractional coverage (θ), the standard rate constant at the bare electrode ($k^o_{\theta=0}$) and the rate constant at the blocked areas (k^o_c), as shown in equation (1.3)[77,78].

$$k^o = k^o_{\theta=0}(1 - \theta) + k^o_c\theta \qquad (1.3)$$

When electron transfer is prevented (or slowed) at the coated portion of the electrode relative to the bare surface, i.e. $0 \leq k^o_c < k^o_{\theta=0}$, decreased electron transfer kinetics may be observed. The size and spacing of these active and inactive sites influences the apparent electron transfer rates. When electroactive regions are small and closely spaced relative to the diffusion layer thickness, cyclic voltammograms in which the heterogeneous rate constant is a weighted average of that at the active and inactive (or partially active) sites result[51,77]. Similarly, when the rate of electron transfer at covered portions of the

electrode is increased relative to the bare surface, ($k^{o}_{c} > k^{o}_{\theta=0}$), enhanced kinetics may be seen.

Considering all these factors it should be noted that an observed increase in the rate of electron transfer at a modified electrode surface can only arise from catalysis, favourable double layer effects, or by slow diffusion leading to mass transport (versus electron transfer) control of the reaction. Conversely, an observed decrease in the electron transfer rate might arise from blocking of catalysis, a switch to electron tunneling, unfavourable double layer effects, or a mixture of the above at a partially modified surface.

1.3 Electrochemical pretreatment (ECP) of carbon electrodes

Carbon is the electrode material of choice for many electrochemical analyses. Forms of carbon commonly used as electrodes are glassy carbon (GC), highly ordered pyrolytic graphite (HOPG), pyrolytic graphite, carbon fibre, graphite epoxy (GE), and carbon paste. The characteristics of these materials have recently been reviewed by McCreery[51]. Carbon electrodes exhibit a moderately wide potential window. Particularly, in the positive direction, they allow measurement of many oxidisable species in aqueous conditions. They may be used over a range of pH, are robust, and relatively inert. Hence, some form of carbon electrode is often used when measuring analytes of clinical interest.

The electron transfer kinetics of many analytes at carbon electrodes appear sluggish compared with metal electrodes. Much effort has been directed at systematically determining the effect of carbon electrode surface character on the electron transfer reactivity of a range of redox couples[51,79]. In particular the role of surface functional groups has been investigated. Figure 1.13 shows some of the oxide functional groups which may be present at polished carbon electrode surfaces. Strategies aimed at elucidating the influence of surface groups have included the specific derivatisation of functional groups, non-specific adsorption of charged and neutral moieties, and non-specific removal of oxides by argon sputtering[79]. The extent to which changes in carbon surface functionalities are manifested depends on the redox systems studied. For couples undergoing simple outer-sphere electron transfers e.g. $Ru(NH_3)_6^{3+/2+}$ and $IrCl_6^{2-/3-}$, electron transfer rates show little dependence on electrode treatment. Conversely, dramatic changes in electrode kinetics are observed for couples such as $Fe(CN)_6^{3-/4-}$, catechol derivatives, AA and other species undergoing proton-coupled electron transfers. However, it appears that for the majority of redox couples, oxygen functionalities are not necessary for the observation of fast electrode kinetics, and the cleanliness of the surface is the most important factor. Thus a generally accepted conclusion is that the acceleration of electrode kinetics observed for many redox couples after electrode pretreatment, is due to

the exposure of active "pristine" carbon sites[82,90]. Well established exceptions are aquated metal ions $Fe_{(aq)}^{2+/3+}$, $V_{(aq)}^{2+/3+}$and $Eu^{2+/3+}$ [79] and redox proteins.

Figure 1.13 : Summary of functionalities which may be present at carbon electrode surfaces[a]

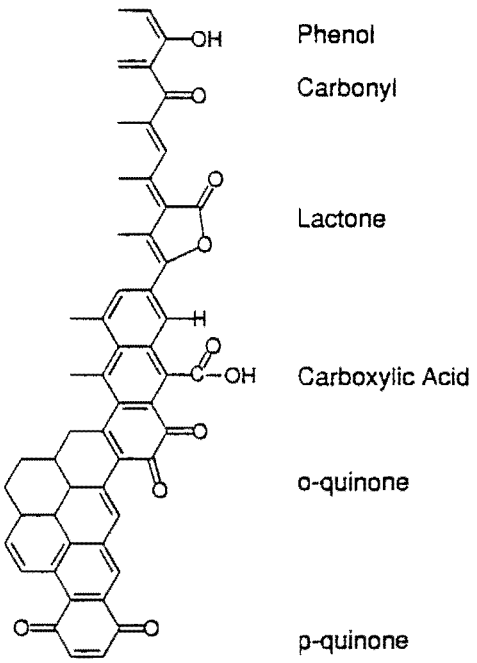

[a]from reference 51

Despite lacking a clear understanding of the reasons for poorly defined electrochemistry at carbon surfaces, it was recognised many years ago that an apparent improvement in electron transfer kinetics (with concomitant improvement in sensitivity and resolution) was attainable by "activating" the electrode. This has been achieved by high-speed polishing[80], radio frequency plasma, vacuum heat treatment (VHT), laser activation[81], and electrochemical pretreatments (ECPs)[82-94].

Electrochemical pretreatment is a popular method of activating carbon electrodes. It requires equipment already available to the electrochemist and may be performed in situ. Lord and Rogers[95] (1954) reported the use of ECP in the first paper describing graphite electrodes for voltammetric studies. Numerous ECPs have been described since; the variables being: the potential limits to which the electrode is exposed, electrolyte composition, and the length of time that the electrode is held at the pretreatment potentials. Electrochemical pretreatments are known to change the carbon microstructure, remove impurities, and form surface oxides, all of which are known to affect electron transfer rates

at carbon electrodes[79]. General features of changes induced by ECP are described below and ECPs are discussed further in Chapter Eight.

Oxidative electrochemical pretreatments performed in acid[82-87] and neutral[89-92] electrolytes are typically characterised by the formation of a non-electroactive, porous, permeable layer known as electrochemical graphite oxide (EGO). The thickness of the EGO layer increases with electrolysis time, and surfaces have high oxygen content. For example, an increase in O/C ratio from 0.084 on polished GC to 0.22 has been observed following ECP[90]. Additionally, surface waves attributed to redox reactions of quinone functionalities are commonly observed after ECP, and the electrode surface is often coloured and is more hydrophilic[86,90]. Organic cations and neutral species adsorb at these surfaces, and high background currents are typically present. Reduction of this layer is necessary to improve the electrochemistry of some analytes[90]. For EGO formed in strong acid conditions, reduction is thought to cause irreversible damage to the graphite lattice[51].

Electrochemical pretreatments performed in basic solutions yield activated surfaces which have lower oxygen content and backgrounds (compared with ECPs in acidic and neutral solutions)[88,93,94]. These surfaces are also non-porous. It has been suggested that although an EGO layer can be formed in base, it is unstable in these conditions and dissolves, exposing clean carbon surfaces. Thus, Anjo et al noted that the adsorption of dopamine at an EGO surface was decreased after soaking the electrode in 1 M NaOH[94].

An alternative ECP strategy involved the rapid cycling between "extreme" potentials (typically ± 6 V) in chloride media[91]. The resultant surface showed high activity and microscopic examination revealed the development of a pitted surface.

1.4 Characteristics of voltammetric response

For the work described in this thesis, the voltammetric responses of analytes are investigated using various electrochemical techniques, and information about the kinetics of electron transfer is deduced. Therefore, some diagnostic characteristics of voltammetric data (T = 298 K) are briefly summarised below for the redox process:

$$O + n\bar{e} \xrightarrow{k^o} R$$

Cyclic voltammetry of solution species. A typical cyclic voltammogram for a chemically reversible redox couple is shown in Figure 1.14, and Table 1.1 summarises the observed relationships for electrochemically reversible, quasi-reversible and irreversible processes.

Figure 1.14: Cyclic voltammogram for a reversible process, where O is initially present in solution[a]

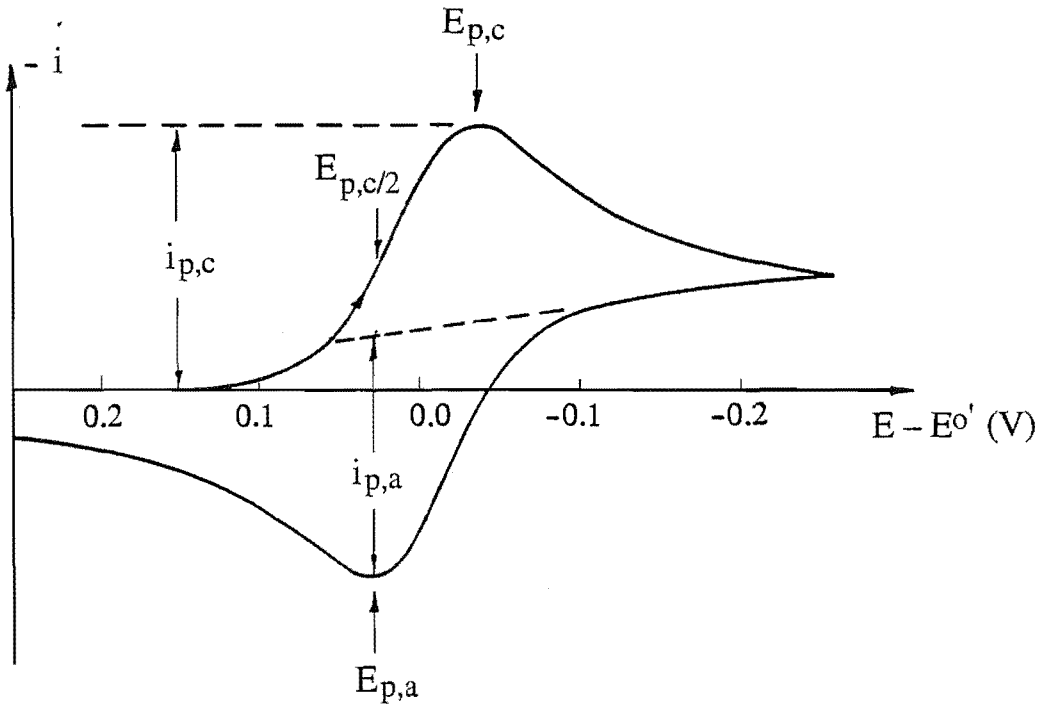

[a]adapted from reference 96

Table 1.1 Diagnostic relationships for cyclic voltammograms of chemically reversible processes[a]

reversible: the rate of electron transfer is fast compared to the rate of mass transport and does not control the overall rate.
$\lvert E_{p,a} - E_{p,c} \rvert = \Delta E_p = 59/n$ mV, where n = number of electrons
$i_{p,a}/i_{p,c} = 1$
$i_p \propto \nu^{1/2}$
E_p is independent of ν
$E_{1/2} \approx E^{o'}$
quasi-reversible: the rate of electron transfer and mass transport are similar and both control the overall rate.
$\Delta E_p > 59/n$ mV and increases with scan rate
ΔE_p increases as the standard heterogenous rate constant, k^o, decreases
totally irreversible: the rate of electron transfer is slow compared to the rate of mass transport and controls the overall rate.
no reverse peak
$i_p \propto \nu^{1/2}$
$E_{p,c}$ moves negative with increasing scan rate
$E_{p,c}$ moves negative as k^o decreases

[a] ν = scan rate

Cyclic voltammetry of adsorbed species. When the response arises from electrochemically reversible species adsorbed at the electrode surface, a cyclic voltammogram such as that shown in Figure 1.15 may be obtained. In this case, the free energies of adsorption for oxidised and reduced forms are the same, and adsorption follows a Langmuir isotherm. Hence $E_{p,a} = E_{p,c}$ and $i_{p,c} = (n^2F^2\Gamma_o\nu)/(4RT)$, where Γ_o is the surface excess of oxidised species before the sweep.

Figure 1.15 : Cyclic voltammogram for the reduction of adsorbed O and re-oxidation of adsorbed product[a]

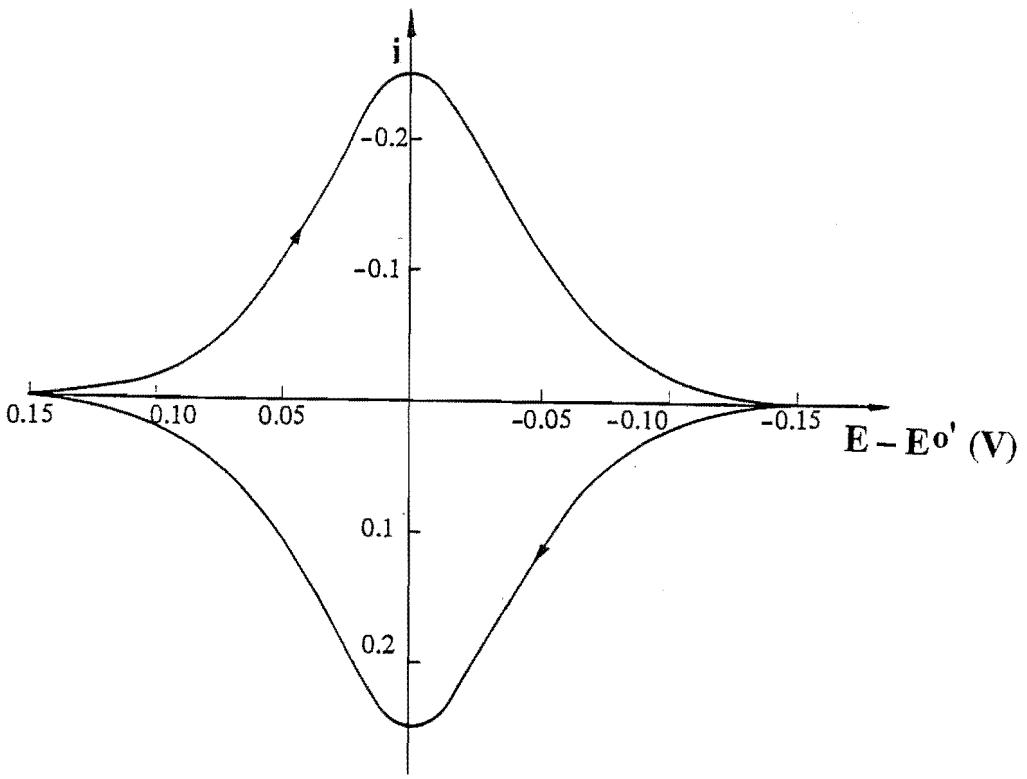

[a]free energies of reactant and product are the same and adsorption follows the Langmuir isotherm. Adapted from reference 96

Hydrodynamic voltammograms. For an electrochemically reversible couple; $|E_{3/4} - E_{1/4}| = 59/n$ mV, and $E_{1/2} \approx E^{o'}$. When the couple is not electrochemically reversible, $|E_{3/4} - E_{1/4}| > 59/n$ mV, and $E_{1/2} < E^{o'}$.

1.5 Electrochemistry of some biologically significant compounds

The electrochemistry of some biological analytes of interest are summarised below. Uric acid and ascorbic acid, which are present to varying extents in plasma, urine and extracellular fluid of the brain, are common interferrents in electrochemical analyses of drugs and neurotransmitters. However, their levels in biological fluids are also important indicators of physical well-being.

1.5.1 Ascorbic Acid

L-Ascorbic acid (vitamin C) is anionic at neutral pH (pKa = 4.10)[44]. It undergoes an electrochemically irreversible oxidation at mercury and carbon electrodes to produce dehydroascorbic acid. This involves the loss of two electrons and one proton, followed by a rapid solvation reaction (see Figure 1.16). The rate constant for chemical decomposition (k_r), given by $k_r = (Dk_f)^{1/2}$ where k_f is the rate of the hydration reaction ($1.4 \times 10^3\ s^{-1}$), is thirty times greater than the rate constant for diffusion (k_d). The first step in the mechanism proposed by Deakin et al[97] is loss of an electron. A proton is then released to form a radical anion followed by loss of the second electron.

Figure 1.16: Ascorbic acid oxidation at physiological pH

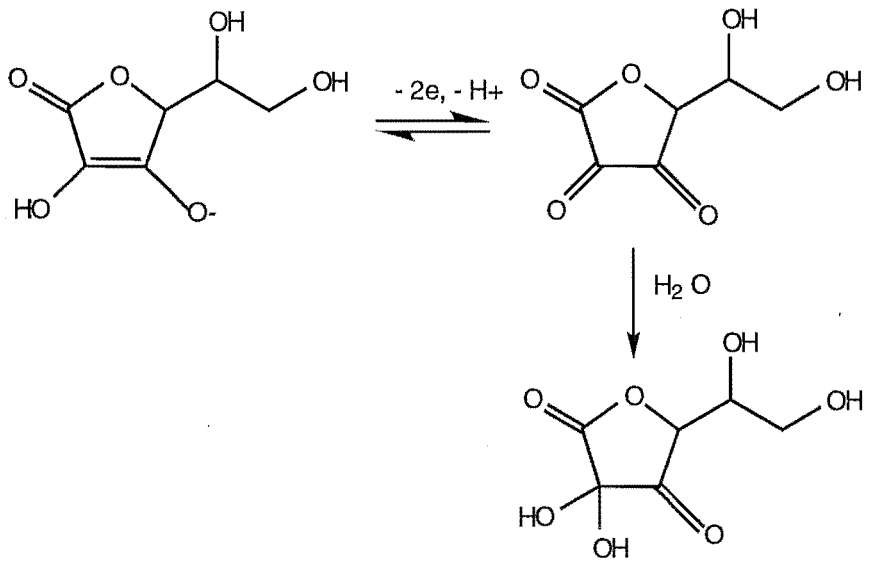

1.5.2 Uric Acid

Uric acid is the final metabolic product of purine derivatives in humans. It is negatively charged at physiological pH (pK_{a1} = 5.40 ± .02 and pK_{a2} = 9.80 ± .02)[98]. In phosphate buffer pH > 7 it undergoes a quasi-reversible two-proton, two-electron oxidation to form an unstable product. This may be reduced at very negative potentials (ca. -1.3 V vs SCE) with concomitant dehydration to give the parent compound (see Figure 1.17). Alternatively the reactive intermediate can rearrange in several steps to form allantoin[3].

Figure 1.17: Uric acid oxidation at physiological pH

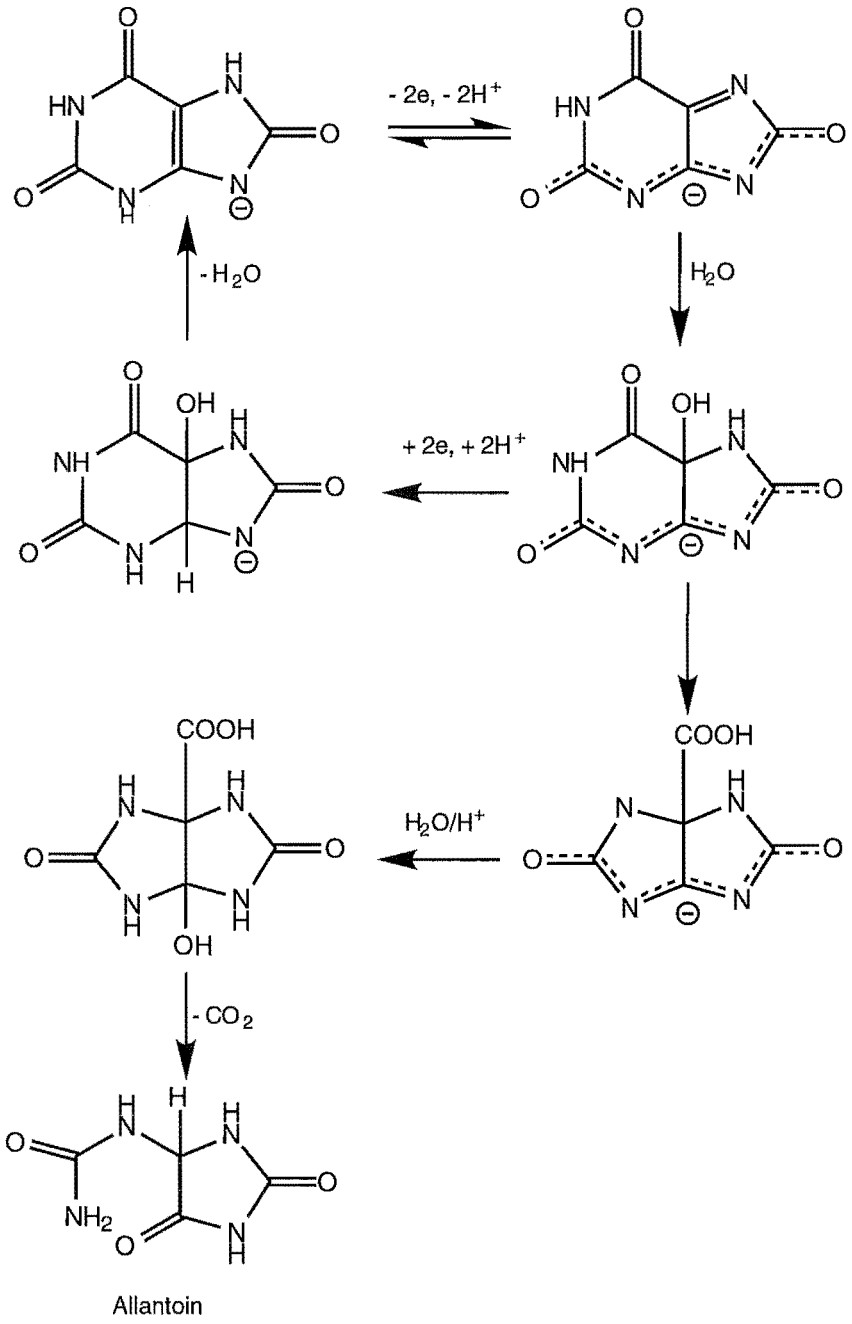

1.5.3 Acetaminophen

The electrochemistry of acetaminophen is shown in Figure 1.18. Acetaminophen (or paracetamol as it is also named) is commonly used as an aspirin substitute. It is known to cause kidney and liver damage when administered in large amounts, and its electroanalysis has been extensively studied. Acetaminophen is oxidised in a pH dependent, two-electron, two-proton process to N-acetyl-p-quinoneimine (NAPQI)[99] which is largely uncharged in the 0 – 8 pH range. At pH 6 or higher, quasi-reversible cyclic voltammograms are observed at scan rates of 40-250 mV s^{-1} indicating that the product is stable on these timescales. At lower pH, NAPQI is protonated to give a less stable electroactive species (III) which is rapidly hydrated to (IV). This product (which is non-electroactive between -0.2 V to 1.0 V vs Ag/AgCl) may then decompose to yield benzoquinone[99].

Figure 1.18: Acetaminophen oxidation

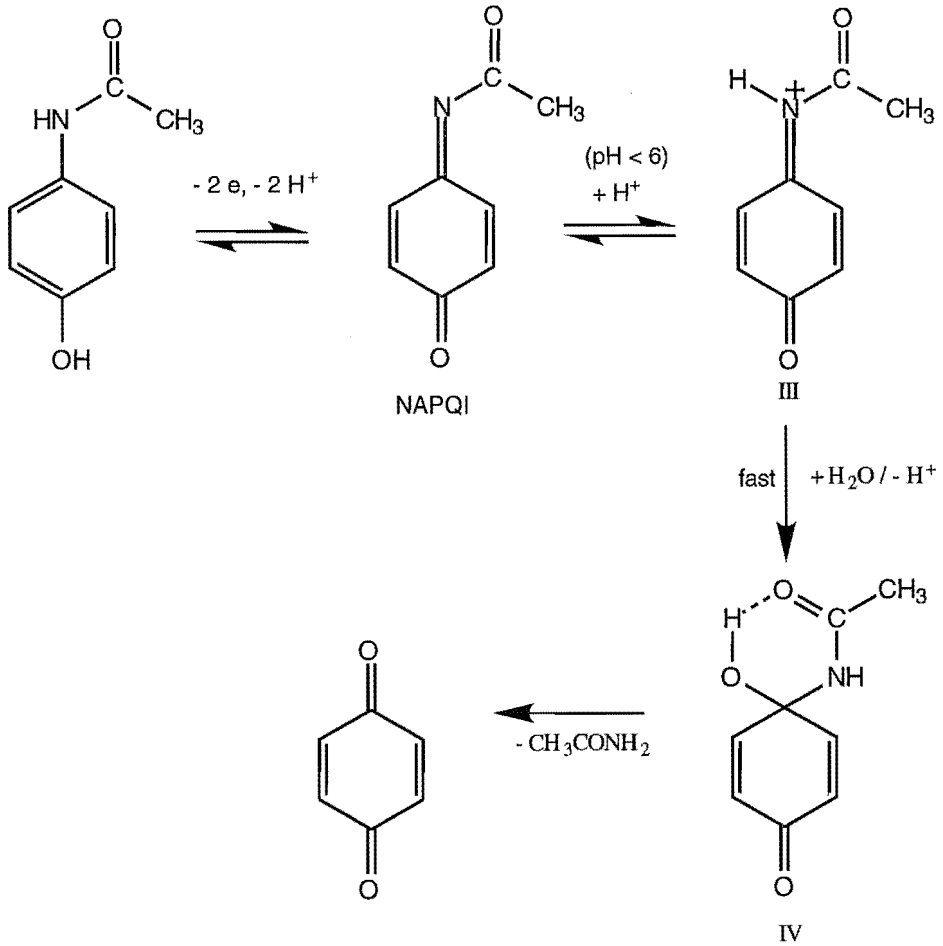

1.5.4 Chlorpromazine

Chlorpromazine (CPZ) belongs to a major group of phenothiazine-based tranquillisers. At neutral pH, CPZ is cationic. It undergoes three one-electron oxidations in phosphate buffer at $E^{o'}$ = + 0.65V, + 0.90V and + 1.10V vs SCE[100]. The first step is quasi-reversible, yielding a small reverse peak. The second oxidation is attributed to a CPZ^+–supporting electrolyte adduct and the third to CPZ sulfoxide (CPZO). These oxidation products are shown in Figure 1.19.

Figure 1.19: Products of stepwise chlorpromazine oxidation

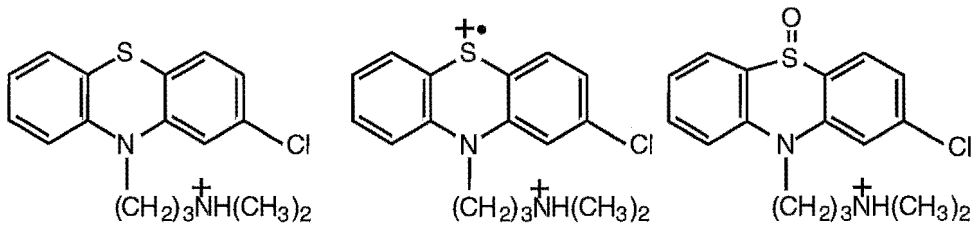

1.5.5 Derivatives of Catechol (3,4-dihydroxybenzene)

At pH 7, catechol derivatives undergo electrochemically quasi-reversible two-electron, two-proton oxidations producing the corresponding *o*-quinones (as shown in Figure 1.20). The mechanism at carbon electrodes suggested by Deakin et al[97] for 3,4-dihydroxyphenylacetic acid (DOPAC), 3,4-dihydroxybenzylamine (DHBA) and 6-hydroxydopamine (6-OHDA), involves initial loss of a proton, followed by an electron. This gives an uncharged radical intermediate which then releases another proton and finally the second electron. The resulting *o*-quinones of catecholamines dopamine (DA) and norepinephrine (NE) rapidly intracyclise to 5,6-dihydroxyindolines. The rate of cyclisation is pH dependent. The resulting 5,6-dihydroxyindolines are very reactive and may be rapidly oxidised in a disproportion reaction by the *o*-quinone to produce an aminochrome[101]. Rates for this disproportionation process on planar electrodes (at pH 7.4) have been reported as 0.07 ± 0.03 and 0.49 ± 0.21 s^{-1} for DA and NE respectively[101]. In most cases the disproportion reaction of DA is too slow to be observed[51,101].

Figure 1.20: Oxidation of 3,4-dihydroxybenzene derivatives

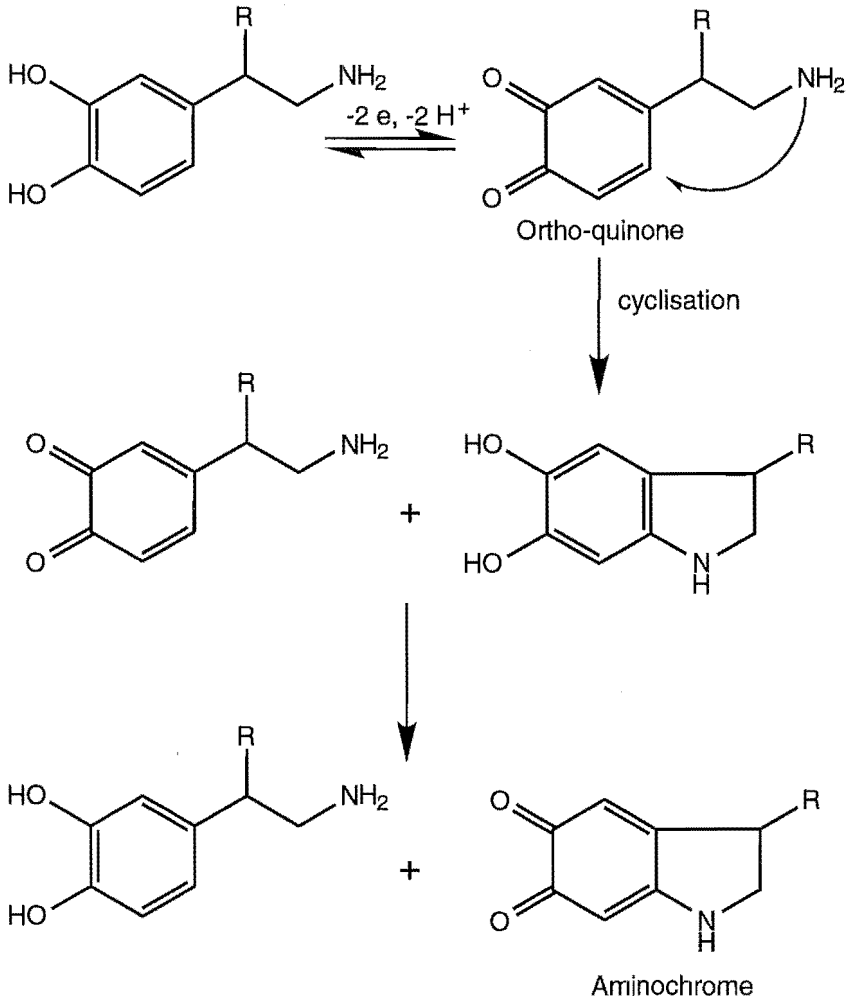

R = H dopamine
OH norepinephrine

1.6 Scope of this work

In this study, several of the problems associated with direct measurement in biological fluids (outlined in this introductory chapter) are addressed. Much of the work described is concerned with investigating the properties, and analytical utility of covalently modified glassy carbon electrodes prepared using the diazonium salt coupling procedure shown in Figure 1.5.

Glassy carbon electrodes modified with monolayers of *p*-phenylacetate groups and *p*-benzoate moieties are characterised using electrochemical techniques. The responses of the CMEs to analytes of biological interest and to probe analytes with fast electrode kinetics are investigated. The CMEs are also examined to identify analytically useful responses, and the basis of the observed selectivity of response at the CMEs is assessed.

The suitability of *p*-phenylacetate and *p*-benzoate CMEs as probes for the measurement of DA in neurological environments where there is a large excess of AA is examined in detail. Conventional-size CMEs are used for experimental simplicity, and the modification is also applied to carbon fibre microelectrodes. The analytical usefulness of the CME is assessed by evaluating response time to DA, selectivity for DA over AA, and sensitivity to DA using electrochemical techniques routinely applied to DA measurements *in vivo*.

Chemically modified electrodes are also prepared by attachment of *p*-alkylbenzene moieties to the electrode surface (using the diazonium salt procedure). The selectivity of response at these CMEs is investigated using a series of probe analytes. The origin of electrochemical response for different probe analytes is explored and a model describing the CME microstructure is proposed.

Para-phenylacetate and *p*-alkylbenzene CMEs are applied to measurements in flow injection analysis systems. The selectivity of response of the modified detectors to acetaminophen and CPZ in the presence of biological interferents AA and UA is investigated. Both aqueous and mixed aqueous/organic carrier solutions are used, the latter to simulate conditions present when using electrochemical detection following reversed-phase HPLC. A retention-time based strategy is applied to separate the response of target analyte (acetaminophen or CPZ) from interfering species and a covalently modified multi-detector array is used to simultaneously measure acetaminophen, UA, and AA in synthetic solutions and a diluted urine sample.

A fundamental study investigating protein adsorption at CMEs is described. Modified GC surfaces are prepared using direct diazonium salt coupling methods and by utilising carboxylate functionalities produced by covalent modification as the basis for further reactions at the electrode surface. A novel method of assessing protein adsorption is used which relies on observing electrochemical response perturbation of a probe analyte in the presence of protein. The importance of the charge, distance of extension from the electrode surface, and density of attached groups for reducing protein adsorption is elucidated.

Further protein adsorption studies are conducted at various unmodified carbon electrode materials, GC surfaces which have been electrochemically pretreated and CMEs prepared by methods other than diazonium salt modification. In the latter category are basal plane graphite surfaces modified with charged surfactants, graphite epoxy with incorporated ionic surfactants, and cellulose acetate coated electrodes. The suitability of these modifications for electroanalysis in solutions containing protein is examined.

Chapter Two: Experimental

2.1 Instrumentation

2.1.1 Electrochemical apparatus used with conventional-size electrodes

Cyclic voltammetry (CV) was performed using a PAR Model 173 Potentiostat coupled to a home-built waveform generator or a PAR Model 174 A Polarographic Analyzer coupled to a PAR Model 175 Universal Programmer. Ouput was recorded on either a Graphtec WX1200 or PAR 0092 recorder. Alternatively a computer-interfaced PAR Potentiostat/Galvanostat Model 273 A was utilised.

Differential pulse voltammetry (DPV) was performed using a PAR 174 A Polarographic Analyzer or a PAR Model 273 A Potentiostat/Galvanostat. Chronoamperometric and chronocoulometric experiments were also performed with the PAR Model 273 A Potentiostat/Galvanostat.

Flow injection analysis (FIA) experiments and ECPs in acid and base utilised the PAR 174 A and PAR 173 set-ups. For square-wave ECP, an Exact Elect Inc. Waveform Generator Model 7030 was coupled to the PAR Model 173 potentiostat.

2.1.2 Nuclear magnetic resonance (^{1}H NMR)

Proton ^{1}H NMR measurements were made using a Varian Unity 300 Spectrometer.

2.2 Electrodes and cells

A standard three-electrode cell was used in experiments involving conventional-size electrodes. This consisted of a working electrode, platinum wire auxiliary electrode and home-made saturated calomel reference electrode (SCE) shown in Figure 2.1. Experiments with microelectrodes used a platinum wire auxiliary and Ag/AgCl (3M NaCl) reference electrode. The diazonium electrode modification in acetonitrile utilised a platinum wire auxiliary electrode and a Ag/Ag^+ (10 mM $AgNO_3$ in CH_3CN/0.1 M tetra-*n*-butylammonium fluoborate) reference electrode.

Figure 2.1: Saturated calomel electrode

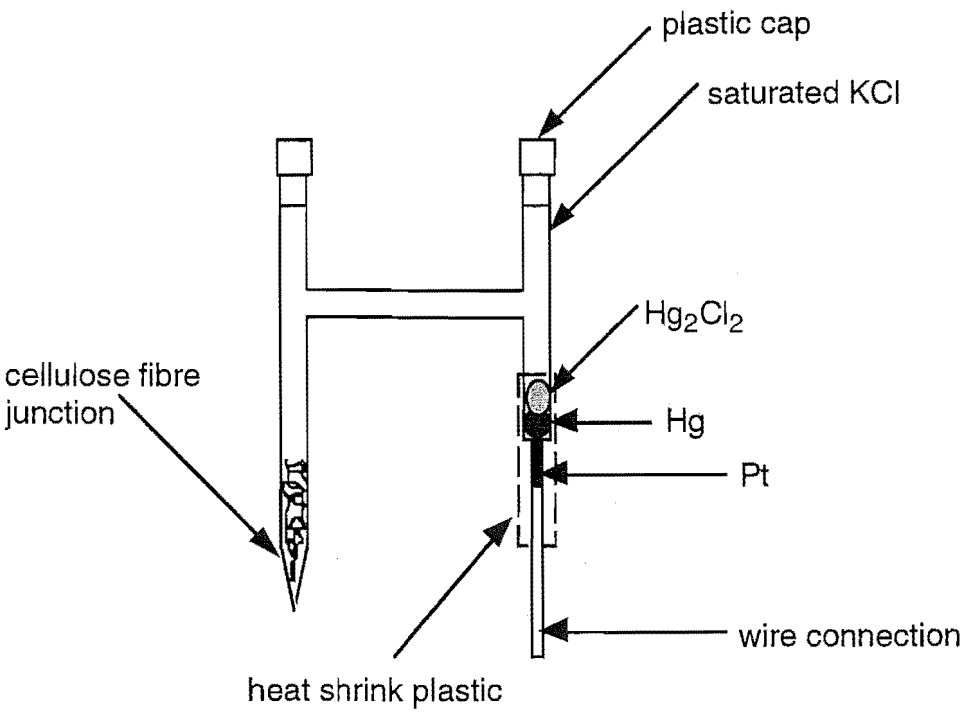

2.2.1 Perspex cells

Stationary experiments in aqueous solutions were performed in home-made perspex cells (shown diagramatically in Figure 2.2). These were tapered to allow convenient measurement of small sample volumes and inner sections of the lids were interchangeable to accommodate different sized electrodes. Non-aqueous diazonium modification procedures used glass cells with Teflon lids.

Figure 2.2: Perspex cell

2.2.2 Carbon electrodes

Conventional-size glassy carbon (GC) electrodes were constructed by sealing glassy carbon rod (0.3 cm diameter; Atomergic Chemetals, VC-10) in Teflon. Contact to the glassy carbon was made with a brass rod. Single microdisk electrodes were fabricated from 11 μm diameter glassy carbon fibre sealed into glass[102]. The random array microdisk (RAM) electrode was a gift from Dr S. Fletcher, CSIRO, Port Melbourne, Australia.

Preparation of temporary GC and graphite electrodes. Temporary GC electrodes were prepared for use in electrochemical studies involving severe ECPs. A length of 3 mm diameter carbon rod (ca. 0.5 cm) was sealed onto a glass cylinder using heat-shrink Teflon or plastic tubing. Electrical connection was made by placing a drop of mercury onto the carbon and contacting this with copper wire. The open end of the glass tube was then sealed with wax. The same procedure was used to prepare the high density graphite (PAR G0091) electrodes which had an electrode area of 0.33 cm^2.

Preparation of graphite epoxy and GE-surfactant electrodes. Graphite epoxy electrodes were fabricated by filling one end of a glass tube with Dylon Grade RX epoxy-bonded graphite. The graphite epoxy was a combination of 1:1.1 w/w accelerator and epoxy resin. The two components were mixed until a homogeneous product was obtained (ca. 10 min). The mixture was then divided into portions and a known amount (typically 10% w/w) of surfactant was added and thoroughly mixed into the epoxy. The epoxy was packed into a length of glass tubing and copper wire was inserted to make the electrical connection. The electrode was cured overnight at 70°C then polished using polishing papers of increasing fineness. The geometric electrode area was either 0.025 or 0.05 cm^2.

Preparation of carbon paste electrodes. Carbon paste was prepared by mixing 1 g of UCP-1M Ultra Microcrystal Grade graphite powder and 1.5 mL of Nujol. This mixture was packed firmly into a Teflon cavity which was in contact with a brass rod. The cavity was ca. 4 mm in depth with a diameter of 3.8 mm giving a geometric electrode area of 0.11 cm^2. A new electrode surface was generated by replacing the outer layer of carbon paste (approximately 2 mm in depth).

Polishing procedures. Newly prepared GC electrodes were polished to a mirror finish using graded sanding papers followed by 9, 6, 3 then 1 μm diamond paste on LECO Lecloth. Between experiments, GC electrodes were polished with 1 μm diamond paste and rinsed in acetone followed by doubly distilled water. The same procedures were utilised for GC detectors in flow cells. Polishing procedures for carbon fibre microelectrodes and the carbon microdisk array are described in Chapter Four.

2.3 Flow injection analysis (FIA) apparatus

Manifold (1). An Alitea C4-XV peristaltic pump was used with a two channel manifold consisting of a reference solution (0.1 M KCl) and the carrier (buffer) solution. A home-built six-port rotary injection valve made from Dalron was utilised with either a 50 µL or 30 µL sample loop.

Manifold (2). A similar two channel set-up was used as for manifold (1) with a Rheodyne Teflon six-port rotary injection valve. The sample loop was 15 µL. This manifold was used with several GC amperometric detectors at different times. Manifolds 1 and 2 are illustrated in Figure 2.3.

Figure 2.3: Diagram of manifolds 1 and 2 used in flow injection analysis

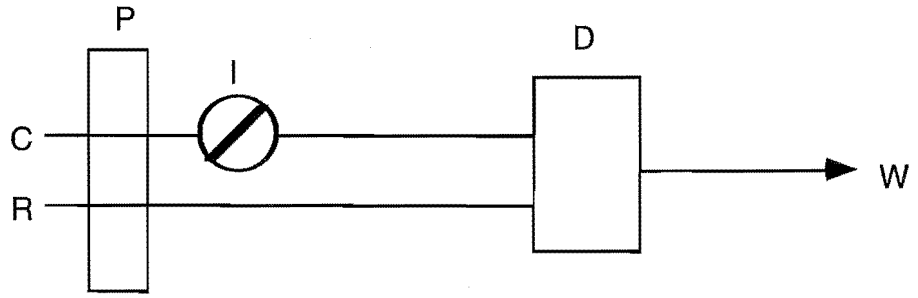

C = carrier solution, R = reference solution (0.1 M KCl), P = pump, I = injection valve, D = detector and W = waste

Detectors.

(a) Ag/AgCl referenced detector

The home-built detector was fabricated from two blocks of Dalron (10 x 20 x 32 mm) separated by a 0.76 mm Teflon spacer. Three electrodes were aligned on one block. A wall-jet configuration was used. The electrodes were 0.3 cm diameter glassy carbon, platinum auxiliary (0.5 mm) and 0.6 mm Ag wire for the Ag/AgCl reference electrode (0.1 M KCl).

(b) SCE referenced flow cell

A glassy carbon electrode (0.3 cm) with wall-jet configuration was the working electrode. A stainless steel spacer formed the auxiliary electrode and the reference electrode was an SCE in contact with the flowing solution.

(c) Multi-electrode detector

This home-built flow cell consisted of four individually addressable GC (0.3 cm diameter) working electrodes. Each working electrode was housed in Teflon with connection made by a brass rod. These GC electrodes were removable to allow individual modification. A configuration of two opposing parallel electrodes was used (see Figure 2.4). A rectangular flow channel with dimensions 4 x 20 x 0.2 mm directed the flowing solution. The detector block comprised two pieces of Dalron having dimensions 4.0 x 1.2 x 3.0 cm. A stainless steel spacer was used for the auxiliary electrode and a Ag disk (1 mm diameter) was used for a Ag/AgCl (0.1 M KCl) reference electrode.

Figure 2.4: Assembled and disassembled views of the multi-detector electrode array

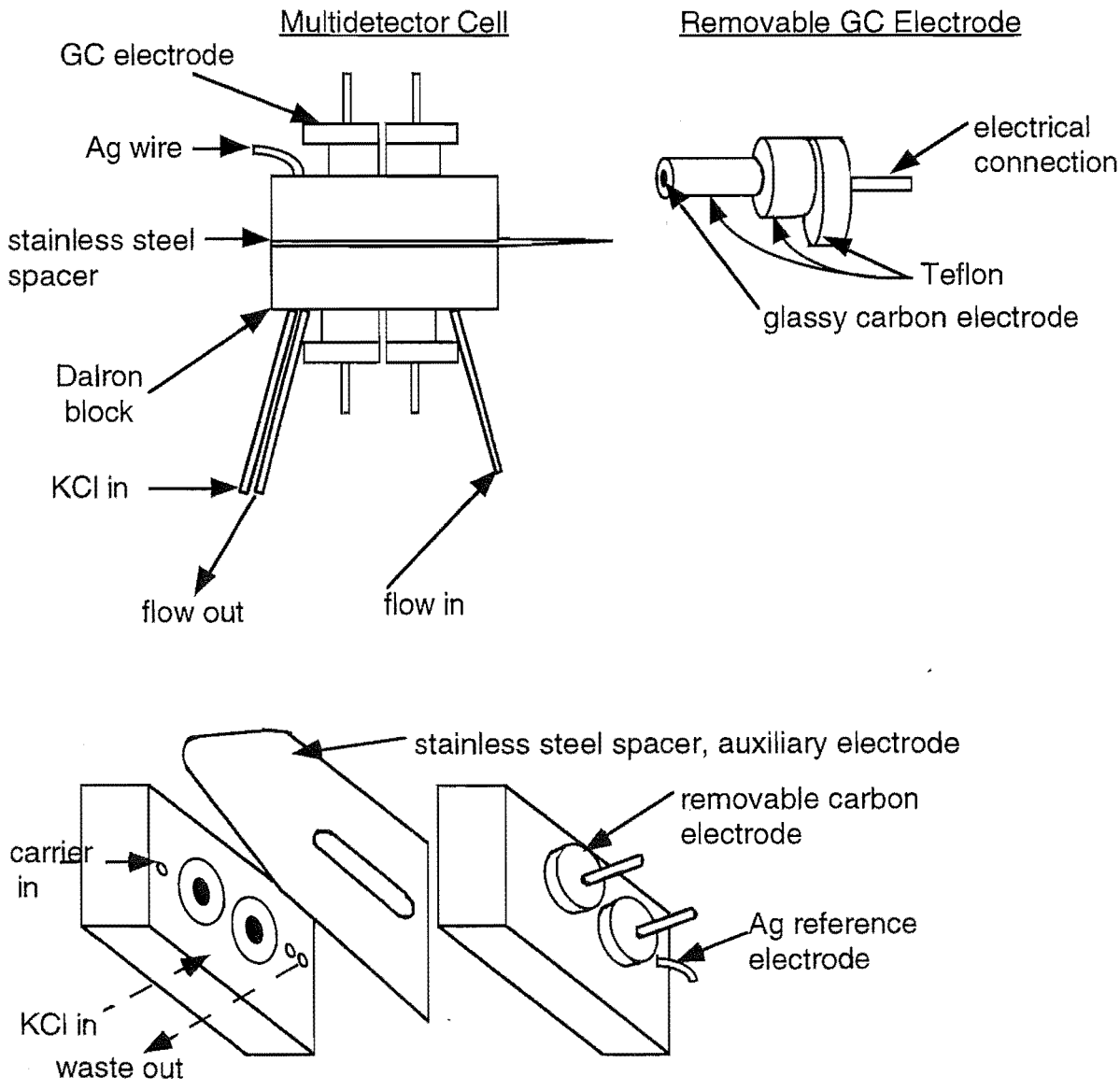

Flow rates were measured by weighing the amount of water collected after a known time (typically 5 or 10 min) for a given pump speed. The specific density of water (at 25°C) was then used to calculate the volume of water passed through the flow apparatus.

2.4 Cleaning procedures

2.4.1 Perspex cells

Perspex cells were briefly rinsed in ethanol followed by distilled water and then soaked in a 10% nitric acid/doubly distilled water (DDW) bath. Cells were soaked in, or thoroughly rinsed with, DDW and allowed to dry prior to use.

2.4.2 Glassware

All glassware was "B" grade. Cleaning procedures involved either washing with detergent followed by rinsing in acetone and soaking in 10% nitric acid or soaking in a base bath (isopropyl alcohol saturated with KOH), prior to a final DDW wash.

2.5 Reagents and solutions

2.5.1 Reagents

Chlorpromazine (CPZ), dopamine hydrochloride (DA), 1,2-dihydroxy-anthraquinone-3-sulfonate (DASA), 3,4-dihydroxyphenyl acetic acid (DOPAC), 4-methylcatechol (4-MC), sodium lauryl sulfate (SDS), ferrocenemonocarboxylic acid (FCA), bovine serum albumin (BSA) (a 20 g dL^{-1} solution stabilised with sodium azide), 2-bromoethylamine hydrobromide and 1-cyclohexyl-3-(2-morpholino-ethyl) carbodiimide metho-*p*-toluenesulfonate (CMCT), were used as supplied from Sigma.

Cellulose acetate (39.8% acetyl content), 4-aminophenylacetic acid, 4-butylaniline, 4-heptylaniline, and 4-decylaniline, 4,4'-bipyridine and 4-(aminomethyl)pyridine were obtained from Aldrich and were used as supplied.

Ferrocenemethanol (FcOH), N,N-dimethylaminomethylferrocene methiodide (FcAm) and hexaammineruthenium(III) trichloride were used as supplied from Strem Chemicals.

Triton X-100, catechol, 1,2-dihydroxybenzene-3,5-disulfonate (tiron) 1,2-naphtho-quinone-4-sulfonic acid (NQS), fluoboric acid (~40%), tetra-*n*-butylammonium hydroxide,

(all reagent grade) were obtained from BDH. Poly(ethylene glycols), AA and UA (analytical reagent grade) were also obtained from BDH.

Chloroform used in amine syntheses was analytical reagent grade. Iodomethane was lab reagent grade from May & Baker.

Acetonitrile was dried by stirring over CaH_2 for two days followed by distillation onto fresh CaH_2 (5 g L^{-1}) and refluxing for at least two hours. It was then distilled onto P_2O_5 (10 g L^{-1}), re-distilled and stored over CaH_2 in a nitrogen atmosphere. The solvent was freshly distilled from this solution immediately prior to use.

Tetra-*n*-butylammonium fluoborate ($TBABF_4$) electrolyte was used for non-aqueous electrochemistry. This was prepared by mixing diluted solutions of tetra-*n*-butyl-ammonium hydroxide and fluoboric acid. Tetra-*n*-butylammonium hydroxide (20 mL of a 40% solution) was diluted to 100 mL with DDW. Fluoboric acid (5 mL of a 40% solution) was diluted to 25 mL with DDW. These two solutions were mixed with constant stirring and the precipitated salt was collected. This was thoroughly washed with DDW and dried under vacuum at ~ 80 °C for two days.

2.5.2 Phosphate buffer electrolyte solutions

Four varieties of phosphate buffer solutions were used as supporting electrolytes:

(1) Phosphate-buffered saline (PBS) pH 7.4. Phosphate buffer (0.04 M) with 0.1 M NaCl added electrolyte was prepared by dissolving analytical grade KH_2PO_4 (1.179 g), Na_2HPO_4 (4.302 g), both dried at 40°C, and 5.844 g NaCl in 1 L of DDW.

(2) Phosphate buffer (0.5 M) pH 7. This was prepared by dissolving 18.281g KH_2PO_4 and 16.419 g Na_2HPO_4 in 500 mL of DDW.

(3) Phosphate buffer (0.05 M) pH 7.4. A 1 L solution was made by dissolving 1.514 g KH_2PO_4 and 5.518 g Na_2HPO_4 in DDW.

(4) Phosphate buffer (0.1 M) pH 7.4. A 1 L solution was made by dissolving 3.028 g KH_2PO_4 and 11.037 g Na_2HPO_4 in DDW.

2.5.3 Bovine serum albumin solutions

The general method of preparing analyte/BSA solutions was as follows. The analyte solution in PBS was prepared and O_2 was removed by bubbling with N_2. For stationary measurements, 5.0 mL was transferred into an electrochemical cell and 100 μL of stock BSA solution (liquid 200 g L^{-1}, obtained from Sigma) was added giving a final concentration of 4 g L^{-1}. To avoid contamination, separate sets of cells, reference and auxiliary electrodes were used for BSA and non-BSA solutions.

2.6 Diazonium salt preparation and standard modification procedure

Para-substituted diazonium tetrafluoborate salts were synthesised from the corresponding aromatic amines using two variations of the "direct method"[103]. Syntheses were performed behind a safety shield and dried products were stored under vacuum in a dessicator in the absence of light.

(1) Fluoboric acid method. The aromatic amine (5 mmol) was added to 2 mL of 40% fluoboric acid pre-diluted with 2 mL of water and the solution was then cooled in an ice-bath. A solution of 0.346 g (5 mmol) sodium nitrite in 0.7 mL water was added slowly to the stirred solution maintaining the temperature around 10°C. The mixture was then cooled to ~ 0°C in a salt/ice bath. The precipitate was collected on a sintered glass filter which had been cooled with ice-water and washed with 1 mL volumes of cold 5% fluoboric acid followed by ice-cold methanol and ether. The product was thoroughly air-dried prior to storage in a dessicator.

(2) Hydrochloric acid method. The aromatic amine (3.3 mmol) was dissolved in 1 mL HCl (12 M) and minimum water with heating. Once completely dissolved the solution was cooled in an ice-bath and the corresponding chloride precipitated. Sodium nitrite 0.253 g (3.7 mmol) dissolved in minimum water was then slowly added to the stirred suspension being careful that the mixture did not overheat. As soon as the precipitate was fully dissolved sodium fluoborate 0.49 g (4.3 mmol) was added and the mixture stirred for a further 30 s. It was then rapidly cooled below 0°C in a salt/ice bath. The product was collected on a sintered glass filter and washed with cold 5% (w/v) $NaBF_4$ followed by ether and stored as described above.

2.6.1 Synthesis procedures and characterisation of diazonium salts

Para-benzoate diazonium salt was prepared from *p*-aminobenzoic acid using the fluoboric acid method (1) described above. A 60% yield of light yellow/brown product was collected. ^{1}H NMR (CD_3CN): δ 8.49 (*d*, 2H, CH), 8.62 (*d*, 2H, CH). The *p*-phenylacetate diazonium salt was synthesised from 4-phenylacetic acid by the hydrochloric acid method (2). Typical yields were ca. 70% of light brown crystals. ^{1}H NMR (CD_3CN): δ 4.0 (*s*, 2H, CH_2), 7.90 (*d*, 2H, CH), 8.47 (*d*, 2H, CH).

Para-alkylbenzene substituted diazonium salts were synthesised from their corresponding amines by the methods described above: *Para*-methylbenzene diazonium fluoborate (*p*-CH_3): method (1) using *p*-toluidine gave white crystals, 62% yield. ^{1}H NMR (CD_3CN): δ 2.24 (*s*, 3H, CH_3), 7.80 (*d*, 2H, CH), 8.40 (*d*, 2H, CH). *Para*-butylbenzene diazonium fluoborate (*p*-$(CH_2)_3CH_3$): method (2) using 4-butylaniline (liquid at room temperature) gave a brown wax-like product, 77% yield. ^{1}H NMR (CD_3CN): δ 1.80, 2.10 (*m*, 6H, CH_2), 8.20 (*d*, 2H, CH), 8.60 (*d*, 2H, CH). *Para*-decylbenzene (*p*-$(CH_2)_9CH_3$) diazonium fluoborate: method (1) using 4-decylbenzeneaniline (liquid at room temperature) gave light brown crystals, 57% yield. ^{1}H NMR (CD_3CN): δ 1.22, (*m*, 3H), 1.63 (*m*, 5H), 1.98 (*m* 3H), 2.28 (*m*, 7H), 3.21 (*m*, 3H, CH_3), 8.07 (*d*, 2H, CH_2), 8.68 (*d*, 2H, CH_2).

Para-methoxybenzene (*p*-OCH_3) diazonium salt was prepared from recrystallised *p*-anisidine using the fluoboric acid method (1). An 80% yield of light pink/brown crystals was obtained.

2.6.2 Standard procedure for electrode modification

Electrodes were polished with 1 μm diamond paste and sonicated in acetone for approximately 5 min prior to modification. Diazonium salt solutions used for modification (5 mM with 0.1 M $TBABF_4$ in freshly distilled acetonitrile) were prepared daily. A three electrode cell consisting of a platinum wire auxiliary and Ag/Ag^+ reference was used. The glassy carbon electrode was held at -0.94 V vs Ag/Ag^+ (i.e. -0.7 V vs SCE) for 5 min in the modifying solution. Following this, electrodes were rinsed and sonicated in acetone for a further 5 min.

2.6.3 Preparation of pyridinium and bipyridinium salts

Standard procedures for alkylation of pyridine derivatives were used to prepare amine modifiers[104].

4-aminomethyl-N-methyl pyridinium iodide 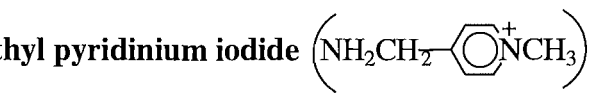

4-(aminomethyl)pyridine (9.3 mM, 1.00 g) and equimolar iodomethane (0.58 mL) were refluxed for 17 h in 20 mL chloroform. A yellow (hygroscopic) precipitate was collected and proton ^{1}H NMR confirmed that the product was the methylated starting material. ^{1}H NMR (D_2O):δ 3.07 (*t*, 2H, CH_2), 4.17 (*s*, 3H, CH_3), 7.40 (*d*, 2H, CH), 8.50 (*d*, 2H, CH).

4-(4'-pyridyl)-N-n-ethylamine pyridinium hydrobromide 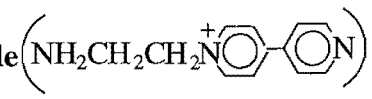

4,4'-bipyridine (3.3 mM, 0.51 g) and 2-bromoethylamine hydrobromide (3.3 mM, 0.67 g) were refluxed for ca. 42 h in 13 mL of dry acetonitrile. A yellow precipitate was collected and shown to be a mixture of the singly and doubly quaternised salt. The filtrate was evaporated to dryness and the acetonitrile soluble portion was isolated and dried. Cyclic voltammetry of this product in 0.1 M PBS and acetonitrile/0.1 M $TBABF_4$ gave a single reduction process ($E_{1/2}$ = -0.75 V vs SCE, ν = 100 mV s^{-1}) consistent with a monoquaternised salt.

N-n-ethylamine-N'-methyl-4,4'-bypyridinium iodide hydrobromide

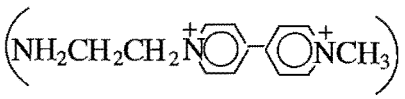

4,4'-bipyridine (3.3 mM) and iodomethane (3.3 mM, 0.204 mL) were stirred in 10 mL chloroform with ca. 0.5 mL DMF for 15 h at room temperature. A yellow precipitate resulted and was separated by filtration. The filtrate was evaporated to dryness and the solid recrystallised from acetonitrile. This product was then refluxed for 14 h in dry acetonitrile in the presence of equimolar (0.26 g) 2-bromoethylamine hydrobromide. A yellow precipitate was collected and the cyclic voltammogram in 0.1 M PBS showed the expected two reduction processes for the doubly quaternised bipyridinium at $E_{1/2}$ = -0.64 V vs SCE, ΔE_p = 60 mV and $E_{1/2}$ = -0.96 V vs SCE, ΔE_p = 65 mV.

2.6.4 Cellulose acetate coatings.

Base-hydrolysed cellulose acetate coatings. A 2% w/v cellulose acetate (CA) solution was prepared by dissolving 1.0 g of CA in 50 mL of 50/50 v/v cyclohexanone/acetone solution. A (2 μL) volume of this solution was applied to the freshly polished GC electrode or GC detector in a flow cell using a microsyringe and allowed to dry for 1 h. This was then hydrolysed by immersion in a stirred solution of 0.06 M KOH for 40 min, rinsed thoroughly in DDW and the flow cell was carefully assembled.

Phase-inversion cellulose acetate coatings. Phase-inversion coatings were prepared following a reported procedure[37]. A solution of 96.8% acetone, 1.9% (w/v) $Mg(ClO_4)_2$ and 1.3% (w/v) cellulose acetate was made by dissolving 0.125 g of cellulose acetate in 9.7 mL acetone and adding 1.7 mL of an aqueous $Mg(ClO_4)_2$ solution (0.52 M). A known volume of this solution (typically 2 μL) was applied to the electrode surface using a microsyringe and allowed to dry for a 20 – 30 s. The electrode was then placed in DDW at room temperature for 15 min then removed and cooled in ice-water for 1 h. Coated electrodes were stored in DDW at room temperature prior to use.

Chapter Three: Characterisation of *para*-phenylacetate and *para*-benzoate modified electrodes

3.1 Introduction

The modification of glassy carbon (GC) surfaces by covalent attachment of modifying species forms the basis of the work described in this thesis. The method used is that reported by Pinson et al [42,43]. In this procedure, a *para*-substituted aryl diazonium salt is electrolysed at -0.94 V vs Ag/Ag^+ in anhydrous acetonitrile with 0.1 M tetra-*n*-butylammonium fluoborate electrolyte. Attachment of modifying groups to the carbon surface is thought to proceed via a one-electron reduction of the adsorbed diazonium salt. The resulting radical species eliminates N_2 and reacts with the carbon surface forming a covalent bond.

Figure 3.1: Proposed mechanism for covalent modification of GC electrodes

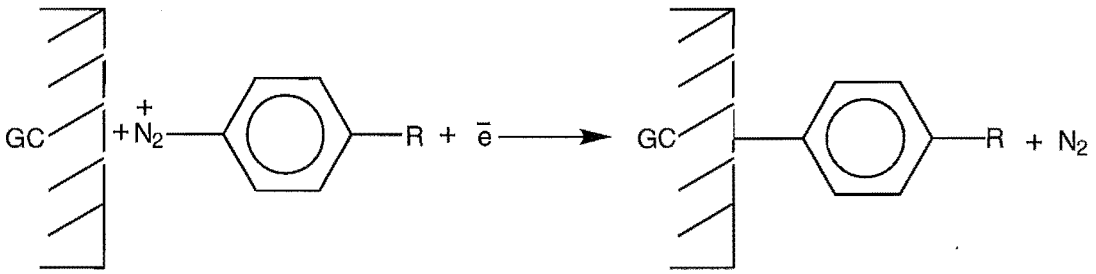

In the initial report, the modification of surfaces with 4-nitro, 4-cyano, 4-carboxy, 4-benzoyl, 4-bromo, 4-carboxymethyl, 4-acetamidobenzene and 4-nitro-naphthalene aryl functionalities was described[42]. The modification was also applied to carbon fibres, carbon powder, and both basal and edge planes of highly ordered pyrolytic graphite. The modified electrodes were characterised by cyclic voltammetry and/or X-ray photoelectron spectroscopy (XPS). Direct measurement of surface group coverage was achieved using an electroactive *p*-nitro modifier. Integration of cyclic voltammetric data indicated a surface coverage of 14 x 10^{-10} mol cm^{-2}. Direct evidence of covalent bonding was not demonstrated. However, adsorption of the diazonium salt prior to reduction and the stability of the aryl radical to reduction at the electrolysis potentials applied, favour this reaction[42].

In later work, the modification procedure was used to immobilise the enzyme glucose oxidase on GC electrodes[43]. This was achieved by coupling *p*-phenylacetate moieties to the electrode surface, followed by carbodiimide activation and reaction with the peripheral amino groups of the enzyme. The activity of the enzyme-modified electrode

was then determined by performing enzymatic electrocatalysis using ferrocenemethanol to mediate electron transfer.

The pKa of the surface groups of the *p*-phenylacetate CME has been studied by other workers[105]. Chronocoulometric measurement of adsorbed ruthenium hexaammine was used to assess the degree of deprotonation of *p*-phenylacetate groups as a function of pH. No accumulation of ruthenium hexaammine was observed at low pH values (pH < 2.8) where the *p*-phenylacetate groups are expected to be predominantly protonated. The amount of adsorbed ruthenium hexaammine (and by inference, the extent of deprotonation) increased with pH and a sigmoidal curve resulted giving a pKa ≈ 5. Although the actual pKa values of individual surface groups are expected to vary widely according to their specific environment, this gives an intrinsic pKa of the modified surface. This may be compared with a value of 4.19 for phenylacetic acid[106]. Markedly different values for apparent dissociation constants between monolayer functional groups and soluble related species are well documented for other CMEs[107-109].

Covalent attachment has important advantages for preparation of CMEs. These advantages mainly arise from the high stability of the attachment, enabling measurements to be made over long time periods, under vigorous hydrodynamic conditions and in organic media. Hence, we have investigated the aryl diazonium modification strategy for preparation of CMEs with useful properties for analysis.

In this chapter, the characterisation of *p*-phenylacetate and *p*-benzoate modified glassy carbon electrode surfaces is described. The conditions for reproducible electrode modification are established, the assessment of surface coverage is described and the accumulation of analytes at the CMEs is investigated. The effect of surface modification on the responses of ferrocene derivatives and several analytes of clinical significance are also examined. The aims of these latter experiments were to identify practically useful responses and to attempt to elucidate the mechanism of electron transfer at the modified electrode and the influence of the coating on electron transfer kinetics.

3.2 Experimental

3.2.1 Diazonium salt preparation and modification procedure

The preparations of *p*-phenylacetate and *p*-benzoate diazonium salts are described in Chapter Two. The standard modification procedure (also given in Chapter Two) was used in these experiments.

3.2.2 Flow injection analysis

Several FIA manifolds and detector cells are described in Chapter Two. Setup (A) utilised manifold (1) with detector (a); setup (B) manifold (2) was used with detector (a); setup (C) utilised manifold (2) with the SCE referenced detector (b) and finally (D) combined manifold (2) with the multi-electrode detector cell. Pump rates between 0.7 and 0.8 mL min^{-1} were used. Hydrodynamic voltammograms were obtained using 2 x 10^{-4} M analyte starting at the lowest potential. The reported peak current values are the average of at least three repeat injections at each electrode potential.

3.2.3 Chronocoulometry

Chronocoulometric experiments were performed using the PAR Model 273 A Potentiostat/Galvanostat. The supporting electrolyte was either phosphate buffered saline (PBS) or phosphate buffer (0.05 M) at pH 7.4. Surface coverages quoted are based on the geometric area of the glassy carbon electrodes (0.07 cm^2).

Chronocoulometry to obtain surface coverage. Electrodes were placed in thoroughly degassed 1 mM analyte solutions, stirred for 5 min and allowed to equilibrate for 10 s prior to measurement. A 200 ms potential step was applied from 0 to -0.6 V for ruthenium(III) hexaammine and from 0 to 1.0 V vs SCE for dopamine (DA). Potential steps in buffer only, collected prior to exposing electrodes to analyte solutions, were subtracted to correct for the charge due to the double layer.

3.2.4 Cyclic voltammetry

Cyclic voltammetry with low analyte concentrations. Cyclic voltammetry of adsorbed species was performed in degassed 6 μM ruthenium(III) hexaammine, 8.8 μM DA and 4-MC and 20 μM DOPAC. The modified electrode was stirred at open circuit in this solution prior to scanning. Generally stirring times of 5 min were used after which no increase in peak height was observed. Scan rates of ν = 100 mV s^{-1} or 200 mV s^{-1} were used.

Cyclic voltammetry with high analyte concentrations. Analytes were prepared as either 1 mM or 2 mM solutions. The electrode was placed in the solution and stirred for ca. 10 s, followed by a rest period of approximately 10 s. A scan rate of 100 mV s^{-1} was used and the experimental data quoted is an average of three scans obtained with stirring ca. 10 s between.

3.3 Results

3.3.1 Modification of electrodes

The first and second cyclic voltammograms recorded at freshly cleaned GC with ν = 200 mV s^{-1} in a 10 mM *p*-phenylacetate modifying solution are shown in Figures 3.2 (A) and (B). The comparatively large peak observed in initial scans of diazonium salts at polished electrodes have been reported to show characteristics of an adsorption wave[42]. Hence, the peak at $E_{p,c}$ = -0.78 V vs Ag/Ag^+ is attributed to reduction of surface adsorbed *p*-phenylacetate diazonium salt. Small peaks present at $E_{p,c}$ = -0.32 V and -1.32 V arise from the reduction of solution diazonium species and a small amount of dissolved oxygen, respectively. The response due to the reduction of *p*-phenylacetate diazonium salt is no longer observed on the second scan (Figure 3.2 (B)), indicating further adsorption can not occur.

Figure 3.2: Cyclic voltammetric responses of GC electrodes in 10 mM *p*-phenylacetate diazonium salt modifying solution recorded at ν = 200 mV s^{-1}

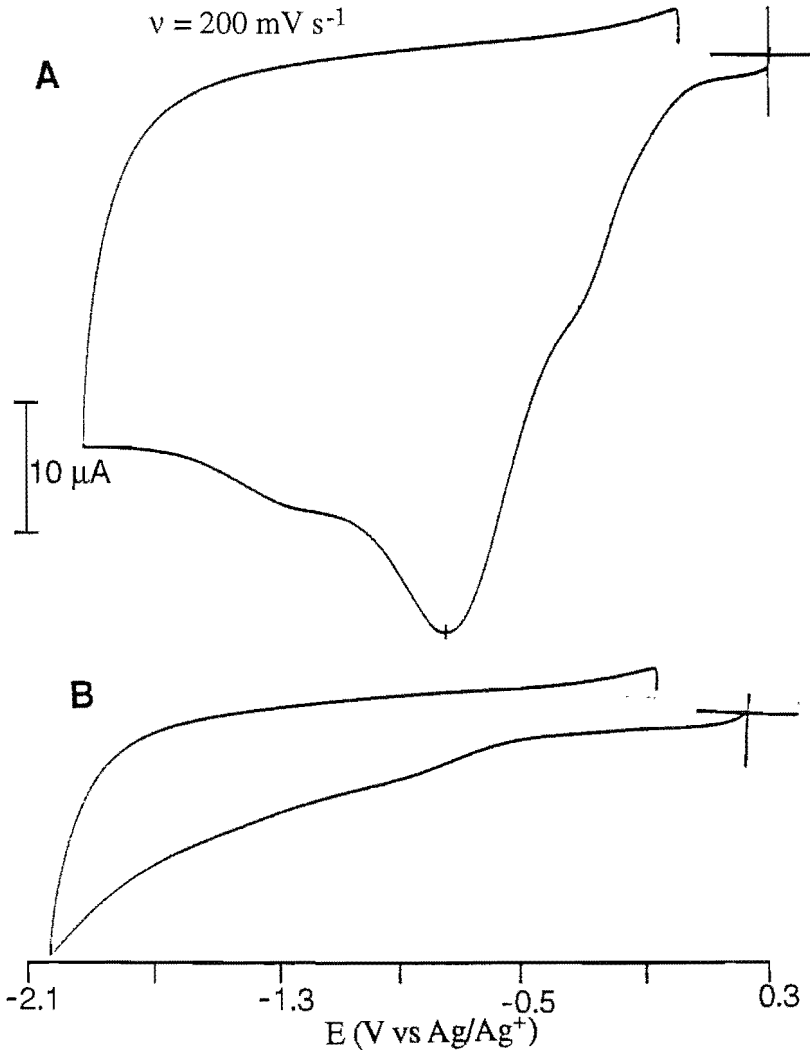

Observations during modification. The *p*-phenylacetate diazonium salt (acetonitrile) solution, which was a light pink colour when first prepared, became a deeper red with time. The colour change of the *p*-benzoate diazonium salt was less pronounced, changing from an almost colourless solution, to a pale yellow. These colour changes occurred even when the solutions were kept under pressure of N_2 and are presumably due to decomposition of the diazonium salt. The deeply coloured solutions resulted in modifications which were indistinguishable from those in the freshly prepared solutions.

3.3.2 Evidence for modification

Para-phenylacetate and *p*-benzoate moieties are not electroactive in the accessible potential range in aqueous solution, pH 7.4. At this pH, the modified surface is expected to be negatively charged. Hence indirect evidence for electrode modification was obtained by recording the cyclic voltammetric response of cationic ruthenium hexaammine accumulated at the electrode surface from a 6 μM solution (PBS, pH 7.4). Alternatively, modification was indicated by a change in the shape of the cyclic voltammogram of ferrocenemonocarboxylic acid (FCA).

Cyclic voltammetry of accumulated ruthenium hexaammine. Ruthenium hexaammine was chosen as the probe analyte because it is cationic and has uncomplicated electrochemistry. The cyclic voltammograms of 6 μM ruthenium hexaammine recorded at ν = 200 mV s^{-1} in PBS at the *p*-phenylacetate modified (a) and unmodified (b) electrode are shown in Figure 3.3. Accumulation reached equilibrium after 5 min stirring in the ruthenium hexaammine solution and consequently stirring times of at least 5 min were used in these experiments. A large peak due to the reduction of accumulated ruthenium hexaammine and a smaller coupled oxidation peak appear at $E_{p,a} = E_{p,c}$ = -0.35 V vs SCE on the *p*-phenylacetate electrode. The smaller oxidation peak indicates that the reduced (lower charged) ruthenium species is less strongly held at the electrode surface. The unmodified GC electrode showed no response to 6 μM ruthenium hexaammine. Cyclic voltammograms of 6 μM ruthenium hexaammine recorded at the *p*-benzoate modified electrode were similar to that described above for the *p*-phenylacetate electrode. The background currents of the CMEs were 2-3 times larger than those at the unmodified surface, presumably due to increased capacitance at the anionic modified surface.

Figure 3.3: Cyclic voltammograms (ν = 200 mV s^{-1}) of 6 μM ruthenium hexaammine/PBS after ≥ 5 min accumulation at the *p*-phenylacetate CME (a) and unmodified electrode (b)

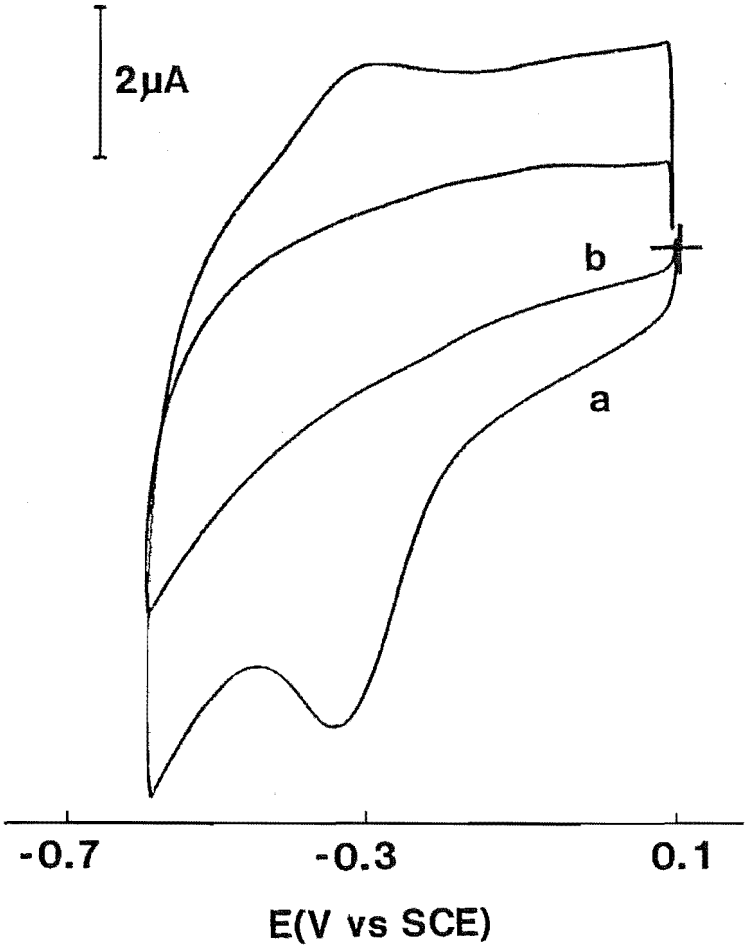

Cyclic voltammetry of ferrocenemonocarboxylic acid. Indirect evidence of electrode modification was also obtained by observing a change in the cyclic voltammetric response of FCA. A saturated solution of FCA in PBS was prepared with an estimated concentration of ca. 0.7 mM. Ferrocenemonocarboxylic acid undergoes a one-electron oxidation at unmodified GC with ΔE_p values ranging from 60-110 mV, depending on the particular glassy carbon electrode (Figure 3.4 (a)). As shown in Figure 3.4 (b), the cyclic voltammogram of FCA at the modified electrode has a sigmoidal shape on the forward sweep (similar shaped voltammograms were observed at both *p*-phenylacetate and *p*-benzoate CMEs). A sigmoidal response may be indicative of steady state behaviour and this possibility was investigated by observing the effect of scan rate on the plateau current for oxidation[105]. The current increased with scan rate over the range ν = 50 – 500 mV indicating that steady-state conditions do not hold. Further investigations of the FCA response at the CME were not undertaken.

Figure 3.4: Cyclic voltammetric response of FCA (~0.7 mM/PBS) at unmodified (a) and *p*-phenylacetate modified (b) electrodes recorded at $\nu = 100$ mV s^{-1}

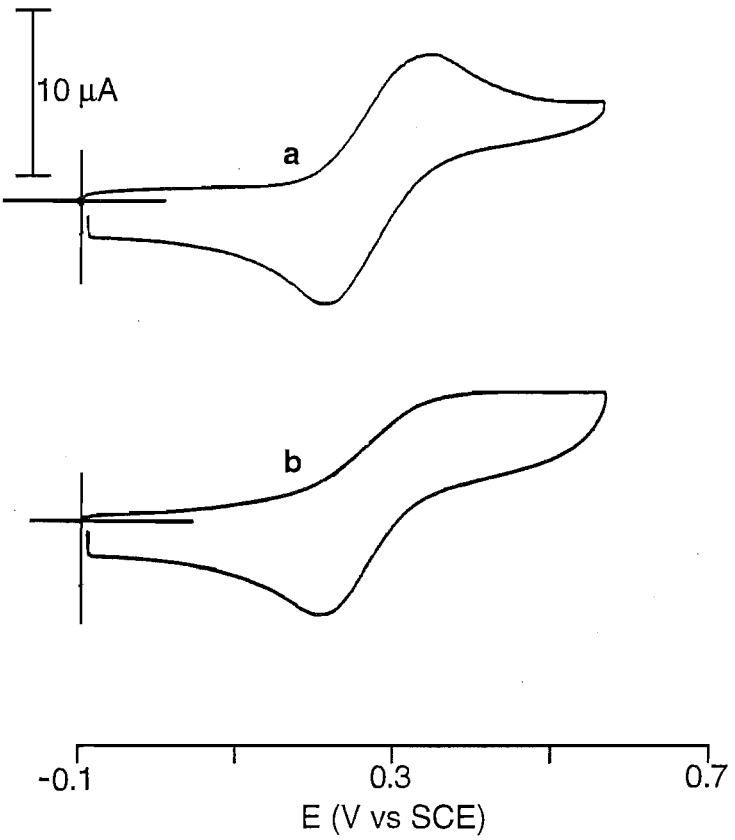

3.3.3 Coverage of surface groups

Ruthenium hexaammine was used as the probe analyte in experiments to estimate surface coverage. Use of this species, however, raises the question of whether $Ru(NH_3)_6^{3+}$ fully compensates for the charge of the surface groups (i.e. coverage of COO^- is 3 times the surface excess of ruthenium hexaammine) or whether solution anions e.g. Cl^- partially compensate for the charge of $Ru(NH_3)_6^{3+}$. A further complication may arise from limitations to ruthenium hexaammine accumulation due to steric factors. Hence the coverage of negatively charged surface groups is assumed to correspond to 1 – 3 times the amount of accumulated ruthenium hexaammine.

Chronocoulometry of ruthenium hexaammine. The amount of a redox active species adsorbed or accumulated at an electrode surface may be determined by the chronocoulometric method of Anson[110]. The potential is stepped into the diffusion controlled region for the redox process and the charge (Q) at (relatively) long times (i.e. the linear region of a Q vs $t^{1/2}$ plot) is extrapolated back to zero. The y-axis intercept gives the charge at time zero and this is due to the redox reaction of the adsorbed or accumulated species. The Q vs $t^{1/2}$ plots resulting from single step chronocoulometric experiments performed using unmodified and *p*-phenylacetate modified electrodes in 1 mM ruthenium

hexaammine/PBS are shown in Figures 3.5 and 3.6 respectively. In these experiments a 200 ms potential step from 0.0 to -0.6 V vs SCE was applied. For the unmodified electrode, subtraction of the charge arising from the double layer (Q_{dl}) in buffer from that observed in the presence of analyte, yields a small non-zero intercept corresponding to 0.077 μC. Using the relation $\Gamma = Q/nFA$ and the geometric area of the electrode, A (0.07 cm^{-2}), this equates to a coverage of $\Gamma = (1.1 - 3.3) \times 10^{-11}$ mol cm^{-2} assuming that between one and three surface charges are compensated by ruthenium hexaammine. This may indicate a small amount of reactant adsorption. Alternatively it could result from extrapolation errors and/or errors in the assumption that Q_{dl} is the same in the presence and absence of ruthenium hexaammine[110]. Chronocoulometric experiments for the *p*-phenylacetate CME result in a charge due to adsorbed species of 3.67 μC which equates to 3.8×10^{-11} moles of ruthenium hexaammine. This gives a range of surface coverage of $\Gamma = (5.4 - 16) \times 10^{-10}$ mol cm^{-2}.

Chronocoulometric experiments at the *p*-benzoate modified electrode (shown in Figure 3.7) gave a charge associated with the adsorbed layer of 4.65 μC, which is equal to 4.8×10^{-11} moles of ruthenium hexaammine and a range of surface coverage of $\Gamma = (6.9 - 21) \times 10^{-10}$ mol cm^{-2}.

Figure 3.5: Q vs $t^{1/2}$plot of PBS only (a) and 1 mM ruthenium hexaammine/PBS (b) at unmodified GC

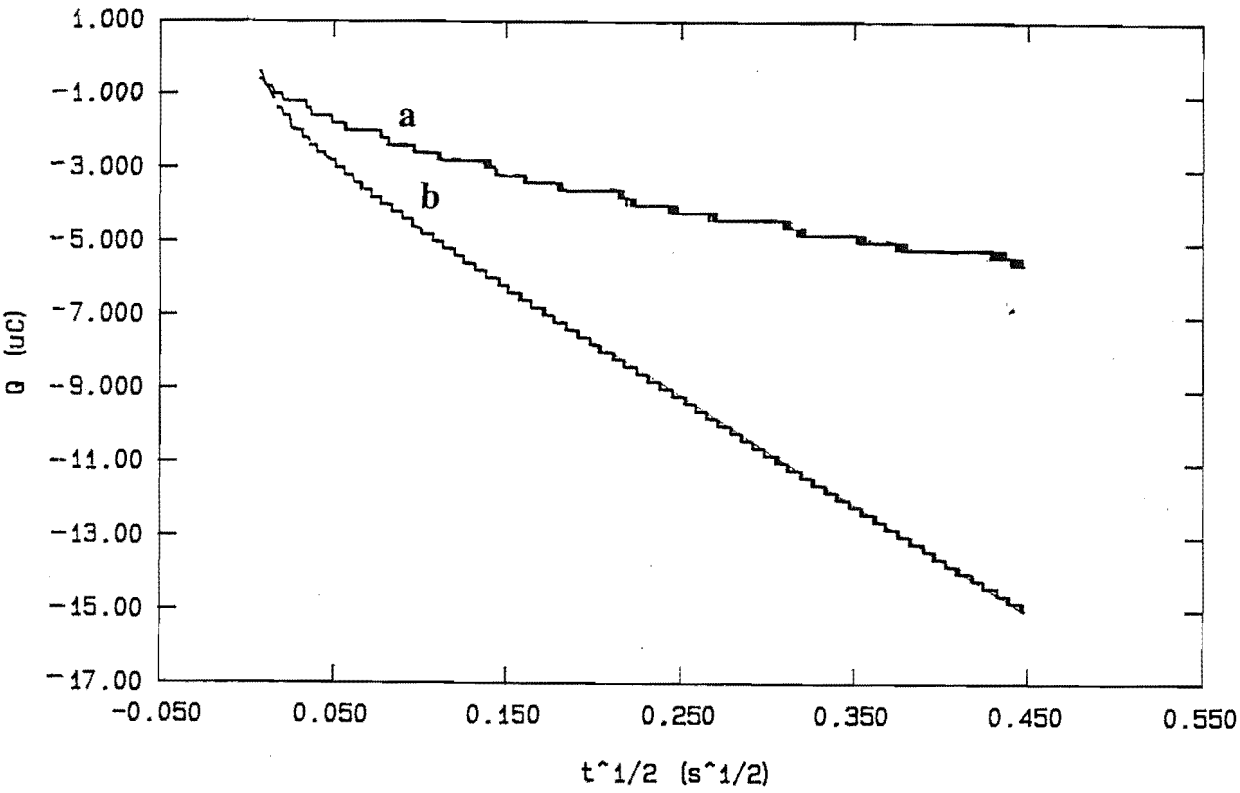

Figure 3.6: Q vs $t^{1/2}$plot of PBS only (a) and 1 mM ruthenium hexaammine/PBS (b) at the *p*-phenylacetate CME

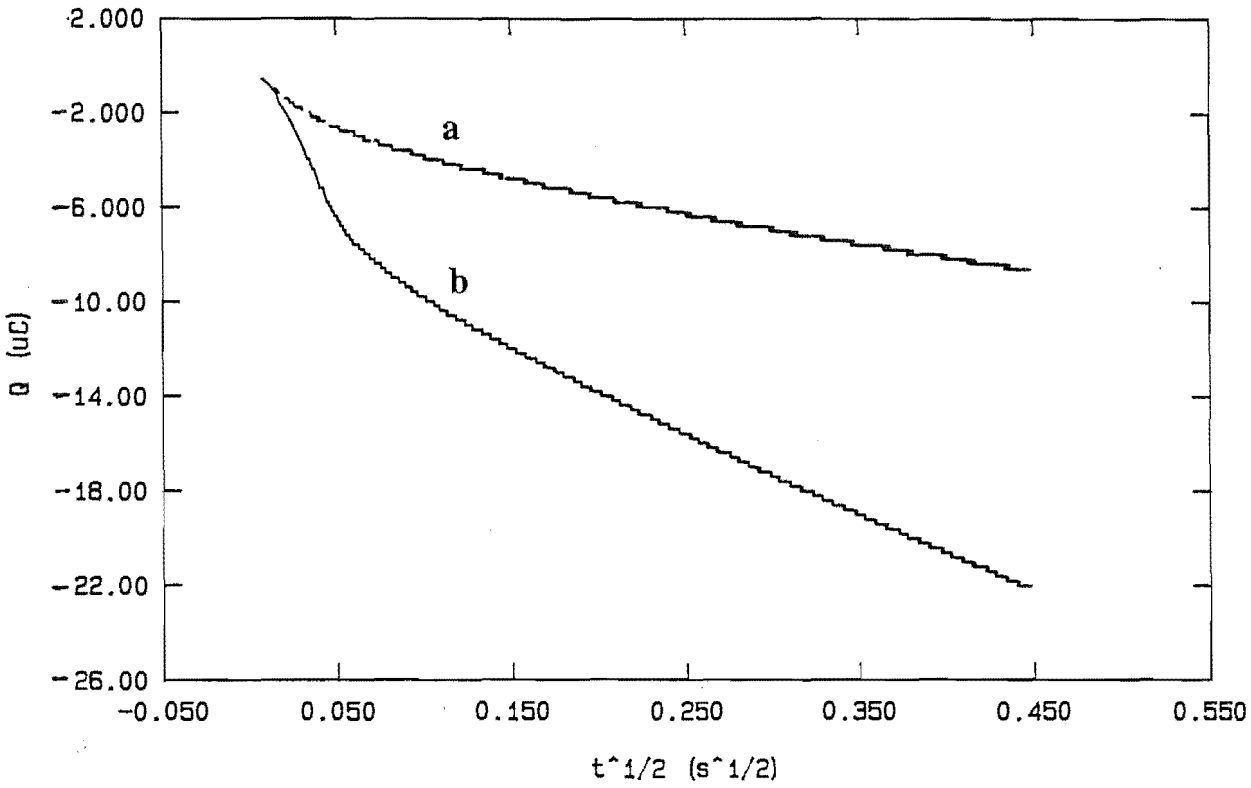

Figure 3.7: Q vs $t^{1/2}$plot of PBS only (a) and 1 mM ruthenium hexaammine/PBS (b) at the *p*-benzoate CME

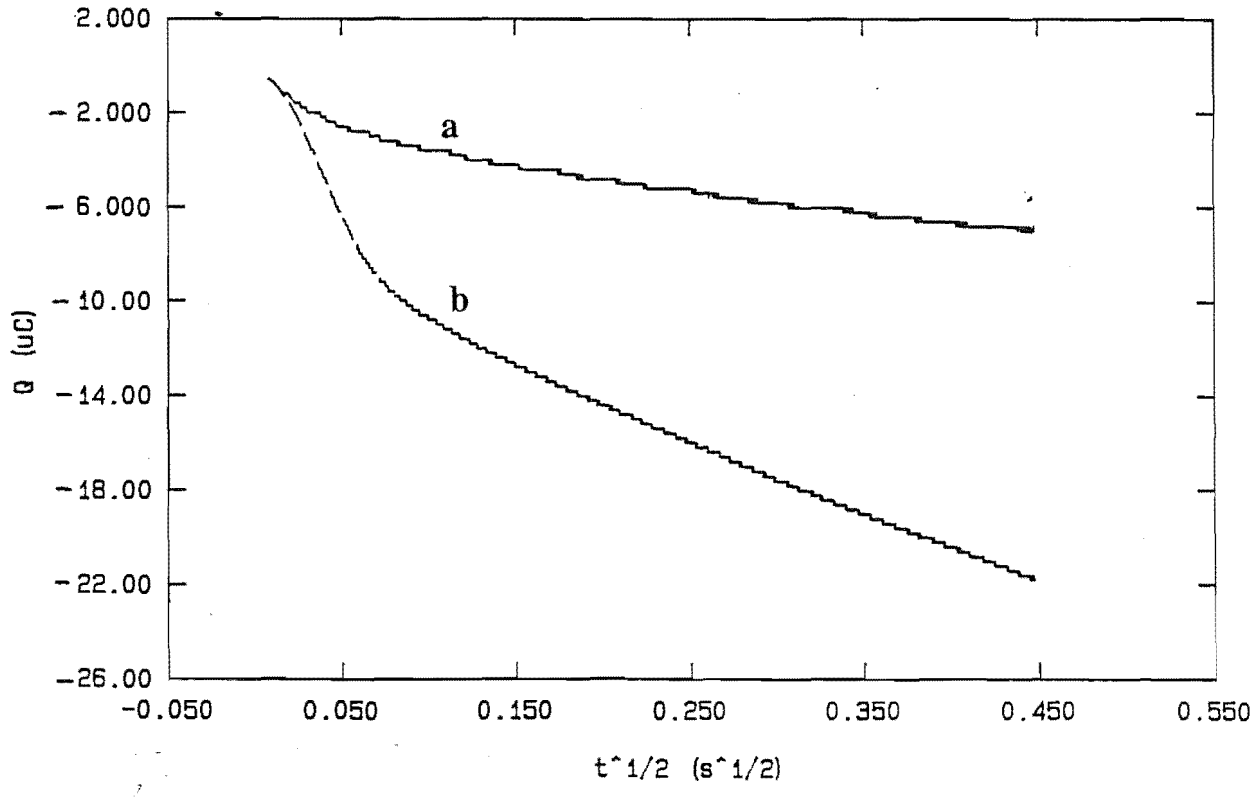

Chronocoulometry of dopamine. Chronocoulometric experiments were also performed at the *p*-phenylacetate CME using the monocation DA. Relatively large amplitude potential steps (-0.1 – 1.0 V vs SCE) were required for diffusion controlled behaviour (i.e. linear i vs $t^{-1/2}$ plots) to be observed. Under these conditions 2.45 x 10^{-11} moles of DA were oxidised which corresponds to a coverage of Γ = 3.5 x 10^{-10} mol cm^{-2}. This lower result, compared with those arising from ruthenium hexaammine adsorption, may be explained by a decreased affinity for adsorption of this lower charged species.

Cyclic voltammetric methods to evaluate accumulated ruthenium hexaammine. Integration of the cathodic cyclic voltammetric peak arising from accumulated ruthenium hexaammine at the *p*-phenylacetate CME (see Figure 3.3 (a)) gives 2.59 x 10^{-11} moles of ruthenium hexaammine and a surface coverage Γ = (3.7 – 11) x 10^{-10} mol cm^{-2}. The coverage of *p*-benzoate groups, also calculated by integrating the peak arising from reduction of accumulated ruthenium hexaammine gives 3.08 x 10^{-11} moles, equating to a surface coverage of Γ = (4.4 – 13) x 10^{-10} mol cm^{-2}.

3.3.4 Reproducibility of preparation and CME stability

The reproducibility of the preparation *p*-phenylacetate CME was also investigated by indirect methods. A polished GC electrode was modified using the standard procedure (Chapter Two) and the electrode contacted with a 6 μM ruthenium hexaammine solution as described in Section 3.3.2. The reduction of ruthenium hexaammine accumulated at the modified surface was then recorded using CV at ν = 100 mV s^{-1}. The electrode was repolished with 1 μm diamond paste and the above modification and accumulation repeated. The peak areas arising from reduction of accumulated ruthenium hexaammine were measured and five separate electrode modifications gave an RSD of 7% for the amount of accumulated analyte.

Stability of modification. The modification was stable to sonication in organic solvents such as benzene, toluene, acetonitrile and acetone but was removed by mild mechanical polishing (for example: 1 min using 1 μm diamond paste). Modified electrodes could be stored on the bench for use without deterioration for as long as necessary without affecting performance.

The stability of the *p*-phenylacetate modification in the flow system was examined by indirect methods. A GC detector was modified using the standard procedure and soaked for 5 min in a stirred solution of 6 μM ruthenium hexaammine. The current arising from accumulated ruthenium hexaammine was recorded by CV and the flow cell was assembled. A constant voltage of 0.6 V vs Ag/AgCl was applied and phosphate buffer (0.05 M) was flowed over the detector for 1 h. The flow cell was then disassembled and accumulation of ruthenium hexaammine at the CME was examined by the same method as prior to the flow experiment. The resulting current due to surface-confined ruthenium

hexaammine after exposure in the flow system was 88% of the original value. The decrease in the amount of cation accumulated at the CME is assumed to arise from the desorption of modifiers which were not covalently bonded to the electrode surface.

3.3.5 Adsorption properties of the *p*-phenylacetate CME

Cationic species, ruthenium hexaammine and dopamine are adsorbed at the CME at pH 7.4 suggesting that adsorption is based on electrostatic interactions. To investigate this further, adsorption of other analytes were examined by CV using low concentrations where the response due to accumulated species dominates over that of diffusing species. Using the expressions for the peak currents for diffusion control and adsorption control (equations 3.1 and 3.2 respectively) equation 3.3 can be derived, showing the relationship between the currents arising from the adsorbed and solution species, as a function of various system parameters.

$$i_p = (2.69 \times 10^5) n^{3/2} A D_o^{1/2} \nu^{1/2} C_0 \quad (3.1)$$

$$i_{(p)surf} = \frac{n^2 F^2 \nu A \Gamma}{4RT} \quad (3.2)$$

$$\therefore \quad \frac{i_p}{i_{(p)surf}} = \frac{(1.08 \times 10^6) D_o^{1/2} C_o RT}{n^{1/2} F^2 \nu^{1/2} \Gamma} \quad (3.3)$$

Assuming: $\Gamma = 6 \times 10^{-10}$ mol cm^{-2}; $D_0 = 5 \times 10^{-6}$ cm s^{-1}; $\nu = 0.1$ V s^{-1}; T = 298 K and n = 2, for $i_p/i_{(p)surf} \leq 1/10$:

$$C_o \leq 4 \times 10^{-8} \text{ mol cm}^{-3}$$

$$\text{i.e. } C_o \leq 4 \times 10^{-5} \text{ mol L}^{-1}$$

Hence, assuming approximately monolayer coverage of adsorbed species, a two-electron redox process, a "typical" diffusion coefficient and a scan rate of 100 mV s^{-1}, at analyte concentrations of 40 μM or less the current arising from adsorbed species dominates.

Adsorption of 3,4-dihydroxybenzene derivatives. Catecholates are important analytes for this work and hence the responses due to 8.8 μM DA and 4-methylcatechol (4-MC) and 20 μM 3,4-dihydroxyphenylacetic acid (DOPAC) were compared at unmodified and *p*-phenylacetate modified electrodes. These species are similar except for

their side-chain structure and charge; DA is a monocation at pH 7.4, DOPAC is a monoanion and 4-MC is neutral. All species undergo a two-electron oxidation, as described in Chapter One. Figure 3.8 shows the results of CV experiments (ν = 100 mV s^{-1}). The signal of DA is increased at the modified electrode, that of 4-MC is unchanged and the response of the DOPAC anion is decreased below the baseline and cannot be detected. These results are consistent with electrostatic control of surface interactions.

Figure 3.8: Cyclic voltammetric responses of 3,4-dihydroxybenzene derivatives/ PBS at unmodified (A) and *p*-phenylacetate modified (B) electrode after 5 min accumulation. Scan rate = 100 mV s^{-1}

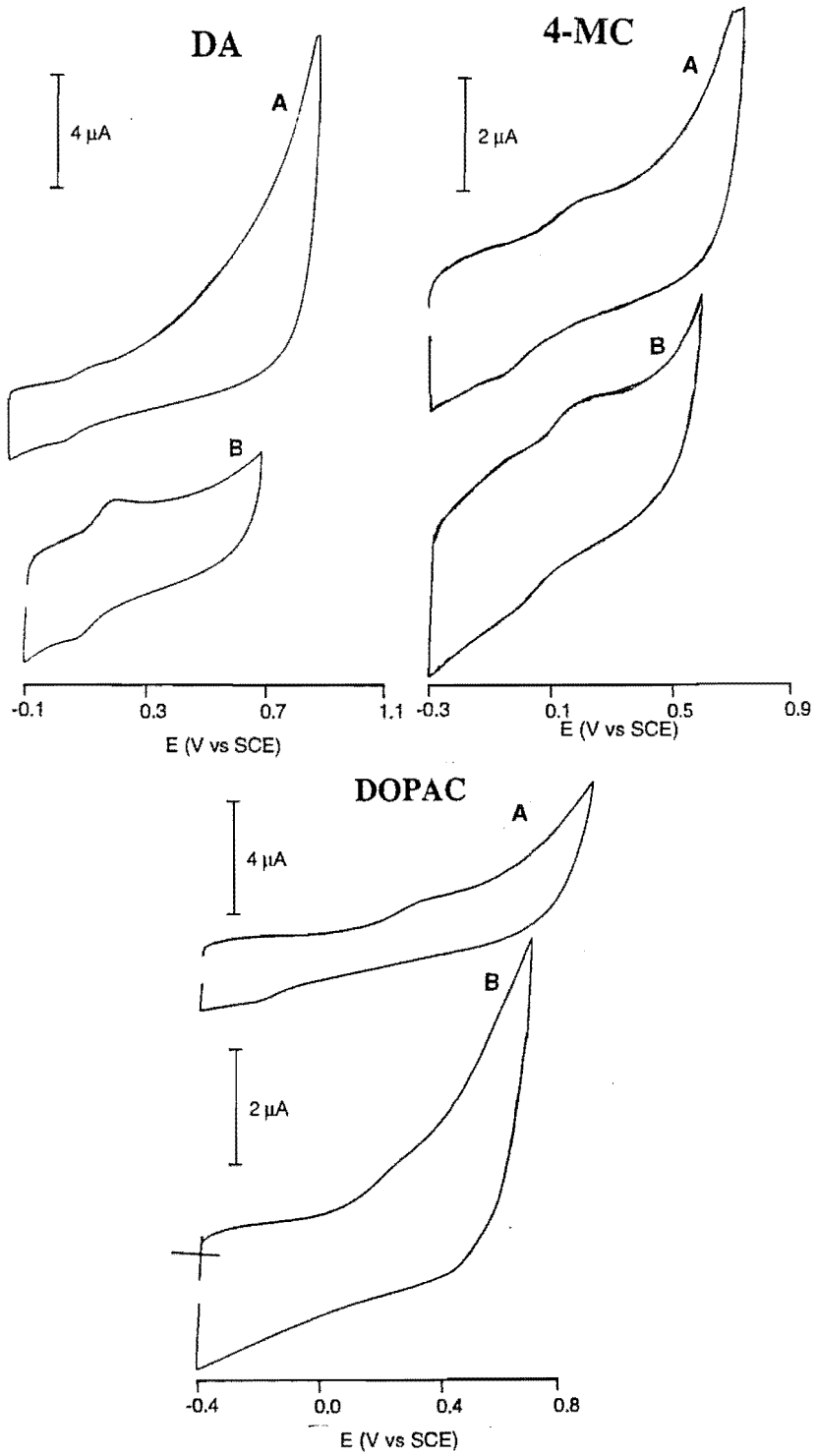

3.3.6 Cyclic voltammetry and hydrodynamic voltammetry of solution species at the CME

Most of the work presented in this section was performed at the *p*-phenylacetate CME. Cyclic voltammograms of the analytes 4-MC, DA, DOPAC, ascorbic acid (AA), uric acid (UA), acetaminophen, FCA, ferrocenemethanol (FcOH) and N,N-dimethylaminomethylferrocene methiodide (FcAm) were recorded (using $\nu = 100$ mV s^{-1}) at unmodified and *p*-phenylacetate modified electrodes. The structures of the ferrocene derivatives are shown in Figure 3.9 and Figure 3.10 shows cyclic voltammograms of the above analytes (excluding FCA). The cyclic voltammetric response of FCA is shown earlier in Figure 3.4. At the solution concentrations used i.e. 1 mM or 2 mM, the response due to diffusing species dominates over that due to adsorbed species (see equation 3.3). Hence, the electrode kinetics can be examined without the complicating effects of adsorption.

Control experiments, which involved soaking a polished electrode in the diazonium salt modifying solution for 5 min (without electrolysis) followed by the usual sonication procedures, were performed. The cyclic voltammetric responses of all analytes described below (except AA and UA) were unaffected by this treatment. The peak potentials for oxidation of AA and UA were typically shifted positive by ca. 100 mV and $i_{p,a}$ decreased to ~80% of their values prior to exposure to the diazonium salt solution.

Cyclic voltammetric responses of 3,4-dihydroxybenzene derivatives at unmodified and p-phenylacetate modified GC electrodes. Cyclic voltammograms of 1 mM DA and 4-MC and 2 mM DOPAC in PBS were obtained at unmodified and *p*-phenylacetate modified electrodes (see Figure 3.10). A summary of the electrochemical data is presented in Table 3.1. The responses of these analytes at the modified electrode appear to be influenced by electrostatic effects. Thus, DA shows an apparent increase in electron transfer kinetics at the CME relative to the unmodified electrode as evidenced by a 50 mV decrease in ΔE_p, a 5 μA increase in $i_{p,a}$ and a 50 mV negative shift in $E_{p,a}$. The electrochemical response of 4-MC is unchanged at the modified surface, whilst DOPAC is poorly resolved at the CME relative to the unmodified electrode; $E_{p,a}$ and ΔE_p increase and $i_{p,a}$ decreases, consistent with a decreased rate of electron transfer at the modified electrode.

Table 3.1: Cyclic voltammetric data of 3,4-dihydroxybenzene derivatives at unmodified and *p*-phenylacetate electrodes recorded at ν = 100 mV s^{-1} in PBS

	UNMODIFIED			MODIFIED		
analyte	$E_{p,a}$ (V)	ΔE_p (mV)	$i_{p,a}$ (μA)	$E_{p,a}$ (V)	ΔE_p (mV)	$i_{p,a}$ (μA)
DA[a]	0.33	300	25.0	0.28	250	30.0
4-MC[a]	0.29	340	24.8	0.29	335	24.3
DOPAC[b]	0.33[c]	360[d]	43.0	0.58[c]	730[d]	32.0

[a]1 mM [b]2 mM [c]$E_{p,a/2}$ for broad wave [d]$\Delta E_{p,a/2} = E_{p,a/2}(ox) - E_{p,a/2}(red)$

Cyclic voltammetric responses of 3,4-dihydroxybenzene catechol derivatives and ascorbic acid at unmodified and p-benzoate modified GC electrodes. Cyclic voltammetric experiments were recorded at ν = 100 mV s^{-1} in PBS at the *p*-benzoate CME and the resulting electrochemical data are presented in Table 3.2. Similar effects on the apparent electron transfer kinetics for analytes DA, 4-MC and DOPAC were observed at this electrode and the *p*-phenylacetate CME. Several carbon electrodes with different initial responses to the probe analytes were also examined. As shown by the data in Table 3.2, the magnitude of change in probe analyte response after modification was influenced by the activity of the unmodified glassy carbon electrode. Importantly, the variation in activity of the different electrodes was dramatically reduced by modification. Further, in cases where the unmodified GC electrode had a poor electrochemical response to 4-MC, modification enhanced the apparent electron transfer kinetics of this neutral analyte.

Table 3.2: Cyclic voltammetric data of 3,4-dihydroxybenzene derivatives at unmodified and *p*-benzoate modified electrodes recorded at $\nu = 100$ mV s^{-1} in PBS

	UNMODIFIED			MODIFIED		
analyte	$E_{p,a}$ (V)	ΔE_p (mV)	$i_{p,a}$ (μA)	$E_{p,a}$ (V)	ΔE_p (mV)	$i_{p,a}$ (μA)
DA[a]	0.285	245	25.5	0.25	200	31.5
	0.40	390	22.0	0.26	220	31.5
4-MC[a]	0.21	210	30.0	0.22	240	27.0
	0.37	450	24.5	0.25	280	27.0
	0.45	550	23.0	0.26	295	28.5
DOPAC[b]	0.27[c]	280[d]	45.0	0.43[c]	590[d]	23.0
	0.34[c]	400[d]	42.5	0.54[c]	740[d]	26.0
AA[b]	0.23[c]	—	43.0	0.39[c]	—	24.0
	0.26[c]	—	38.5	0.46[c]	—	30.0

[a]1 mM [b]2 mM [c]$E_{p,a/2}$ for broad wave [d]$\Delta E_{p,a/2} = E_{p,a/2}(ox) - E_{p,a/2}(red)$

Cyclic voltammetric responses of uric acid, acetaminophen and ascorbic acid at the p-phenylacetate CME. Cyclic voltammetric data for the biologically significant compounds UA, AA and acetaminophen, at unmodified and *p*-phenylacetate electrodes, are summarised in Table 3.3 and the cyclic voltammograms are shown in Figure 3.10. The responses of anions UA and AA at the *p*-phenylacetate CME are consistent with electrostatic interactions leading to an apparent slowing of electron transfer kinetics. Thus the potentials at half wave height, $E_{p,a/2}$, (quoted for comparison as flattened peaks at the CME prevent measurement of $E_{p,a}$) at modified electrodes are shifted positive and decreased peak currents are observed relative to values at unmodified electrodes. Surprisingly, the neutral analyte, acetaminophen, shows similar (although much smaller) effects at the CME with a 30 mV positive shift in $E_{p,a}$, a 140 mV increase in ΔE_p and 4.2 μA decrease in $i_{p,a}$ after electrode modification.

Table 3.3: Cyclic voltammetric data of 1 mM analyte recorded at ν = 100 mV s^{-1} in PB (0.05M) at unmodified and *p*-phenylacetate modified electrodes

	UNMODIFIED			MODIFIED		
analyte	$E_{p,a}$ (V)	ΔE_p (mV)	$i_{p,a}$ (μA)	$E_{p,a}$ (V)	ΔE_p (mV)	$i_{p,a}$ (μA)
acet	0.47	440	29.0	0.50	580	24.8
UA	0.28[a]	—	29.5	0.43[a]	—	15.7
AA	0.11[a]	—	18.3	0.30[a]	—	12.2

[a] $E_{p,a/2}$

Cyclic voltammetric responses of ferrocene derivatives at the p-phenylacetate CME. Ferrocene and its derivatives are often used in electrochemical studies as they have simple one-electron, chemically reversible electrochemistry. The cyclic voltammetric responses of ferrocenemonocarboxylic acid (FCA), ferrocenemethanol (FcOH) and N,N-dimethylaminomethylferrocene methiodide (FcAm) were recorded at unmodified and *p*-phenylacetate modified electrodes. The resulting electrochemical data are presented in Table 3.4. The structures of these analytes are shown in Figure 3.9. Ferrocenemonocarboxylic acid is anionic at pH 7.4, FcOH is neutral and FcAm is a cation. Low peak currents for FCA and FcOH at unmodified GC are due to the limited solubility (~0.7 mM for a saturated solution) of these analytes at pH 7.4. As noted in Section 3.3.2, the cyclic voltammogram of FCA shows a sigmoidal shaped oxidation at the modified electrode and $E_{p,a/2}$ values of both the peaked CV at the unmodified electrode and sigmoidal CV are quoted in Table 3.4 for comparison. The cyclic voltammetric responses of FcOH and FcAm are not significantly altered at the CME relative to unmodified GC, though the oxidation peak resolution of FcAm is improved due to a positive shift in the iodide oxidation signal (see Figure 3.10).

Table 3.4: Cyclic voltammetric data of ferrocene derivatives (~0.7 mM FCA and FcOH) and 1 mM FcAm, in PB (0.05M) recorded at ν = 100 mV s^{-1}

	UNMODIFIED			MODIFIED		
analyte	$E_{p,a}$ (V)	ΔE_p (mV)	$i_{p,a}$ (μA)	$E_{p,a}$ (V)	ΔE_p (mV)	$i_{p,a}$ (μA)
FCA	0.27[a]	110	9.6	0.27[a]	—	6.3
FcOH	0.26	110	12.25	0.26	110	11.8
FcAm	0.46	100	14.5	0.45	100	14.5

[a] $E_{p,a/2}$(ox)

Figure 3.9: Structure of ferrocene derivatives

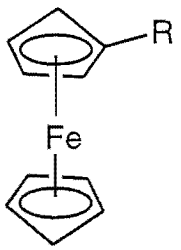

FcOH R = CH_2OH
FCA R = COOH
FcAm R = $CH_2NH(CH_3)_2^+I^-$

Figure 3.10: Cyclic voltammetric responses of probe analytes at unmodified (A) and *p*-phenylacetate modified electrodes (B). Scan rate = 100 mV s^{-1}

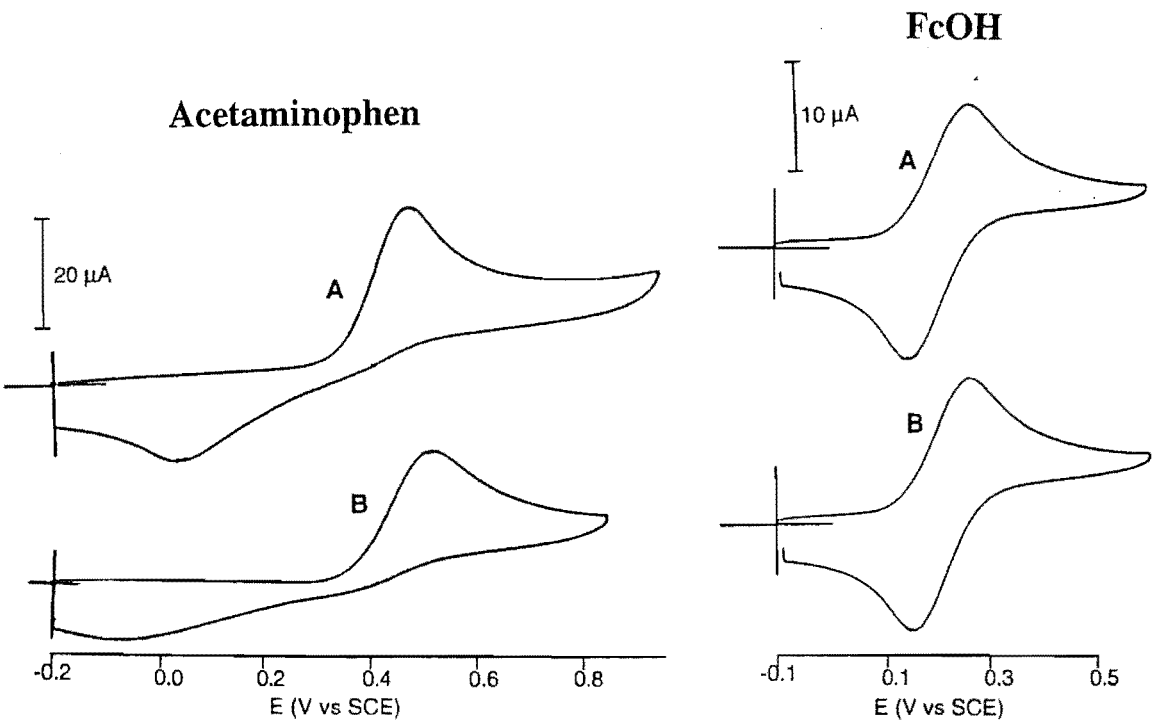

Figure 3.10: Cyclic voltammetric responses of probe analytes at unmodified (A) and *p*-phenylacetate modified electrodes (B). Scan rate = 100 mV s^{-1}

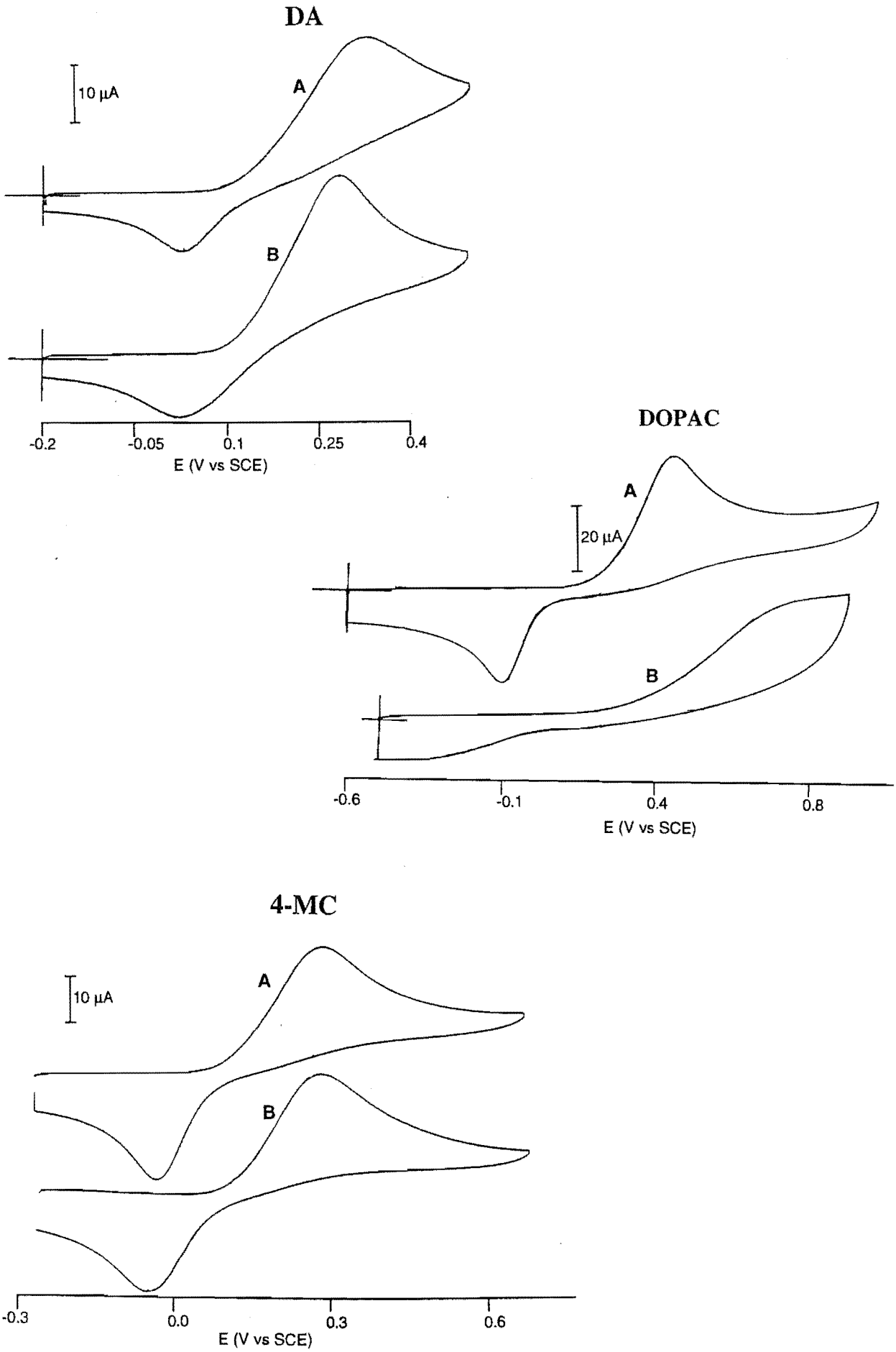

Figure 3.10: Cyclic voltammetric responses of probe analytes at unmodified (A) and *p*-phenylacetate modified electrodes (B). Scan rate = 100 mV s^{-1}

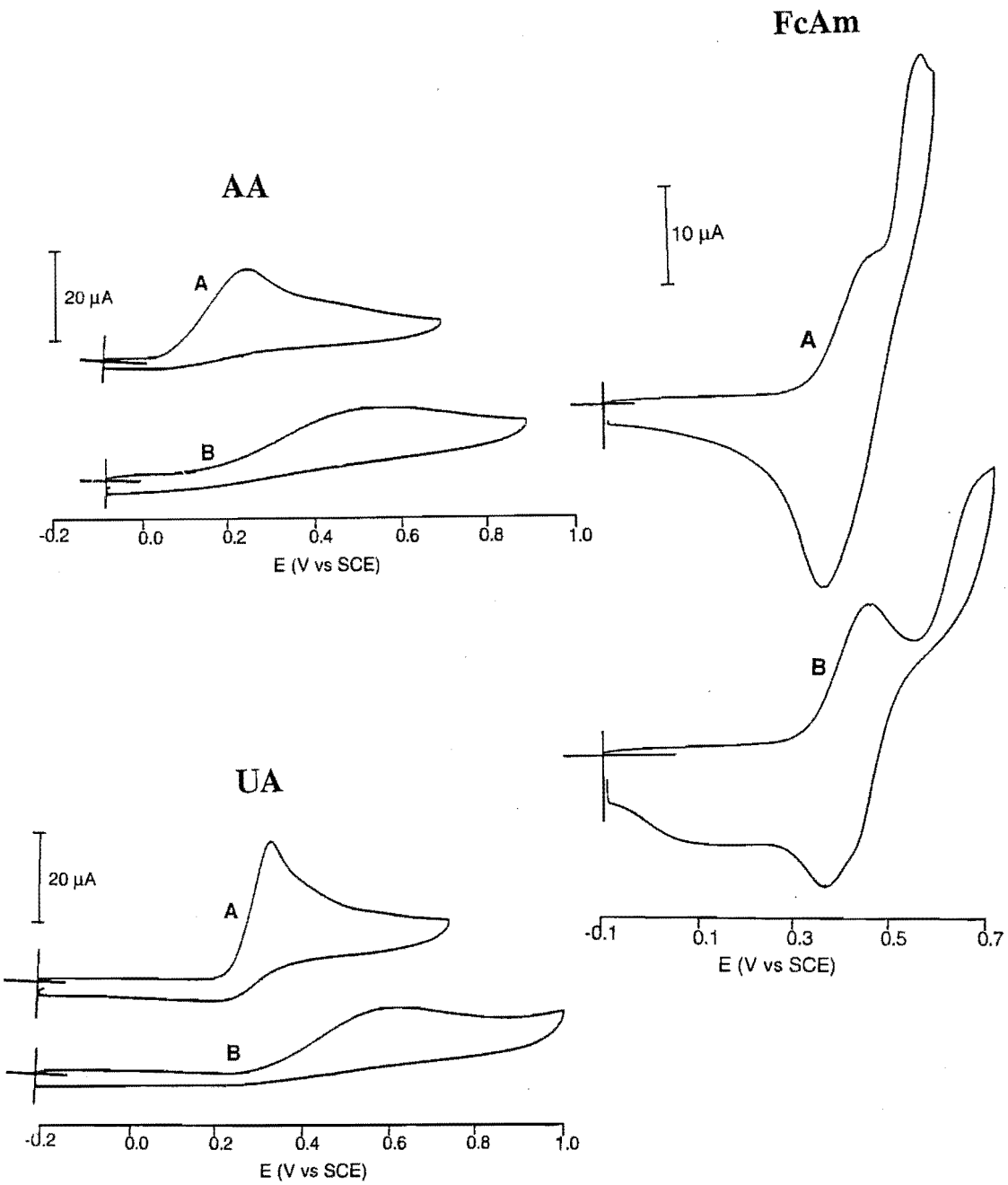

Hydrodynamic voltammetry at the p-phenylacetate CME. Hydrodynamic voltammetry was performed using a flow injection analysis (FIA) system. The different manifolds and detectors used are summarised in the Experimental section and described in detail in Chapter Two. The results of hydrodynamic voltammetry of probe analytes on unmodified and *p*-phenylacetate modified GC detectors are presented in Table 3.5 and summarised in Table 3.6. Representative hydrodynamic voltammograms (HDVs) are

shown in Figures 3.11 to 3.13. Analytes (2 x 10^{-4} M in PB) were injected into the buffer carrier and the peak height used was an average of at least 3 injections at each potential. The standard procedure for GC electrodes was used to modify flow cell detectors except that the electrolysis time was increased from 5 to 10 min. Electrochemical parameters for comparison of HDVs are the potential at half the plateau current (i.e. half-wave potential, $E_{1/2}$), the difference in potential at one quarter and three quarters plateau current ($E_{3/4}$-$E_{1/4}$) and the limiting plateau current (i_l). A variation of ± 10 mV in the $E_{1/2}$ values of HDVs was observed at unmodified detectors in these experiments, presumably due to shifts in the Ag/AgCl reference electrode potential and/or small differences in cell geometry after cell disassembly and reassembly.

Table 3.5: Hydrodynamic voltammetric data for probe analytes (2 x 10^{-4} M) at unmodified and *p*-phenylacetate modified flow detectors

	UNMODIFIED			MODIFIED		
analyte	$E_{1/2}$ (V)	i_l (μA)	$E_{3/4}$-$E_{1/4}$ (mV)	$E_{1/2}$ (V)	i_l (μA)	$E_{3/4}$-$E_{1/4}$ (mV)
DA[a]	0.39	2.86	188	0.29	3.35	175
DA[d]	0.28	1.94	140	0.22	2.52	93
Acet[a]	0.57	2.13	125	0.52	3.25	123
Acet[b]	0.61	1.25	129	0.48	3.10	124
UA[a]	0.52	3.00	128	—	—	—
4-MC[d]	0.26	1.47	90	0.18	1.76	83
DOPAC[d]	0.48	1.10	93	0.46	1.33	97
FCA[b]	0.37	2.80	95	0.35	2.5	103
FcOH[b]	0.26	2.45	85	0.24	2.45	90
FcAm[c]	0.41	2.0	83	0.43	2.0	83

[a] FIA setup (A) [b] FIA setup (B) [c] FIA setup (C) [d] FIA setup (D)

Table 3.6: Summary of results for hydrodynamic voltammograms recorded at unmodified and *p*-phenylacetate modified electrodes

analyte	$E_{1/2}$ at modified relative to unmodified	$E_{3/4}$-$E_{1/4}$ at modified relative to unmodified	i_l at modified relative to unmodified
DA	less positive	decrease	larger
Acet	less positive	no change	larger
UA	more positive	increase	not at plateau
4-MC	less positive	no change	larger
DOPAC	no change	no change	larger
FCA	no change	no change	small decrease
FcOH	no change	no change	no change
FcAm	no change	no change	no change

The origin of increases in the plateau currents for HD voltammograms at CMEs was investigated. Because all HD voltammograms were recorded beginning at the lowest potential, measurements at the plateau potentials were made on electrodes at which a significant number of measurements had been made. Hence, it is reasonable to assume that fouling of the electrode surface by reaction products might account for the lower plateau current at unmodified detectors. To investigate this possibility, measurements at freshly polished and modified detectors at 0.5 V vs Ag/AgCl (i.e. the plateau region) were made. Shown in Figure 3.14 is the result of 5 repeat injections of 1 x 10^{-4} M DA in PB (0.05 M) at the unmodified (A) and *p*-phenylacetate electrode (B). Flow injection analysis setup (A) was utilised with a 30 μL sample loop. There was a progressive decrease in peak currents at the unmodified electrode and the peak current for the fifth injection of DA was 89% of the first peak. The modified electrode gives a more stable response to DA and the RSD was 1% (n = 5). Similar results were observed for UA, acetaminophen and AA under the same experimental conditions.

Figure 3.11: Hydrodynamic voltammograms of catechol derivatives (2 x 10^{-4} M/PB) recorded at unmodified and *p*-phenylacetate detectors

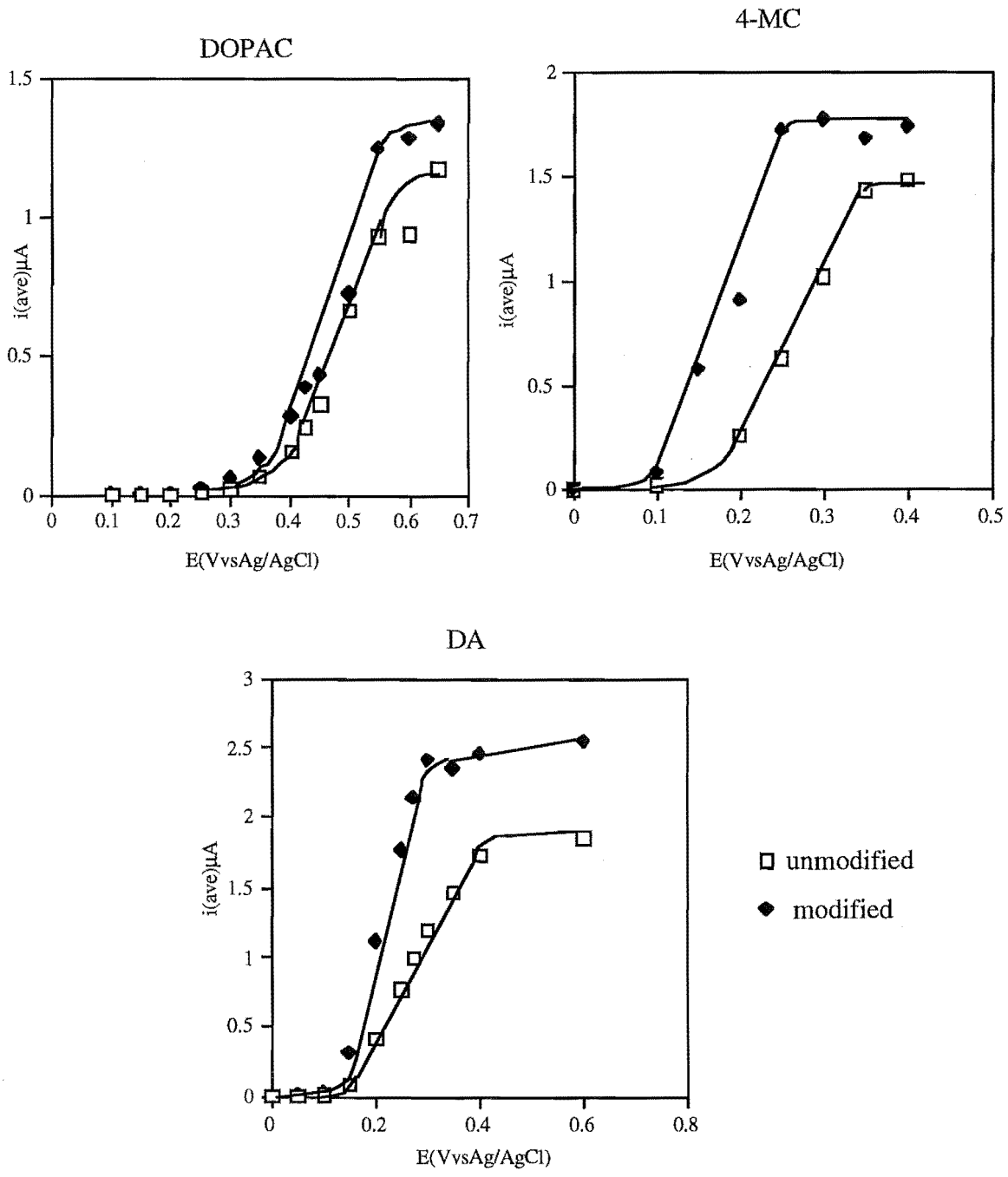

Figure 3.12: Hydrodynamic voltammograms of biological analytes (2 x 10^{-4} M/PB) recorded at unmodified and *p*-phenylacetate detectors

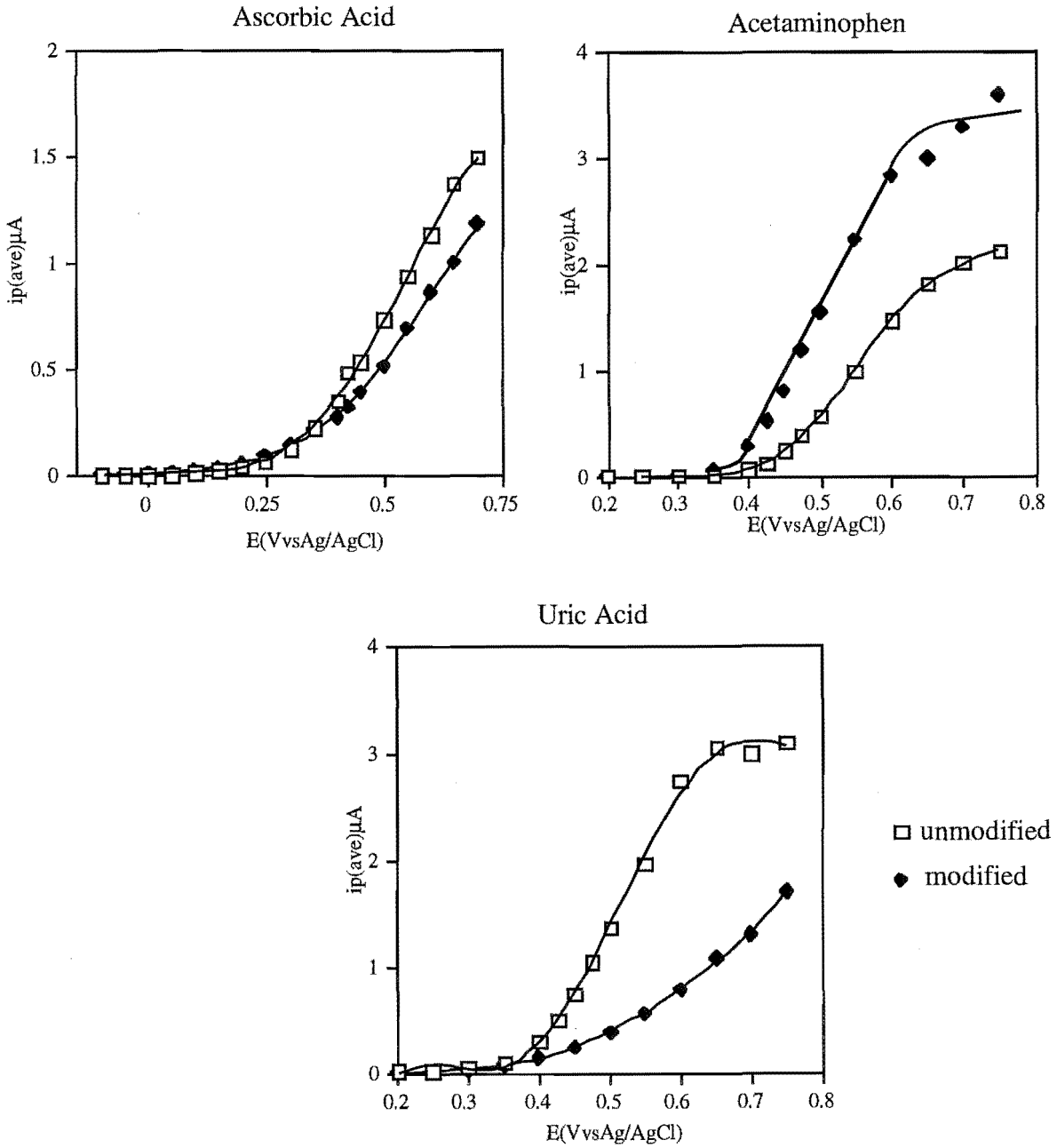

Figure 3.13: Hydrodynamic voltammograms of ferrocene derivatives
(2×10^{-4} M/PB) recorded at unmodified and *p*-phenylacetate detectors

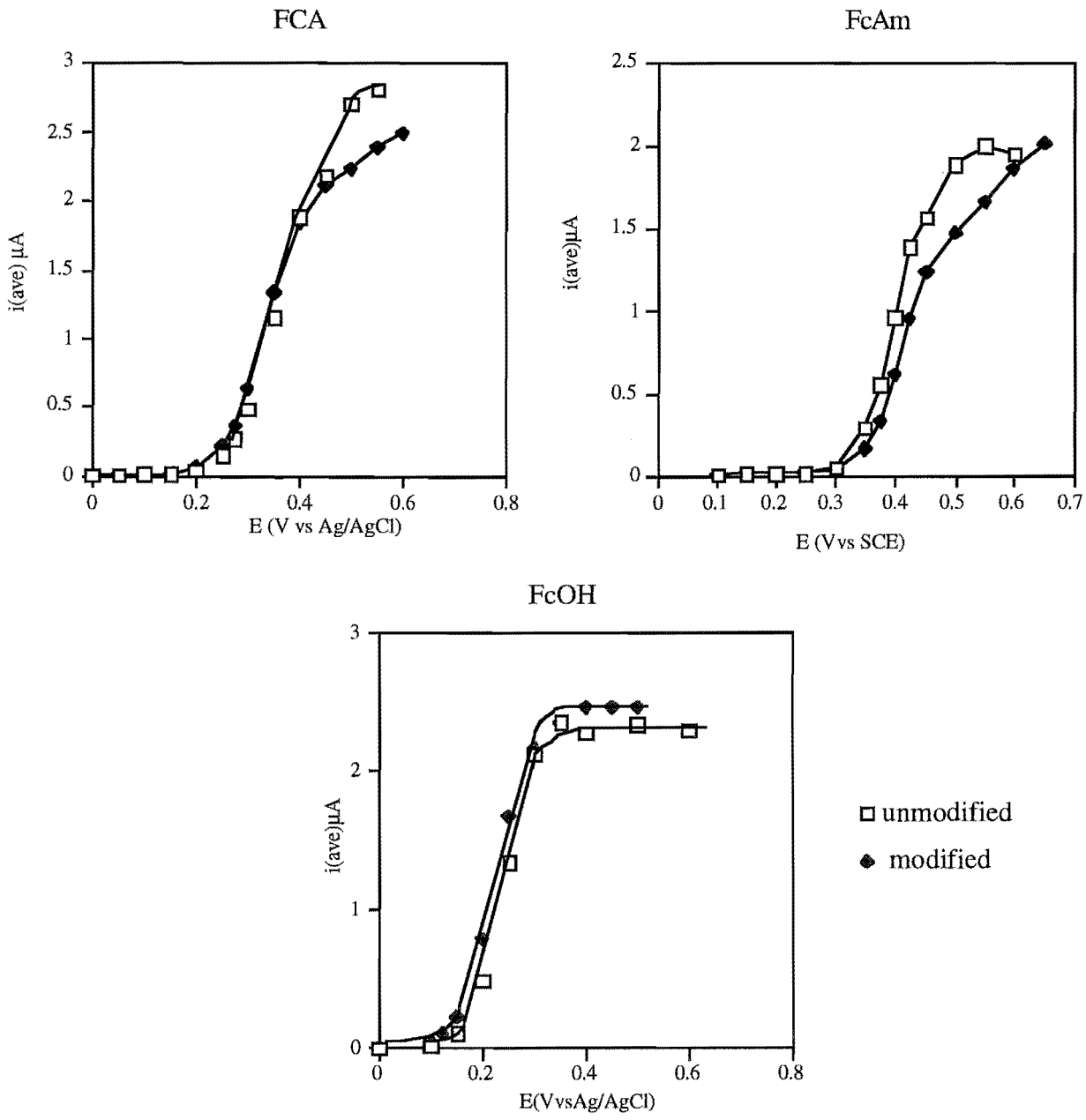

Figure 3.14: Repeat injections of 1 x 10^{-4} M DA in PB (0.05 M) at unmodified (A) and *p*-phenylacetate modified (B) electrodes with an applied voltage of 0.5 V vs Ag/AgCl and a flow rate of 0.73 ml min^{-1}

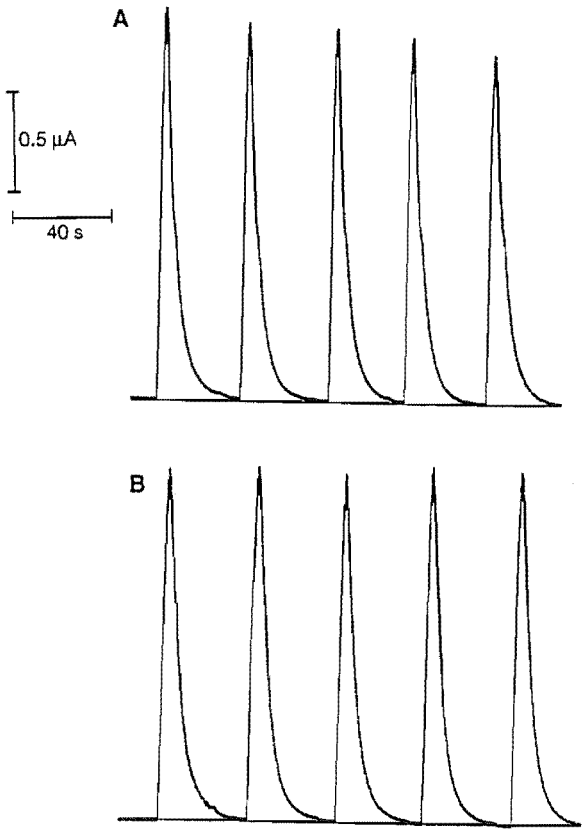

3.4 Discussion

3.4.1 Characteristics of the modified electrodes

Surface coverage. Typical values for monolayer coverage of adsorbed species on platinum and carbon electrodes are 1 – 5 x 10^{-10} mol cm^{-2} [19,23,111,112], although higher coverage (7.9 ± 0.5 x 10^{-10} mol cm^{-2}) has been reported for alkanethiols self-assembled on Au[113]. In their initial publication[42], the original authors of the aryl diazonium modification procedure reported a surface coverage of *p*-nitro groups of 14 x 10^{-10} mol cm^{-2}. This was attributed to a densely packed monolayer but appears larger than usually observed for monolayer coatings. Due to the uncertainty of ruthenium hexaammine charge compensation, a range of surface coverage of 3.5 – 21 x 10^{-10} mol cm^{-2} was obtained at *p*-phenylacetate and *p*-benzoate CMEs in the present study. Hence, it is reasonable to assume that modifiers were present in monolayer, or close to monolayer, quantities.

A higher surface coverage of *p*-benzoate modifiers relative to the *p*-phenylacetate electrode was shown in both chronocoulometry (CC) and CV experiments involving

analysis of accumulated ruthenium hexaammine. Generally, self-assembled monolayers (such as those formed by alkanethiols on Au) show increased density and stability as the chain length of the modifier is increased[45]. The diazonium method of attachment, however, is thought to proceed by initial adsorption of the diazonium salt onto the electrode, followed by reduction and reaction with the surface[42]. Hence, the increased coverage of *p*-benzoate modifiers may be attributed to an increased number of smaller modifiers adsorbed prior to covalent attachment.

There are differences between surface coverage for CMEs calculated from accumulated ruthenium hexaammine using CC and CV methods. The results obtained for the *p*-phenylacetate electrode using CV is 69% of the CC value. Similarly, the *p*-benzoate electrode gave a coverage using CV which was 64% of that calculated from CC experiments. There may be errors arising from the assumption that Q_{dl} is the same in the presence and absence of accumulated species in CC experiments. In the case where reactant but not product adsorption occurs at the electrode, double step chronocoulometry may be used to ascertain Q_{dl} ,[110] however, as shown by cyclic voltammetric experiments, the reduction product of ruthenium hexaammine is also adsorbed at the CME (see Figure 3.3). Alternatively, the low ruthenium hexaammine concentration could cause low coverage in CV experiments if the surface sites are not saturated but rather an equilibrium between surface-confined and solution species was present.

Reproducibility and stability. The reproducibility of CME preparation, as measured by surface coverage of anionic groups using indirect methods gave an RSD of 7%. This is within the range typically observed for preparation of CMEs[114] and for GC when commonly used polishing procedures are employed.

Direct evidence of covalent bond formation was not provided in this work. However, the stability of the modification to flow injection analysis conditions and in organic solvents is consistent with covalent bond formation between the carbon electrode and modifying groups.

3.4.2 Effect of CMEs on analyte response

Cyclic voltammetry and hydrodynamic voltammetry at the CMEs. Voltammetry can be used to provide information about electron transfer processes. Relating carbon surface structure and electron transfer rates is often difficult due to uncertainty about the carbon electrode interface and mechanisms of electron transfer.

In CV experiments, the apparent electron transfer kinetics of DA were found to be enhanced at the CME. As discussed in Chapter One, increased electron transfer rates may result from catalysis, favourable double layer effects or slow film diffusion leading to a switch from electron transfer to diffusion control. It seems most likely that double layer

effects are responsible for the observed changes in reaction rates of the probe analytes. There are two ways in which double layer effects can influence the apparent electron transfer rate i.e. by changing the effective driving force for the reaction (the ϕ_2–effect) and by altering the concentration of electroactive species near the electrode surface due to electrostatic interactions. Since the electrochemical probes used in this study were oxidised, the ϕ_2–effect will operate in the same direction for all analytes i.e. modification with an anionic monolayer is expected to increase the effective driving force for oxidative electron transfer. Hence, electrostatic interactions seem to be the most important factor affecting analyte response at the CME. Thus, the apparent reaction kinetics of DA were increased due to attractive electrostatic interactions whilst that of DOPAC, AA and UA, which are anionic at pH 7.4, were decreased at the CME. It was not possible to ascertain whether electron transfer was occurring at a homogeneous, fully covered CME surface or at sites with different electron transfer rates (e.g. bare and modified electrode regions) which are small and closely spaced.

This explanation does not account for the CV results of neutral analytes 4-MC and acetaminophen. The response of 4-MC was either unchanged or showed an enhanced electron transfer rate (when initial unmodified electrode response was poor). In this instance, the enhancement may be due to the modification procedure removing blockages (with poor electron transfer properties) from the bare electrode. The reason for the apparent decrease in electron transfer kinetics for acetaminophen at the CME is not understood.

Ferrocene derivatives, which have faster electrode kinetics, were less affected by electrode modification. Ferrocenemonocarboxylic acid, however, showed a characteristic change in voltammogram shape at the modified electrode. This provides a simple and rapid method for demonstrating successful modification of the electrode.

The flow system can be used to study kinetic effects of electrode modification under conditions where reactant adsorption and accumulation are assumed to be less important. Increased rates of electron transfer in HDV experiments are indicated by a decrease in $E_{1/2}$ (for oxidation) and a decreased value for $E_{3/4}$-$E_{1/4}$. As shown in Tables 3.5 and 3.6, enhanced rates of electron transfer in HDV experiments were observed at the CME for many of the analytes examined. The possible origins of these increased reaction rates are the same as discussed above for CV experiments, however, effects of electrode fouling must also be considered in HDV studies. The presence of electrode fouling was indicated by different plateau currents for analytes at the unmodified and modified detectors. Repeat injections of DA at the unmodified and *p*-phenylacetate modified detectors confirmed that unmodified surfaces were more prone to fouling by reaction products. Deactivation of electrode surfaces by catecholamines and other organic analytes is well documented, as are examples of electrochemical detector fouling in flow injection analysis[27,87,115].

Unfortunately, interpretation of electron transfer kinetics in hydrodynamic voltammetric experiments is complicated by electrode fouling as adsorption of reaction products decreases the electroactive surface area and slows apparent electron transfer rates causing positive shifts in $E_{1/2}$ (for oxidation) and increased $E_{3/4}$-$E_{1/4}$ values.

The HDV experiments with catechol derivatives and biological analytes at the modified surface showed the same trends as described above for CV measurements. Under HDV conditions, UA and AA gave decreased responses at the CME due to unfavourable electrostatic interactions. The response of DOPAC was similar at the unmodified and modified detector despite electrostatic effects, as a result of decreased fouling by reaction products at the CME. An apparent enhancement of kinetics occurred for neutral analytes 4-MC and acetaminophen presumably because of the increased driving force for electron transfer (ϕ_2-effect) and decreased fouling at the CME. Dopamine showed the greatest enhancement of electron transfer rate at the modified electrode due to favourable electrostatic interactions and decreased electrode deactivation. Electrode fouling by the ferrocene derivatives is not expected to contribute to the HDV responses and as with CV experiments these analytes were not as affected by electrode modification due to their faster electron transfer kinetics.

3.5 Conclusions

The CMEs described in this Chapter have very useful properties for analytical purposes. The calculated range of modifier coverage was typical of that expected for a monolayer. Apparent electron transfer kinetics of probe analytes at the modified electrode were consistent with electrostatic control of electron transfer rates. Hence, these CMEs would be expected to be selective for cationic analytes relative to anionic species. Importantly, modification of GC surfaces with very different initial activities resulted in surfaces which gave similar behaviour to probe analytes in CV experiments, thus this seems to be a useful method of generating reproducible GC surfaces. These CMEs were also shown to be very stable in hydrodynamic conditions suggesting covalent attachment was achieved. Importantly, these experiments indicate that the CME is less prone to adsorption of reaction products, relative to unmodified GC, under flow injection analysis conditions.

Chapter Four: Application of CMEs to the measurement of dopamine in the presence of ascorbic acid

4.1 Introduction

The *in vivo* monitoring of neurotransmitters in brain extracellular fluid (ECF) using electrochemical techniques has been of interest since 1973 when Kissinger and co-workers first demonstrated voltammetric recording in brain tissue[116]. Voltammetry is well suited to *in vivo* monitoring as electrodes can be easily miniaturised and many species of interest undergo electron transfer reactions at accessible potentials. Further, the measurement of dynamic changes in neurological fluids is possible using fast timescale electrochemical techniques.

Electroactive species present in mammalian brain extracellular fluid include neurotransmitter catecholamines; dopamine (DA) and norepinephrine (NE, also commonly called noradrenaline), their metabolites 3,4-dihydroxyphenylacetic acid (DOPAC), 3-methoxytyramine (3 MT) and homovanillic acid (HVA), the hydroxyindole neurotransmitter 5-hydroxytryptamine (5 HT), its metabolite 5-hydroxyindoleacetic acid (5 HIAA), the purine metabolite uric acid (UA) and the natural anti-oxidant ascorbic acid (AA). Figure 4.1 shows the structures (at pH 7.4) of some neurotransmitters and their metabolites. Basal levels reported for each of these compounds are generally agreed to be in the ranges shown in Table 4.1, although concentrations vary according to the location in the brain and with the level of anaesthesia. The potential ranges over which oxidation of these analytes occur are also presented in Table 4.1. These values are dependent on the thermodynamic standard redox potential of the substrate and the kinetics of electron transfer at the working electrode.

Figure 4.1: Chemical structures of some neurotransmitters and their metabolites present in ECF

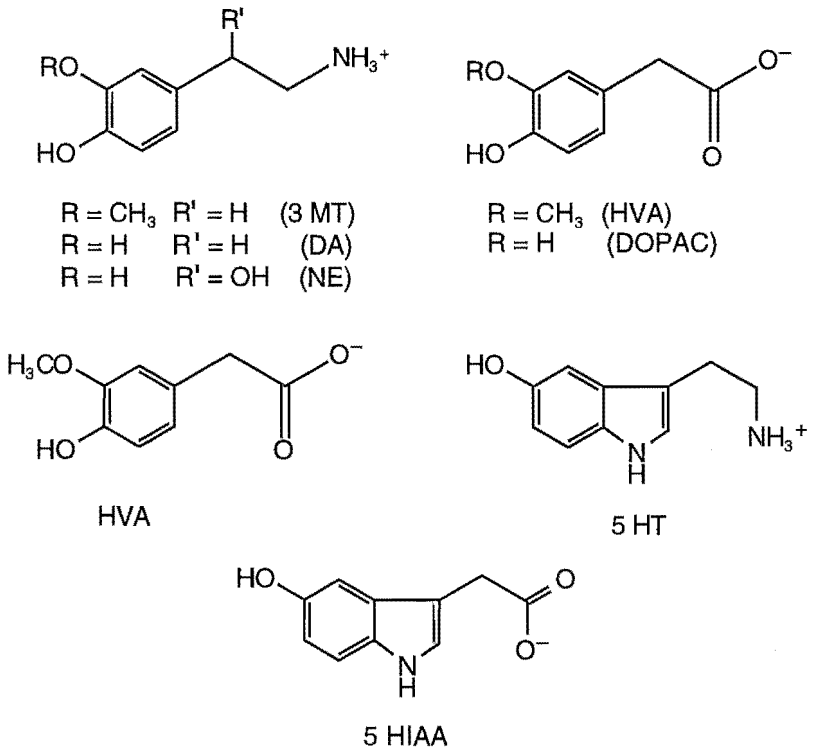

Table 4.1: Concentrations and electrochemical data for the most common species detected voltammetrically in extracellular fluid of the brain[a]

Analyte	Charge[b]	Oxidation potential[c] (mV vs SCE)	Concentration in ECF (μM)
AA	–	–100 to +400	100-500
DA, NE	+, +	+100 to +250	0.001-0.05
DOPAC	–	+100 to +250	1-20
5 HT	+	+300 to +400	0.001-0.01
5 HIAA	–	+300 to +400	1-10
UA	–	+300 to +400	1-50
3 MT, HVA	+, –	+500 to +600	1-10

[a] adapted from ref 15, [b]At physiological pH (7.4), [c]data for $E_{p,a}$ from DPV and CV, and $E_{1/2}$ from NPV measurements

The measurement of the catecholamine neurotransmitter dopamine (DA) has been the focus of much research. Dopamine is the transmitter for a group of neurons involved with muscular activity. Parkinson's disease, which is characterised by muscular tremors and weakness, is associated with a decrease in the number of DA producing neurons and thus with a low level of DA, in certain areas of the brain[117]. The usual protocol for voltammetric monitoring of DA levels is to place the electrode in a region which is rich in DA-releasing neurons[6,9,10,12] and has low levels of other neurotransmitters. Therefore, the major problem is to overcome interference from AA which is present in much greater concentrations than DA. Other factors which complicate DA measurement under neurochemically significant conditions include fouling of the electrode surface by adsorption of tissue components and large molecular weight organic species present in ECF, and the catalytic oxidation of AA by oxidised DA (dopamine-*ortho*-quinone). This reaction, which is summarised in Scheme 4.1, may lead to an enhanced DA signal which is related to the concentration of AA near the electrode surface.

Scheme 4.1: Mechanism for dopamine oxidation in the presence of ascorbic acid

$$DA \longrightarrow DA_{(ox)} + 2\,\bar{e}$$

$$DA_{(ox)} + AA \longrightarrow DA + AA_{(ox)}$$

Three general strategies aimed at overcoming problems associated with DA measurement have emerged: (i) optimisation of measurement technique, electrode dimensions and material, with or without electrochemical pretreatment (ECP) of the carbon electrode, (ii) modification of working electrodes with anionic films such as Nafion[33,34] or poly(ester sulfonic acid)[118] and (iii) application of anionic monolayers. Monolayers have received comparatively little attention. Stearate modified carbon paste electrodes have been reported to exhibit excellent discrimination between AA and DA in vitro[67,119] but later studies demonstrated that exposure to surfactants (such as lipids) removed stearate and pasting oil from the electrode[68]. Self-assembled monolayers of ω-mercaptocarboxylic acids on Au have also been proposed as suitable probes for DA detection[45].

Measurements of both basal DA levels in ECF and DA released after some form of stimulation (e.g. electrical stimulation of a neurological pathway or K^+ stimulated release) are of interest. To monitor DA released after strong stimulation (which typically generates micromolar concentrations) an electrode which responds rapidly to changing DA concentrations and a short timescale electrochemical technique are required. Hence, fast scan rate cyclic voltammetry (FCV) or chronoamperometry at bare or thin Nafion film coated carbon fibre microelectrodes are commonly utilised[4,7-14]. Measurement of basal DA concentrations requires more sensitive electrochemical techniques coupled with the use of electrodes which preconcentrate DA. This usually involves differential pulse

voltammetry (DPV) with Nafion coated, electrochemically pretreated carbon fibre electrodes[4].

In this chapter, experiments aimed at establishing the suitability of *p*-phenylacetate and *p*-benzoate CMEs as DA probes are described. Studies outlined in Chapter Three indicated that the *p*-phenylacetate and *p*-benzoate CMEs showed electrochemical behaviour consistent with electrostatic control of electron transfer kinetics. Hence, the apparent rate of DA oxidation increased whilst that of AA and DOPAC decreased at the CMEs. Therefore, these CMEs seemed promising as probes for DA. Further, the covalent attachment of modifying species was expected to provide a surface with good mechanical stability and anti-fouling properties.

For experimental simplicity the response of DA is characterised at conventional-size CMEs in synthetic solutions using differential pulse voltammetry and chronoamperometry. Optimum conditions for DA determination in the presence of a large excess of AA are established and limits of detection, reproducibility and response times of the CME are evaluated. The effect of surfactants on CME performance is also investigated. The *p*-phenylacetate modification is applied to glassy carbon fibre and RAM (random array of microdisks) electrodes. Fast scan rate cyclic voltammetry and DPV are used in conjunction with modified microelectrodes.

4.2 Experimental

4.2.1 Measurements using microelectrodes and microelectrode arrays

Modification procedure for microelectrodes. Diazonium salt solutions were passed through activated carbon prior to use for modification. The standard modification procedure for conventional-size GC (described in Chapter Two) was used to modify carbon fibre micro- and RAM electrodes.

Polishing procedures. Microdisk and random microdisk array (RAM) electrodes were polished on a damp polishing cloth with either alumina (0.05 μm) or cerium oxide. They were then briefly wiped across a clean moist polishing cloth and in some cases the RAM electrode was dipped in 10% HNO_3 prior to use.

When glassy carbon fibre electrodes developed large background currents they were re-surfaced by polishing on a mechanically driven wheel to restore their initial responses. RAM electrodes were polished with 0.05 μm alumina for extended periods (i.e. at least 1 h) to reproduce their initial performance.

Experimental apparatus. Cyclic voltammetry measurements utilised a Cypress systems Model CS-1090 computer-controlled Electroanalytical system; DPV was performed with a BAS 100 Electrochemical Analyzer equipped with a preamplifier (model PA-1) and a Faraday cage. A conventional three electrode cell was used with a platinum wire auxiliary electrode and Ag/AgCl (3 M NaCl) reference electrode. Differential pulse voltammetry was performed using the following settings: pulse amplitude = 25 mV, sample width = 20 ms, pulse width = 60 ms, pulse period = 0.5 s and scan rate = 5 mV s^{-1}.

Experiments with carbon fibre micro- and RAM electrodes were performed in phosphate buffer (0.04 or 0.1 M) at pH 7.4.

4.2.2 Response time measurements

Flow injection analysis manifold (1) was used with GC detector (a) as described in Chapter Two. A 30 μL sample loop was utilised in these experiments. Dopamine (0.2 μM) in PBS was injected into the PBS carrier stream and passed over the detector which had an applied voltage of 0.6 V vs Ag/AgCl (0.1 M KCl). The flow rate was 1.12 mL min^{-1} and the time-base of the recorder was operated at 0.5 cm s^{-1}.

4.2.3 Differential pulse voltammetric calibration of DA responses at conventional-size GC electrodes

The settings for DPV were as described above for microelectrodes. Phosphate buffered saline was degassed and 5.0 mL pipetted into a perspex cell. The concentration of DA was changed by addition of aliquots of stock DA (1 mM, freshly prepared and kept under N_2). The modified electrode was suspended in this solution throughout the experiment. After an aliquot of DA was added, (with the electrode at open circuit) the solution was stirred for 5 min and the first DP voltammogram recorded. At least 3 repeat DP voltammetric scans were recorded at each DA concentration with stirring for 1 min between each scan and the average response used.

4.2.4 Chronoamperometry

Chronoamperometric measurements were performed on a computer interfaced PAR Potentiostat/Galvanostat Model 273A. Step times of 200 ms were applied and the background transient recorded in electrolyte only was subtracted from responses of analyte solutions. Currents at 20 ms were used to construct calibration curves. For optimisation experiments sets of three solutions were used. These were either: (1) 5 mM AA; (2) 50 μM DA and (3) 5 mM AA plus 50 μM DA, or (1) 1 mM AA; (2) 10 μM DA and (3) 1 mM AA plus 10 μM DA. Prior to each potential step, the solution was stirred for 10 s followed by a rest period of 10 s at open circuit and 5 s equilibration at the initial potential. Care was taken to ensure that no stirring of the solution by N_2 occurred and the magnetic stirrer

was disconnected prior to application of the potential step to avoid electrical interference. Chronoamperometry measurements were made in triplicate.

Chronoamperometric calibrations were performed using optimised step potentials for *p*-phenylacetate (-0.1 to 0.225 V vs SCE) and *p*-benzoate (-0.1 to 0.25 V vs SCE) modified electrodes. Measurements were made in triplicate with stirring for ca. 10 s between experiments and the average currents at 20 ms on the i vs t transients were used. A degassed solution of 10 μM DA in PBS was prepared and 10.0 mL was pipetted in the electrochemical cell. Calibrations were then conducted in the absence or presence of 200 μM AA by adding aliquots of DA from a 1 mM DA stock solution. Following each concentration increment, solutions were stirred for 1 min at open circuit and then allowed to become quiescent prior to measurement.

4.3 Results

4.3.1 Differential pulse voltammetry at conventional-size CMEs

Differential pulse voltammetric responses of DA and AA at the p-phenylacetate CME. Representative differential pulse voltammograms for oxidation of 20 μM DA and 2 mM AA at unmodified and modified conventional-size GC electrodes are shown in Figure 4.2. The oxidation peak potential for DA is the same at both unmodified GC and the CME ($E_{p,a}$ = 0.15 V vs SCE). The sensitivity to DA, however, increases approximately sixfold at the CME with the peak current changing from 0.18 μA at unmodified GC to 1.07 μA at the *p*-phenylacetate electrode. The response due to AA, over the same potential range, decreases significantly (note the change in current scales in Figure 4.2) and the peak potential is shifted from 0.31 V to ca. 0.65 V. It is assumed that the increase in the surface concentration of cationic DA at the modified electrode is responsible for the observed increased DA current.

Although these results appear useful for discrimination of DA over AA, a solution containing both analytes gives a single large signal. This is assumed to arise from catalytic oxidation of AA by dopamine-*ortho*-quinone and hence the signal size will depend on both DA and AA concentrations. Clearly these conditions are not satisfactory for quantitation of DA in the presence of AA.

Figure 4.2: Differential pulse voltammograms of A), B) 20 μM DA and C), D) 2 mM AA in PBS recorded at A), C) unmodified and B), D) modified GC electrodes

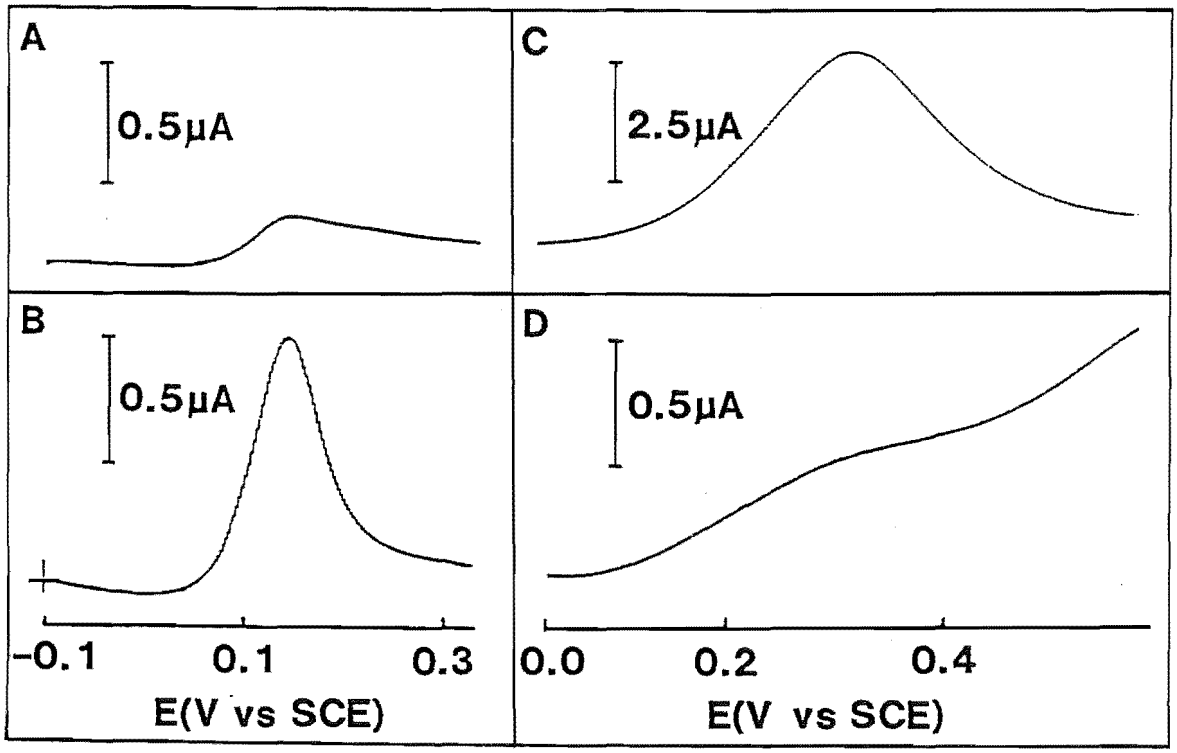

Calibration curve for DA at the p-phenylacetate CME using DPV. The calibration curve for DA (0.2 μM – 0.64 mM in PBS) is presented in Figure 4.3 and the linear region is shown in Figure 4.4. Each point is an average of at least three repeat DPV scans at each concentration. A stirring time of 5 min was used for the first scan at each concentration, with 1 min stirring between subsequent voltammograms. Stirring for less than 1 min resulted in successively smaller peaks whilst times of 1 min or 5 min gave similar currents and a detection limit (measured as 3σ for 0.2 μM DA) of 90 nM was obtained. The linear working range was 0.45 – 32.0 μM (r^2 = 0.994). The small y-intercept (49 nA) matches the observed blank. The RSD (n = 6) for peak currents of repeat DPVs in 1.2 μM DA was 7%.

Figure 4.3: Calibration curve for DA in PBS at the *p*-phenylacetate CME using differential pulse voltammetry

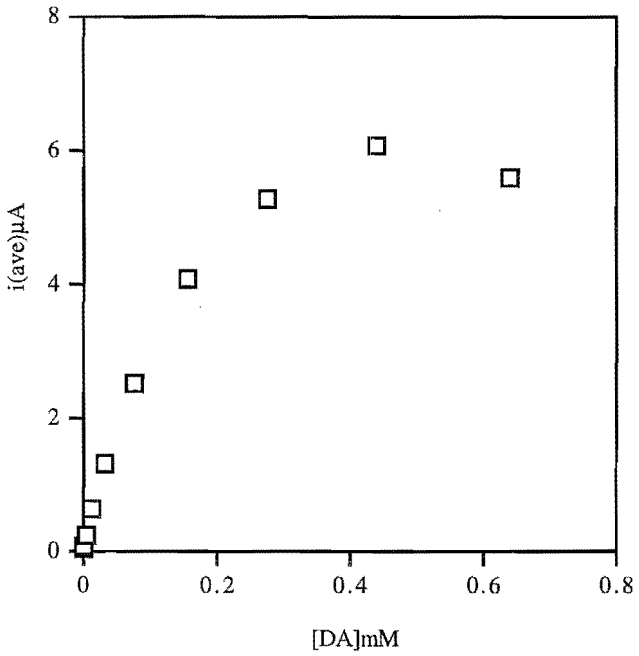

Figure 4.4: Linear region of the calibration curve for DA on the *p*-phenylacetate CME using differential pulse voltammetry

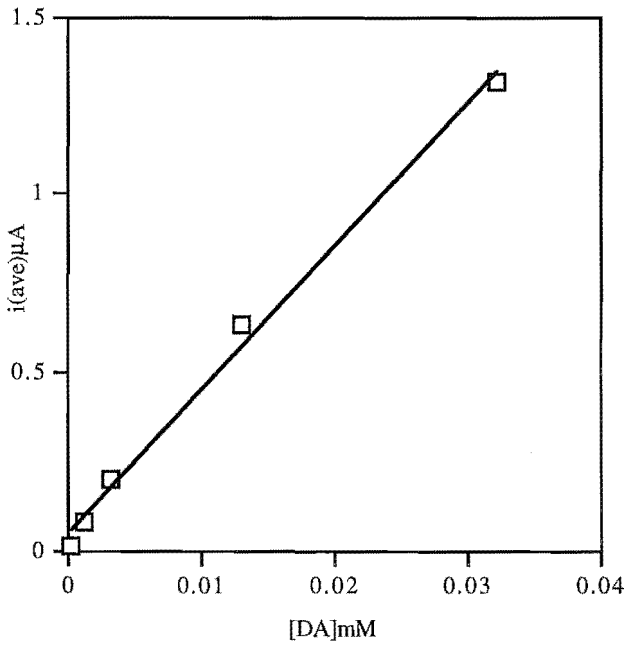

The observed curvature of the plot in Figure 4.3 at DA concentrations greater than 32 μM may arise from saturation of negative sites on the CME and electrode fouling by reaction products at high concentrations.

4.3.2 Chronoamperometric studies at conventional-size electrodes

Optimisation of step potential for DA discrimination in the presence of AA at the CME. Chronoamperometry is a short timescale technique (when measurement occurs soon after the potential step) which can be used with conventional-size electrodes. Thus the chronoamperometric determination of DA in the presence of AA should be less affected by catalytic enhancement than DP measurements. In addition, this technique is used *in vivo* for measurement of DA released after stimulation[4]. The optimal step potential (E_{step}) to maximise DA response relative to AA was evaluated at the *p*-phenylacetate and *p*-benzoate CMEs by measuring the currents at 20 ms after application of the step. This time represents a compromise between good reproducibility for repeat measurements and discrimination of DA response over AA response. An initial step potential ($E_{initial}$) of -0.1 V vs SCE was always used. Separate solutions of DA, AA and, in some instances, a mixture of the two analytes were examined. The concentration of DA was always 100 times less than that of AA. The standard procedure for these experiments involved modifying the electrode and applying several potential steps in PBS until a stable response was observed (typically 5 – 7 steps were required). The electrode was then placed in an analyte solution and triplicate measurements were made. The CME was removed, rinsed in DDW and background transients were again recorded in PBS prior to measurement in the next analyte solution. To compensate for changes in background responses with time, transients in PBS recorded prior to each analyte solution were subtracted from the response in the presence of analyte. Some representative chronoamperometric results, for varying E_{step} values at the *p*-benzoate CME, are shown in Figure 4.5 A (E_{step} = 0.4 V) and B (E_{step} = 0.275 V). For *p*-phenylacetate and *p*-benzoate CMEs, changing the magnitude of E_{step} resulted in the relative sensitivities of AA to equimolar DA shown in Figure 4.6. The usual notation for quantifying the relative sensitivities to the two analytes is adopted here[33]. This is expressed as (response to AA)/(response to equimolar DA) x 100%. Thus the smaller this value, the higher the selectivity to DA relative to AA.

Figure 4.5: Chronoamperometric transients of 10 μM DA (a) and 1 mM AA (b) in PBS at the *p*-benzoate CME with $E_{initial}$ = -0.1 V vs SCE and E_{step} = 0.4 V (A), and 0.275 V (B)

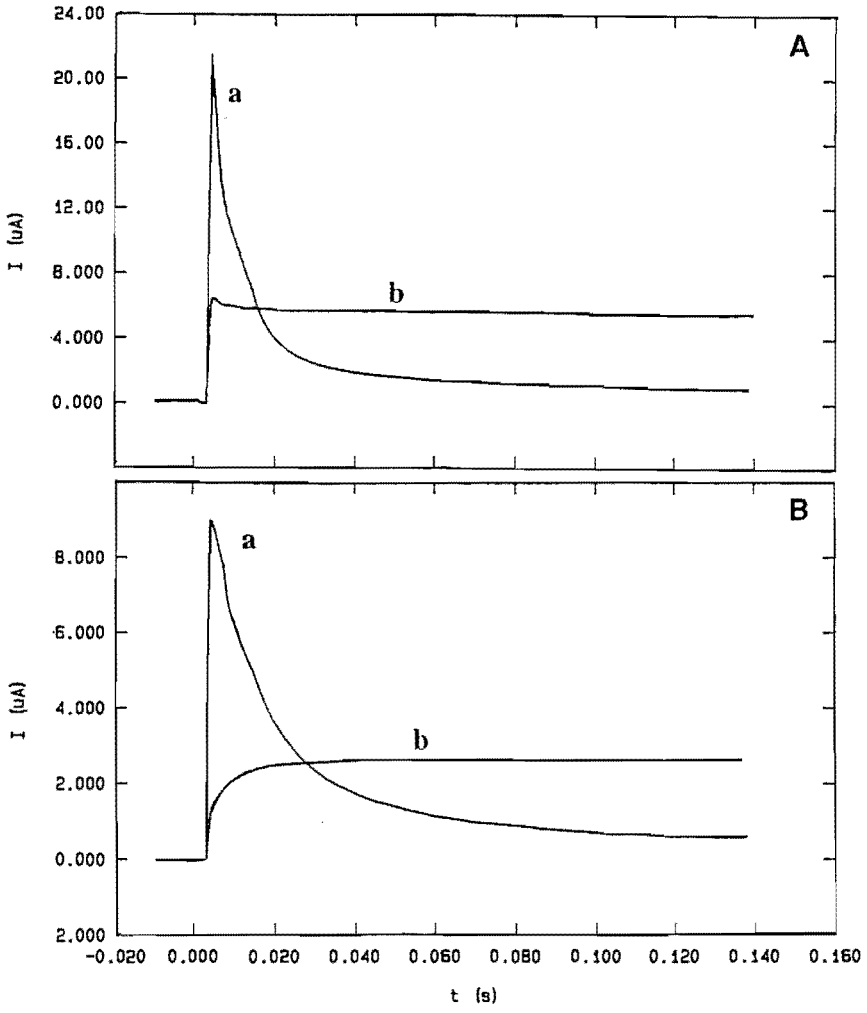

Figure 4.6: Variation in the current ratios at 20 ms for AA:DA (expressed as a percentage) with $E_{initial}$ = -0.1 V vs SCE

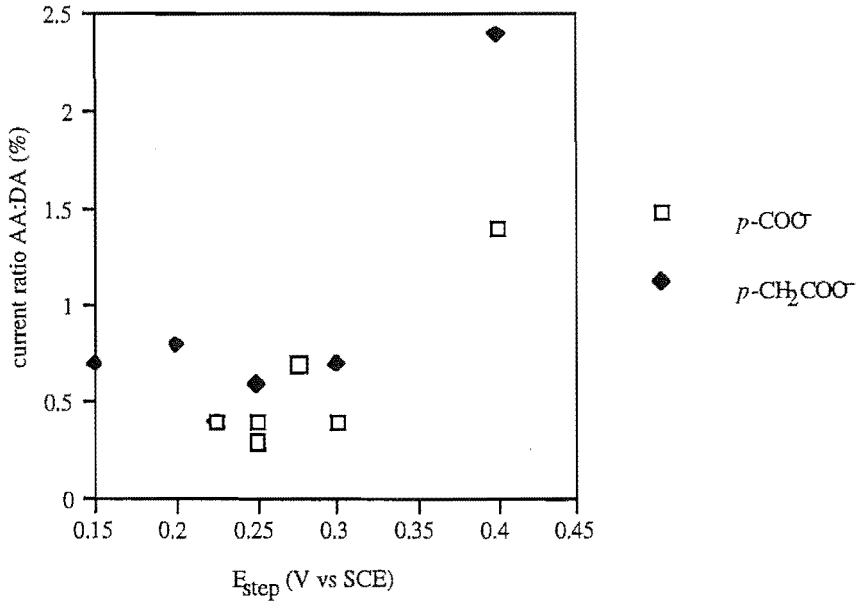

Potential steps to less positive values (≤ 0.3 V vs SCE) resulted in the highest DA currents compared to those of AA i.e. lower relative sensitivities to AA. Under these conditions, the electrode response of DA was under mixed (mass transport and electron transfer) control (a plot of i vs $t^{-1/2}$ was non-linear) and that of AA was electron transfer controlled (i independent of t). When E_{step} was increased to 0.4 V a higher relative sensitivity to AA was obtained. The lowest relative sensitivities to AA observed were 0.4 ± 0.1% (E_{step} = 0.225 V) at the *p*-phenylacetate CME and 0.3 ± 0.1% (E_{step} = 0.25 V) at the *p*-benzoate modified electrode. These optimised step potentials were used for all subsequent chronoamperometric experiments. The constant error of ± 0.1% associated with each relative sensitivity value was estimated from repeat experiments at different preparations of the CME. The analyte solutions (in particular those of AA) were very susceptible to oxidation and this probably contributed to the variability of response, even though solutions were kept under nitrogen and fresh analyte solutions were prepared daily.

The transients arising from chronoamperometric measurements of 10 μM DA, 1 mM AA and a mixture of the two analytes in PBS at *p*-phenylacetate modified (Figure 4.7 (A)) and unmodified (Figure 4.7 (B)) electrodes are shown below. Clearly, modification increases the current for DA oxidation and decreases that of AA relative to the unmodified electrode. The response due to 10 μM DA plus 1 mM AA (i.e. a mixed solution) at the *p*-phenylacetate electrode was 118 ± 10% that of the sum of the individual responses whereas the DA plus AA solution was ca. 140% of the sum of the individual responses at the unmodified electrode. Values greater than 100% indicate that enhancement of the DA response by the catalytic reaction with AA is occurring. The poor reproducibility for the mixed solution at the CME reflects both the variability in solution concentrations (due to aerial oxidation) as well as differences arising from separate CME preparations. Nevertheless, it is always found that modification decreases the importance of the catalytic reaction.

Figure 4.7: Chronoamperometry of a) 10 μM DA, b) 1 mM AA and c) 10 μM DA plus 1 mM AA at A) *p*-phenylacetate modified and B) unmodified GC electrodes. Potential was stepped from -0.1 to 0.225 V vs SCE

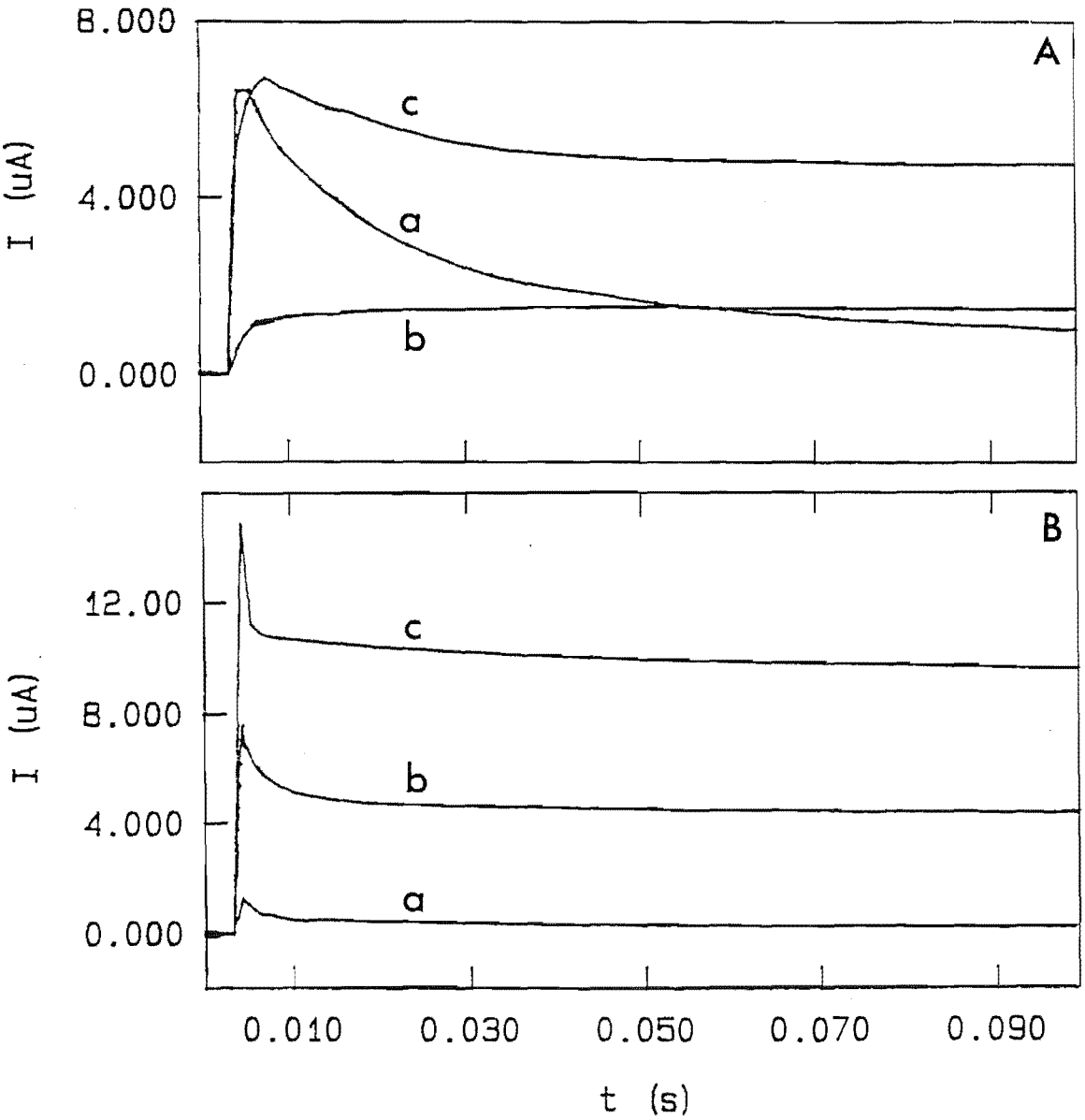

Calibration curve for DA at the p-phenylacetate CME using chronoamperometry. A calibration curve for DA was obtained at the *p*-phenylacetate CME using the chronoamperometric response at 20 ms. Triplicate measurements were made using $E_{initial}$ = -0.1 V and E_{step} = 0.225 V vs SCE and each point is background corrected by subtraction of the current recorded in PBS prior to the addition of analyte. A range of DA concentrations between 1 and 20 μM were measured in the presence or absence of 200 μM AA and the resulting regression lines are shown in Figure 4.8. Each calibration curve was obtained using a different CME.

Figure 4.8: Calibration curves for DA and DA/AA in PBS at the *p*-phenylacetate CME using the chronoamperometric response at 20 ms

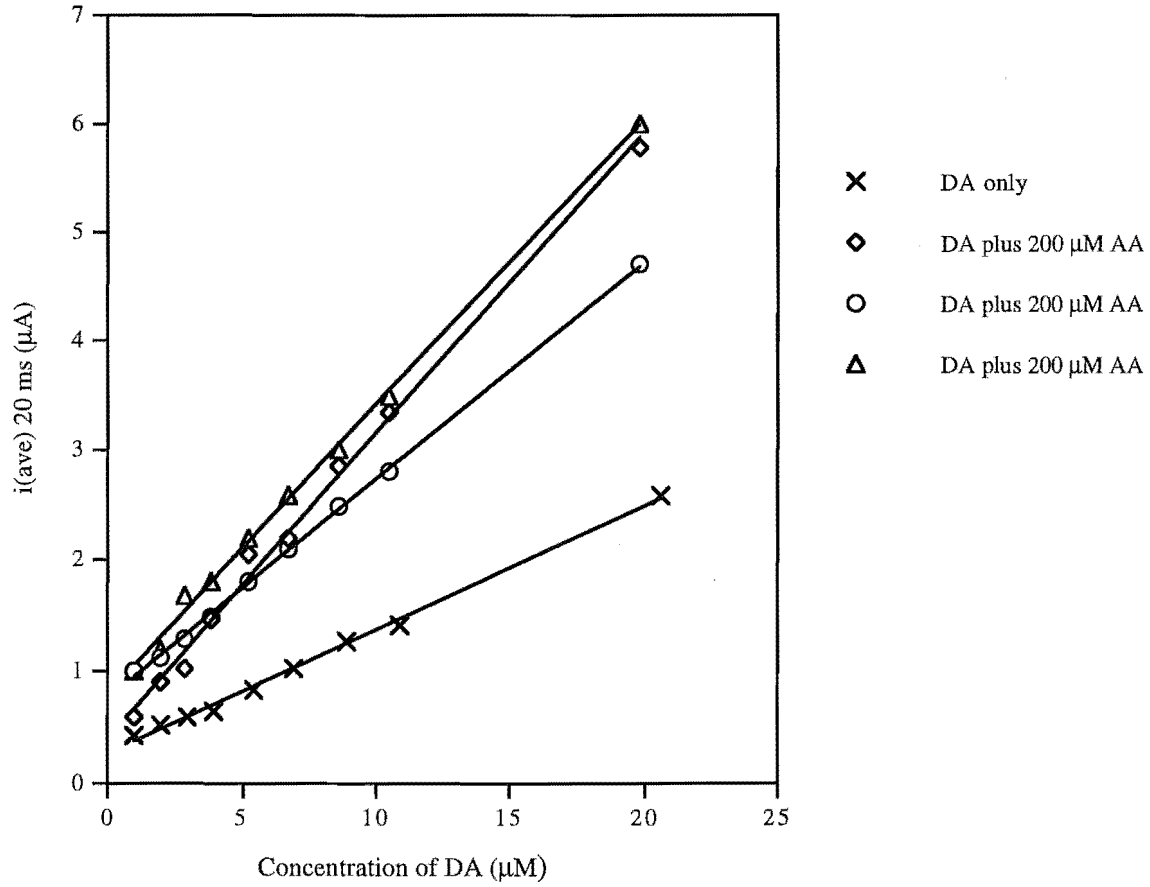

The resulting equations for lines of best fit and r^2 coefficients for calibrations performed in the presence of 200 μM AA were: (◇) i(20 ms) = 0.227[DA](μA) + 0.388(μA) (r^2 = 0.995); (O) i(20 ms) = 0.199[DA](μA) + 0.76(μA) (r^2 = 0.999) and (Δ) i(20 ms) = 0.263[DA](μA) + 0.794(μA) (r^2 = 0.998). This gives an RSD for slope of 17% (n = 3). In the absence of AA (X), the equation of the calibration line was i(20 ms) = 0.112[DA](μA) + 0.260(μA) (r^2 = 0.995). Non-zero intercepts were consistently observed and are assumed to arise from differences in the subtracted background value (recorded in PBS) and the contribution of background current in the presence of analyte. The slopes of the regression lines in the presence of AA are approximately twice those in its absence and the greater slopes are attributed to the effect of the catalytic reaction with AA. For a solution of 2 μM DA and 200 μM AA, repeat chronoamperometric measurements gave an RSD of 1% (n = 7) for the current at 20 ms. The detection limit, calculated as 3 times the standard deviation, for a solution of 2 μM DA/200 μM AA, was 72 nM.

The calibration curves for DA obtained at the *p*-benzoate CME by the same procedure described above are shown in Figure 4.9. For these measurements $E_{initial}$ = -0.1 V and E_{step} = 0.25 V. The equation for the line of best fit with 200 μM AA present (◇) was i(20 ms) = 0.390[DA](μA) + 0.015(μA) (r^2 = 0.996). Dopamine calibrations in the absence of AA (X) and (O), obtained at different *p*-benzoate CMEs, resulted in regression lines; i(20 ms) = 0.269[DA](μA) + 0.288(μA) (r^2 = 0.998) and i(20 ms) = 0.318[DA](μA) + 0.739(μA) (r^2 = 0.992), respectively. The addition of AA at the *p*-benzoate electrode affects the slope less than is observed at the *p*-phenylacetate CME. This may be due to the greater density of negative charges at the *p*-benzoate surface (arising from a larger surface coverage) decreasing the effective concentration of AA near the electrode. Similarly, an enhanced electrostatic effect at the *p*-benzoate CME may explain the increased slope of calibration curves for DA only, relative to that at the *p*-phenylacetate CME.

Figure 4.9: Calibration curves for DA and DA/AA in PBS at the *p*-benzoate CME using the chronoamperometric response at 20 ms

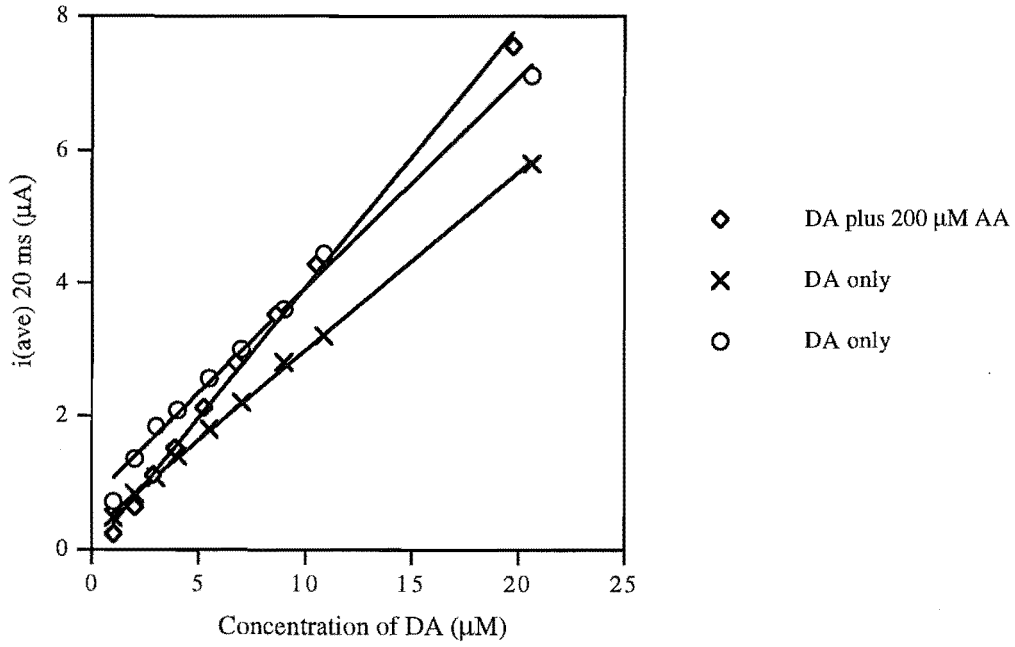

4.3.3 Response of the CMEs after exposure to surfactants and lipids

When microelectrodes are used for *in vivo* measurements of neurotransmitters it is always found that electrode response deteriorates after contact with the brain tissue[34,68,118,120]. This has been attributed to adsorption of high molecular weight species on the electrode surface. To investigate the effect of foulants on the CMEs presently under study, chronoamperometric experiments were performed at *p*-phenylacetate and *p*-benzoate

CMEs following 24 hours stirring in a 0.1% solution of the non-ionic surfactant Triton X-100 plus 0.3 g L^{-1} bovine serum albumin. Following surfactant treatment, sensitivity to DA and AA decreased to 65 ± 15% of the original value and the relative response to AA was unchanged. The changes observed at the CME upon exposure to surfactants are consistent with a reduction in active electrode area by adsorption. The chronoamperometric responses of the *p*-benzoate CME before (A) and after (B) 24 h stirring in the surfactant solution are shown in Figure 4.10.

Figure 4.10: Chronoamperometry of a) 10 µM DA, b) 1 mM AA and c) 10 µM DA plus 1 mM AA at the *p*-benzoate CME A) before and B) after 24 h exposure to the surfactant solution. Potential was stepped from -0.1 to 0.25 V vs SCE

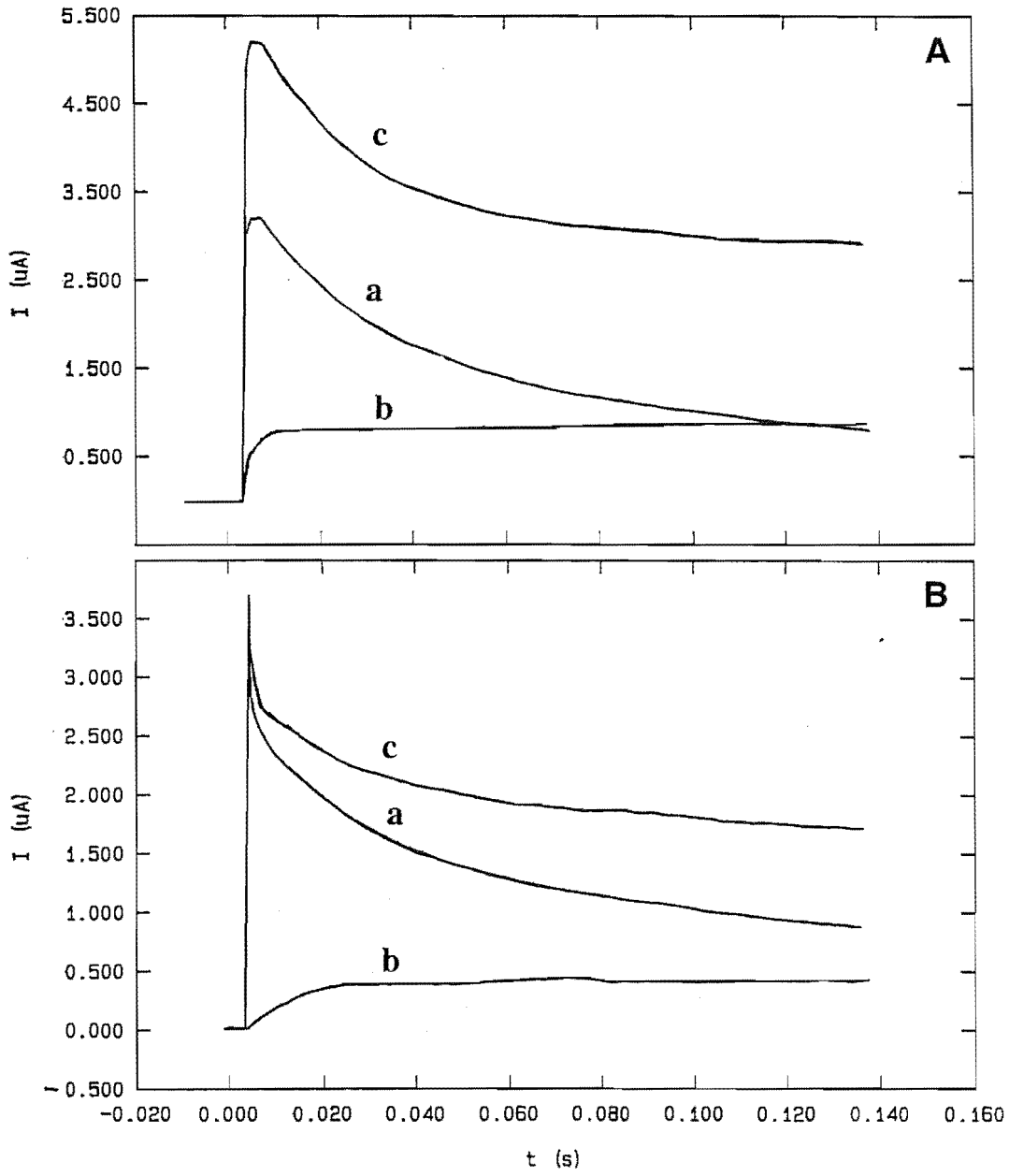

4.3.4 Response times of the CMEs to DA

To be useful as probes for measuring rapid changes in DA concentration, modified electrodes must respond quickly. The response times of the CMEs were investigated using flow injection analysis (FIA) with electrochemical detection. The FIA manifold was adjusted to give minimum sample dispersion and hence an approximately rectangular sample zone at the detector. The distance between the injection valve and the detector was made as small as practicable given that noise at the detector increased as the distance between the detector and pump decreased. A 30 μL sample of 0.2 μM DA in PBS was injected into the carrier stream (PBS) and passed over the modified or unmodified GC detector operated at an applied voltage of 0.6 V vs Ag/AgCl. Elapsed times from the foot of the peak to 90% of the maximum (T_{90}) and from the maximum down to 10% of its value (T_{10}) were compared at the unmodified and modified detectors.

Para-phenylacetate and *p*-benzoate CMEs showed the same response time characteristics. Peak currents for DA oxidation were greater at the modified electrodes (0.046 μA) compared to the unmodified response (0.039 μA). The T_{90} values however, were the same for the CMEs and unmodified electrodes (1.8 s); T_{10} was increased by 0.5 s at the CMEs (relative to the unmodified electrode) giving a value of 10.5 s. It is assumed that the i vs t response recorded at the unmodified electrode accurately reflects the concentration profile of the sample zone as it flows over the detector, i.e. the sample zone is not rectangular, and the electrode response is fast on the timescale of the measurement. The larger value for T_{10} at the modified electrode therefore represents a small lag in response.

4.3.5 Studies at microelectrodes and microelectrode arrays

Microelectrodes must be used for *in vivo* measurements of neurotransmitters. Hence an obvious extension of this work was to apply the modification to microelectrodes. All modifications to microelectrodes involved *p*-phenylacetate groups. Single glassy carbon fibre disk electrodes (11 μm diameter) and an electrode composed of a random array of carbon fibre microdisks (RAM) were used in these experiments. The main aims of this work were to demonstrate that the modification could be applied to microelectrodes and to investigate whether responses at these were consistent with the macroelectrode results.

The RAM electrode, illustrated in Figure 4.11, has a total diameter of approximately 1 cm and obviously is not suitable for *in vivo* use. The spacing of microdisks on this electrode is such that diffusion zones do not overlap and hence it behaves like a microelectrode but with a surface area of the additive disk areas. Additionally, random noise at each microdisk should cancel out. Therefore, electrode behaviour relevant to single carbon fibres can be observed with the benefits of much larger currents and an enhanced signal to noise ratio.

Figure 4.11: Random array of microdisks (RAM) electrode

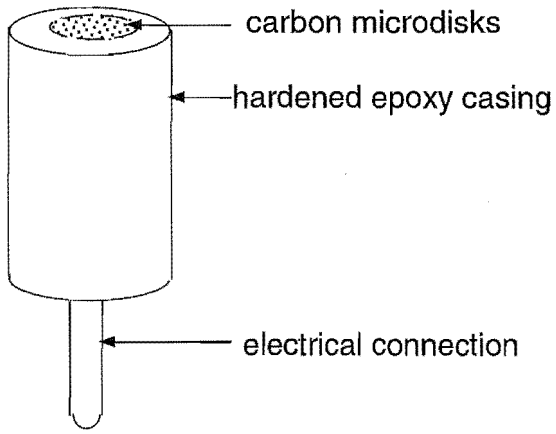

Electrode modification. Initial attempts to modify micro- and RAM electrodes with *p*-phenylacetate groups were unsuccessful, although conventional-size CMEs could be prepared using the same diazonium salt solutions. Hence *p*-phenylacetate modifying solutions which were very brightly coloured (pink/red) when first prepared, were passed through activated carbon decreasing the colour of the solution. Modification of micro- and RAM electrodes using diazonium salt solutions treated in this way were successful. It is assumed that blockage of the microelectrode surface by high molecular weight impurities prevents covalent modification and that these are largely removed by treatment with activated charcoal. The standard electrolysis conditions (described in Chapter Three) were used. The best results were obtained for microelectrodes when 10 s sonication in AR acetone followed modification. All experiments performed with modified micro- and RAM electrodes were undertaken with the *p*-phenylacetate groups.

Electrochemical behaviour at unmodified micro- and RAM electrodes. Considerable difficulty was encountered in the use of micro- and RAM electrodes. There were two main problems: performance of the electrodes and the difficulty of measuring very small currents. As a consequence, reproducibility of the experiments described below was generally poor. Response deteriorated rapidly with each scan recorded at the unmodified electrode and routine polishing did not restore performance. Worsening of electrode response involved increased background currents, decreased kinetics for oxidation of 1 mM DA (monitored by CV with ν = 50–200 mV s^{-1}) and the appearance of additional oxidation peaks (at ca. -0.08 V vs Ag/AgCl) presumably due to surface oxides. The effect was more pronounced for single fibre electrodes. The performance of electrodes after modification was strongly affected by the condition of the electrodes prior to modification; a "good" response prior to modification resulted in a "good" response after modification and vice versa.

It is well-known that oxidation of carbon surfaces increases background currents and that oxidation of chloride at carbon results in surface corrosion. Hence, all micro- and RAM electrode measurements were made in chloride-free PB solutions and scans were

limited to the lowest possible positive potential. Despite these conditions it was necessary to regularly re-surface electrodes by exhaustive polishing. For single fibre electrodes, this was carried out by polishing using cerium oxide on a mechanical polishing wheel. RAM electrodes could be restored to their initial performance by prolonged polishing (typically > 1 h) with 0.05 μm alumina or cerium oxide on a wet cloth. Results described in the following sections were obtained at freshly re-surfaced electrodes.

4.3.6 Differential pulse voltammetry at micro- and RAM electrodes

The DPV responses of 20 μM DA in PB (0.04 M) were obtained at the unmodified and modified RAM electrode (see Figure 4.12). The peak current ($i_{p,a}$) due to DA at the unmodified electrode was 2.2 nA and a peak potential for oxidation ($E_{p,a}$) of 0.13 V vs Ag/AgCl was observed. After modification, $i_{p,a}$ = 9.9 nA and $E_{p,a}$ = 0.125 V.

The DP voltammogram for oxidation of 1 mM AA gave $E_{p,a}$ > 0.6 V at the unmodified RAM electrode. Hence the AA response does not overlap with the signal for oxidation of 20 μM DA . This contrasts with the results obtained at conventional-size GC and presumably this is due to the type of carbon fibre used in the construction of the electrode.

Figure 4.12: Differential pulse voltammograms obtained at the RAM electrode for 20 μM DA/PB before (A) and following (B) modification

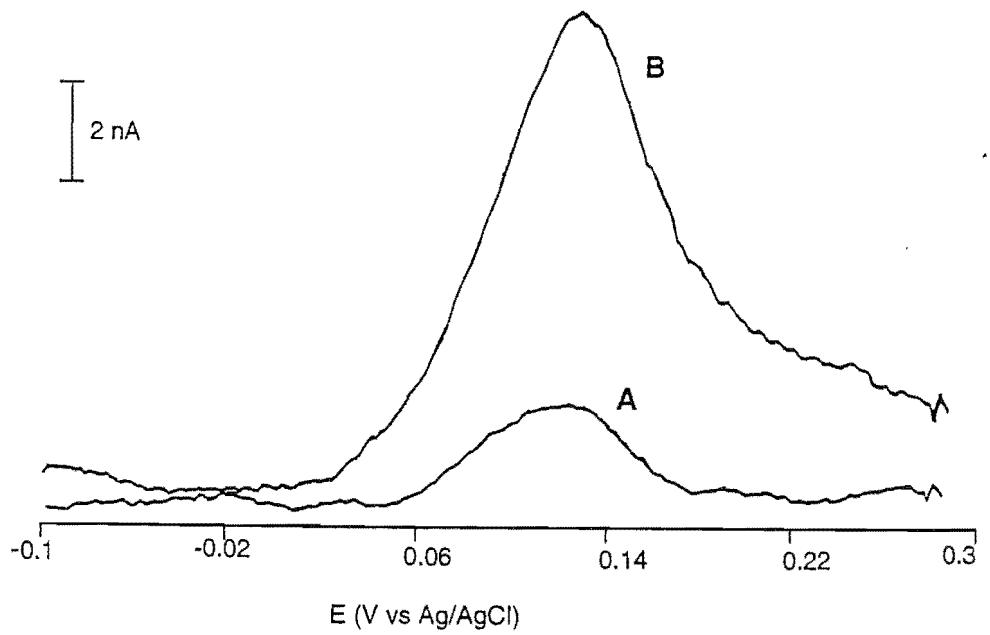

Differential pulse voltammetric studies were also carried out at the single glassy carbon fibre electrode. In this case the oxidation responses of DA and AA overlap at the unmodified electrode. Modification of a freshly re-surfaced carbon fibre microelectrode resulted in a 3 to 6 fold enhancement of $i_{p,a}$ for 20 μM DA whilst the response of 2 mM AA was decreased and $E_{p,a}$ was shifted more positive, relative to the unmodified carbon fibre. Representative DP voltammograms of a 20 μM DA plus 2 mM AA solution in 0.1 M PB at the modified (Figure 4.13 A) and unmodified (Figure 4.13 B) carbon fibre are shown below. The data for repeat DP scans at the modified carbon fibre are given in Table 4.2. At the unmodified carbon fibre, the DA signal is obscured by that of AA whereas the DA response is resolved after modification. Two observations suggest that the large peak at the unmodified carbon fibre is due to AA rather than a catalytically enhanced DA signal: $E_{p,a}$ occurs at the potential expected for AA and $i_{p,a}$ is consistent with that observed for a solution of 2 mM AA only at the unmodified carbon fibre.

Figure 4.13: Differential pulse voltammograms of a solution of 20 μM DA and 2 mM AA in 0.1 M PB at A) modified and B) unmodified carbon fibre microelectrodes

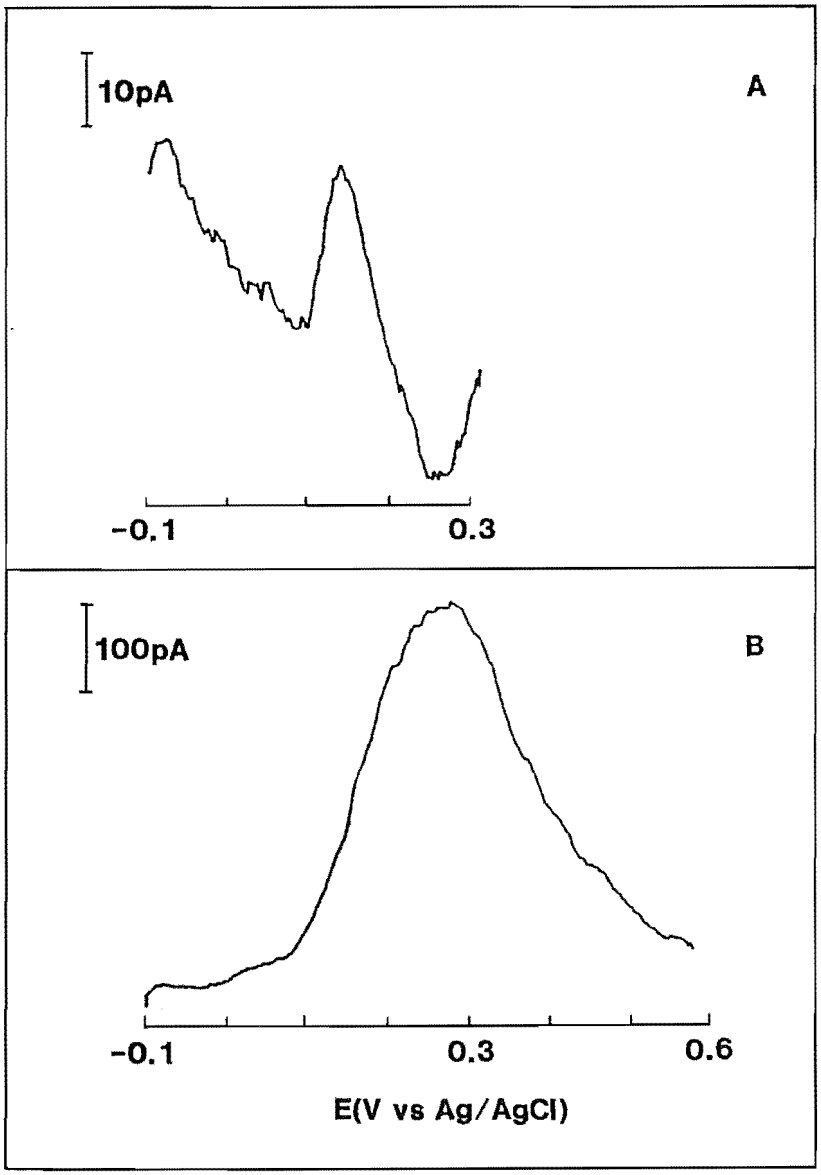

Table 4.2: Repeat differential pulse voltammograms of 20 μM DA plus 2 mM AA at the modified carbon fibre microelectrode

DPV scan no.	$E_{p,a}$ (V)[a]	$i_{p,a}$ (pA)
1	0.160	23.3
2	0.152	29.2
3	0.147	32.0
4	0.147	30.7

[a] $E_{p,a}$ (V vs Ag/AgCl)

The RSD for $i_{p,a}$ (n = 4) at the modified carbon fibre was 13% which is the same as that obtained at the unmodified carbon fibre. The current due to DA oxidation increased over the first three DP voltammograms and $E_{p,a}$ was shifted less positive but appeared to stabilise on the forth scan. Hence, several "conditioning" scans prior to analysis would be expected to improve the sensitivity and reproducibilty of DP measurements.

4.3.7 Fast scan rate cyclic voltammetry at micro- and RAM electrodes

Fast scan rate voltammetry (FCV) is a routine method for measuring DA released after strong stimulation *in vivo*. This technique was used to investigate the effect of modification of the RAM electrode. Figure 4.14 shows the responses of the modified (a) and unmodified (b) RAM electrode to 10 μM DA in PB (0.04 M) at 270 Vs^{-1}. Several voltammograms were recorded in PB prior to use in the DA solution (for both the unmodified and modified electrodes) and these were subtracted from the resulting voltammogram recorded in the presence of DA. The voltammograms are the best obtained after background subtraction.

Figure 4.14: Fast scan rate voltammograms at a modified (a) and unmodified (b) RAM electrode recorded at $\nu = 270$ V s^{-1} in 10 μM DA/PB (0.04 M)

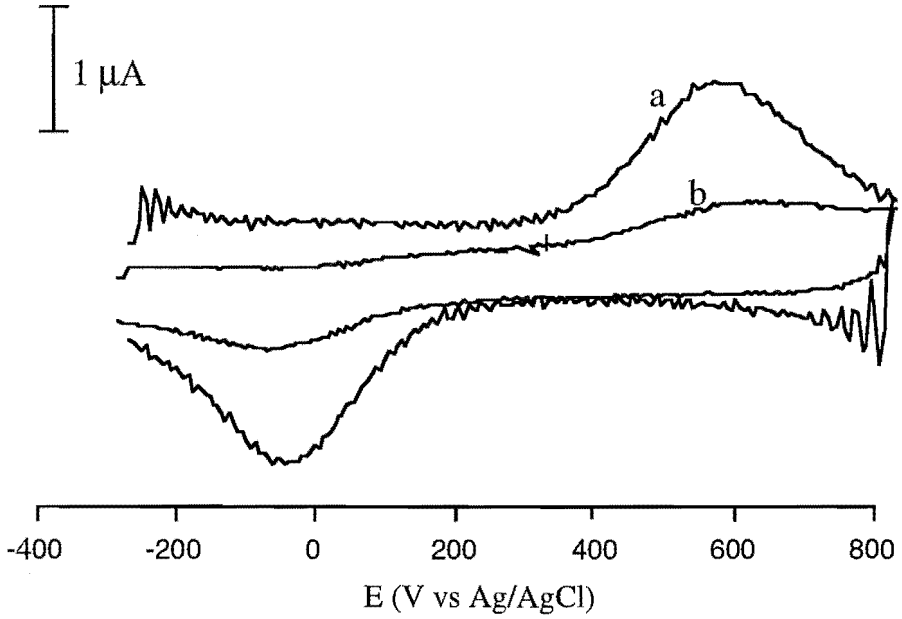

To investigate whether the response at the RAM electrode was due to surface adsorbed species, the effect of changing scan rate on the peak current for oxidation was examined. Voltammograms were recorded at scan rates between 1 and 270 V s^{-1} in 10 μM DA/PB (0.04 M). Increasing the PB concentration to 0.1 M did not affect the peak potentials at $\nu = 270$ V s^{-1}, hence it is assumed that the relatively low buffer concentration (0.04 M) did not contribute to solution resistance. The resulting plot of log peak current vs log scan rate is shown in Figure 4.15. In the case of weak adsorption, the slope will lie between 0.5 (for a purely diffusion-controlled process) and 1.0 (for a purely adsorption-controlled response)[121]. The graph obtained was linear ($r^2 = 0.999$) and had a slope of 0.737(V s^{-1}) indicating that both adsorbed DA and diffusing species contributed to the peak current at scan rates of 1 – 270 V s^{-1}. (Note that the linearity of the plot suggests that slow electrode kinetics or solution resistance are not influencing the response. These phenomena are expected to become increasingly important with scan rate, thus causing curvature of the plot.)

Figure 4.15: Log-log plot showing the effect of varying scan rate on the peak current for oxidation of DA (10 μM) at the modified RAM electrode

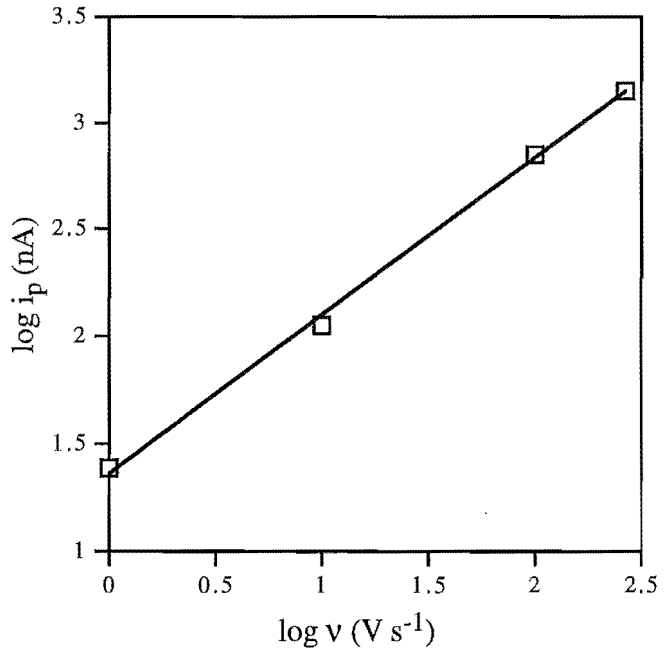

Fast scan rate cyclic voltammetry experiments (270 V s^{-1}) were also carried out at the single GC fibre electrode. A freshly re-surfaced carbon fibre electrode, which gave negligible response to 10 μM DA (see Figure 4.16 B), consistently gave an observable DA signal after modification (Figure 4.16 A). Further, $i_{p,a}$ at the modified electrode increased and became more peaked with stirring time in DA solution indicating that this response was due to adsorbed DA.

Figure 4.16: Cyclic voltammograms of 10 μM DA in 0.1 M PB recorded at ν = 270 V s^{-1} at A) modified and B) unmodified carbon fibre microelectrode

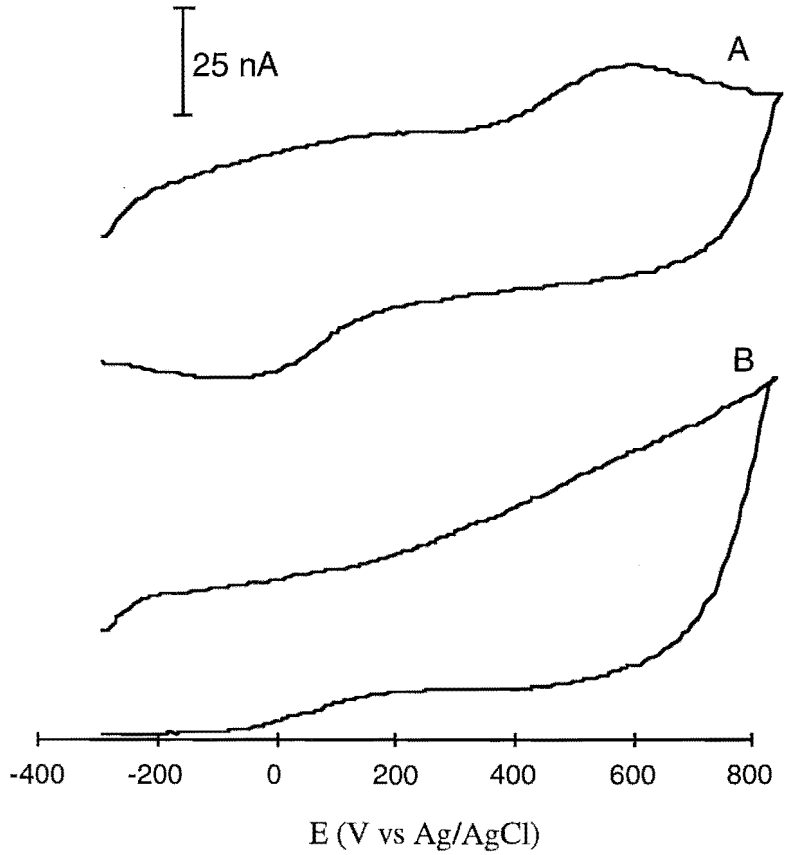

4.4 Discussion

4.4.1 Performance of the conventional-size CME

Differential pulse voltammetric experiments at *p*-phenylacetate modified conventional-size GC electrodes show that DA is not measurable in the presence of 100 fold concentrations of AA due to the catalytic enhancement of DA response. The detection limit for DA (90 nM) suggests that basal DA levels in the neurochemical environment would not be measurable at a chemically modified microelectrode with the same properties. It may be possible to detect DA using DPV after strong stimulation in conjunction with pharmaceutical inhibition of DA metabolism (which typically generates micromolar concentrations) with the CMEs. The sensitivity of this measurement, however, would not be expected to be as high as that obtainable with a Nafion coated, electrochemically pretreated carbon fibre[34].

Para-phenylacetate and *p*-benzoate CMEs showed good discrimination for DA at short times (20 ms) in chronoamperometric experiments. At $E_{step} \geq 0.225$ V, DA was under mixed electron transfer and diffusion control whilst AA was under electron transfer control indicating a much faster rate of electron transfer for oxidation of DA than AA. The relative response ratios to AA at *p*-phenylacetate and *p*-benzoate electrodes showed little dependence on E_{step} ranges between 0.15 to 0.3 V vs SCE. The most favourable response ratios observed, $0.4 \pm 0.1\%$ (*p*-phenylacetate) and $0.3 \pm 0.1\%$ (*p*-benzoate), are comparable to other DA probes designed for use with fast timescale electrochemical techniques[33,34]. For example, a relative sensitivity ratio to AA (over DA) of 0.33% was reported for electrochemically pretreated Nafion coated carbon fibre electrodes. Analyte responses were measured by integrating chronoamperometric currents between 70 and 100 ms after application of the potential step. Similarly, Nafion thin film electrodes used in chronoamperometric experiments by other workers[33] gave relative sensitivities to AA over DA of 0.5 – 0.7%. Although lower ratios were attainable at thicker Nafion films, these were not used because response times were excessively high.

In the present study, the *p*-benzoate CME generally gave lower relative response to AA than that of *p*-phenylacetate and this probably reflects the denser coating of anionic groups at the *p*-benzoate CME. Greater slopes in calibration curves, with only DA present, at the *p*-benzoate CME and the decreased effect of AA on regression line gradients, compared to *p*-phenylacetate, are consistent with a larger electrostatic effect. A (decreased) catalytic current, compared with unmodified GC, was observed in chronoamperometric experiments at the CME. The catalytic reaction increased gradients in calibration curves but linear responses to changing DA concentration were obtained at constant AA concentration.

Exposure to surfactants decreased the DA oxidation current by ~ 35% at both CMEs. These results can be compared to those reported for other DA probes under similar conditions. Stearate-modified carbon paste electrodes which give well resolved DA and AA signals (ca. 600 mV separation of peaks in CV measurements) show poor resolution of responses after exposure to lipids and surfactants (typically 150 to 300 mV separation of peaks)[120]. After 2-12 h exposure to brain tissue, electrochemically pretreated carbon fibers typically retain approximately 50% of their initial sensitivity[34]. This value is unaltered by the presence of Nafion coating, and untreated and unmodified fibres are also reported to undergo deterioration to the same extent[122]. Hence, the CMEs described here appear to have similar fouling resistance to these probes.

Electrode response times are important when applying short timescale electrochemical techniques, such as FCV, to measure transient analyte concentrations. Carbon fibre electrodes with thin Nafion coatings are commonly used for these experiments in the neurochemical environment[4]. In this case DA must diffuse through the coating to be measured at the electrode surface and the response time of the electrode is increased (relative to an unmodified surface). A range of response times for Nafion coated carbon fibres have been reported in the literature. For example, T_{90} is reported to increase by 1 – 2 s (relative to a bare electrode) in some cases[34] whereas in other instances T_{90} for DA is increased by only 0.5 s[32]. It is reasonable to assume that Nafion film characteristics will be affected by the casting method and the structure of the underlying carbon electrode. Response times at electrochemically pretreated carbon fibres are reported to increase from 1.1 to 10.6 s[34]. In comparison, the *p*-phenylacetate and *p*-benzoate CMEs showed no significant change in T_{90} and only small increases in T_{10} values, indicating these surfaces appear well-suited for short timescale measurements of DA.

The purpose of this work was to establish whether monolayer modification with *p*-phenylacetate and/or *p*-benzoate groups produces electrodes with useful properties for *in vivo* neurotransmitter measurements. Modified single fibre microelectrodes must be used *in vivo* and experiments conducted at macro- and RAM electrodes were for experimental simplicity. This assumes that results at these electrodes can be meaningfully extended to microelectrodes taking into account fundamental differences in the mass transport characteristics of the different sized electrodes. At the microelectrode, at sufficiently long times, radial diffusion dominates over linear diffusion leading to an increased rate of mass transport[123]. One consequence is to reduce the effects of coupled homogeneous reactions because the redox products are rapidly removed from the vicinity of the electrode. To compare the behaviour of the different electrode types used in these experiments, Table 4.4 summarises the observations made at the conventional-size CME, carbon fibre micro- and RAM electrodes.

Table 4.4: Summary of DA experiments made with different electrodes and using different electrochemical techniques

	GC	RAM	C Fibre
		Differential pulse voltammetry	
unmodified	DA, AA overlap	no overlap of DA/AA	DA, AA overlap no catalysis for DA + AA
modified	DA, AA overlap enhanced DA (20 μM) AA shifted positive catalysis for DA + AA	enhanced DA (20 μM)	enhanced DA (20 μM) AA shifted positive no catalysis for DA + AA
		Fast scan rate/cyclic voltammetry	
modified	enhanced DA signal at low [DA] faster DA kinetics ([DA] = 1 mM) decreased response to AA	enhanced DA signal at low[DA]	enhanced DA signal at low[DA]
		Chronoamperometry	
modified	faster DA kinetics decreased catalytic reaction	not examined	not examined

All electrodes (when modified) gave enhanced response to low concentrations of DA in DPV experiments. Using DPV, both unmodified GC and GC fibre microelectrodes showed overlapping DA and AA responses whereas the RAM electrode did not. Several different procedures may be used to fabricate carbon fibres and this affects their cross-sectional structure and ultimately their electrochemical behaviour[51]. Hence different sources of carbon fibre materials can be expected to give different degrees of resolution for

DA and AA. The carbon fibre used in the construction of the RAM electrode would be a useful material for the development of *in vivo* probes; the type of fibre is confidential to the manufacturer of the RAM electrodes. Unlike the situation at the conventional-size electrode, there was no evidence of catalytic reaction of DA at either the unmodified or modified carbon fibre microelectrode in DPV experiments. This is the expected consequence of rapid radial diffusion of oxidised DA away from the electrode surface preventing the catalytic reaction with AA.

Fast scan rate cyclic voltammetry (and CV for GC), resulted in enhanced currents for DA present at micromolar concentrations. There is evidence that under these conditions adsorbed DA is being measured.

Chronoamperometry was experimentally too difficult to perform using the carbon fibre microelectrode however it is anticipated that the relative sensitivity to AA over DA will decrease at the modified microelectrode, relative to the macroelectrode. The expected current due to oxidation of DA at the microelectrode of radius (r) can be estimated from equation (4.1), assuming diffusion control of DA response[124]. Note this expression is only approximate for currents at an 11 μm diameter electrode, 20 ms after application of a potential step. The first term in equation 4.1 describes the current arising from linear diffusing species at time t and the second term is the contribution of radial diffusing species. For r = 5.5 μm and t = 20 ms, the contribution of radial diffusion is calculated to be approximately equal to linear diffusion (D = 5 x 10^{-6} cm^2 s^{-1}). Hence the current density due to oxidation of DA should be approximately doubled at a microelectrode compared to the conventional-size electrode.

$$i = r^2\pi^{1/2}nFCD^{1/2}t^{-1/2} + r\pi nFCD \qquad (4.1)$$

On the other hand, at the modified electrode the oxidation of AA is under electron transfer control and hence the current will be unaffected by radial diffusion. These considerations lead to the prediction that the relative sensitivity to AA at the modified microelectrode will be approximately half that of the conventional-size electrode i.e. ~ 0.2%. The catalytic reaction is not expected to be important in chronoamperometric measurements at microelectrodes due to the enhanced rate of mass transfer arising from radial diffusion.

4.5 Conclusions

Measurements at *p*-phenylacetate modified conventional-size and carbon fibre microelectrodes indicate modified microelectrodes may be useful for *in vivo* measurement of neurotransmitters. The selectivity of the *p*-phenylacetate and *p*-benzoate CMEs are similar to that reported for *in vivo* probes currently in common use, namely, carbon fibres which are coated with thin layers of Nafion. The single most important feature of the CMEs discussed in this work is their fast response time to DA. Modification with an anionic monolayer does not increase T_{90} relative to unmodified GC. Compared to the Nafion coated carbon fibres, the *p*-phenylacetate and *p*-benzoate CMEs possess similar discrimination for DA over AA and comparable stability to the neurochemical environment but have decreased response times to DA. Thus these CMEs seem well-suited for fast timescale measurements *in vivo*.

Chapter Five: Characterisation of *para*-alkylbenzene modified electrodes

5.1 Introduction

Chemically modified electrodes incorporating hydrophobic surface groups are of interest for two reasons: the determination of hydrophobic analytes, and as a way of studying electron transfer at blocked surfaces.

Several methods have been utilised to generate hydrophobic electrode surfaces including adsorption of phospholipids onto carbon materials[56-58], self assembly of alkanethiols on gold electrodes[49,50], and physical incorporation of hydrophobic modifiers into electrode materials such as carbon paste[64,65].

Typically phospholipids are cast onto the electrode surface from chloroform solutions[56-58]. Hydrophobic analytes are preferentially accumulated from aqueous solutions. Consequently, these CMEs have been used to analyse drugs in the presence of hydrophilic biological interferents such as ascorbic and uric acids. Selectivity on the basis of charge may also be achieved using lipid modifiers with differently charged head groups[56] and by incorporation of charged surfactants into the phospholipid coatings[125]. In these studies selectivity of analytes was based on electrostatic interactions and hydrophobicity/hydrophilicity. Thus the anionic metalloprotein, ferrodoxin, was measurable at phospholipid/cholesterol/dodecylbenzeneamine coated electrodes whilst it was not observed in the absence of dodecylbenzeneamine[125].

Physical incorporation of compounds such as fatty acids, surfactants and phospholipids into carbon paste materials is a common method of generating hydrophobic CMEs. Modified carbon paste electrodes prepared in this way have been utilised extensively to measure biologically important compounds such as the phenothiazines, marcellomycin and ergot alkaloid drugs [64,65]. Predominantly, applications have involved adsorptive stripping batch analysis and have been applied to water, diluted urine and plasma samples buffered at acidic or neutral pH.

Phospholipids typically have hydrocarbon chains composed of ca. 17 carbons therefore, the above hydrophobic CMEs are thick mono- or multilayers. They are suitable for adsorptive stripping analysis when the target analyte can partition into the coating and typically accumulation times of 3–5 min are employed for measurements[56,57,65]. The apparent electron transfer kinetics of analytes in CV experiments at these thick coatings, however, are decreased due to resistive effects (which lower the potential driving force of the reaction). For analytical applications, there is a general need for CMEs which can

measure hydrophobic analytes under fast timescale conditions and give fast electron transfer kinetics.

Much research has focussed on hydrophobic CMEs prepared by self-assembly of alkanethiol monolayers on Au[49,50,126]. Generally, this method of modification is used for long chain alkanethiols, and produces blocking films at which diffusion of analytes to the electrode surface is severely retarded. Hence, as discussed in Chapter One, these CMEs have been used in kinetic studies to examine nonadiabatic electron transfer processes across the film, which acts as a non-conducting spacer[46,47].

Recently, Au electrodes modified with very thin (~0.8 nm) spacer layers have been prepared by self-assembly of 1,2-dithiolane-3-pentanoic acid compounds. These CMEs are designed to minimise the kinetic effects of electron transfer through space. The film hydrophobicity was altered by varying the amount of uncharged thiol present in the coating. The effect of this change on the kinetics of both hydrophilic and hydrophobic analytes was discussed[49]. It was anticipated that thin hydrophobic films might allow the selective determination of hydrophobic analytes. However, it was found that the responses of benzoquinone, DA and DOPAC were decreased at the hydrophobic SAMs. The most hydrophobic CMEs were very resistive, giving effective double layer capacitance values 7 – 70 times less than those observed at unmodified Au surfaces. This effect was assumed to be important to the observed slow electrode kinetics of analytes in CV experiments.

In this chapter, studies at *p*-alkylbenzene CMEs prepared using the diazonium salt modification procedure, are described. The mode of electron transfer at the CMEs is examined and the selectivity of these modified surfaces is investigated using probe analytes of varying hydrophobicity/hydrophilicity and charge. The analytical utility of *p*-alkylbenzene CMEs is discussed.

5.2 Experimental

5.2.1 Modification procedures

The general modification procedure described in Chapter Two was used to prepare *p*-alkylbenzene CMEs. An electrolysis potential of -0.94 V vs Ag/Ag^+ was applied in a diazonium salt/acetonitrile solution with 0.1 M $TBABF_4$ electrolyte. Electrolysis times of 15 s, 30 s, 90 s, 5 min or 10 min were used with 0.5 or 5.0 mM diazonium salt solutions. Electrolysis for 5 min in 5 mM diazonium salt solution was used to obtain a densely coated CME. Control experiments were carried out by submerging polished electrodes in the diazonium salt solution for the appropriate time and repeating the sonication treatments used after modifications. The synthesis of *p*-alkylbenzene diazonium salts are described in Chapter Two.

5.2.2 Normal pulse voltammetry

Normal pulse voltammetry (NPV) was performed using either a PAR Potentiostat/Galvanostat Model 273 A or PAR 174 A Polarographic Analyzer. A scan rate of 20 mV s^{-1} and drop time of 0.5 s were employed. Analytes were present at 0.5 mM or 1 mM concentrations in 0.5 M PB (pH 7). Triplicate measurements of each probe analyte were made at the modified electrode. The initial scan was recorded immediately in the analyte solution, after which the solution was stirred for 5 min and the second scan recorded. Following measurement of all analytes at the CME, the electrode was polished and the responses of analytes were recorded at the unmodified surface. Solutions of 1,2-dihydroxyanthraquinone-3-sulfonate (DASA) and naphthaquinone-4-sulfonic acid (NQS) were prepared immediately prior to measurement, as they were unstable over longer times All solutions were degassed with N_2 to remove O_2.

5.2.3 Variable temperature experiments

Cyclic voltammograms of FcOH (1 mM) in 0.5 M PB were recorded at the *p*-decylbenzene CME at temperatures of 5, 21 and 45°C. Solutions were cooled by suspending the electrochemical cells in ice water, and temperatures above ambient were attained by placing cells in a water bath.

5.3 Results

5.3.1 Choice of probe analytes

The chemical structures of analytes used in these studies and their charges at pH 7 are shown in Figure 5.1. Probe analytes of varying molecular weights, charge and hydrophobicity/hydrophilicity were used to investigate the selectivity of *p*-alkylbenzene modified electrodes.

The analytes 4-MC, catechol and FcOH are uncharged at pH 7; 4-MC and catechol are small compared to FcOH. Ascorbic acid, uric acid (UA) and ferrocyanide, $Fe(CN)_6^{4-}$, represent small, intermediate and large hydrophilic species respectively. Tiron (1,2-dihydroxybenzene-3,5-disulfonate) has an aromatic ring but also two large anionic sulfonate groups, so it is considered as hydrophilic. The structures of NQS and DASA are similar i.e. they are contain an anionic sulfonate group and have regions of aromaticity but DASA is larger and more hydrophobic. Chlorpromazine (CPZ) is both cationic and hydrophobic; as is the iron-tris-2,2'-bipyridine complex, $Fe(bpy)_3^{2+}$, which is comparatively larger.

Probe analytes can further be classified according to the simplicity of their electron transfer reactions. Ruthenium(III) hexaammine, FcOH, $Fe(bpy)_3^{3+}$ and CPZ have uncomplicated outer-sphere electron transfer reactions whilst DASA, NQS, 4-MC, catechol, UA, tiron and AA have complex, proton-coupled electron transfer reactions at pH 7. The electron transfer of $Fe(CN)_6^{4-}$ also appears to involve electrode-mediated inner-sphere processes[127,128].

Figure 5.1: Chemical structures of probe analytes used to examine *p*-alkylbenzene CMEs

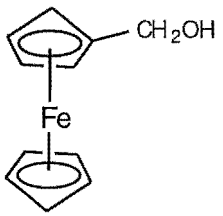

FcOH

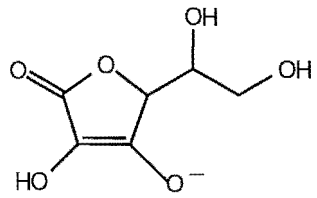

AA

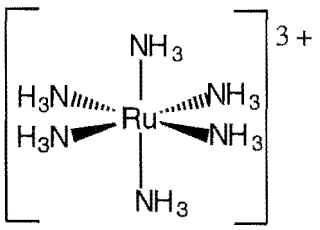

Ruthenium hexaammine

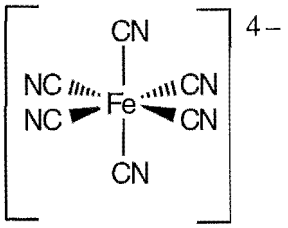

Ferrocyanide

Figure 5.1: Chemical structures of probe analytes used to examine *p*-alkylbenzene CMEs

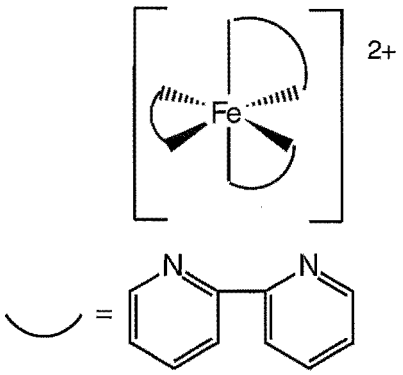

$Fe(bpy)_3^{2+}$

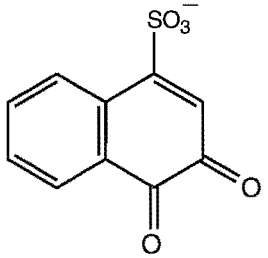

NQS

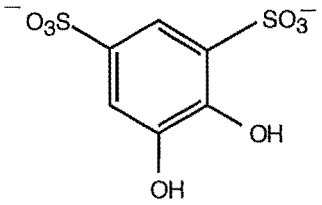

Tiron

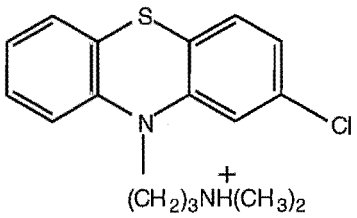

CPZ

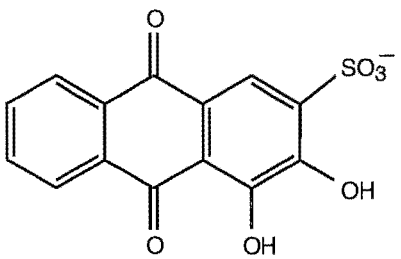

DASA

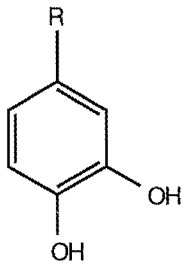

R = CH_3 4-MC
R = H catechol

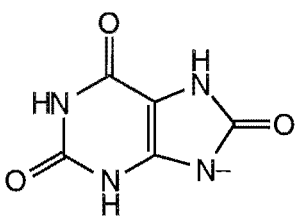

UA

5.3.2 Cyclic voltammetry at *p*-methylbenzene and *p*-decylbenzene CMEs

Background currents at CMEs. The background currents in CV experiments can be used to compare double layer capacitance at unmodified and modified electrodes[47,49]. Modification with *p*-methylbenzene moieties did not alter the background currents relative to unmodified GC, implying that solvent and electrolyte are able to freely penetrate the modifying layer. Hence, film resistance and potential drop across the coating are expected to be low. The longer-chained *p*-butylbenzene and *p*-decylbenzene CMEs showed small decreases in currents compared to the unmodified electrode. Therefore a more resistive/hydrophobic environment is assumed to be present within these coatings, compared to the *p*-methylbenzene CMEs. This contrasts with self-assembled monolayers of alkanethiols on Au which typically give large reductions in capacitance after modification[47,49].

Cyclic voltammetric response of probe analytes at densely coated p-methylbenzene CMEs . Cyclic voltammograms of probe analytes (1 mM in 0.5 M PB) were recorded at *p*-methylbenzene CMEs prepared by 5 min electrolysis in 5 mM diazonium salt solution. These conditions were shown to give coatings of maximum density. The electrochemical data are summarised in Table 5.1 and cyclic voltammograms are shown in Figure 5.2. Control experiments, performed by immersing an unmodified GC electrode in diazonium salt solution and applying the usual sonication procedures used for modification, gave unchanged electrochemical response for 4-MC. For AA however, which is known to be very sensitive to changes in the electrode surface, $E_{p,a}$ shifted 60 mV positive and $i_{p,a}$ decreased to 78% of its value prior to the control experiment. This implies that some diazonium salt was adsorbed on the GC electrode but that this effect was not responsible for the CME behaviour. Note that for experimental convenience, two electrodes (one modified and the second unmodified) were used for these experiments. Prior to modification, the electrodes gave similiar responses to the probe analytes. However, the electrode which was not subsequently modified exhibited smaller background currents.

Table 5.1: Cyclic voltammetry of 1 mM analyte/0.5 M PB at unmodified and *p*-methylbenzene modified electrodes recorded at $\nu = 100$ mV s^{-1}

	UNMODIFIED			MODIFIED			
analyte	$i_{p,a}$ (μA)	$E_{p,a}$ (V)[a]	ΔE_p (mV)	$i_{p,a}$ (μA)	$E_{p,a}$ (V)[a]	ΔE_p (mV)	$i_{p(m)}/i_{p(u)}$
4-MC	29.0	0.19	80	1.0+ 3.3	0.21+ 0.78	90 + 1150	0.03 + 0.11
DA	27.0	0.20	60	2.0[b]	0.81[b]	> 1500	0.07
$Fe(CN)_6^{4-}$	10.0	0.26	100	no signal	—	—	0.0
$Fe(bpy)_3^{2+}$	11.5	0.88	65	10.8	0.93	120	0.94
CPZ	33.0	0.64	—	20.0	0.82	—	0.61
AA	17.5	0.47	—	no signal	—	—	0.0
UA	23.0	0.42	—	1.75	0.87	—	0.08
FcOH	16.0	0.26	60	8.0	0.30	160	0.50
$Ru(NH_3)_6^{3+}$	$i_{p,c}$ 17.0	$E_{p,c}$ -0.29	65	$i_{p,c}$ 10.0	$E_{p,c}$ -0.32	120	0.59

[a] V vs SCE

[b] very small response also observed at 0.21 V

Figure 5.2: Cyclic voltammograms of 1 mM analyte/0.5 M PB at the unmodified (A) and *p*-methylbenzene modified (B) electrode

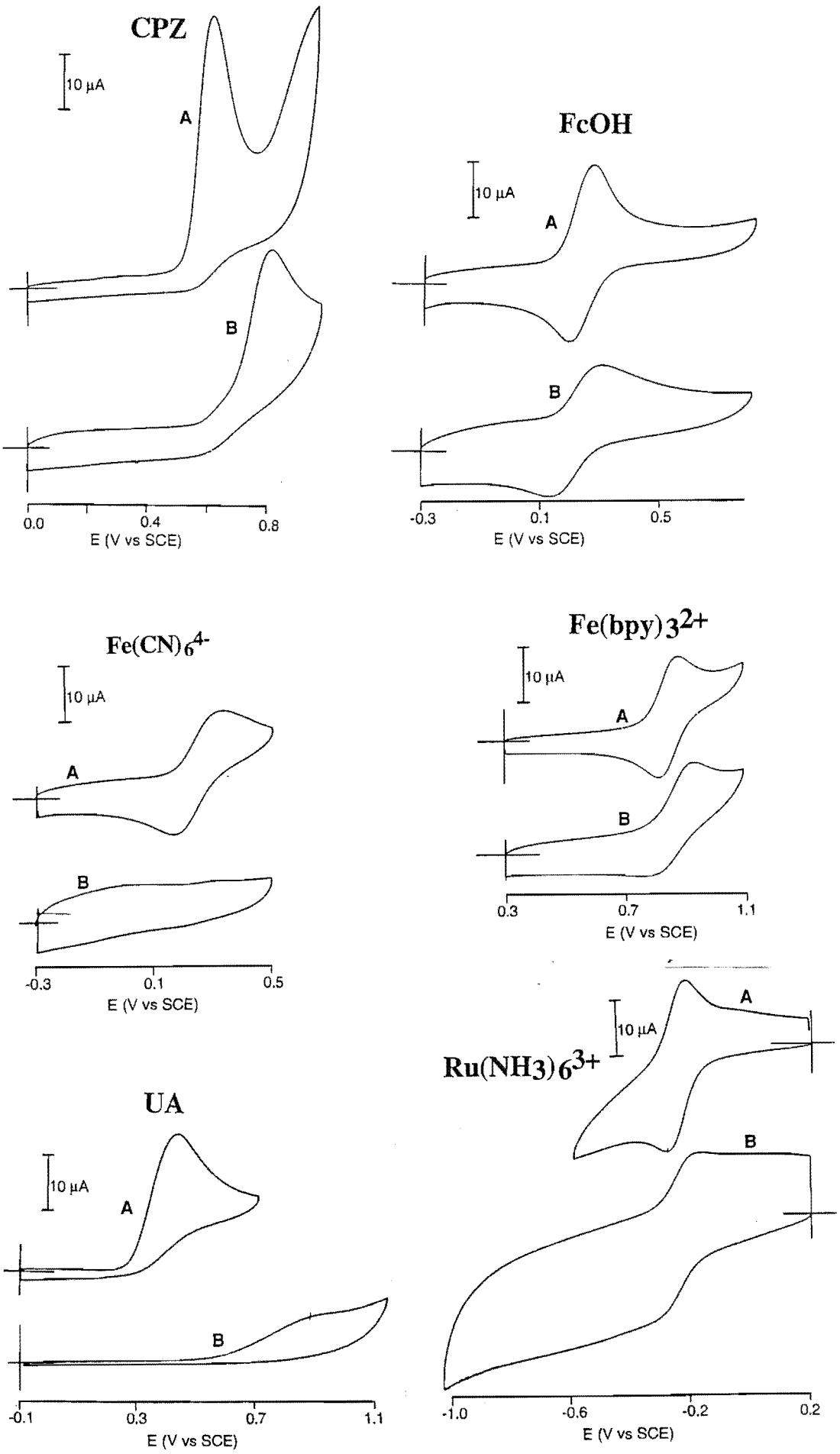

Figure 5.2: Cyclic voltammograms of 1 mM analyte/0.5 M PB at the unmodified (A) and *p*-methylbenzene modified (B) electrode

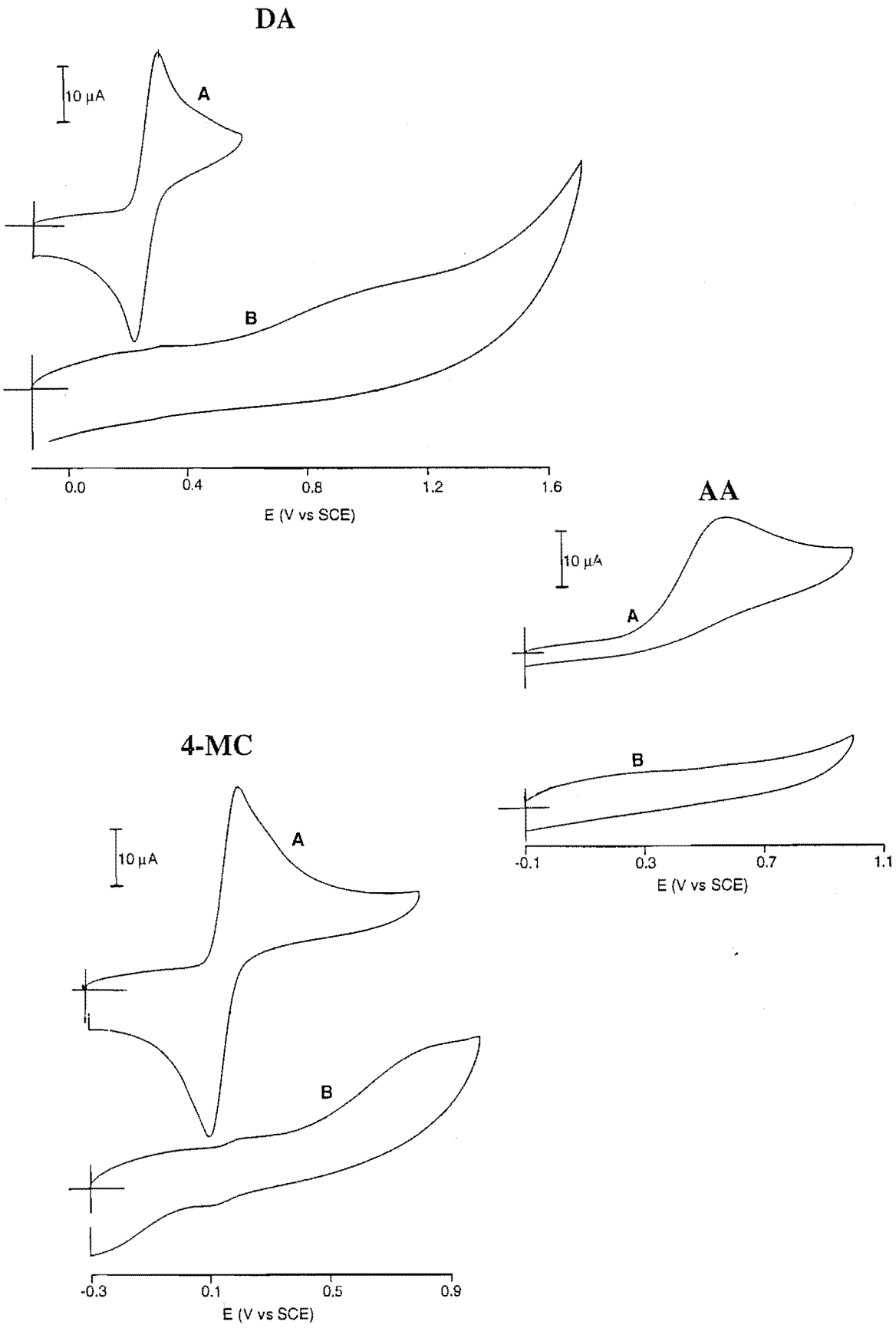

Large cationic hydrophobic analytes ($Fe(bpy)_3^{2+}$ and CPZ) and the hydrophilic cationic species (ruthenium hexaammine) gave the greatest response at the CME. Ferrocenemethanol, and to a lesser extent 4-MC, DA and UA, were also observed at the CME. The responses of AA and $Fe(CN)_6^{4-}$ were completely suppressed in CV experiments. For all species exhibiting chemically reversible behaviour at the unmodified electrode, ΔE_p increased markedly at the modified electrode; for chemically irreversible processes $E_{p,a}$ moved to more positive potentials. This can be ascribed to electron transfer occurring from a greater distance of closest approach, compared to that at an unmodified electrode, plus the additional effect of the resistance of the spacing layer (this resistance is assumed to be small). On the basis of bond lengths, and assuming that the modifier is aligned perpendicular to the electrode surface, the thickness of the *p*-methylbenzene modifying layer is expected to be < 0.7 nm.

The voltammogram of $Fe(bpy)_3^{2+}$ at the CME did not show the normal reduction peak observed at unmodified GC. Similarly, a changed voltammogram shape was observed for ruthenium hexaammine which also gave a less peaked response at the CME. Distorted voltammograms for species undergoing electron transfer at modified electrodes is often reported in the literature. Changes in cyclic voltammogram shape indicate that coating-analyte interactions are influencing the response although the nature of these interactions is generally not understood. These film-analyte interactions may be important only when the reacting species is in a certain oxidation state (i.e. has a particular charge or conformation) hence influencing the response as the reaction proceeds in one direction but not the other. Further, a change in the mode of reactant diffusion as a result of electrode modification may alter voltammogram shapes. To investigate this possibilty, voltammograms for oxidation of $Fe(bpy)_3^{2+}$ were recorded at scan rates between ν = 10 – 1000 mV s^{-1}. The resulting graph (Figure 5.3) shows a linear dependence of $i_{p,a}$ on $\nu^{1/2}$ at slow scan rates whilst at $\nu \geq 100$ mV s^{-1} the peak current of $Fe(bpy)_3^{2+}$ is less than that expected for a linear diffusion controlled response. The decreased slope at fast scan rates may be due to the resistive effect of the non-conducting coating becoming increasingly important.

Figure 5.3: Variation in the peak current for oxidation of $Fe(bpy)_3^{2+}$ with scan rate ($\nu^{1/2}$) at the *p*-methylbenzene CME

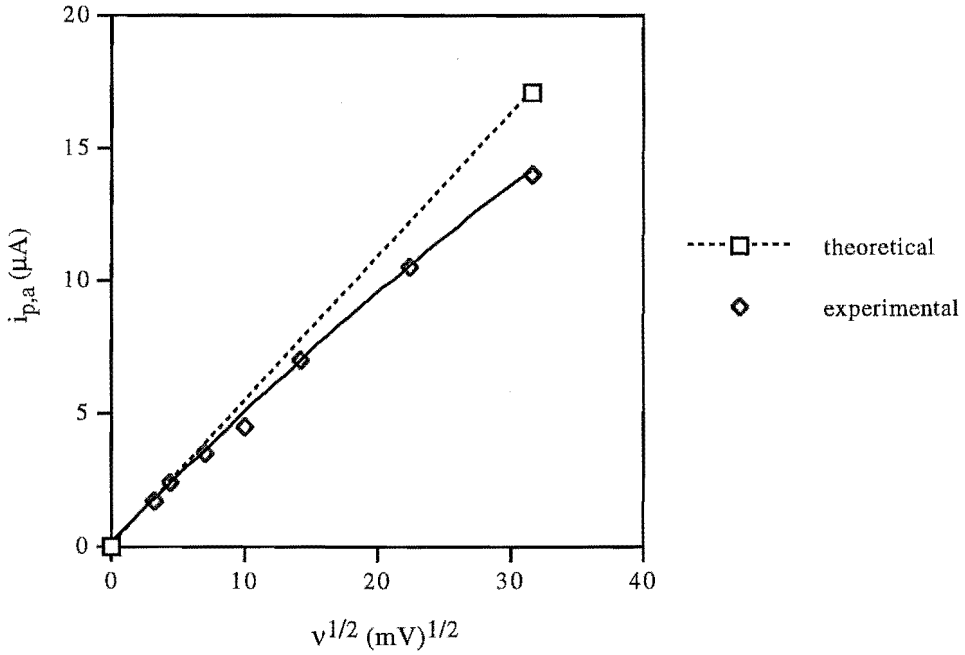

At the unmodified electrode, the current for CPZ oxidation is 2–3 times larger than expected for a one-electron oxidation and the peak is very sharp. These observations are consistent with reactant adsorption. The peak current of CPZ decreases after electrode modification suggesting a decrease in adsorbed material. The positive shift in $E_{p,a}$ at the CME may be due to a change from adsorption to diffusion control of the response in addition to the resistive effect of electron transfer over a distance. The voltammogram for FcOH was similar to that obtained at unmodified GC, although it became less electrochemically reversible. Dopamine and 4-MC showed two oxidation peaks at the modified electrode the first of which occurred near $E^{o'}$ and the second at more positive potentials. Uric acid was observed at the CME but the response was markedly decreased and shifted positive.

Selectivity of response at the p-methylbenzene CME. The magnitude of the ratio of cyclic voltammetric peak currents at modified and unmodified electrodes, ($i_{p(m)}/i_{p(u)}$), can be used to assess the selectivity of the CMEs. The controlling factor for selectivity of response at the *p*-methylbenzene modified electrode appears to be the nature of the electron transfer step; hydrophobicity of the analyte also has an effect. Thus $Fe(bpy)_3^{2+}$, ruthenium hexaammine, FcOH and CPZ all undergo uncomplicated single electron transfers and exhibit relatively unperturbed responses at the CME. The larger value of $i_{p(m)}/i_{p(u)}$ for $Fe(bpy)_3^{2+}$ compared to ruthenium hexaammine however, suggests that the more hydrophobic analyte interacts more favourably at the CME. In contrast, the response of $Fe(CN)_6^{4-}$, AA, UA, DA and 4-MC, which undergo complex electron transfer reactions, were suppressed dramatically at the CME. This may be due to blocking of specific interactions between analyte and the electrode surface. The observation that the oxidation of $Fe(CN)_6^{4-}$ was also suppressed indicates that discrimination at the CME is not simply confined to proton-coupled electron transfer reactions.

Cyclic voltammetry at the densely coated p-decylbenzene CME. Electrodes modified with longer alkylbenzene chains gave decreased background currents and were more resistive than *p*-methylbenzene CMEs. Cyclic voltammograms of probe analytes were recorded immediately after placing the CME in solution and again following 5 min stirring. Electrochemical data obtained from the 5 min stirred voltammogram are shown in Table 5.2. A control experiment was performed (as described previously) using the response of ferrocyanide to indicate change in electrode behaviour arising from adsorbed diazonium salt. The $i_{p,a}$ of ferrocyanide decreased to 64% of its value prior to exposure to the modifying solution, ΔE_p increased by 210 mV and $E_{p,a}$ shifted 120 mV positive. Hence, as may be expected due to its hydrophobic nature, the *p*-decylbenzene diazonium salt adsorbs at the GC electrode. This effect alone, however, does not cause the behaviour observed at the CME.

Table 5.2: Cyclic voltammetry of 1 mM analyte/0.5 M PB at unmodified and *p*-decylbenzene modified electrodes recorded at $\nu = 100$ mV s^{-1}

	UNMODIFIED			MODIFIED			
analyte	$i_{p,a}$ (μA)	$E_{p,a}$ (V)[a]	ΔE_p (mV)	$i_{p,a}$ (μA)	$E_{p,a}$ (V)	ΔE_p (mV)	$i_{p(m)}/i_{p(u)}$
4-MC	29.0	0.19	80	1.45	0.18	—	0.05
$Fe(CN)_6^{4-}$	10.0	0.26	100	no signal	—	—	0.0
$Fe(bpy)_3^{2+}$	11.5	0.88	65	2.5	0.93	130	0.22
CPZ	33.0	0.64	—	17.1	1.14	—	0.52
FcOH	16.0	0.26	60	3.0 + 3.0	0.34 + 0.70	155[b]	0.19 + 0.19
$Ru(NH_3)_6^{3+}$	$i_{p,c}$ 17.0	$E_{p,c}$ -0.29	65	$i_{p,c}$ 2.04	$E_{p,c}$ -0.50	350	0.12

[a] V vs SCE [b] ΔE_p^1 for the first oxidation

Selectivity at the p-decylbenzene CME. The selectivity of response at this CME is assumed to be governed by the same considerations as discussed for the *p*-methylbenzene modified electrode, namely simplicity of electron transfer reaction and hydrophobicity of the probe species. When the probe analyte is restricted to the outside of the film, the non-conducting spacer layer imposes a significant distance over which electron transfer must occur. Hence, probes which partition into the layer may show a significantly enhanced response, relative to those unable to penetrate the layer. Thus, based on ΔE_p values, it may be deduced that $Fe(bpy)_3^{2+}$, CPZ and FcOH readily partition into the film whereas ruthenium hexaammine does not.

The $i_{p(m)}/i_{p(u)}$ of CPZ was least affected by modification with long *p*-alkylbenzene moieties. This analyte is known to effectively partition into and diffuse through hydrophobic films[65] and was the only probe to show a significant increase in current after 5 min stirring. A large positive shift in $E_{p,a}$ was observed at the CME, presumably due to decreased adsorption and resistive effects.

Two oxidations were observed for FcOH. The first occurred near $E_{p,a}$ for the unmodified electrode, and the second at more positive potentials. These separate responses are described in more detail in the following section. The total current arising from FcOH oxidation (i.e. the sum of the two responses) resulted in an $i_{p(m)}/i_{p(u)}$ value which was greater than that of $Fe(bpy)_3^{2+}$. This contrasts with observations at *p*-methylbenzene modified electrodes at which $Fe(bpy)_3^{2+}$ gave the greatest response. Both the larger size and positive charge of $Fe(bpy)_3^{2+}$ may contribute to its decreased response.

Only one oxidation (near $E_{p,a}$ observed at unmodified GC) was observed for 4-MC. The response was similar in magnitude to the corresponding signal at the *p*-methylbenzene CME. Hence, 4-MC may permeate through the coating, but can only react at sites on the electrode which are not blocked by modifying groups.

Ferrocyanide oxidation was not observed at the modified electrode. Cyclic voltammograms recorded over the entire accessible potential range, in the presence and absence of ferrocyanide, gave no detectable response to this analyte. This is consistent with the inability of this hydrophilic species to penetrate the surface film, or the lack of across-film electron transfer by the blocking of electrode surface-probe interactions.

Investigation of the origin of the two FcOH oxidations at the CME. To obtain further information about the origin of the two separate oxidations observed for FcOH at the *p*-decylbenzene CME, the effect of temperature and scan rate on response was investigated.

The cyclic voltammetric response of FcOH at unmodified GC was not very temperature dependent between 5 and 65 °C. The density and coherence of the electrode coating, however, may change with temperature. Hence changes in peak current arising from temperature variation must indicate a dependence on the electrode coating. A dense coating was applied to the electrode (5 mM diazonium salt, 10 min electrolysis) and cyclic voltammograms were recorded at ν = 100, 500 and 1000 mV s^{-1} at temperatures of 5, 21 and 45°C. The resulting electrochemical data are shown in Table 5.3.

Table 5.3: Temperature and scan rate dependence of the 1st and 2nd oxidation peak of FcOH (1 mM/0.5 M PB) at the *p*-decylbenzene CME

ν (mV s^{-1})	temperature (°C)	$E_{p,a}{}^1$ (V)	$E_{p,a}{}^2$ (V)	$i_{p,a}{}^1$ (μA)	$i_{p,a}{}^2$ (μA)
100	5	0.31	0.86	2.6	0.6
	21	0.29	0.80	1.5	1.6
	45	0.27	0.65	1.3	4.0
500	5	0.42	0.97	3.2	a
	21	0.33	0.92	2.4	2.4
	45	0.32	0.77	2.0	9.8
1000	5	0.43	a	3.5	a
	21	0.34	a	3.6	a
	45	0.32	0.83	2.8	12.8

[a] not measurable

The peak current for the first FcOH oxidation, $i_{p,a}{}^1$, was independent of temperature and showed a weak dependence on scan rate (i.e. less than $\nu^{1/2}$). In contrast, $i_{p,a}{}^2$ was strongly dependent on temperature (see Figure 5.4) and showed proportionality to $\nu^{1/2}$ giving ($r^2 = 0.996$) for the line of best fit for results obtained at 45 °C. Hence, the first oxidation appears to be controlled by a combination of linear ($i_p \propto \nu^{1/2}$) and radial diffusion (i_p independent of ν) consistent with electron transfer occurring at pinholes in the film. Most likely there is a range of pinhole sizes. Radial diffusion may occur at small holes and linear diffusion at larger uncoated regions. The second oxidition is assigned to analyte which has partitioned (i.e. dissolved) into the film and undergoes electron transfer in a resisitive environment. Hence, temperature dependence may arise from a change in diffusion coefficient within the film and/or increased resistance in the coating due to variation in the "compactness" of the modifying layer with temperature.

Figure 5.4: Cyclic voltammetric response of 1 mM FcOH recorded at $\nu = 100$ mV s^{-1} at temperatures of 5 (A), 21 (B) and 45 °C (C)

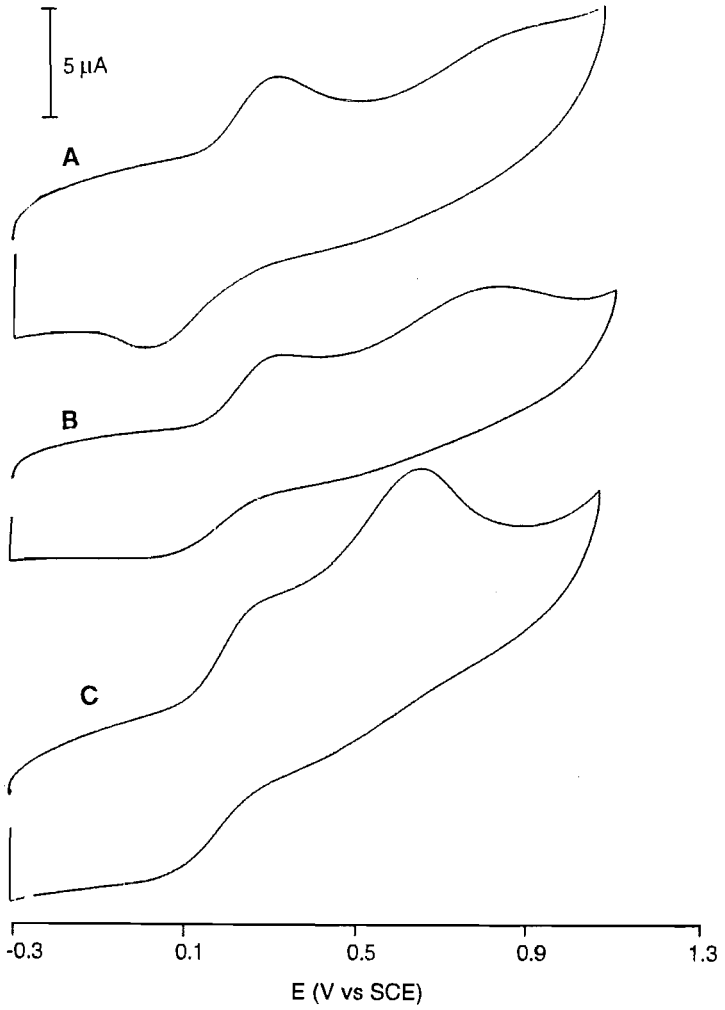

5.3.3 Analytical utility of *p*-alkylbenzene CMEs

Cyclic voltammetry is a useful technique for gaining information about electrode processes but pulse techniques are more appropriate for analytical applications. In this section, normal pulse and differential pulse voltammetry are used to assess the analytical utility of CMEs.

Normal pulse voltammetry at densely coated p-methylbenzene CMEs. A densely coated CME was prepared using the standard procedure. The electrochemical data for probe analytes at 1 mM are given in Table 5.4 and some normal pulse voltammograms are shown in Figure 5.5.

Table 5.4: Normal pulse voltammetric response of 1 mM analytes/0.5 M PB at unmodified and *p*-methylbenzene modified electrodes[a]

	UNMODIFIED			MODIFIED			
analyte	$i_{l\,(u)}$ (μA)	$E_{1/2}$ (V)[a]	$E_{3/4} - E_{1/4}$ (mV)	$i_{l\,(m)}$ (μA)	$E_{1/2}$ (V)[a]	$E_{3/4} - E_{1/4}$ (mV)	$i_{l\,(m)}/i_{l\,(u)}$
4-MC	90.0	0.20	65	35.0	0.83	180	0.39
DA	70.0	0.30	120	no signal	—	—	0.0
$Fe(CN)_6^{4-}$	45.0	0.28	80	no signal	—	—	0.0
$Fe(bpy)_3^{2+}$	30.0	0.85	60	30.0	0.90	80	1.0
CPZ	60.0	0.61	50	60.0	0.84	90	1.0
AA	40.0	0.36	150	no signal	—	—	0.0
FcOH	41.0	0.23	60	35.0	0.21	120	0.85
$Ru(NH_3)_6^{3+}$	34.0	-0.27	60	14.0	-0.27	60	0.41

[a] pulse amplitude = 25 mV, pulse width = 57 ms and $\nu = 20$ mV s^{-1}

The ratio of limiting currents, $i_{l\,(m)}/i_{l\,(u)}$, shows similar trends to that observed for $i_{p(m)}/i_{p(u)}$ in CV experiments. Thus FcOH, CPZ and $Fe(bpy)_3^{2+}$ gave large plateau currents at the modified electrode. For CPZ, the voltammogram at the unmodified surface was peaked, most probably due to adsorption of reactant and/or oxidation products. A well-defined plateau is observed after modification. 4-MC was measurable at the CME and the $E_{1/2}$ of the resulting voltammogram was shifted 630 mV positive, compared to unmodified GC. Presumably, the response arises from the same process as gives rise to the second oxidation peak observed in CV. No signal for AA, DA or ferrocyanide was observed at the CME in the potential scan range of 0 to 1.5 V.

Figure 5.5: Normal pulse voltammograms of 1 mM analyte/0.5 M PB at unmodified (A) and *p*-methylbenzene modified (B) electrodes

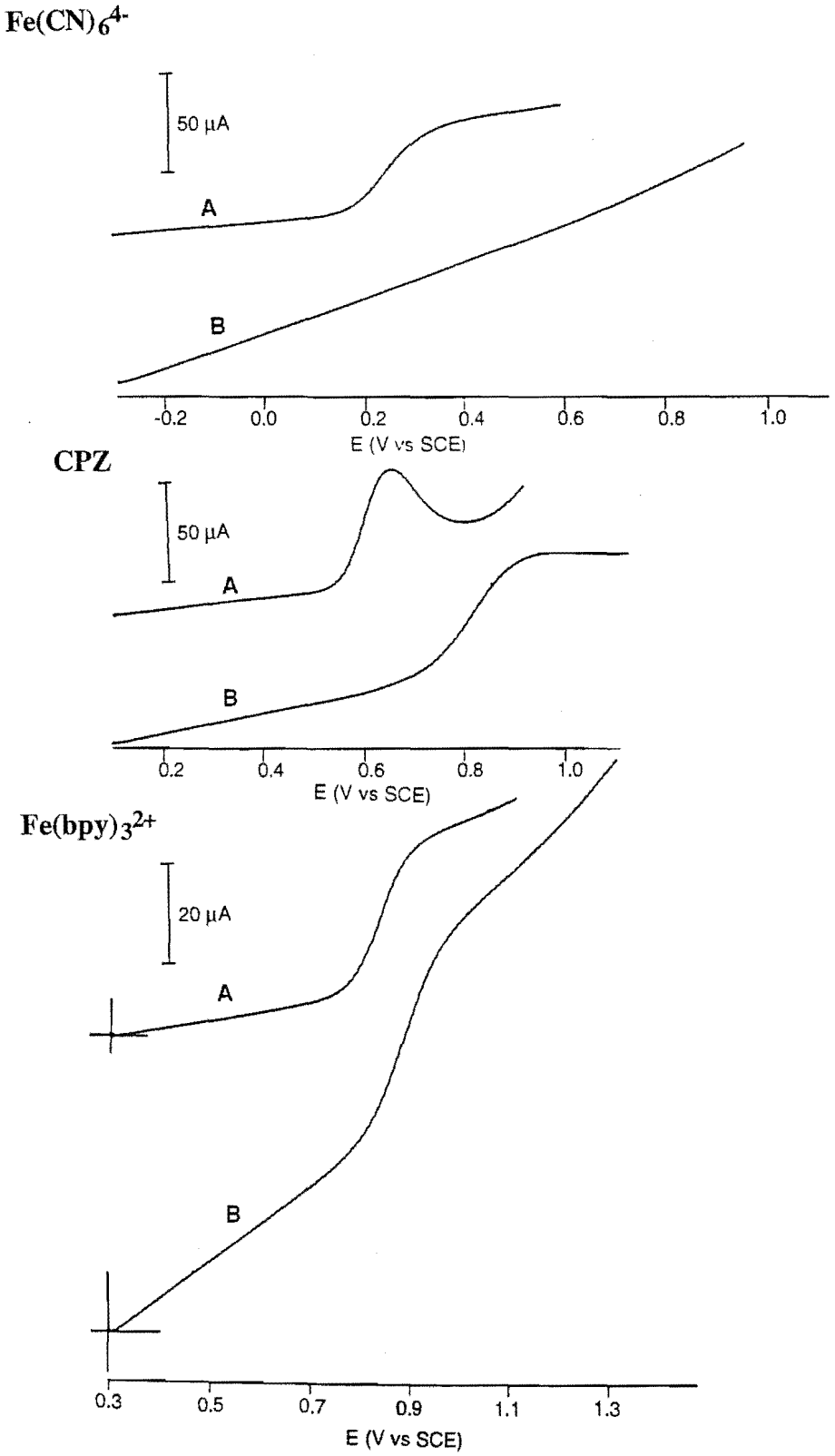

Figure 5.5: Normal pulse voltammograms of 1 mM analyte/0.5 M PB at unmodified (A) and *p*-methylbenzene modified (B) electrodes

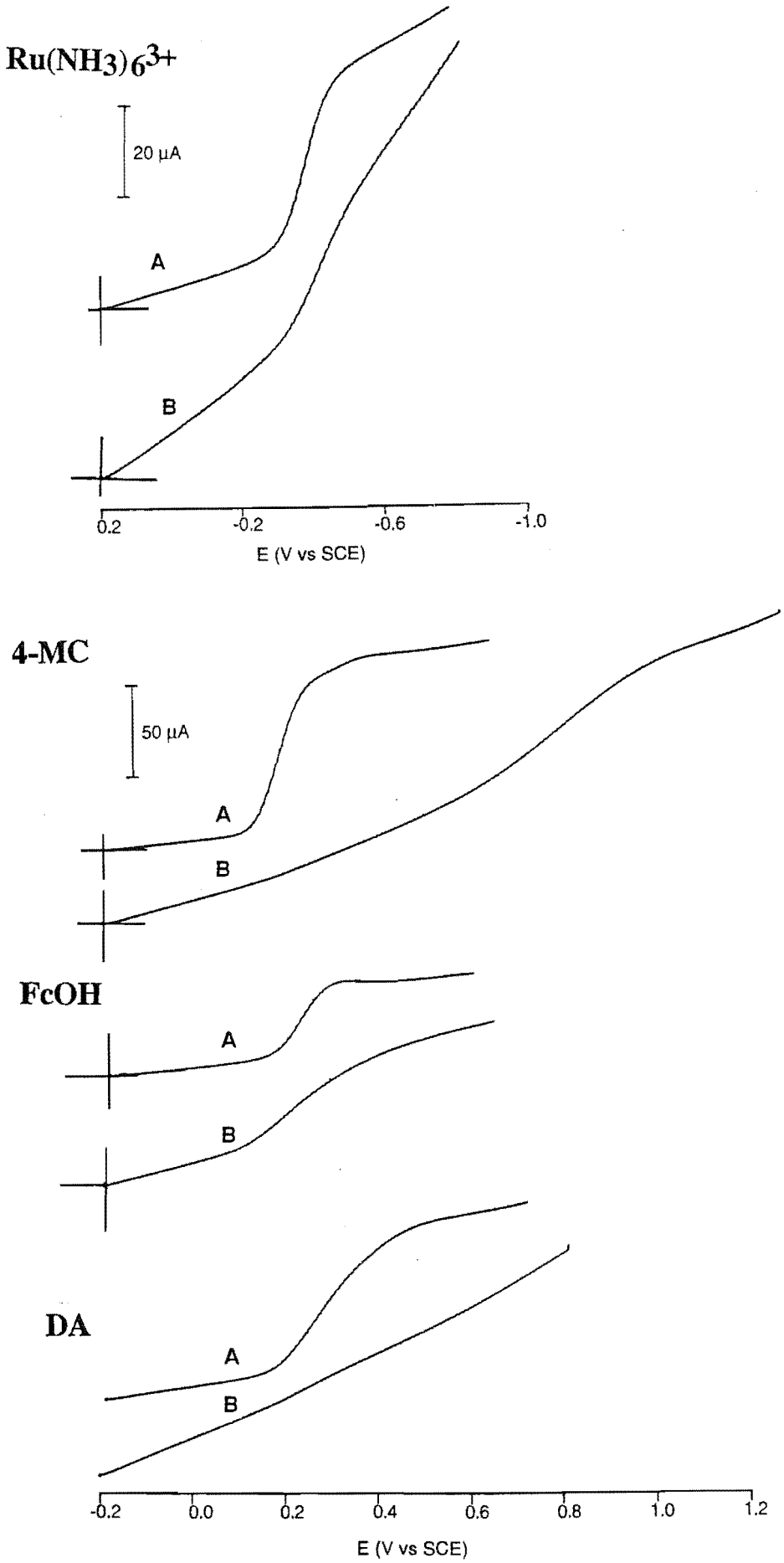

Differential pulse voltammetry at the densely coated p-methylbenzene CME. The electrochemical data arising from DPV of probe analytes at the densely coated *p*-methylbenzene CME are shown in Table 5.5. The largest $i_{p(m)}/i_{p(u)}$ value was obtained for $Fe(bpy)_3^{2+}$. Ruthenium hexaammine, FcOH and CPZ also gave readily discernible responses. The oxidations of 4-MC and DA were seen at the CME and a small peak was observed for ferrocyanide. Of the analytes examined, AA was the only species not detected at the CME when DPV was used. Chlorpromazine was the only analyte for which a significant shift in peak potential was observed.

Table 5.5: Differential pulse voltammetry of 1 mM analyte/0.5 M PB at unmodified and *p*-methylbenzene modified electrodes[a]

	UNMODIFIED		MODIFIED		
analyte	$i_{p,a(u)}$ (μA)	$E_{p,a(u)}$ (μA)	$i_{p,a(m)}$ (μA)	$E_{p,a(m)}$ (μA)	$i_{p(m)}/i_{p(u)}$
4-MC	6.9	0.18	1.25	0.18	0.18
DA	7.4	0.19	0.9	0.21	0.12
$Fe(CN)_6^{4-}$	4.9	0.25	0.25	0.26	0.005
$Fe(bpy)_3^{2+}$	6.4	0.83	3.4	0.87	0.53
CPZ	9.6	0.58	2.8	0.71	0.29
AA	1.4	0.28	no signal	—	—
FcOH	9.2	0.22	3.4	0.23	0.37
$Ru(NH_3)_6^{3+}$	9.0	-0.29	3.8	-0.29	0.42

[a] pulse amplitude = 25 mV, pulse width = 57 ms and $\nu = 5$ mV s^{-1}

Clearly, the choice of electrochemical technique affects the relative responses of probe analytes. A summary of the current ratios for various analytes obtained using CV, NPV and DPV at the same CME preparation is presented in Table 5.6. Of these techniques, DPV is generally the choice for analytical applications due to its sensitivity and peak shaped output. However, increased discrimination between analytes was obtained using NPV.

Table 5.6: Summary of the current ratios obtained at *p*-methylbenzene modified and unmodified electrodes using different electrochemical techniques

analyte	CV	NPV	DPV
	$i_{p(m)}/i_{p(u)}$	$i_{l(m)}/i_{l(u)}$	$i_{p(m)}/i_{p(u)}$
4-MC	0.11[a]	0.39	0.18
DA	0.07[a]	0.0	0.12
$Fe(CN)_6^{4-}$	0.0	0.0	0.005
$Fe(bpy)_3^{2+}$	0.94	1.0	0.53
CPZ	0.61	1.0	0.29
AA	0.0	0.0	0.0
FcOH	0.50	0.85	0.37
$Ru(NH_3)_6^{3+}$	0.59	0.41	0.42

[a] ratio of current for the second oxidation

Normal pulse voltammetry at the densely coated p-decylbenzene CME.

The response of probe analytes (0.5 mM/0.5 M PB) using NPV at a densely coated *p*-decylbenzene CME are summarised in Table 5.7.

Table 5.7: Normal pulse voltammetric data of 0.5 mM analyte/0.5 M PB at unmodified and densely coated *p*-decylbenzene modified electrodes

	UNMODIFIED			MODIFIED			
analyte	$i_{l\,(u)}$ (μA)	$E_{1/2}$ (V)	$E_{3/4} - E_{1/4}$ (mV)	$i_{l\,(m)}$ (μA)	$E_{1/2}$ (V)	$E_{3/4} - E_{1/4}$ (mV)	$i_{l\,(m)}/i_{l(u)}$
4-MC	34.5	0.29	90	4	0.23	40	0.12
catechol	39.3	0.39	105	2.8	0.30	45	0.07
$Fe(bpy)_3^{2+}$	13.6	0.83	60	1.2	0.91	a	0.09
CPZ	22.0	0.61	35	5.9	0.69	40	0.27
DASA	8.0	0.43	30	0.7	0.49	a	0.09
FcOH	17.8	0.21	50	1.2	0.24	a	0.07

[a] values can not be accurately measured

The ratios of plateau currents, $i_{l\,(m)}/i_{l(u)}$, decreased (relative to those at the *p*-methylbenzene modified electrode) for all analytes observed at this CME. For 4-MC and catechol, $E_{1/2}$ is decreased and voltammograms appear more electrochemically reversible. These responses are thought to arise from analyte which is undergoing electron transfer at uncoated regions of the electrode surface. Other analytes show positive shifts in $E_{1/2}$ of 30 – 80 mV and it is presumed that these species partition into the coating and react in the more resisitive environment. The response of CPZ is increased relative to all other probe analytes which dissolve into the coating (rather than accessing a hole in the film) indicating that the hydrophobic conditions favour partitioning of this species.

Normal pulse voltammetric response of probe analytes at p-methylbenzene and p-decylbenzene CMEs of varying density. The effect of changing modifier density on the response of analytes was examined using NPV. The density of surface modifying groups was controlled by changing the concentration of diazonium salt solutions and by varying electrolysis times. The resulting $i_{l(m)}/i_{l(u)}$ values at each modified surface, for a series of probe analytes at *p*-methylbenzene and *p*-decylbenzene CMEs, are summarised in Figure 5.6 and 5.7 respectively.

Figure 5.6: Plateau current ratios in NP voltammetric experiments for probe analytes at *p*-methylbenzene CMEs of varying density

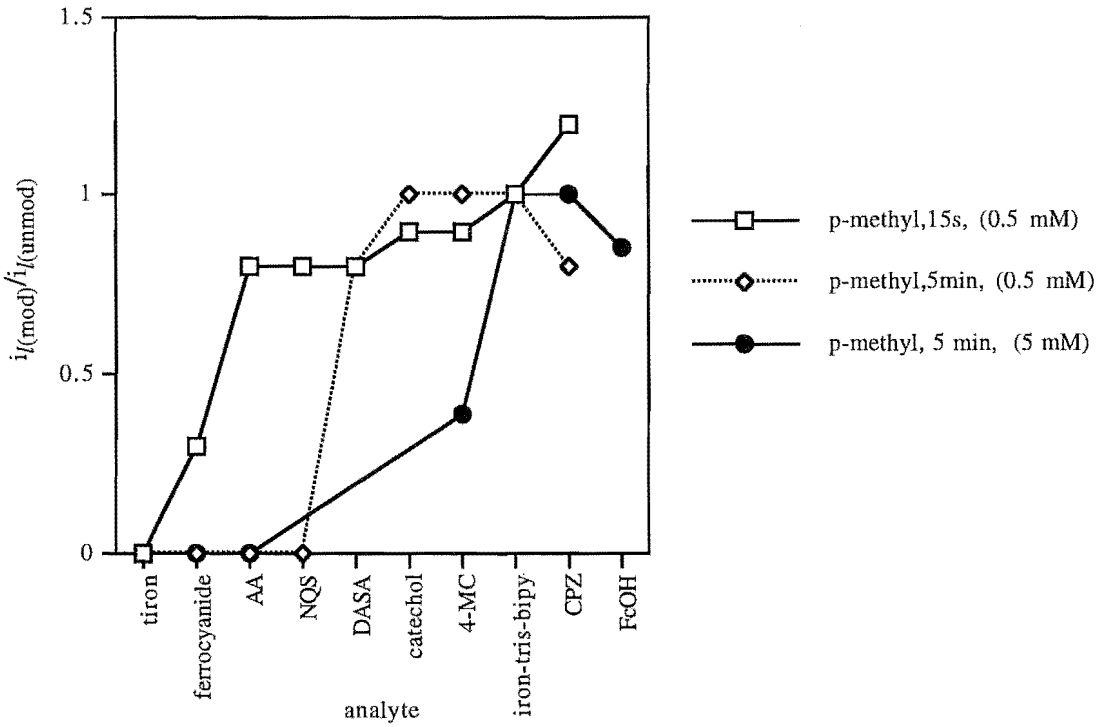

Figure 5.7: Plateau current ratios in NP voltammetric experiments for probe analytes at *p*-decylbenzene CMEs of varying density

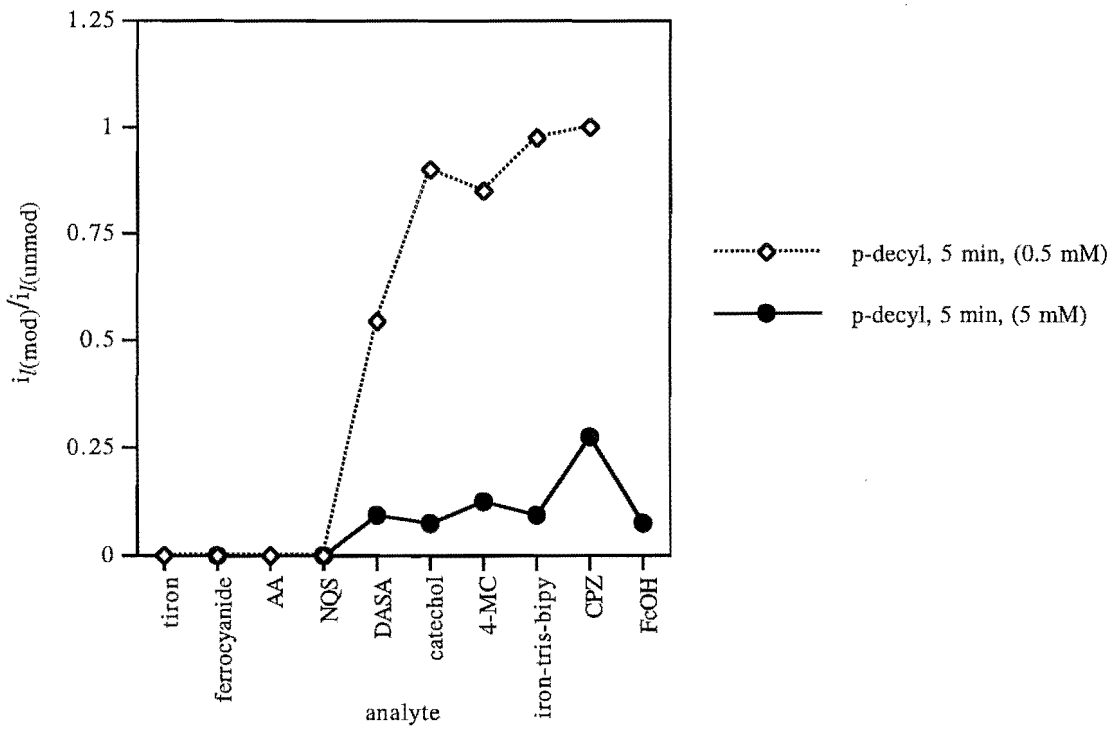

At the CME prepared by the shortest treatment procedure i.e. *p*-methylbenzene with 15 s electrolysis in 0.5 mM diazonium salt solution, most analytes gave $i_{l(m)}$ similar to the unmodified electrode. The exceptions are tiron, which was completely suppressed and ferrocyanide which had a $i_{l(m)}/i_{l(u)}$ value of 0.3. Modified electrodes prepared by 5 min electrolysis in 0.5 mM *p*-methylbenzene or *p*-decylbenzene diazonium salt solutions showed similar response to all analytes; both excluded AA, ferrocyanide and tiron. Increasing the concentration of diazonium salt solution affected the sensitivity of the *p*-decylbenzene CME to a greater extent than the *p*-methylbenzene CME. This is not surprising considering that a dense blocking film which is thick is likely to have a greater effect on analyte behaviour than one which extends a short distance from the electrode surface.

Reproducibility of repeat CPZ measurements at the p-methylbenzene CME and regeneration of electrode performance. The *p*-methylbenzene CMEs prepared by 5 min electrolysis in 0.5 or 5 mM diazonium salt solution, and the *p*-decylbenzene CME prepared by 5 min electrolysis in 5 mM diazonium salt solution, show high sensitivity to CPZ and very low sensitivity to AA. Thus the CMEs might be useful for determining phenothiazine drugs in the presence of high concentrations of AA and UA (e.g. in urine). In addition to selectivity, reproducibility and linearity of electrode response are important for practical applications. Preliminary experiments were undertaken to investigate these features of the CME.

Repeat cyclic voltammograms of 1 mM CPZ were recorded at the densely coated *p*-methylbenzene CME. The first voltammogram was obtained without stirring in the CPZ solution and 30 s stirring was used prior to the next scan. An increase in $i_{p,a}$ from 9.0 μA to 11.5 μA was observed. This indicates that either the coating was not at equilibrium at the time of the first scan, or that time-dependent adsorption was occurring. Longer stirring times (5 min) did not increase $i_{p,a}$. To determine reproducibility, 30 s stirring was used between voltammograms. An RSD for $i_{p,a}$ of 7% (n = 15) was obtained. Over the 15 repeat voltammograms $i_{p,a}$ deceased from 11.5 to 8.75 μA, and $E_{p,a}$ shifted from 0.86 to 0.94 V vs SCE.

Although the CME was still responding to CPZ, the cyclic voltammetric response of $Fe(bpy)_3^{2+}$ and ruthenium hexaammine were completely suppressed, possibly due to blocking of the electrode by CPZ oxidation products. The regeneration of $Fe(bpy)_3^{2+}$ response was examined at this surface. A simple protocol of 5 min sonication in acetone completely restored the electrode response to $Fe(bpy)_3^{2+}$ whilst maintaining discrimination against ferrocyanide.

Calibration curve for CPZ at the p-methylbenzene CME. In order to establish that the electrode equilibrates with the analyte in the bulk solution, even after repeat use, a calibration curve was obtained at a densely coated *p*-methylbenzene modified electrode using NPV. Chlorpromazine concentrations between 0.05 and 1 mM were measured in 0.5 M PB. The CME was sonicated in acetone for 30 s and stirred in the CPZ solution for 1 min prior to each NP voltammogram. The line of best fit through the experimental data points gave an r^2 coefficient of 0.996 (see Figure 5.8). Repeat voltammograms in 0.1 mM CPZ gave an RSD of 4.9% (n = 6).

Figure 5.8: Normal pulse voltammetric calibration curve for CPZ at the *p*-methylbenzene modified electrode

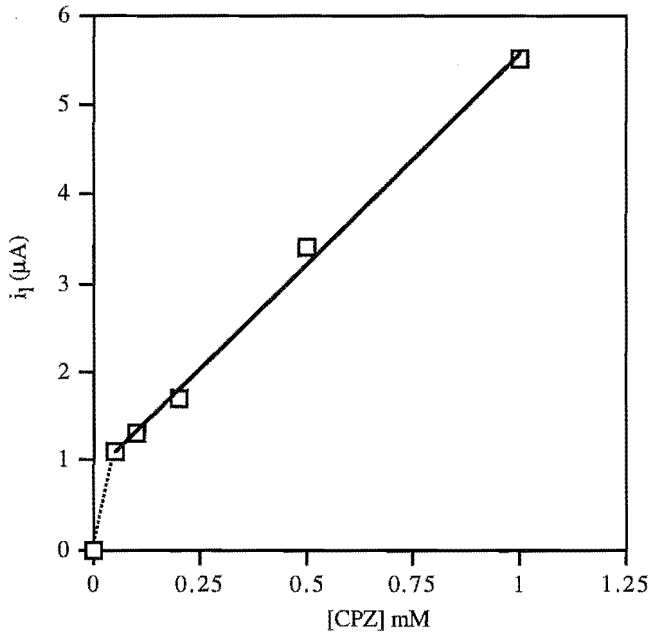

At the lowest concentration measured in the experiment (0.05 mM), the CPZ response at the CME was sigmoidal and well-defined compared to that at the unmodified electrode where the voltammogram was peaked. A line of greater slope was obtained when the amount of CPZ in solution was low, suggesting that somewhere in the region between 0 and 0.05 mM CPZ, the response switched from an adsorption controlled, to a diffusion controlled process[56].

Reproducibility of CMEs prepared with short modification times. To investigate the reproducibility of preparing *p*-methylbenzene CMEs, when short modification times were applied, the cyclic voltammetric response of 0.5 mM 4-MC in 0.5 M PB was recorded at three separate electrode preparations. An electrolysis time of 30 s and a diazonium salt concentration of 0.5 mM were used.

At the unmodified electrode, 4-MC gave $i_{p,a}$ = 7.0 μA, $E_{p,a}$ = 0.31 V vs SCE and ΔE_p = 300 mV. Two oxidations were present at the CME the first of which was coupled to a reduction. The RSD (n = 3) for the peak current of the initial oxidation was 22% and that of the second oxidation was 42%.

Reproducibility of dense electrode coatings. The reproducibility of electrode coatings was investigated at *p*-butylbenzene CMEs. The usual modification procedure to make dense coatings was used. The cyclic voltammetric response of 1 mM FcOH was recorded at 5 different electrode preparations. Scans were made in triplicate with initial stirring times of 3 min followed by stirring for ca. 10 s between subsequent voltammograms. Ferrocenemethanol showed two separate responses as observed at the *p*-decylbenzene CME. Averaged data for the anodic processes are reported in Table 5.8.

Table 5.8: Electrochemical data for 1 mM FcOH/0.5 M PB for different *p*-butylbenzene CME preparations recorded at $\nu = 100$ mV s^{-1}

electrode number	$E_{p,a}{}^1$ (V vs SCE)	$E_{p,a}{}^2$ (V)	$i_{p,a}{}^1$ (μA)	$i_{p,a}{}^2$ (μA)
1	0.26	0.73	0.93	3.73
2	0.30	0.74	0.87	4.27
3	0.31	0.78	1.27	2.80
4	0.29	0.73	1.07	3.33
5	0.28	0.83	1.00	2.30
unmodified	0.23		17.2	

Relative standard deviations (n = 5) of 15% and 23% were obtained for the peak currents $i_{p,a}{}^1$ and $i_{p,a}{}^2$ respectively, at different CME preparations. A 50 mV range in $E_{p,a}{}^1$ was observed whilst $E_{p,a}{}^2$ varied by 100 mV.

5.4 Discussion

5.4.1 Characterisation of *p*-alkylbenzene CMEs

The aim of this work was to prepare hydrophobic CMEs by grafting *p*-alkylbenzene substituted moieties onto GC surfaces using the diazonium salt procedure. The covalent attachment was expected to provide a highly stable surface and it was anticipated that the hydrophobic modifier would create a coating with selective permeability to hydrophobic species. Although the results described above show that the hydrophobicity of the modifier does not appear to be the major factor controlling the electrode response, the CMEs are of interest for two reasons. Firstly, the nature of the analyte-CME interactions giving rise to the observed response are of fundamental interest and secondly, the selectivity of the CMEs appears to be analytically useful.

Unlike CMEs prepared by other workers using self-assembly of alkanethiols on Au, modification with *p*-alkylbenzene moieties did not give highly resistive monolayers. This is not surprising considering the comparative roughness of the GC surface prior to modification (in contrast to the very smooth Au substrates prepared to promote uniform self-assembled monolayers[49]). Therefore, an electrode surface which has some regions of modifiers oriented at varying angles, other areas of aligned groups, and some unmodified regions, may be an appropriate model for the CME.

Despite the apparent "openness" of the modification, selectivity of response was observed at these CMEs. It is proposed that the major factor governing selectivity is the same for both *p*-methylbenzene and *p*-decylbenzene CMEs i.e. discrimination of analytes with simple electron transfer reactions over those which have complex mechanisms. Analyte hydrophobicity has less influence on selectivity but still remains a minor controlling factor and becomes more important at the *p*-decylbenzene CMEs. *Para*-butylbenzene CMEs showed behaviour similar to *p*-decylbenzene modified electrodes. The proposed origin of electrochemical response for the probe analytes used in this study is shown diagramatically in Figure 5.9 and explained below the figure.

Figure 5.9: Diagram of the proposed origins of electrochemical response at *p*-methylbenzene and *p*-decylbenzene CMEs

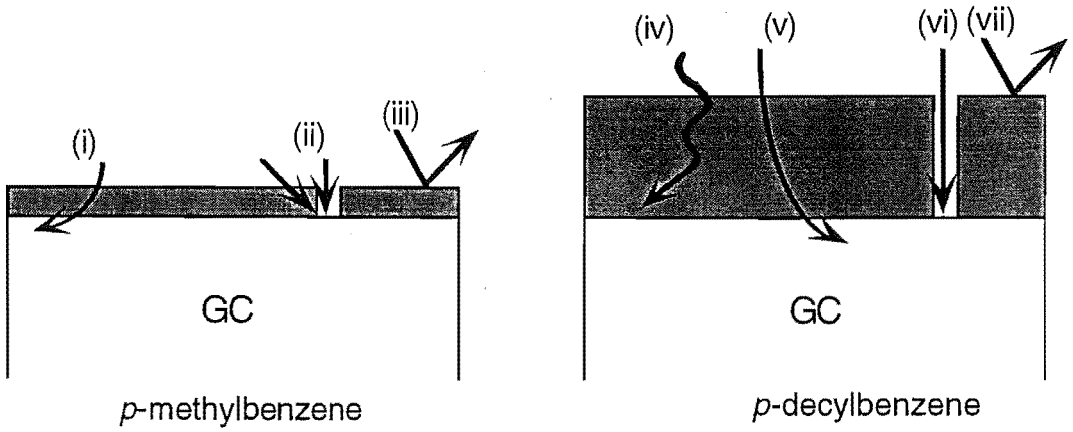

(i) Electron transfer across an ultra-thin spacing layer (< 0.7 nm) at the electrode surface. This is the main mechanism of electron transfer for probes which do not need specific interactions with the electrode surface. Increasing the distance of closest approach results in an observed decrease in electron transfer kinetics. Additionally there may be a small influence due to the resistance of the coating. Probe species which are proposed to react via this process are: FcOH, CPZ, $Fe(bpy)_3^{2+}$ and ruthenium hexaammine.

(ii) Electron transfer at bare regions of the electrode i.e. at pinholes in the coating. This is the assumed source of response for small, hydrophobic analytes which undergo complex, proton coupled electron transfer reactions e.g. 4-MC, DA and catechol. Pinholes are selective for hydrophobic species, thus AA and ferrocyanide are not observed. Other hydrophobic probes discussed in (i) above may also use this mode of transfer and the extent to which this occurs depends on the size and density of pinholes i.e, will vary for different CME preparations.

(iii) No observed response at the CME for analytes which have unfavourable interactions with the coating and are required to undergo mediated electron transfer reactions at the underlying electrode (AA, ferrocyanide).

(iv) Electron transfer from hydrophobic analytes that can dissolve into the coating. Responses are indicative of a resistive environment (relative to the unmodified electrode). Analytes reacting in this way are: CPZ, $Fe(bpy)_3^{2+}$ and FcOH.

(v) Electron transfer from a long distance over a spacing layer for analytes which do not need mediated transfer and cannot partition into the coating i.e. ruthenium hexaammine.

(vi) Diffusion through pinholes in the coating. This mode of electron transfer is assumed to be responsible for the small 4-MC signal and the first oxidation of FcOH.

(vii) As for (iii) above.

5.4.2 Analytical utility

As noted in the introduction to this chapter, there is a need for CMEs which selectively measure hydrophobic analytes, without decreasing the observed electrode kinetics. It has been suggested that a non-resistive, hydrophobic monolayer is needed to achieve this[49]. Thin monolayers self-assembled on Au have been shown to be resistive and to decrease the response of the small hydrophobic analytes benzoquinone, DA and DOPAC. The *p*-methylbenzene CME examined in the present study is assumed to be "open" allowing solvent molecules and ions to permeate into the coating. The cyclic voltammetric responses of DA and 4-MC at the *p*-methylbenzene modified electrode, however, were suppressed (see Table 5.1). As discussed in the previous section, this behaviour is assumed to arise from blocking of specific analyte-electrode interactions which are involved in electron transfer reactions of these analytes at carbon surfaces. The large responses of hydrophobic species which undergo simple, outer-sphere electron transfer reactions at the *p*-methylbenzene CME ($Fe(bpy)_3^{2+}$, CPZ), demonstrates that the CME does meet the requirement for sensitive measurement of hydrophobic species (for a limited range of analytes).

The most important results relevant to use of the CMEs for analytical applications are those shown in Figures 5.6 and 5.7. Clearly, with the appropriate choice of coating, selective measurement of some analytes in the presence of biological interfering species is possible.

Probe analytes $Fe(bpy)_3^{2+}$, ruthenium hexaammine, FcOH and CPZ gave good response in CV experiments at the *p*-methylbenzene CME. The most analytically important result was the discrimination of CPZ over the biological interferent AA. Hence, at this CME the measurement of CPZ should be possible in the presence of biological interferents with complex electron transfer reactions (for example UA and AA). Repeat cyclic voltammograms of 1 mM CPZ gave an RSD for peak current of 7% (n =15) at the *p*-methylbenzene CME. Although the CME shows significant deactivation, the electrode performance was simply regenerated by sonication in acetone. Cleaning, presumably removes reaction products trapped in the coating or adsorbed on the underlying electrode surface.

Generally the best sensitivity to observed analytes (relative to the response at unmodified electrodes) was achieved using NPV. For the measurement of CPZ, modification gave the added advantage of changing the peaked response obtained at

unmodified GC to a more analytically useful sigmoidal curve. This may arise from decreased adsorption of CPZ at the CME (i.e. the peak comes from surface accumulated species) or may be a result of decreased fouling of the electrode by reaction products (i.e. a dip occurs due to electrode deactivation). Using NPV, the response of CPZ at the *p*-methylbenzene CME was shown to be linear between the concentrations examined (0.05 to 1 mM). Further investigation is needed at the lower concentration range.

Cyclic voltammetry at the *p*-decylbenzene CME also showed a marked preference for CPZ relative to other analytes. Therefore this electrode coating seems suited to flow injection analysis where, at a potential set sufficiently positive, it would be expected to give a large response compared to all other probes investigated in this study (see Table 5.2). Further, it is assumed that the relatively large response of CPZ would be observed for other phenothiazine derivatives of biological interest such as promethazine.

The reproducibility of the modified electrode surface, as measured by variation in peak currents of observable analytes, was generally poor i.e. at densely coated *p*-butylbenzene CMEs RSDs (n = 5) for $i_{p,a}{}^1$ and $i_{p,a}{}^2$ were ca. 20% and shorter electrolysis times gave less reproducible surfaces. This is indicative of coatings containing pinholes the size, density and spacing of which will vary from one preparation to the next. It is assumed that differences in the surface morphology of GC prior to modification affects the orientation and coverage of modifying groups and that there is a steric or surface cleanliness barrier to producing pinhole free coatings. However, the selectivity trends are consistent, although the exact magnitude analyte response may vary from one electrode to another.

5.5 Conclusions

Chemically modified electrodes prepared by coupling *p*-alkylbenzene moieties onto a GC electrode surface using the diazonium salt procedure selectively respond to analytes that undergo simple, unmediated electron transfer reactions. A preference for hydrophobic analytes relative to hydrophilic species is also observed. Electrodes modified with *p*-methylbenzene groups give good response to selected analytes even when fast timescale electrochemical techniques (i.e. CV) are used. *Para*-decylbenzene modified electrodes show a greater affinity for hydrophobic species relative to hydrophilic analytes. The CMEs discussed in this chapter appear useful for the measurement of phenothiazine drugs in the presence of biological interferents AA and UA.

Chapter Six: *Para*-phenylacetate and *para*-alkylbenzene CMEs as detectors in flowing solutions

6.1 Introduction

The development of strategies to extend the application of electrochemical detection in flow injection analysis (FIA) and high performance liquid chromatography (HPLC) is the subject of much ongoing research. Electrochemical detection has desirable features such as high sensitivity, low cost and fast sample throughput. However, the amperometric mode of detection commonly used in flow detectors is not selective with respect to analytes which can be oxidised or reduced at the applied potential[16]. When on-line chromatography (HPLC), masking, or removal of interferences in (FIA) is inefficient or experimentally difficult, selectivity at the detector may be improved by: (i) appropriate modification of the electrode by application of permselective films (with or without immobilisation of a biological sensing agent) (ii) application of films which produce variable retention times for different species and hence result in stretched solute zones at CMEs or (iii) fabrication of arrays of partially selective CMEs which allow multicomponent analysis by pattern recognition methods.

(i) Selectively permeable CMEs in FIA. Special requirements are placed on CMEs designed for use in FIA systems. Fast response times are desirable to achieve high sample throughput and increased demands are placed on coating stability in the vigorous hydrodynamic conditions. Charge and size discriminative properties of polymeric coatings such as cellulose acetate[26,27,39,40] and Nafion[40] have been successfully exploited in flow measurements. Using a hydrophobic lipid/cholesterol modified detector Wang et al[58] were able to measure chlorpromazine and promethazine whilst responses from ascorbic acid, uric acid and acetaminophen were suppressed. These coatings responded rapidly to partitioning analytes and yielded narrow peaks in FIA, indicating efficient "wash-out" of hydrophobic analytes. Self-assembled monolayers of *n*-alkanethiols on gold were also shown to be adequately stable for use as amperometric flow detectors[129]. Another dimension of selectivity has recently been attained by immobilisation of calixarenes on flow detectors[25]. Specific host-guest interactions between calixarenes and neurotransmitters dopamine and norepinephrine allowed good discrimination of these analytes over acetaminophen and anionic interferents. Analyte response was inversely proportional to flow-rate indicating that host-guest binding rate was the controlling factor.

(ii) Selectivity in FIA by induced retention times. A novel approach for enhancing selectivity in flow-injection systems, by inducing increased residence times for the target analyte at CMEs, has been described[130]. It is illustrated diagramatically in Figure 6.1. The sample is selectively dispersed as it passes over the CME resulting in a relatively broad signal. Different stretching profiles result for partitioning and non-partitioning analytes. Non-partitioning analytes give a response over a narrow time range whereas partitioning analytes contribute to the current at the tail of the peak. Thus appropriate choice of measuring time allows measurement of a partitioning analyte without interference from those which do not interact favourably with the coating. Using this protocol, the measurement of CPZ was shown to be possible in the presence of hydrophilic biological interferents at hydrophobic modified detectors[130]. Similarly, catecholamine signals could be resolved from those of AA and UA at Nafion films. Typical residence times of 30 – 75 seconds, however, mean high sample throughputs, usually associated with FIA methods, are sacrificed.

Figure 6.1: Induced gradient based discrimination of an analyte in the presence of an interfering species in FIA conditions[a]

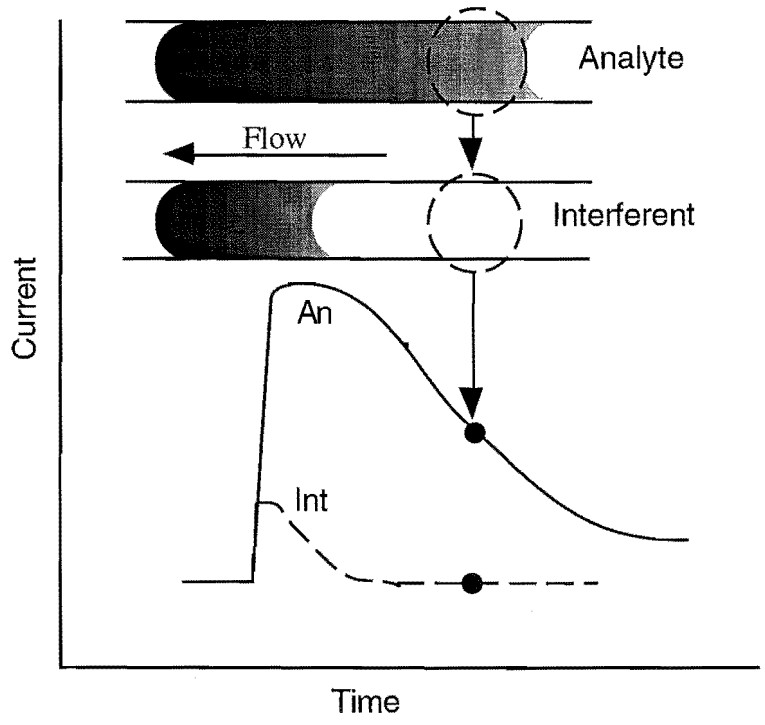

[a] from reference 130

(iii) Detector arrays for multicomponent analysis. Arrays based on different sensing principles have been described. Piezoelectric crystals modified with different adsorbates were used for environmental monitoring of gaseous vapours by Carey et al[131-133]. Hazardous gases were detected by Stetter and co-workers at an amperometric sensor array consisting of four electrodes held at different potentials[134]. Ion-selective electrode arrays for simultaneous determination of metal ions have also been described[135,136]. More recently, Wang et al, have extended the use of sensor arrays to electrochemical multicomponent analysis[137]. A multi-detector flow injection analysis cell was used. Glassy carbon detectors were modified with partially selective films possessing different transport properties (eg Nafion, cellulose acetate, PVP and lipids). The array was applied to two-component mixtures of catechol derivatives and ascorbic acid. Multiple linear regression (MLR) was employed for data analysis yielding relative predictive errors ranging from 1 – 26%. As noted by the author, the chemometric MLR approach requires linear additivity with respect to analyte concentration. Non-linearity may result, for example, from fouling of the electrode surface, changes in reaction mechanisms, chemical reactions between individual solutes and ohmic losses. Data processing methods for amperometric signals arising from individually modified electrodes were studied by Simons et al[138]. Linear scan voltammetry (with rapid stirring) was used to record responses of 117 solutions containing *ortho*- and *meta*-nitrophenols at various concentrations at bare, and rhodium modified Au electrodes. Linear and non-linear multivariate calibration methods were then applied to the experimental data. It was found that the best results (lowest relative mean error) were obtained, in this case, using the non-linear calibration model.

This chapter describes investigations of the analytical utility of *p*-phenylacetate and *p*-alkylbenzene covalently modified electrodes as detectors in flow systems. Considerable effort was aimed at the problem of determining acetaminophen in the presence of AA and UA. The measurement of this drug in plasma and urine is of clinical interest[38,40,72,139,140] and AA and UA are the major electroactive components in these matrices. Further, the ability to measure AA and UA simultaneously in biological fluids is desirable[141,142]. Typical levels for AA and UA in plasma (and serum) are 0.06 mM and 0.29 mM, respectively[142,143]. Average concentrations for AA and UA in undiluted urine are 0.17 mM and 3.5 mM respectively[144] and the levels of acetaminophen in plasma after maximum therapeutic dose (1000 mg) are in the range of 0.1 – 0.2 mM[40]. Hence, experiments aimed at selectively measuring acetaminophen in the presence of UA were performed using gradient flow techniques, and the determination of all three analytes simultaneously was attempted utilising a multi-detector array. Aqueous and mixed aqueous/organic carrier solutions were used and the mixed solution experiments were chosen to reproduce the conditions used in RP-HPLC[17].

Based on the results described in the previous chapter, it was anticipated that *p*-alkylbenzene modified detectors might allow selective measurement of the drug CPZ in the presence of hydrophilic interferents, such as UA, under FIA conditions. This was examined using aqueous carrier solutions and the retention-based procedure was also tested for selective CPZ measurement.

6.2 Experimental

6.2.1 Mixed organic/aqueous carrier solutions

Carrier solutions for FIA. Dimethylbenzene formamide (DMF): Phosphate buffer (0.05 M) 20:80 solution pH 3.4. A 500 mL solution was prepared by mixing 0.7583 g KH_2PO_4 and 2.7918 g Na_2HPO_4 with 400 mL DDW and 100 mL analar reagent grade DMF. The pH was then adjusted to 3.4 by addition of concentrated phosphoric acid.

Methanol: Phosphate buffer (0.043 M) 15:85 solution pH 4.2. Phosphate buffer, 0.05 M, (850 mL) was mixed with spectro grade methanol (150 mL) and the pH was adjusted to 4.2 with concentrated phosphoric acid.

6.2.2 Flow injection analysis

Flow injection analysis used manifold (1) or (2) described in Chapter Two with either detector (a), (b) or (c). Injector valves were fabricated from Teflon. Silicon and Teflon tubing were used in the manifold.

Hydrodynamic voltammograms. Hydrodynamic voltammograms were recorded using either 1 x 10^{-4} M or 2 x 10^{-4} M analyte. Analyte solutions were prepared from degassed carrier solvents and kept under N_2 during the experiment. At least three peaks were obtained at each potential and the average current was used to construct HD voltammograms. Carrier solution was flowed over freshly modified detectors at open circuit for at least 15 min prior to measurements.

6.2.3 Multi-detector array experiments

Calibration curves in 15 % v/v methanol:PB. The usual procedures were followed for *p*-phenylacetate modification and the *p*-decylbenzene CME was prepared by 10 min electrolysis in 5 mM diazonium salt solution. Calibration curves for acetaminophen, UA and AA were obtained at concentrations 4 x 10^{-7} M – 4 x 10^{-4} M on *p*-phenylacetate and *p*-decylbenzene modified electrodes at the potentials subsequently used in the multi-detector experiment. Analyte solutions were prepared from a freshly prepared stock solution, immediately prior to injection. The peak currents used to construct calibration curves were the average of three repeat injections at each analyte concentration.

Treatment of urine sample. The urine sample was collected from a healthy volunteer, immediately filtered through a G-4 glass filter (pore size 2 – 5 μM) and stored in the dark at 4 °C. Before use the sample was diluted 40 fold with degassed carrier solution and, when required, spiked with 5 x 10^{-5} M acetaminophen.

Analysis of acetaminophen, UA and AA using a multi-detector electrode array. Two of the working electrodes of the array were modified with *p*-decylbenzene moieties and the remaining two with *p*-phenylacetate groups. The chosen potential was applied to each electrode individually and the response of individual (5 x 10^{-5} M) and mixed solutions of analytes were recorded in triplicate. The peak currents of a non-spiked and acetaminophen-spiked urine sample were then recorded at each electrode.

6.3 Results

6.3.1 *Para*-phenylacetate modified detectors for acetaminophen measurement in presence of UA and AA

Optimised response for acetaminophen over UA and AA in aqueous conditions. Flow injection analysis was used to compare the currents arising from acetaminophen, UA and AA at unmodified and *p*-phenylacetate modified detectors. Hydrodynamic voltammograms of these analytes, shown in Figure 3.13 (Chapter Three), indicate that the response of acetaminophen is expected to be increased relative to that of AA and UA at the *p*-phenylacetate CME. The sensitivity to acetaminophen relative to its interferents was maximised at 0.5 V vs Ag/AgCl. Table 6.1 compares the peak current ratios for each analyte at the *p*-phenylacetate modified and unmodified detectors $i_{p(m)}/i_{p(un)}$. Analytes (1 x 10^{-4} M in 0.05 M PB) were measured at the modified electrode which was then polished and the responses were recorded at the unmodified detector with the same solutions. The flow rate was 0.87 mL min^{-1}.

Table 6.1: Relative peak currents of acetaminophen, UA and AA (all 1 x 10^{-4} M) recorded at 0.5 V vs Ag/AgCl at *p*-phenylacetate modified and unmodified GC detectors[a]

Analyte	$i_{p,a(m)}$ (μA)	$i_{p,a(un)}$ (μA)	$i_{p(m)}/i_{p(un)}$
Ascorbic acid	0.13	0.39	0.33
Uric acid	0.28	1.72	0.16
Acetaminophen	0.99	0.49	2.02

[a] detector (a)

Under optimal conditions (and assuming the responses are additive when all analytes are present) the peak current of an equimolar acetaminophen, AA and UA solution would arise 71% from acetaminophen, 9% from AA and 20% from UA. This is a signifcant improvement in discrimination for acetaminophen relative to the unmodified detector at the same potential (19% acetaminophen, 15% AA and 66% UA). However, because total discrimination was not achieved it would not be useful as a stand-alone detector for acetaminophen under the described conditions.

Hydrodynamic voltammograms of acetaminophen, UA and AA with mixed organic carrier at p-phenylacetate modified and unmodified detectors. The relative responses of acetaminophen and biological interferents were examined at unmodified and *p*-phenylacetate modified flow detectors using a typical carrier solution employed in RP-HPLC (methanol 15% v/v: PB (0.043 M) at pH 4.2[72]). Analyte concentrations were 1 x 10^{-4} M in 0.05 M PB and the SCE referenced detector (b) was used in these experiments. The HD voltammograms of each analyte, at the modified and unmodified detector, are compared in Figures 6.2, 6.3 and 6.4. The relative response of these analytes at each detector is illustrated by Figure 6.5.

Figure 6.2: Hydrodynamic voltammograms of 2 x 10^{-4} M acetaminophen at the *p*-phenylacetate modified and unmodified detector in 15% v/v methanol:PB

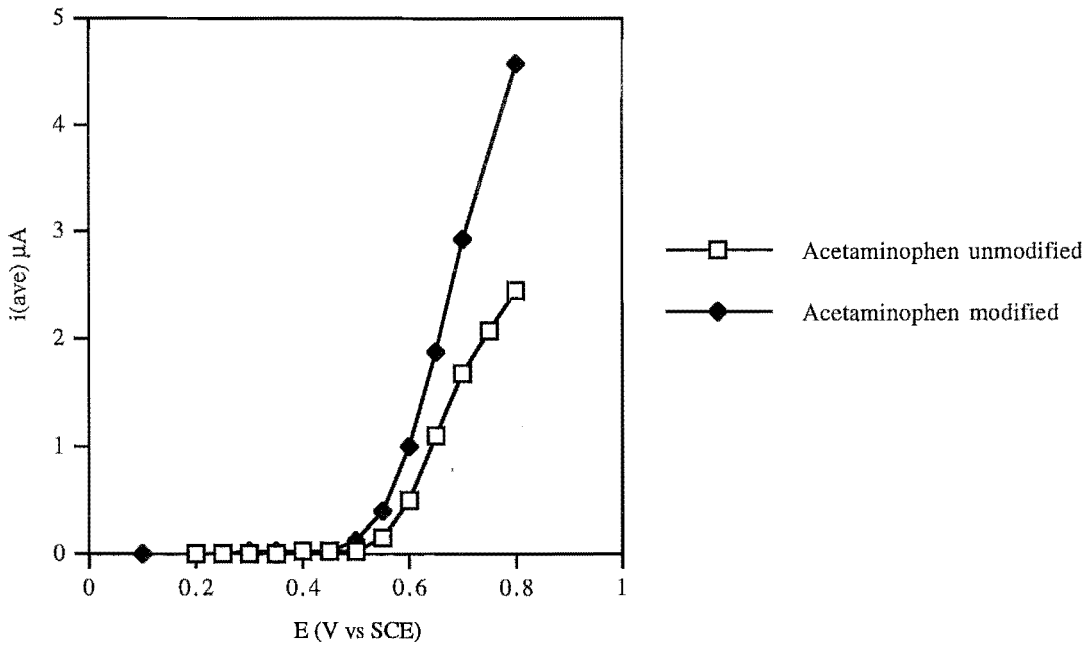

Figure 6.3: Hydrodynamic voltammograms of 2 x 10^{-4} M UA at the *p*-phenylacetate modified and unmodified detector in 15% v/v methanol:PB

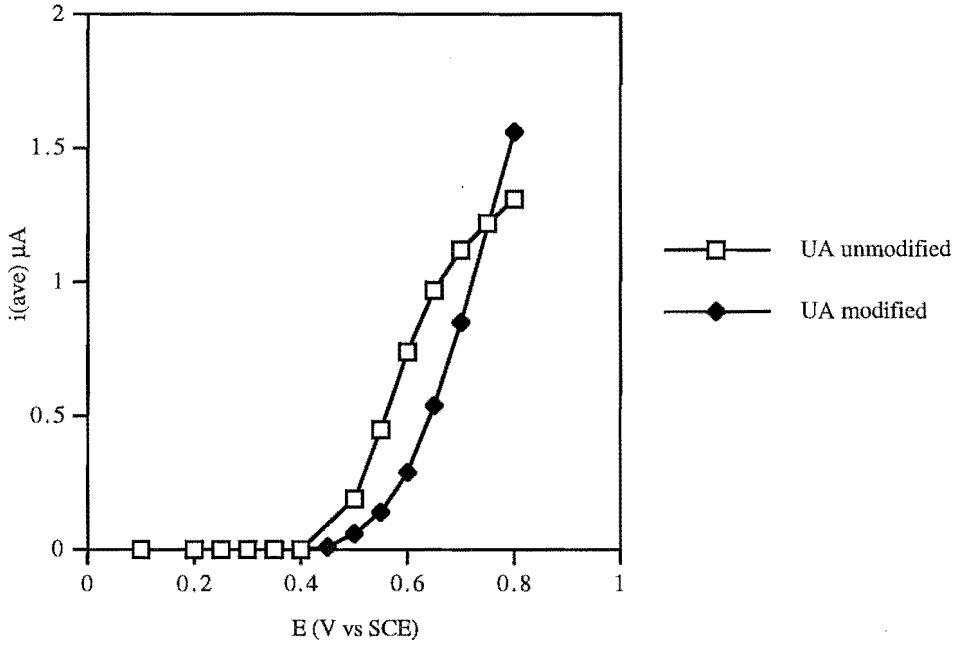

Figure 6.4: Hydrodynamic voltammograms of 2 x 10^{-4} M AA at the *p*-phenylacetate modified and unmodified detector in 15% v/v methanol:PB

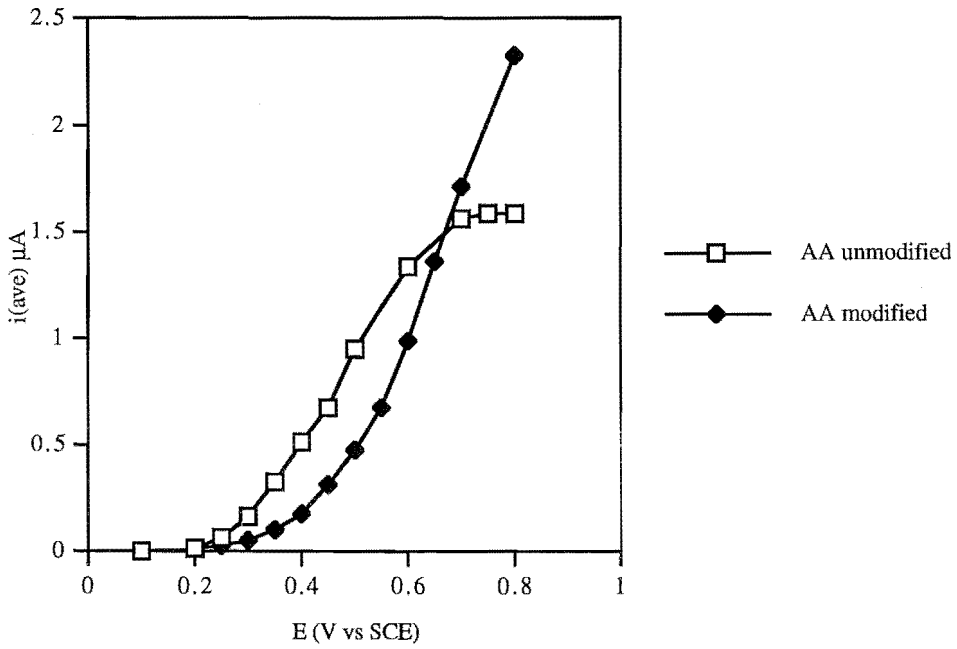

Figure 6.5: Hydrodynamic voltammograms of 2 x 10^{-4} M analytes at the unmodified (a) and *p*-phenylacetate modified (b) in 15% v/v methanol:PB

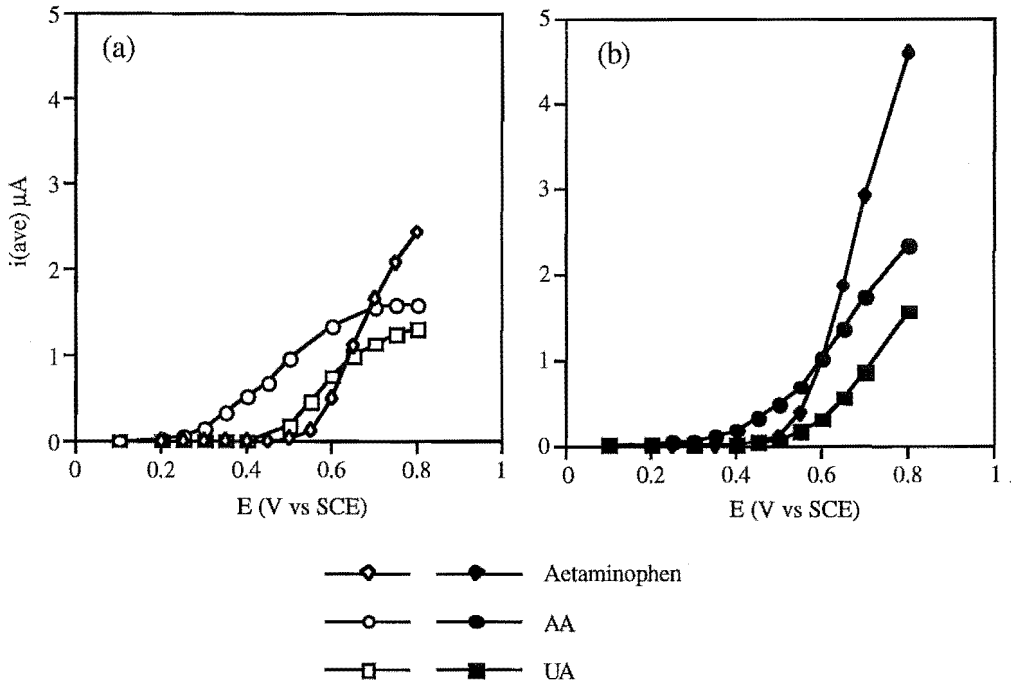

The $E_{1/2}$ values of UA and AA are shifted positive at the modified detector but no comment can be made about the $E_{1/2}$ of acetaminophen as the plateau current was not reached at either the modified or unmodified surfaces. Potentials greater than 0.8 V were not applied as carbon electrodes tend to oxidise under these conditions. The increase in analyte current at high potentials at the *p*-phenylacetate modified detector (relative to the unmodified detector) observed in these experiments, is assumed to be due to decreased electrode fouling by reaction products at the modified surface. This was also found to be the case in earlier HD voltammetric measurements (Chapter Three).

The best potential for acetaminophen measurement in the presence of equimolar AA and UA in the potential range examined was 0.8 V vs SCE. At this potential 55% of the signal would be due to acetaminophen, 27% AA and 18% UA, again assuming linear additivity when all components were present. At the same potential, the unmodified detector gave results of 46% acetaminophen, 30% AA and 24% UA.

Hence, in this carrier solution *p*-phenylacetate modified detectors offered less improvement in the relative sensitivity to acetaminophen compared to that observed in aqueous (0.05 M PB) solutions. The decreased selectivity for acetaminophen in the methanol/PB carrier solution is probably due to protonation of carboxylic acid functionalities on the modified electrode and increased protonation of AA and UA (which have pKa values of 4.1 and 5.4 respectively).

6.3.2 Selectivity of *p*-alkylbenzene modified detectors in aqueous solutions

Para-alkylbenzene CMEs were shown (in Chapter Five) to have some selectivity for hydrophobic analytes relative to hydrophilic species in batch conditions and to be strongly selective towards species undergoing simple electron transfer reactions. Hence, HD voltammograms of biological analytes were recorded at *p*-methylbenzene modified detectors to investigate selectivity in flow injection analysis conditions.

Hydrodynamic voltammograms of acetaminophen and UA at densely coated p-methylbenzene modified flow detectors. To produce a densely coated CME, the detector electrode was modified in 5 mM *p*-methylbenzene diazonium salt for 10 min. Analyte concentrations of 2 x 10^{-4} M/0.05 M PB were used in these experiments with the SCE reference electrode flow cell (detector b, Chapter Two). After recording voltammograms at the modified detector, the flow cell electrode was polished and the HD voltammogram of UA was repeated with the same analyte solution. The results are shown in Figure 6.6.

Figure 6.6: Hydrodynamic voltammograms of acetaminophen and UA (2 x 10^{-4} M/ 0.05 M PB) at dense *p*-methylbenzene modified flow detectors

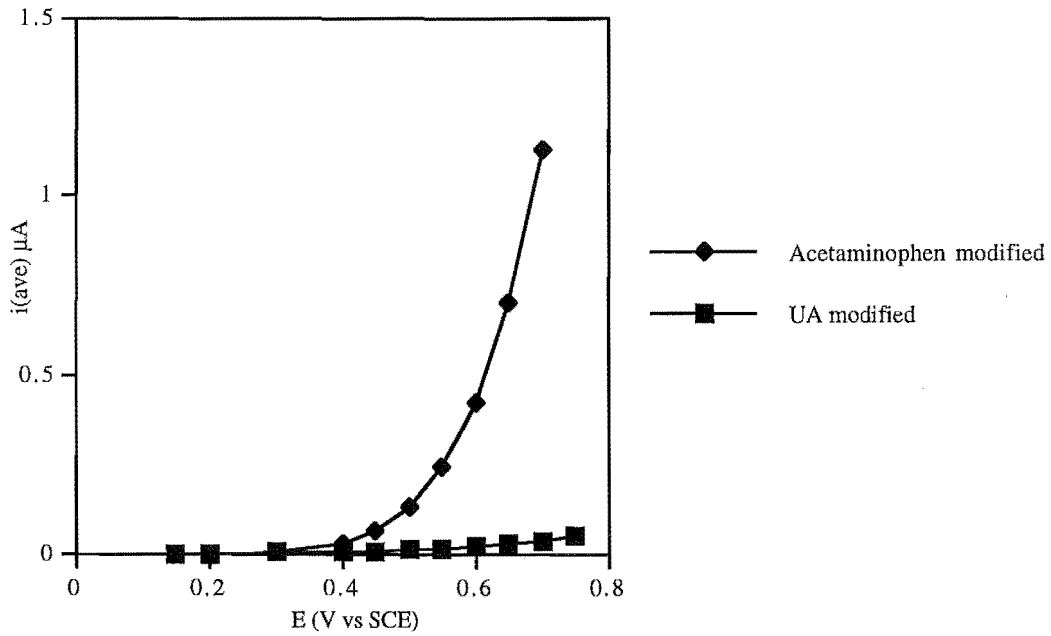

Clearly the densely coated *p*-methylbenzene detector shows some selectivity for acetaminophen response relative to UA and this increases as the applied voltage is increased.

6.3.3 Measurement of acetaminophen, UA and AA at the *p*-phenylacetate and *p*-decylbenzene modified multi-detector array

When complete selectivity for a component in a mixture is not able to be achieved, the partial selectivity can be exploited to obtain information about the relative concentrations of each analyte using an array of detectors. Electrode coatings with different permeability to the analytes of interest can be used with the same applied potential[136] or the responses of analytes at different potentials on the same electrode may be used if the relative sensitivities are sufficiently variable. In this experiment, both strategies were combined for the measurement of acetaminophen, UA and AA in a three-component mixture.

Mixed acetaminophen, UA and AA solutions with 15 % v/v methanol:PB. In preliminary experiments, the peak currents of separate and mixed solutions of equimolar (i.e. 5 x 10^{-5} M) acetaminophen, UA and AA were recorded at unmodified GC detectors.

When 15% v/v methanol:PB was used as the carrier solution, it was found that the peak current arising from the mixed analyte solution was 85 – 90% of the additive currents for the individual responses at both unmodified and modified detectors. This effect was not due to electrode deactivation, as shown by injections of the mixed analyte sample prior to individual solutions. The possibility that non-linear response, at the high overall concentration of the mixed solution, was affecting peak current was considered and shown not to be responsible for the observed behaviour.

To further investigate if specific interactions were occurring between the analytes, combinations of two analytes were examined. Acetaminophen and AA mixed solutions gave peak currents which were experimentally the same as the sum of the separate components whereas solutions with UA present (particularly with AA) gave lower than expected currents. The reasons for this were not investigated.

Calibration curves of acetaminophen, UA and AA at the p-phenylacetate and p-decylbenzene modified detectors. Calibration curves for each analyte were obtained in 15% v/v methanol:PB at the potentials subsequently applied to the electrode of the multi-detector cell. All analytes gave linear plots between concentrations 4 x 10^{-7} M and 1 x 10^{-4} M with r^2 coefficients ranging from 0.995 – 1.000.

Choice of carrier solution for linear additivity of analyte currents. The additivity of acetaminophen, UA and AA response was investigated with other carrier solutions. For 15% and 50% acetonitrile: PB (0.05 M) at pH 4.2 and pH 7 respectively, mixed solutions gave low currents relative to those of the sum of the individual components. This was not observed, however, when 20% DMF: PB (0.05 M) pH 3.4 was

the carrier solution. Therefore this medium was used for further experiments. Two electrodes of the multi-detector flow cell were modified with *p*-phenylacetate groups and the remaining two with *p*-decylbenzene moieties. One of each type of electrode was operated with an applied voltage of 0.8 V and the other two at 0.55 V. Separate solutions of each analyte (5×10^{-5} M) were measured, in turn, at each modified detector (held at the appropriate potential) to obtain the relative responses. Two-component solutions containing 5×10^{-5} M acetaminophen and AA were then measured at each electrode. Following this, the response of an equimolar solution of all three analytes was recorded. Hence, a matrix describing the relative response of each analyte at each electrode was generated (see Table 6.2).

Table 6.2: Relative response of different electrodes of the multi-detector array to 5×10^{-5} M analyte and mixed solutions of AA, acetaminophen and UA

	AA (μA)	**Acet** (μA)	**UA** (μA)	**AA + Acet** (μA)	**AA + Acet + UA** (μA)
Elec 1 *p*-decylbenzene 0.55 V	0.00108	0.00	0.00042	0.00125	0.00154
Elec 2 *p*-decylbenzene 0.8 V	0.00345	0.00325	0.00150	0.00675	0.0080
Elec 3 *p*-phenylacetate 0.55 V	0.07375	0.0020	0.005167	0.07833	0.0850
Elec 4 *p*-phenylacetate 0.8 V	0.3900	0.5625	0.17333	0.97813	1.11667

Data was processed simply by solving a series of simultaneous equations and the closest agreement between actual concentrations and experimental values was obtained by excluding the results from electrode 4 which gave much larger currents than the other three electrodes. The best results are shown in Table 6.3.

Table 6.3: Results of solution composition determinations for two and three component systems using a modified multi-detector electrode array

solution description	calculated concentration (10^{-5} M)	actual concentration (10^{-5} M)
AA + acetaminophen	5.18 + 4.87	5 + 5
AA + UA + acetaminophen	5.31+ 4.50 + 4.71	5 + 5 + 5

A urine sample which had been diluted 40 fold was spiked with 5 x 10^{-5} M acetaminophen and measured at the multi-detector array. The peak currents at the *p*-decylbenzene detectors were observed to decrease with repeat exposure to the diluted urine sample, presumably due to adsorption of organic species which were not removed by the filtering process. To take this into account a post calibration procedure, in which the responses of single analyte solutions were recorded after the urine sample, was used. The data were processed by solving simultaneous equations as above and concentrations of 3.25 x 10^{-6} M AA, 9.8 x 10^{-3} M UA and 4.1 x 10^{-5} M acetaminophen were determined. These equate to concentrations in undiluted urine of 1.3 x 10^{-4} M AA and 9.8 x 10^{-3} M UA and an 82% recovery of the acetaminophen spike. The average levels for AA and UA in urine are 1.7 x 10^{-4} M and 3.5 x 10^{-3} M respectively[144].

6.3.4 Retention time experiments for acetaminophen measurement

Gradient flow techniques may be used to selectively measure components of a sample. This selectivity relies on the different diffusion coefficients of analytes which leads to regions of increased and decreased concentrations in the sample plug[145].

An extension of this methodology is to induce variable dispersion of analytes within a sample zone by coating the flow detector electrode with a modifier which interacts with components to various extents[130]. Hence, hydrophobic coatings will stretch out the sample zones of hydrophobic analytes relative to non-interacting (hydrophilic) species and allow selective measurements to be made at the tail of the current peak.

Retention time based discrimination of acetaminophen over UA and AA at p-decylbenzene detectors in mixed methanol carrier solutions. The following experiments describe studies applying the sample zone stretching strategy, outlined above, to the measurement of acetaminophen. A carrier solution of 15% v/v methanol:PB (pH 4.2) was used because in the absence of organic solvent the permeability of acetaminophen at the very dense, long chained alkylbenzene coatings was very low.

Figure 6.7 compares the flow injection peaks of 2 x 10^{-4} M acetaminophen, UA and AA at unmodified (A) and *p*-decylbenzene modified (B) detectors. The acetaminophen is retained longer at the modified surface allowing it to be measured after the decay of UA and AA giving a current of 1 nA at 38 s. Although the currents at the coated detector are very small, the signal to noise ratio remains high. A higher potential of 0.8 V vs SCE gave optimal response to acetaminophen over interferents as shown by the HD voltammograms in Figure 6.8. The coating gave reproducible peak current responses to acetaminophen (RSD = 4%, n = 20 at 0.7 V) and was stable for the 4 – 5 h during which these measurements were made. The sensitivity to acetaminophen over UA at the *p*-decylbenzene detector, however, does not appear to be sufficient to allow measurement of acetaminophen (when present at therapuetic dosage levels) in urine, where UA concentrations are typically ~15 times higher.

Figure 6.7: Flow injection peaks of 2 x 10^{-4} M acetaminophen, UA and AA in 15% v/v methanol:PB (pH 4.2) at unmodified (A) and *p*-decylbenzene modified (B) detectors recorded at E = 0.8 V, flow rate = 0.48 mL min^{-1}

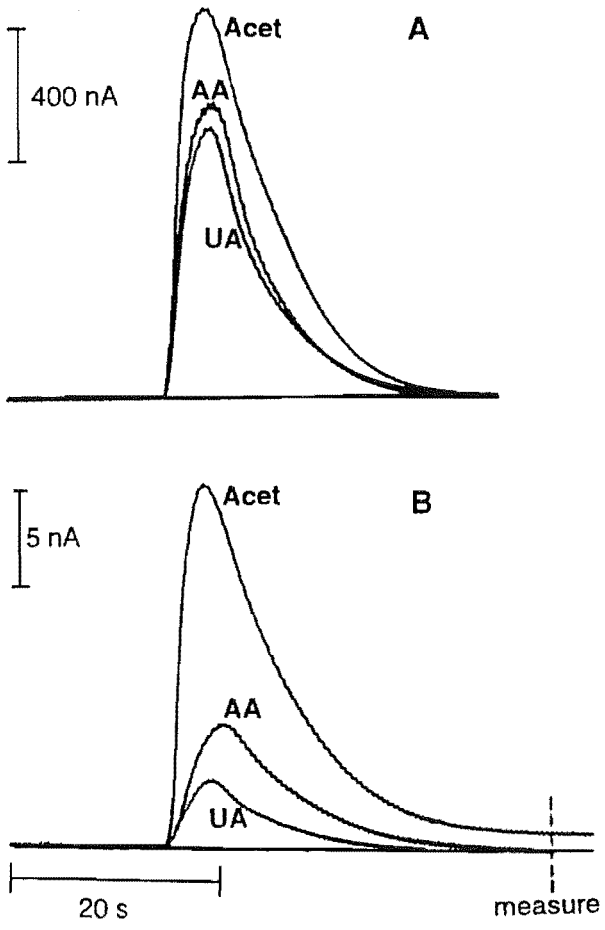

Figure 6.8: Hydrodynamic voltammograms of 2 x 10^{-4} M acetaminophen, UA and AA at the *p*-decylbenzene modified detector in 15% v/v methanol:PB

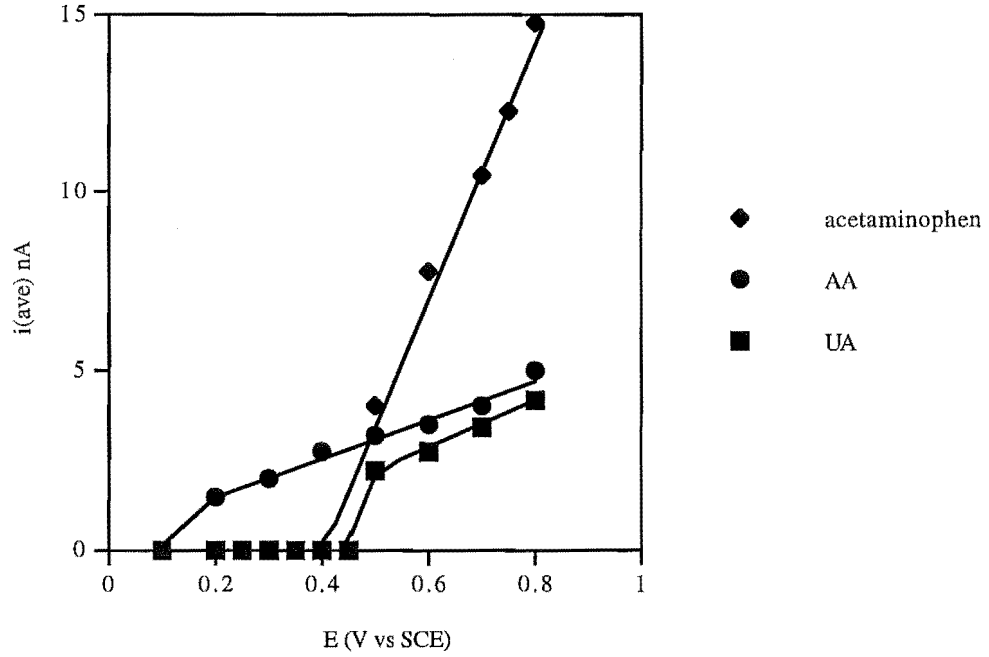

6.3.5 Selectivity of CPZ response at modified detectors

In Chapter Five, *p*-alkylbenzene CMEs were shown to suppress the response of AA whilst allowing the measurement of CPZ in CV experiments. Similarly, the cyclic voltammetric response of UA was decreased at *p*-methylbenzene CMEs. Hydrodynamic voltammograms were recorded at *p*-methylbenzene modified detectors to investigate selectivity in FIA conditions.

Hydrodynamic voltammograms of UA and CPZ at less densely coated p-methylbenzene modified detectors. Glassy carbon flow cell electrodes were modified in 0.5 mM *p*-methylbenzene diazonium salt with 30 s electrolysis. Analyte concentrations of 2 x 10^{-4} M/0.05 M PB were used in these experiments with the SCE reference electrode flow cell . After recording the voltammogram at the modified detector the flow cell electrode was polished and the HD voltammogram was repeated with the same analyte solution.

Cyclic voltammetry of UA was used to assess the condition of the modified detector prior to and following HD voltammograms. This showed that changes in electrode performance after obtaining complete voltammograms were consistent with fouling of the surface by reaction products i.e. $E_{p,a}$ for UA was shifted positive and $i_{p,a}$ decreased. The

HD voltammograms of UA and CPZ at the less densely coated *p*-methylbenzene modified and unmodified detectors are shown in Figures 6.9 and 6.10.

Figure 6.9: Hydrodynamic voltammograms of UA (2 x 10^{-4} M/0.05 M PB) at *p*-methylbenzene modified and unmodified flow detectors

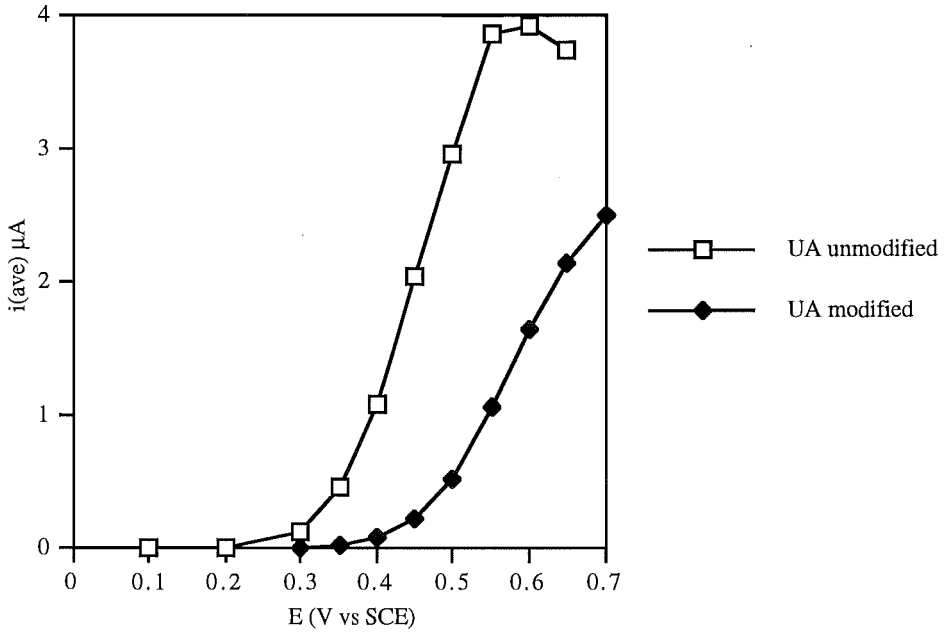

Figure 6.10: Hydrodynamic voltammograms of CPZ (2 x 10^{-4} M/0.05 M PB) at *p*-methylbenzene modified and unmodified flow detectors

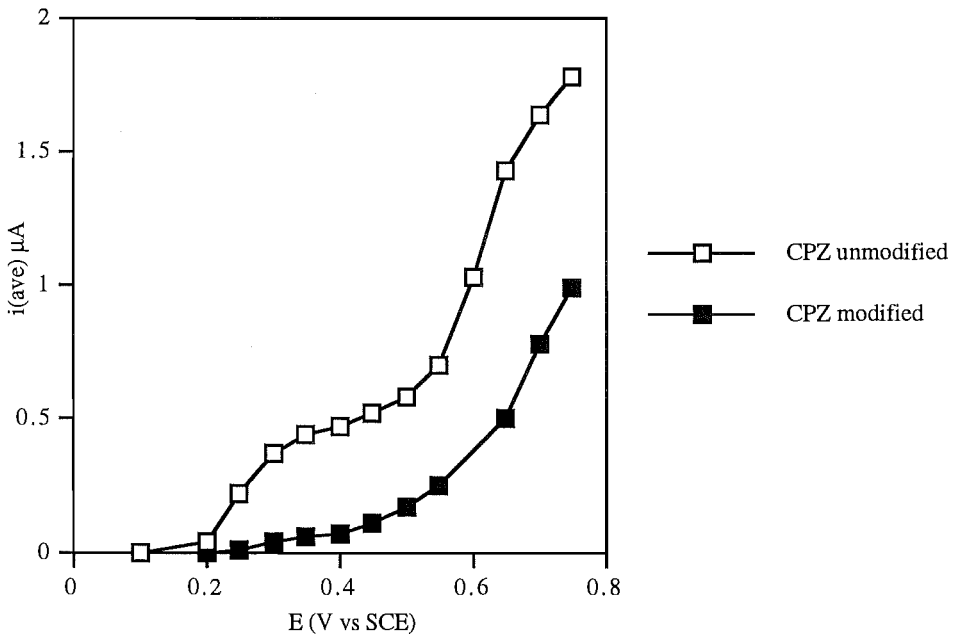

The voltammograms of UA and CPZ at the modified detector showed a similar degree of peak current decrease relative to the unmodified GC detector. These results imply that in hydrodynamic conditions the less densely coated modified electrode has decreased selectivity for hydrophobic species and does not significantly favour the species undergoing simple electron transfer. This may arise from convective diffusion through pinholes in the coating.

6.3.6 Retention time based selectivity for CPZ over UA

In the following experiments, *p*-decylbenzene, *p*-methylbenzene and mixed *p*-methylbenzene/*p*-phenylacetate modified detectors are used to induce stretching of CPZ sample zones. The aim of these experiments is to develop strategies which allow the selective measurement of CPZ in the presence of UA.

Para-methylbenzene modified detectors with aqueous carrier solutions for the selective measurement of CPZ in the presence of UA. Glassy carbon flow detectors were covalently modified with hydrophobic coatings of varying density and the responses of separate solutions of CPZ and UA (2 x 10^{-4} M in 0.05 M PB) were examined. The aim was to increase dispersion of the CPZ peak and decrease that of UA as much as possible, allowing discrimination of the CPZ signal at short times.

All measurements were performed with an applied voltage of 0.7 V vs SCE unless stated otherwise. Lower potentials did not affect the response ratio of CPZ and UA and gave decreased currents. A *p*-methylbenzene coating, prepared using a short electrolysis time in dilute diazonium salt, produced a surface at which equimolar CPZ and UA gave similar peak currents at a flow rate of 0.76 mL min^{-1}. The peak width at half height, $w_{1/2}$, was greater for UA relative to CPZ at all flow rates (0.48, 0.76 and 1.18 mL min^{-1}) and the CPZ peak was not drawn out sufficiently to allow selective measurement. Interestingly, CPZ gave increased peak currents at greater flow rates whilst UA response was unchanged. This suggests that slow diffusion of UA in the coating is controlling its response and CPZ diffusion is relatively fast.

More dense coatings, i.e. those prepared by long electrolysis times in 5 mM diazonium salt modifying solutions, produced surfaces which excluded UA relative to CPZ more successfully and increased the stretching of sample zones. As shown in Figure 6.11 the peak current ratio of CPZ to UA increases with increasing coating density, as measured by the permeability of UA. The maximum ratio of peak currents for CPZ:UA at the *p*-methylbenzene modified detector was 3.8; this compares with 0.3 at the unmodified electrode. The peak currents of both analytes were unaffected by flow rate. Decreasing the flow rate results in a more drawn out response for CPZ relative to UA hence the

greatest sensitivity to CPZ was obtained at low flow rates (0.48 mL min^{-1}) but correspondingly, long times were needed for selectivity to be achieved. Figure 6.12 shows responses of CPZ and UA at unmodified and two modified electrodes of different density.

Figure 6.11: Variation of the peak current ratio of CPZ relative to UA with the density of *p*-methylbenzene modification for 2 x 10^{-4} M analytes in 0.05 M PB with a flow rate of 0.78 mL min^{-1}

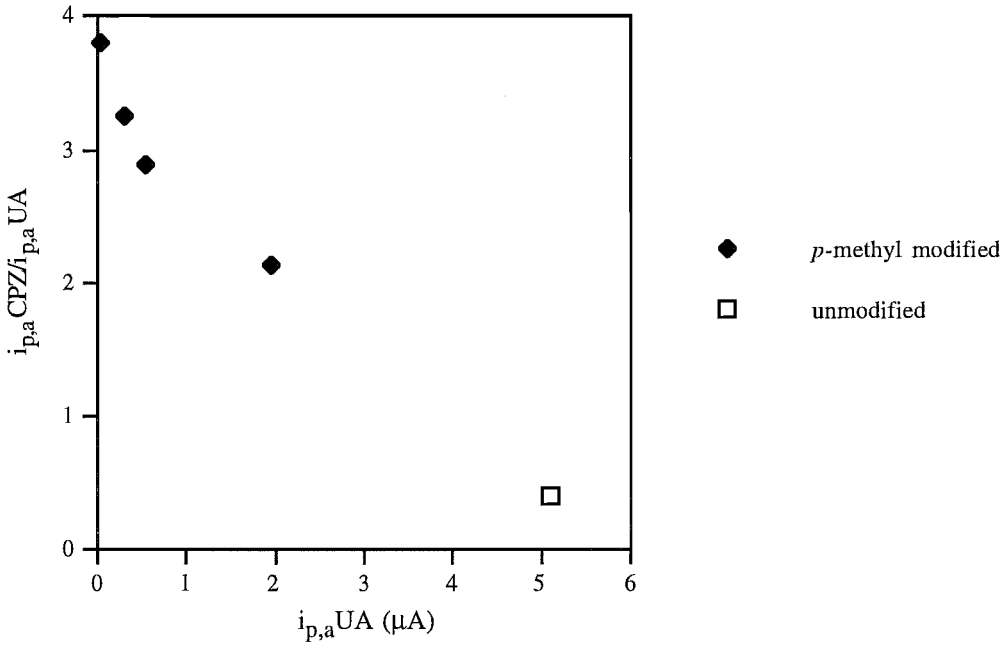

Figure 6.12: Flow injection peaks for CPZ and UA (2 x 10^{-4} M/0.05 M PB) at unmodified (A) and modified detectors of intermediate (B) and high density (C). Flow rates (a) 0.48, (b) 0.76 and (c) 1.18 mL min^{-1}. E = 0.7 V vs SCE. The dotted line indicates the time at which UA current has decayed to zero allowing measurement of CPZ only.

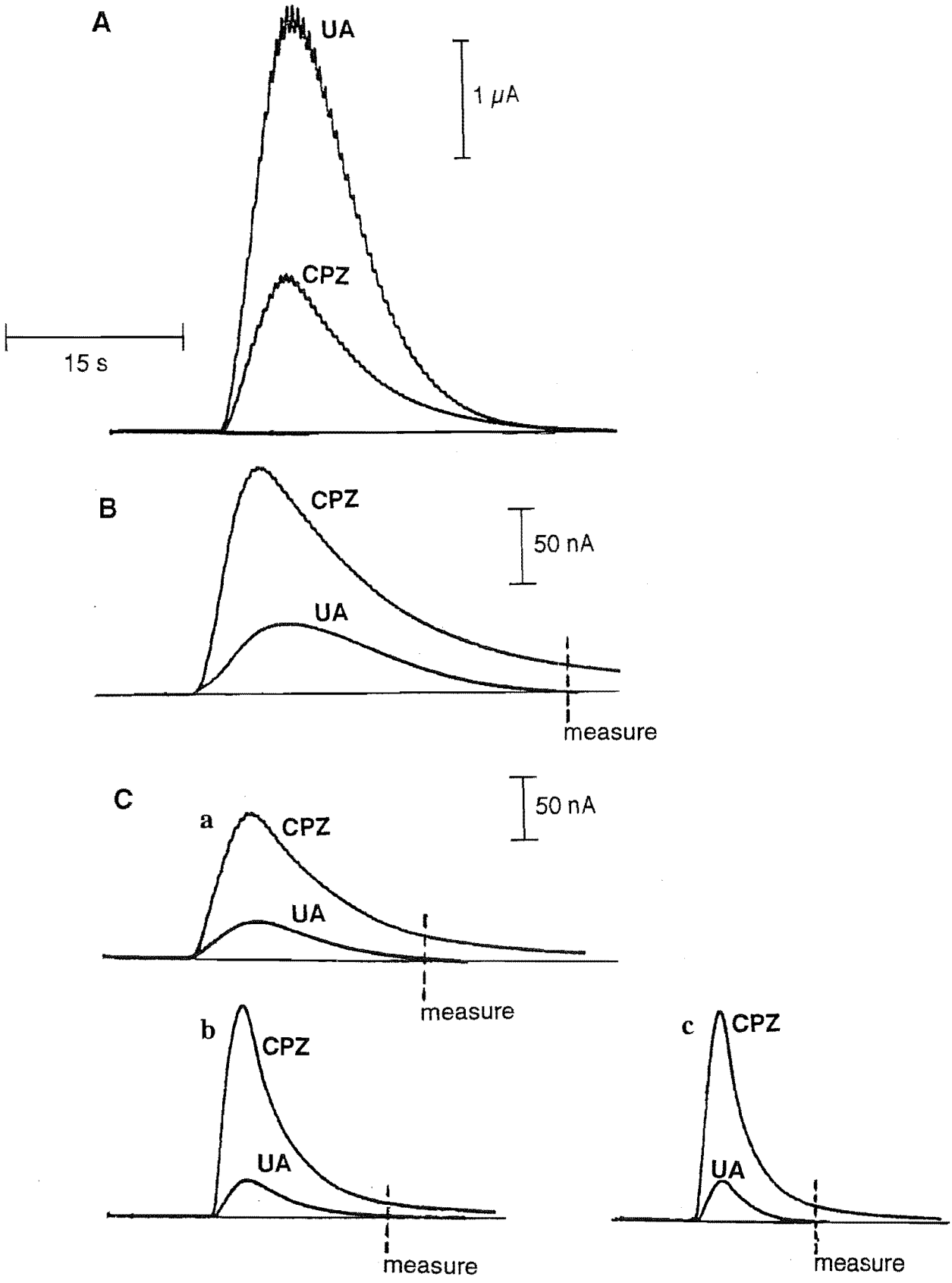

The flow injection peaks for CPZ and UA at the unmodified detector have superimposable tail regions indicating that they interact to a similar extent with the bare electrode. Both modified detectors show an increased stretching of the solute zone for CPZ which allows selective measurement of this analyte at times when the UA current has decayed to zero. At a flow rate of 0.48 mL min^{-1} detector (B) (*p*-methylbenzene modified with intermediate density) gave a current due to CPZ of 20 nA at 32 s. The effect of different flow rates on stretching of sample zones of CPZ and UA is shown for the more dense coating (C). At a flow rate of 0.48 mL min^{-1} a current due to CPZ of 20 nA can be measured at 21 s (i.e. the time taken for the UA to pass over the detector) whereas increasing the flow rate to 1.18 mL min^{-1} results in a 10 nA signal at 10.5 s. Hence, a compromise between sensitivity and sample throughput must be reached.

Para-decylbenzene modified detectors with aqueous carrier solutions for the measurement of CPZ in the presence of UA. The relative permeability of CPZ and UA and stretching of solute zones was also investigated at *p*-decylbenzene modified detectors. The usual modification procedure for dense coatings was applied. The resultant coating gave very low currents to UA (2 nA) and CPZ (10 nA) but improved discrimination for CPZ over UA, relative to *p*-methylbenzene modified electrodes, i.e. a maximum peak current ratio of 5.0 was obtained (compared to 3.8 for the *p*-methylbenzene CME). At a flow rate of 0.48 mL min^{-1} the UA injection peak decayed to zero after 25 s at which time the CPZ current was 3.5 nA. Alternatively, at 1.18 mL min^{-1} a CPZ current of 2 nA could be selectively measured after 15.5 s. The flow injection peaks obtained at a flow rate of 0.48 mL min^{-1} are shown in Figure 6.13. The calibration curve for changing CPZ concentration is shown in Figure 6.14. The CPZ solution was diluted with UA and the total concentration of the two components was 2 x 10^{-4} M. The time required for a 1.6 x 10^{-4} M UA solution to decay to zero was 35 s thus this was used for analysis. The resulting calibration curve showed a linear relationship to CPZ over the concentration range examined i.e. 0.04 to 0.2 mM (r^2 = 0.999 for the regression line).

Figure 6.13: Flow injection peaks of 2 x 10^{-4} M CPZ and UA in PB (0.05 M) recorded at a flow rates of 0.48, with E = 0.7 V vs SCE

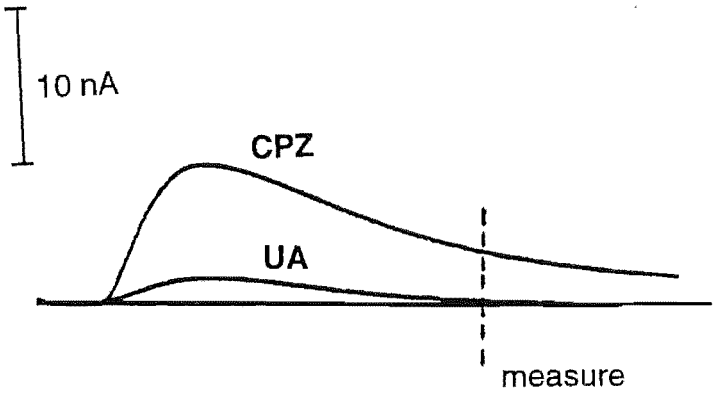

Figure 6.14: Calibration curve for CPZ (0.05 M PB) in the presence of UA measured at 35 s with a flow rate of 0.48 mL min^{-1} and E = 0.7 V vs SCE

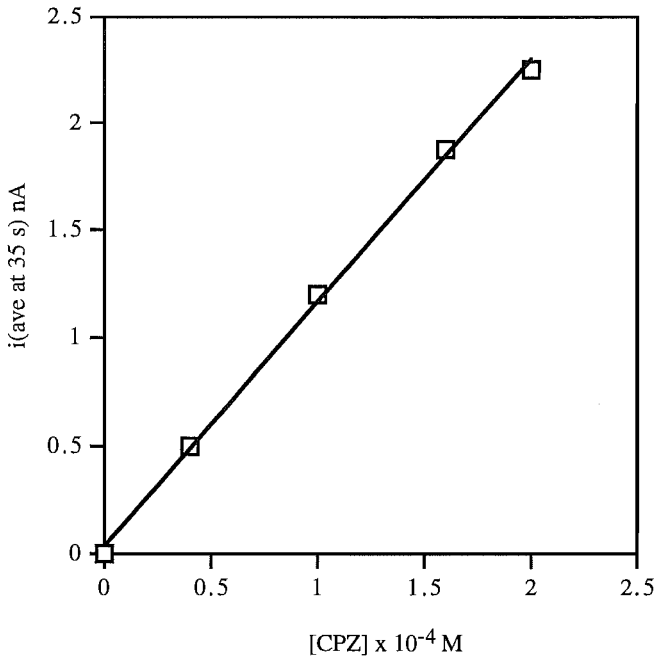

Mixed p-methylbenzene/p-phenylacetate modified detectors with aqueous carrier solutions for the measurement of CPZ in the presence of UA. Mixed *p*-methylbenzene/*p*-phenylacetate coatings were investigated to try and further enhance the response of CPZ over UA by introducing electrostatic interactions. Chlorpromazine is cationic at pH 7.4 whilst UA is anionic and the *p*-phenylacetate coating is largely deprotonated (pKa ≈ 5). Table 6.4 summarises the results of various modification procedures used to generate mixed coatings.

Table 6.4: Modification strategies for generating mixed *p*-methylbenzene/*p*-phenylacetate coatings and the resulting response for CPZ and UA (both 2 x 10^{-4} M/ 0.05 M PB). E = 0.7 V vs Ag/AgCl[a] and flow rate = 0.48 mL min^{-1}

Modification procedure[b]	Time for UA to decay to zero (s)	Current of CPZ at zero current for UA (nA)	Stability of response
(**1**) *p*-phenylacetate diazonium salt (10 min), *p*-methylbenzene diazonium salt (10 min), sonication in acetonitrile	26.5[c]	75	increased currents for repeat CPZ injections
(**2**) *p*-methylbenzene salt (20 min), *p*-phenylacetate (5 min) sonication in benzene	29.5	100	stable for repeat CPZ injections
(**3**) As for (**2**); further treatment in *p*-phenylacetate (5 min), *p*-methyl-benzene (5 min) sonication in acetonitrile	35	125	stable for repeat CPZ injections
(**4**) Modify (**3**) in *p*-methylbenzene (10 min) with stirring, (5 min) sonication in acetone	35	25	stable for repeat CPZ injections
(**5**) Modify in mixed *p*-methylbenzene/ *p*-phenylacetate (2.5 mM) solution (10 min) sonication in acetone	38	75	stable after CPZ injections

[a] FIA detector (a)

[b] modification solutions are 5 mM diazonium salt and electrolysis times are given in parentheses

[c] flow rate = 0.76 mL min^{-1}

Modification with *p*-phenylacetate groups first, produced a coating at which the current of both analytes increased with time. This may be due to adsorption of the *p*-methylbenzene modifiers at the *p*-phenylacetate derivatised surface which are later desorbed as the *p*-phenylacetate groups become deprotonated.

The response of UA was not completely suppressed in any of these experiments although it was decreased markedly. The peak was very drawn out leading to relatively long times for current decay. Modification procedures (2) and (3) which involved total electrolysis times of 25 and 35 min respectively, gave the best results for CPZ measurement. The response of CPZ was readily measurable after 30 to 35 s (at zero UA current) and the signal:noise ratio was high. Hence, these coatings are promising for measurement of CPZ in the presence of common biological interferents.

6.4 Discussion

In this Chapter, the performance of covalently modified detectors was examined in PB and mixed aqueous/organic carrier solutions. The latter were used because reversed phase-HPLC, which is the most commonly applied mode of chromatographic separation, often employs such carrier solutions for the measurement of biological analytes[17].

6.4.1 Performance of modified detectors for acetaminophen measurement

Selectivity for acetaminophen relative to UA and AA at modified detectors in FIA. *Para*-phenylacetate modified flow detectors showed improved selectivity for acetaminophen over UA and AA in PB (0.05 M) at pH 7.4. Total exclusion of interferents, however, was not achieved and hence the modification alone is not sufficient to selectively measure acetaminophen in FIA conditions. When the carrier solution was changed to 15% methanol/PB (pH = 4.2) the relative peak currents of analytes were altered and the *p*-phenylacetate detector was less selective for acetaminophen (compared to its response in 0.05 M PB). The decrease in pH would be expected to shift oxidation potentials more positive (for proton coupled electron transfer reactions) and also increase the degree of protonation of both the electrode surface and analytes (UA and AA). The latter effect may be responsible for the observed decrease in selectivity for acetaminophen in mixed aqueous/organic carrier solutions. Although complete selectivity for acetaminophen was not achieved, the *p*-phenylacetate CME showed very favourable anti-fouling properties with respect to oxidation of acetaminophen, UA and AA (relative to GC). This would make it a suitable detector when RP-HPLC successfully separates these signals. Similarly it would be useful as part of an array of electrodes.

Multi-detector electrode array. The partial selectivities of modified electrodes can be utilised to provide multi-channel information about sample composition. This technique is becoming more established (especially in connection with microelectrodes[138,146]) as a means of obtaining comprehensive analyses of multiple species in a sample. The use of a multielectrode array is attractive because comparatively

low-cost instrumentation is required. Simultaneous determination of AA and UA has been achieved by other workers. For example, Almuaibed et al[141] used FIA with spectrophotometric detection of UA at 293 nm and amperometric detection of AA and UA at 0.6 V to achieve simultaneous measurement of AA and UA in synthetic binary solutions. The concurrent determination of UA and AA in plasma by reversed phase-HPLC using an ion-pairing agent with UV detection, has also recently been reported[142]. In the present study a simple, rapid method for the simultaneous analysis of acetaminophen, UA and AA using a multielectrode detector array was demonstrated. Relative predictive errors were in the range of 2.6 – 10% which can be compared to 1 – 26% attained by other workers when using an electrode array for measurements of neurologically significant analytes in two-component systems[137].

To optimise the simultaneous measurement of acetaminophen, UA and AA in urine using the multielectrode array, the *p*-phenylacetate detector would be utilised but *p*-alkylbenzene detectors, which suffer electrode deactivation from adsorption of high molecular weight organic molecules, would be inappropriate. A coating, such as Nafion, could be applied to decrease fouling by non-electroactive components of the matrix, depending on the organic component of the carrier solution. Alternatively, other covalently modified detectors which are resistant to adsorption of high molecular weight organic species and give different selectivities to the target analytes, may be used.

Retention time based experiments. Selectivity of acetaminophen response over that of UA was possible using retention time based techniques. This was demonstrated using the *p*-decylbenzene modified detector and mixed aqueous/organic carrier solutions. Although the current arising from the oxidation of acetaminophen (2×10^{-4} M) was small (1 nA) at zero UA current, these detectors are characterised by very low background noise. Nevertheless, this method is less sensitive to acetaminophen (compared to the multi-detector strategy above) because measurements are made at the tail of the FIA peak. Hence, although complete selectivity for acetaminophen is achievable, the retention time based method of analysis is less analytically useful when large concentrations of interfering species are present.

6.4.2 Performance of modified detectors for CPZ measurement

Results described in the previous chapter indicated that *p*-alkylbenzene CMEs showed selectivity for CPZ relative to hydrophilic interferents primarily based on the simplicity of its electron transfer reaction. Analyte hydrophobicity was also shown to be a minor controlling factor. It was anticipated that these modifications would give similar discrimination of CPZ response in FIA conditions. Less densely coated *p*-methylbenzene detectors, however, did not give increased selectivity of CPZ response relative to UA (compared to the unmodified electrode). This is ascribed to forced convection of the hydrophilic analyte through pinholes in the coating. As the density of *p*-methylbenzene

modifiers was increased, the relative response ratio of CPZ over UA was also increased and reached a maximum of 3.8 at E = 0.7 V vs SCE. Increasing the hydrocarbon chain length of the modifier (i.e. modifying with *p*-decylbenzene groups) decreased the currents of both CPZ and UA but gave an improved relative response ratio CPZ:UA of 5.0 at maximum coating density. This increased selectivity may be attributed to the greater hydrophobicity of this coating as well as the increased thickness, both of which will disfavour the approach of UA to uncoated regions of the electrode surface.

Retention-based selectivity at modified detectors. The largest CPZ currents (at zero UA response) were obtained at detectors modified with *p*-methylbenzene and *p*-phenylacetate groups. The response of UA at these modified detectors is disfavoured by the barrier properties of the coating, hydrophobicity and repulsive electrostatic interactions. The best results obtained for CPZ discrimination in the presence of UA were comparable to those observed at phospholipid/cholesterol modified detectors[130] using the same retention-based methods. Due to the high concentration of UA (compared to therapeutic levels of drugs) in urine, great demands are placed on selectivity for the target analyte. In these experiments, reasonably high currents were obtained for CPZ after the current of equimolar UA had decayed to zero. It is anticipated that further decreasing the solution flow rate would increase selectivity to CPZ, as would a larger area of modified electrode. Thus, the retention-based method seems promising for CPZ measurement in the presence of UA.

6.5 Conclusions

Para-phenylacetate and *p*-alkylbenzene modified detectors gave increased (though not complete) selectivity to acetaminophen and CPZ relative to the hydrophilic interferents UA and AA, in FIA conditions. The *p*-phenylacetate modified detector, in particular, showed very promising anti-fouling properties upon exposure to diluted urine samples, as well as decreased deactivation from analyte reaction products which was also observed in Chapter Three. Simultaneous measurement of a three-component solution (acetaminophen, UA and AA) was demonstrated using a modified multielectrode detector array. Selective measurement of acetaminophen and CPZ in the presence of UA was possible at the modified detectors using retention time based strategies. However, considering the very high concentration of interferents (especially UA) in urine samples, the multi-detector approach is the more pertinent analytical procedure.

Chapter Seven: Protein adsorption at chemically modified electrodes prepared by the diazonium salt method

7.1 Introduction

The adsorption of high molecular weight species (greater than 5000 Daltons) onto electrode surfaces complicates electrochemical measurements in biological fluids[147]. Electrode fouling causes changes in sensitivity and shifts in redox potentials leading to irreproducibility of response. Polymeric coatings, such as Nafion[30], poly(4-vinylpyridine)[148], poly(ester-sulfonic acid)[149] and cellulose acetate[26,150] have been used to protect electrodes from proteins and other surfactants. These coatings have been applied to anodic[150], and adsorptive[151] stripping analyses and electrochemical detection for flow systems[26,27,58], but their use for direct voltammetric analysis is complicated by slow equilibration of the film with solution species. At present, treatment procedures which remove large molecular weight organic species are routinely used prior to making electrochemical measurements in plasma or serum samples. It is desirable, however, to be able to make electrochemical measurements directly in biological fluids without the need for pretreatment protocols as this will simplify and shorten the time for analysis.

Much work has been directed at understanding the mechanisms of protein adsorption at solid surfaces[152]. Proteins are co-polymers of amino acids of varying hydrophobicity and as such are amphiphilic and generally highly surface active. The literature includes many contradictory results about the relative importance of factors controlling protein adsorption. This is not surprising considering the number of variables which affect adsorption; for example, the type of protein studied, pH, buffers, ionic strength and surface charge[152,153]. Many different proteins are present in plasma and the majority have isoelectric points less than physiological pH i.e. they are negatively charged[154]. The total protein of normal human plasma or serum is 60 – 80 g L^{-1} and albumin constitutes 40 – 48 g L^{-1} of this[154]. Human serum albumin (HSA) and bovine serum albumin (BSA) have been well characterised[155] and are very similar in size, structure and charge having molecular weights of 66 439 and 66 267 Daltons and net charges at pH 7 of -15 and -18, respectively. Hence BSA, which is routinely used in protein adsorption studies[147,153,156-159] was chosen as the model protein in this work.

When surfaces are first exposed to plasma, the adsorption of albumin dominates, but at longer times other proteins which interact more strongly with the surface become important[153]. Generally, albumin will adsorb at hydrophobic or hydrophilic surfaces even when substrate-protein electrostatic interactions appear unfavourable[147-149] and it is

thought that a two step adsorption mechanism operates[157,158]. The first step involves the irreversible adsorption of the protein and the second, the irreversible transformation of the adsorbed proteins to a more covering layer. The adsorption of albumin is entropically-driven and the favourable entropic force arises from the spreading out of the protein and ensuing dehydration as the inner, more hydrophobic regions of the macromolecule interact with the substrate[152,159].

Some of the most well-studied protein resistant surfaces are those covered with poly(ethylene oxides)[160-163], (PEOs). The importance of density and length of PEO modifier has been investigated both theoretically[161,162] and experimentally (by ellipsometry) at well-defined surfaces formed by self-assembly of ethylene glycol terminated ω-functionalised alkanethiols[160,163]. These studies indicate that long chain PEOs are more effective at preventing protein adsorption although shorter modifiers which are more densely assembled do exclude surfactants.

The work described in this chapter is aimed at generating modified GC surfaces that are resistant to protein adsorption and hence give superior electrochemical response (relative to unmodified surfaces) in biological fluids. It was anticipated that monolayer modification would offer protection from fouling without significantly slowing the response time of the electrode, thus permitting use of measurement techniques such as DPV. Neutral, negatively and positively charged electrode coatings were prepared using the diazonium salt coupling procedure.

In order to assess the amount of protein adsorption at the various electrode surfaces, the response of probe analytes were compared in the presence and absence of BSA. If the response is unperturbed by BSA, it may be assumed that there is no significant blocking of the electrode surface by adsorbed protein. Conversely, if the signal is affected by the presence of BSA, either protein adsorption is significant or the analyte interacts with BSA in solution. In the latter case, the effect on the response will depend on the lability of the probe-BSA complex. Thus, for simple interpretation of results, initial experiments identified probe analytes for which interactions with BSA in solution do not influence the electrochemical response. It may then be assumed that any changes in electrochemical response in the presence of BSA arises entirely from protein-surface interactions.

7.2 Experimental

7.2.1 Preparation of solutions

All electrochemical measurements described in this chapter were made in PBS (pH 7.4). The method of preparation of analyte/BSA solutions is given in Chapter Two.

7.2.2 Measurement of analyte/BSA interaction using FIA

Flow injection analysis utilised manifold (1) with detector (a) described in Chapter Two.

Comparison of effective timescales of electrochemical techniques. The ferric chloride and ferric chloride/hydrogen peroxide solutions were prepared in 0.15 M sulfuric acid. The ferric ion reduction was recorded using DPV and HDV techniques. Hydrogen peroxide was then added from a 0.2 M stock solution and the measurements repeated. The potential was changed between 0.3 and -0.5 V vs SCE and the maximum ratio of catalytic current observed in the presence of peroxide to that in its absence (i_k/i_d) was measured using the peak current in DPV experiments and the plateau currents in HDV. Solutions were kept under N_2 and concentrations were 0.2 mM Fe^{3+}/2 mM H_2O_2 (DPV and HDV).

Hydrodynamic voltammograms of probe analytes in the presence and absence of BSA. Analyte concentrations in the range 0.02 – 0.2 mM were used with 4 g L^{-1} BSA. The hydrodynamic voltammogram of the analyte only (in PBS) was recorded at the unmodified GC detector followed by the analyte-BSA solution. A single measurement was made at each potential. All sample solutions were thoroughly degassed and kept under N_2 during the experiment. The flow injection analysis apparatus was cleaned by passing dilute ethanol, nitric acid and finally DDW through the system.

Hydrodynamic voltammograms at cellulose acetate coated GC detectors. The method used to modify GC detector electrodes was based on a previously described procedure[27] and is the same as that described for GC electrodes in Chapter Two. HD voltammograms were recorded in the absence and presence of BSA (4 g L^{-1}) as described above.

7.2.3 Preparation of CMEs.

The GC electrodes were modified with *p*-carboxylic acid groups by the standard procedure using either the *p*-phenylacetate or *p*-benzoate diazonium salts. Carboxylic acid functional groups coupled to the electrode were activated by conversion to an acid chloride or exposure to an aqueous carbodiimide and then reacted with amine pyridinium salts as

described below. The preparations of pyridinium and bipyridinium salts are given in Chapter Two.

Para-phenylacetate CMEs were stirred in 0.1 M CMCT/acetate buffer pH 4.5 for 1 h. The electrode was then rinsed with PBS and stirred overnight in a large excess (50 – 85 mg mL^{-1}) of the amine.

Para-benzoate CMEs were refluxed in a 50/50 v/v mixture of thionyl chloride and dry benzene for 24 h[164]. The electrodes were then stirred in a solution of dry benzene and (ca. 17% w/v) poly(ethylene glycol), PEG, $OH(CH_2–CH_2O)_nH$, n = 200 or 6000 for 40 h. PEGs were dried over molecular sieves (4 Å).

7.2.4 Differential pulse voltammetry

Differential pulse voltammtery was used to measure the oxidation of FcOH or FCA in PBS (pH 7.4) at unmodified and modified electrodes. Scans were between -0.1 and 0.4 V vs SCE at a scan rate of 2 mV s^{-1} with a pulse amplitude of 25 mV and a pulse rate of 0.5 s. Solutions of 2 x 10^{-4} M FcOH (or FCA) with or without BSA (4 g L^{-1}) were used. At least two DP voltammograms were recorded in each of the non-BSA and BSA solutions with brief stirring between scans. Electrode modifications were carried out in triplicate and the averaged results were used.

7.3 Results and discussion

7.3.1 Selection of the model system to assess protein adsorption at electrode surfaces

Choice of probe analytes and model protein. Flow injection analysis with electrochemical detection was used to examine the interactions of potential probe analytes with BSA. The aim of these experiments was to identify analytes with responses which were unaffected by interactions with BSA in solution. In the absence of electrode fouling this will result in superimposable HD voltammograms for the analyte in the presence and absence of BSA. It was anticipated that electrode fouling would be minimised by the short sample/electrode contact times of FIA. Figures 7.1 and 7.2 show HD voltammograms of 2 x 10^{-4} M FCA and FcOH with and without 4 g L^{-1} BSA. In each set of experiments, the HD voltammograms in the absence of BSA was recorded first.

Figure 7.1: Hydrodynamic voltammograms of 2 x 10^{-4} M FCA (PBS) in the absence and presence of 4 g L^{-1} BSA recorded at a flow rate of 0.49 mL min^{-1}

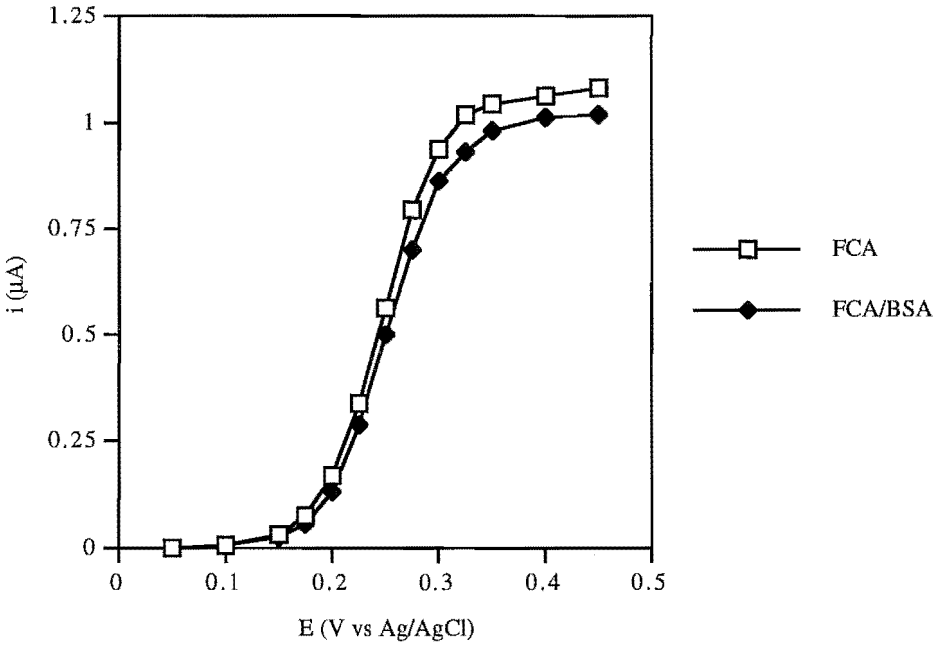

Figure 7.2: Hydrodynamic voltammograms of 2 x 10^{-4} M FcOH (PBS) in the absence and presence of 4 g L^{-1} BSA recorded at a flow rate of 0.49 mL min^{-1}

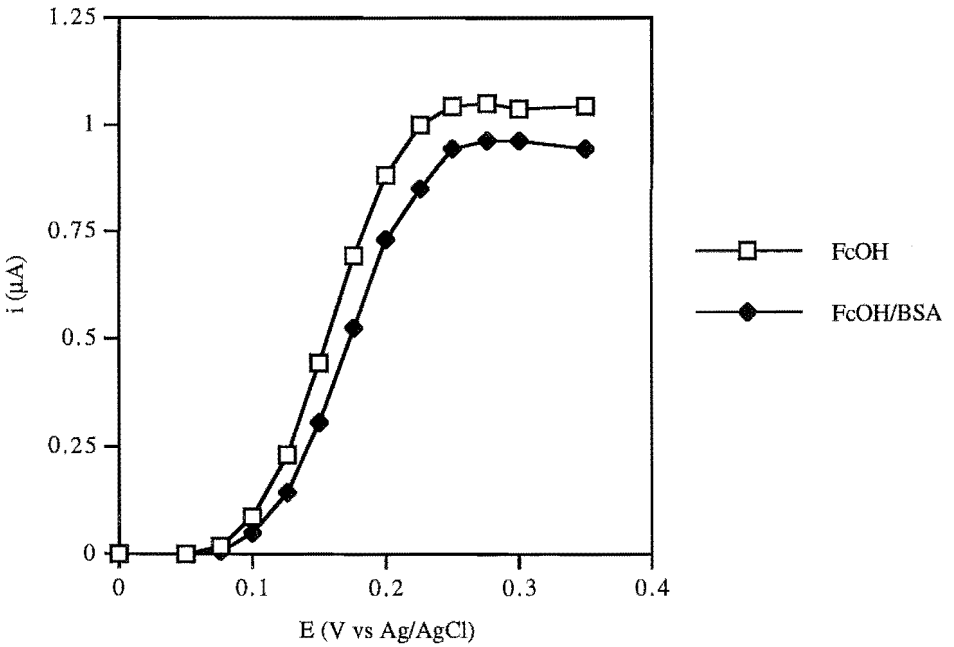

For both analytes, the HD voltammograms are nearly superimposable with a small decrease in currents observed for HD voltammograms recorded in the presence of BSA. This is attributed to some blocking of the electrode surface by protein adsorption during the experiment. Consistent with this, a HD voltammogram of analyte only, measured after the FCA-BSA experiment gave a response which was the same as the analyte-BSA result. Lowering the concentration of BSA produced HD voltammograms which were not significantly different to that in the absence of protein and similarly an FCA concentration of 2×10^{-5} M gave the same HD voltammograms in the absence and presence of BSA (4 g L^{-1}). Thus, for these analytes there was no evidence of analyte-protein interaction in solution.

Hydrodynamic voltammograms of ruthenium(III) hexaammine in the presence of BSA, however, were substantially different to those in its absence. At a BSA concentration of 4 g L^{-1} the plateau current of ruthenium hexaammine was increased relative to that observed in the absence of BSA. This result is shown in Figure 7.3. As noted above some BSA adsorption occurs at the unmodified GC detector at this protein concentration. It appears that ruthenium hexaammine interacts with adsorbed BSA and this enhances the response of this analyte by increasing its effective concentration at the detector surface. To investigate this further, HD voltammograms of ruthenium hexaammine under conditions where protein adsorption should be less important i.e. with a 10 fold lower concentration of BSA (0.4 g L^{-1}) were obtained. Under these conditions, the plateau current arising from the ruthenium hexaammine solution in the presence of BSA was lower than that obtained in the absence of BSA. This suggests that ruthenium hexaammine is interacting with BSA in solution and that the complex is not labile on the timescale of these FIA measurements. Hence, the electrochemical response of ruthenium hexaammine does not give unambiguous information about the amount of BSA adsorption. Therefore all further experiments utilised FCA and FcOH as probe analytes.

Figure 7.3: Hydrodynamic voltammograms of 2 x 10^{-5} M ruthenium hexaammine (PBS) in the absence and presence of 4 g L^{-1} BSA recorded at a flow rate of 0.49 mL min^{-1}

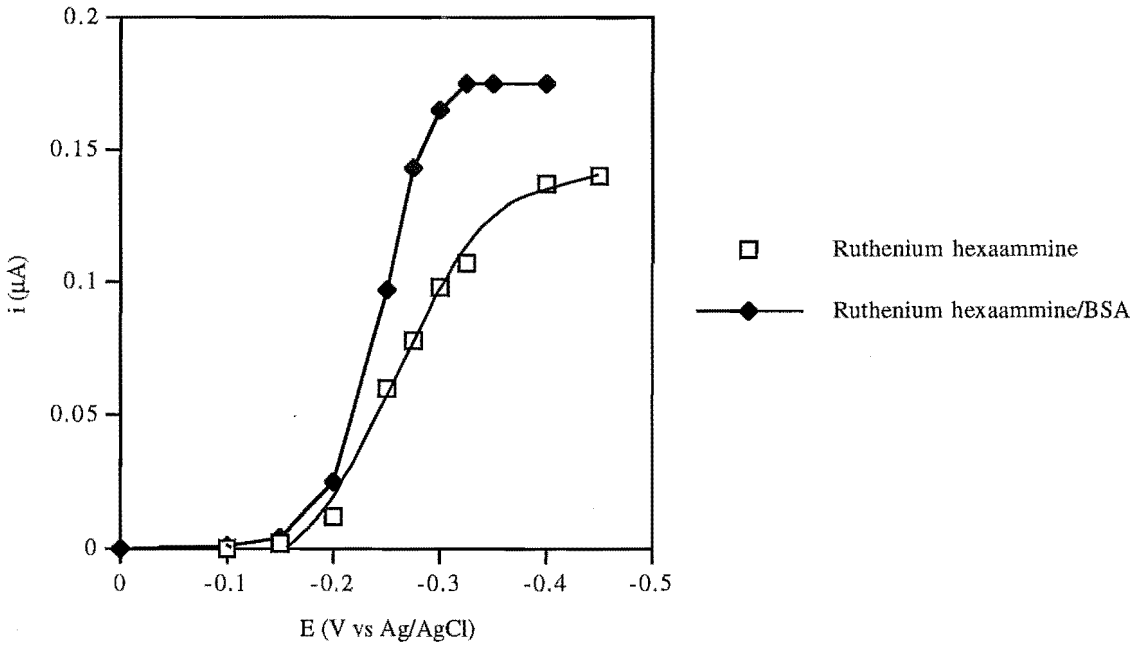

Timescale of the FIA experiment. The absence of detectable FcOH- and FCA-BSA interactions in solution during FIA experiments may arise from the timescale of the technique. To compare timescales of FIA with DPV, the influence of a well-characterised coupled homogeneous reaction on the electrochemical response was measured using each technique.

The reaction chosen to ascertain the effective timescale of FIA was the catalytic oxidation of ferrous ion by hydrogen peroxide which is summarised in Scheme 7.1. In the presence of peroxide, the current for the reduction of ferric ion is enhanced by an amount related to the concentration of peroxide, the rate constant (k_f) and the timescale of the measurement. Thus by keeping all other parameters constant, the amount of current enhancement of Fe^{3+} reduction in the presence of peroxide is an indicator of the effective timescale of the technique. This is expressed quantitatively as the ratio of the kinetically limited current (in the presence of peroxide) to the diffusion limited current in the absence of peroxide), i_k/i_d. Figure 7.4 compares (i_k/i_d) obtained in FIA with that from DPV at different scan rates.

Scheme 7.1: Mechanism for ferric ion reduction in the presence of hydrogen peroxide

$$Fe^{3+} + \bar{e} \rightleftharpoons Fe^{2+}$$

$$Fe^{2+} + 1/2\ H_2O_2 + H^+ \xrightarrow{k_f} Fe^{3+} + H_2O$$

Figure 7.4: Relative timescales of DPV and FIA electrochemical techniques as measured by the ratio of catalytic to non-catalytic current for ferric ion reduction

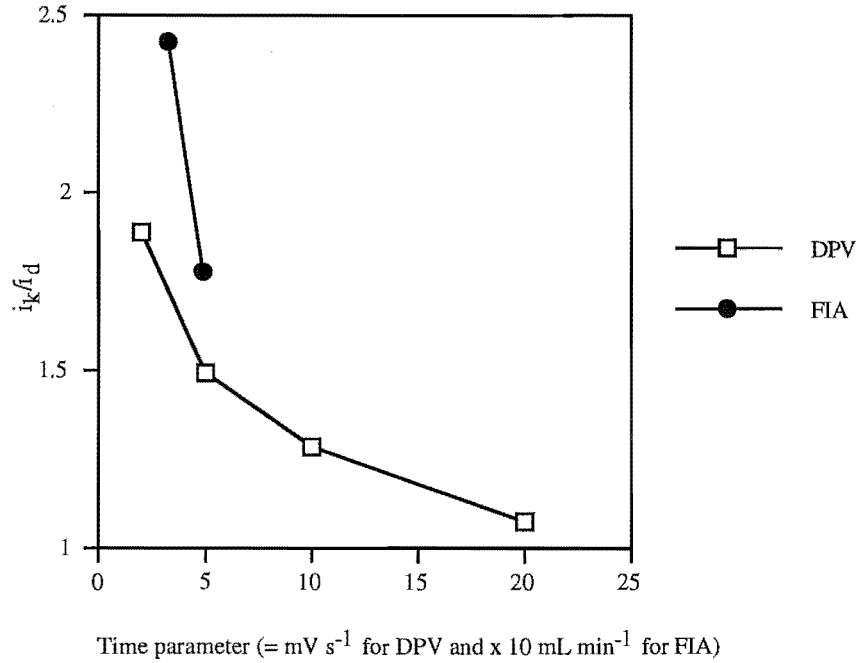

The flow rate of 0.49 mL min^{-1} used in FIA to assess analyte/BSA interaction gives a i_k/i_d ratio of 1.8. The same ratio is expected in DPV experiments with ν = 3 mV s^{-1} (pulse amplitude = 25 mV). Due to instrumental limitations DPV experiments were conducted using ν = 2 mV s^{-1}. Hence, for probe analytes FCA and FcOH which do not interact with BSA on the timescale of the measurement, a decrease in peak height in differential pulse voltammetric experiments when BSA is present in solution can be assumed to result from fouling of the electrode surface by BSA adsorption.

7.3.2 Adsorption of BSA at unmodified GC electrodes

The effect of BSA adsorption on the CV and DPV responses of FCA and FcOH were very similar; Figure 7.5 shows the results for FCA at unmodified GC. On addition of 4 g L^{-1} BSA, cyclic voltammograms (ν = 100 mV s^{-1}) exhibit an increase in ΔE_p from 60 to 68 mV, and $i_{p,a}$ decreases to 82% of its initial value. For DPV, $E_{p,a}$ shifts from 285 to 290 mV on addition of BSA and $i_{p,a}$ decreases to 80% of its initial value. These changes indicate that adsorption of BSA blocks the GC surface.

The response in the presence of BSA was reproducible and stable with time and with repeat scans. For repeat CV experiments (in which the electrode was polished before each scan) the RSD was 3% (n = 15). An RSD of 1% was calculated for 19 consecutive repeat CV scans recorded at an electrode (with stirring for ca. 3 s between) which was freshly polished before the first scan.

Figure 7.5: Differential pulse voltammograms (A) of 2 x 10^{-4} M FCA and cyclic voltammograms (B) of 1 x 10^{-3} M FCA in the absence (a) and presence (b) of 4 g L^{-1} BSA

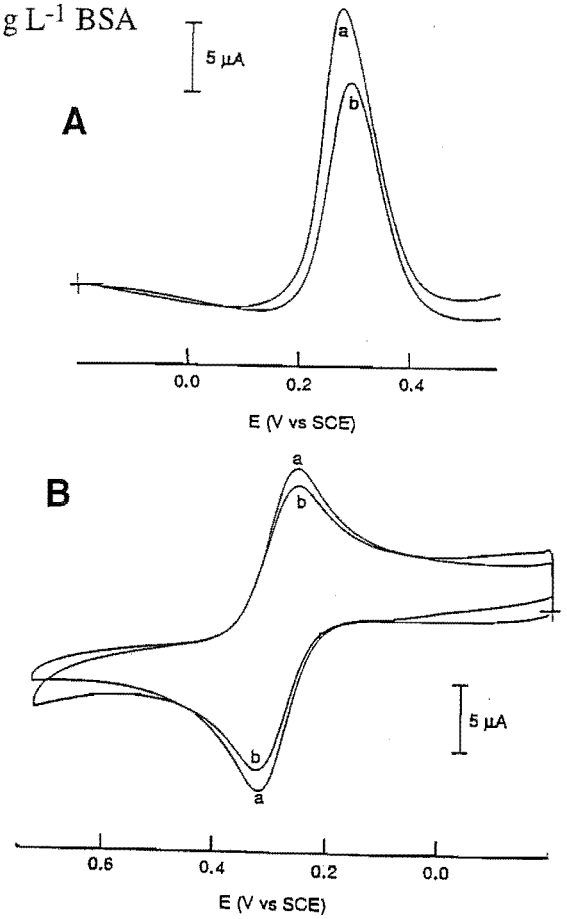

7.3.3 Protein adsorption at CMEs prepared by direct diazonium coupling procedures and aqueous carbodiimide coupling of amines

Protein adsorption was examined at a series of GC electrodes derivatised using the diazonium coupling procedure. The preparations of *p*-benzoate (**I**), *p*-phenylacetate (**II**) and *p*-methoxybenzene (**III**) CMEs were as described previously. Pyridinium and bipyridinium modified surfaces were prepared by reacting carboxylic acid group of a *p*-phenylacetate modified electrode with the corresponding amine. *Para*-phenylacetate was used, as it is reported to be more reactive than the *p*-benzoate functionality[43]. In the first step the carboxylic acid group was activated with an aqueous coupling agent (CMCT).

Following this, the activated group was stirred in an amine solution for ca. 16 h. The attachment of 1-methyl(4-aminomethyl)pyridine is illustrated in Scheme 7.2.

Amine modifiers coupled by this procedure are listed below:

amine modifier	*p*-phenyl substituent	
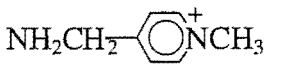	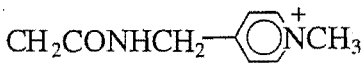	**(IV)**
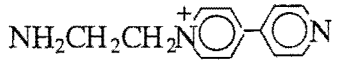	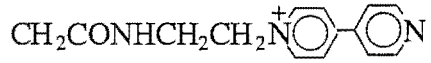	**(V)**
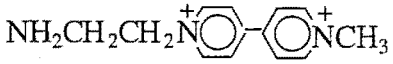	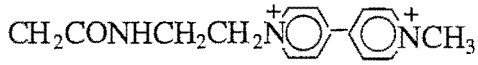	**(VI)**

Scheme 7.2: Reaction scheme for the attachment of 1-methyl(4-aminomethyl)pyridine to the *p*-phenylacetate CME

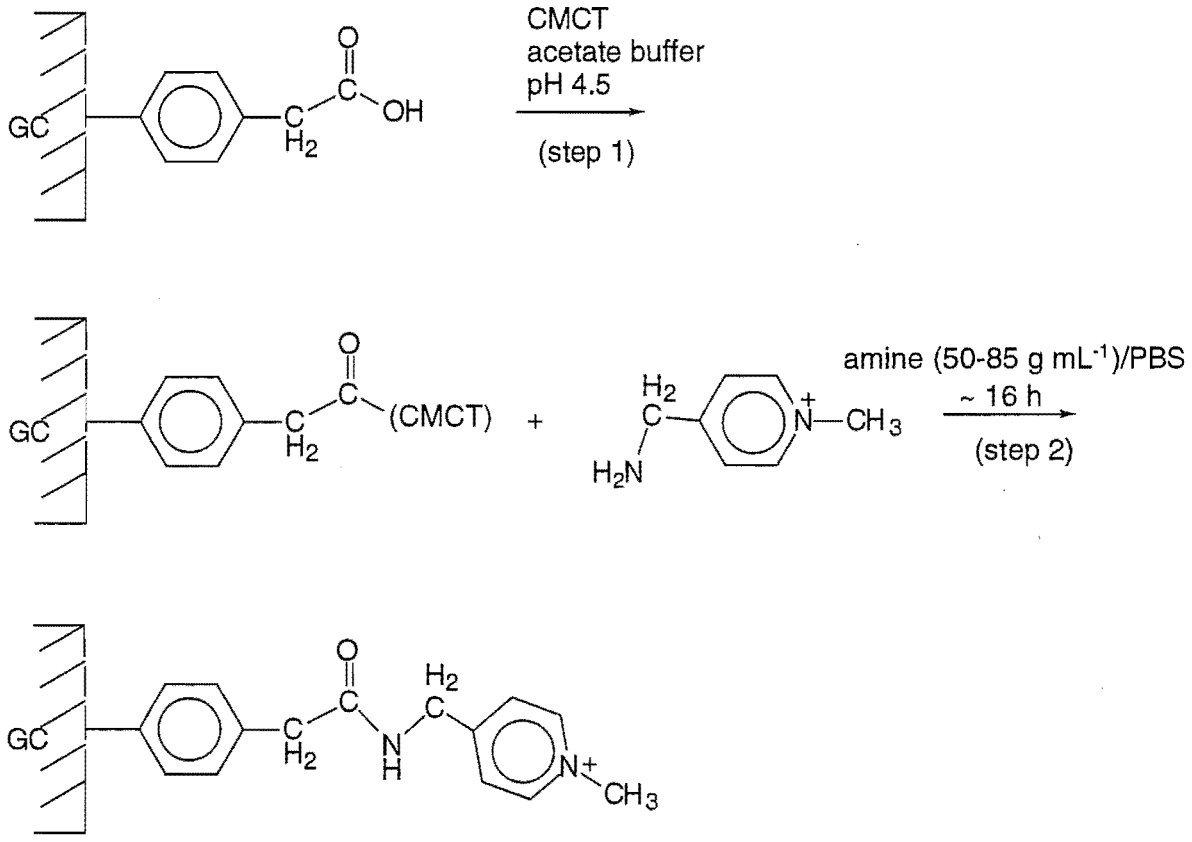

Characterisation of pyridinium and bipyridinium modified electrodes.

The existence of groups on the modified electrodes was established in several ways: for *p*-benzoate **I** and *p*-phenylacetate **II** CMEs, ruthenium(III) hexaammine was accumulated from a 6 μM solution in PBS pH 7.4 and observed with CV. From the enhanced currents at the CME (compared to the unmodified electrodes) it may be deduced that interactions are occurring between the cationic complex and an anionic surface layer. Hence the electrode is successfully modified. The *p*-methoxybenzene **III** and the pyridinium **IV** modifiers are not electroactive and a decrease in CV peak currents for oxidation of FcOH after modification gives indirect evidence that surface groups have been attached. Modification with **V** and **VI** also gave decreased $i_{p,a}{}^{o}$ for FcOH, and the expected electrochemistry of the mono- and diquaternised (bi)pyridinium was observed. The cyclic voltammograms of these CMEs are shown in Figure 7.6 and typical surface coverages, calculated from areas under the cyclic voltammetric peaks, were 3.1 – 3.8 x 10^{-10} mol cm^{-2}. The possibility that the bipyridinium was not covalently bonded but electrostatically attached to the electrode was considered. The bipyridinium electrochemistry persisted on repeat scans and after soaking in 6 μM ruthenium hexaammine there was no evidence for displacement of the bipyridinium or accumulation of ruthenium hexaammine. Thus amide bond formation was assumed to have occurred.

Figure 7.6: Cyclic voltammetric response of CMEs **V** (A) and **VI** (B) in PBS at $\nu = 500$ and 200 mV s^{-1}respectively

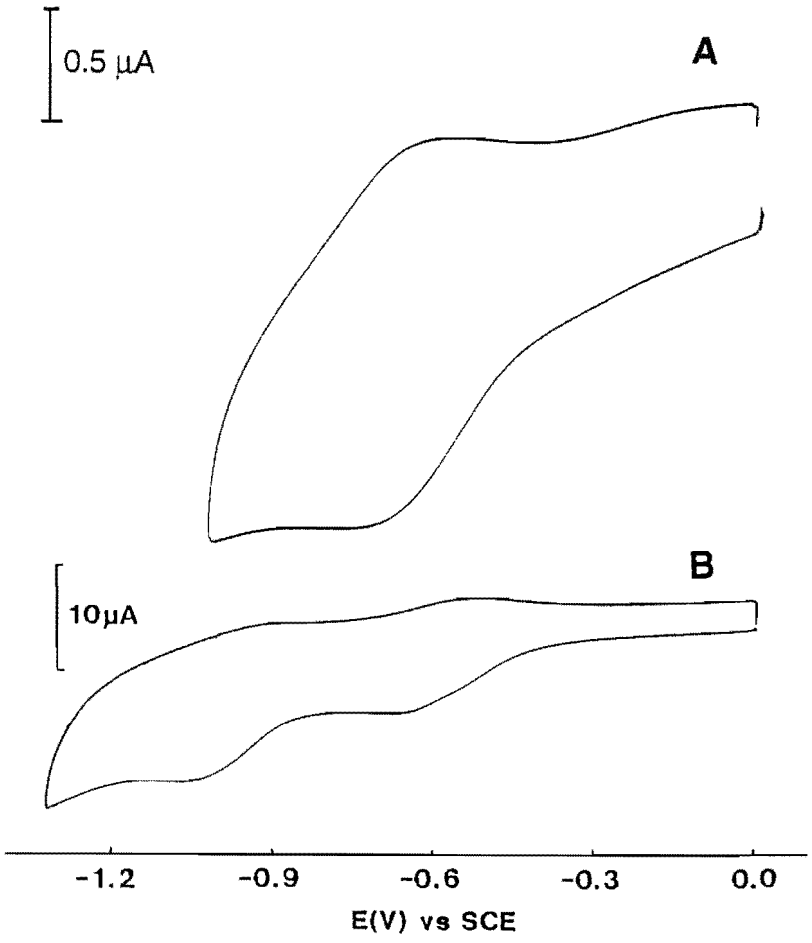

Protein adsorption at the CMEs assessed by FcOH oxidation. Differential pulse voltammetry was used to measure peak currents for oxidation of 2 x 10^{-4} M FcOH in PBS in the absence ($i_{p,a}^{o}$) and presence ($i_{p,a}^{BSA}$) of 4 g L^{-1} BSA at unmodified and modified electrodes. Electrode modifications were made in triplicate and the average results are presented in Table 7.1. Some representative DP voltammograms are shown in Figure 7.7.

Table 7.1: Relative DP voltammetric peak currents for 2 x 10^{-4} M FcOH in the absence and presence of 4 g L^{-1} BSA at unmodified and modified GC electrodes

p-phenyl substituent	$i_{p,a}^{o}$(μA)	$i_{p,a}^{BSA}/i_{p,a}^{o}$
unmodified	2.10±0.03	0.84±0.02
COO^- (**I**)	2.00±0.02	0.83±0.03
CH_2COO^- (**II**)	2.10±0.05	0.92±0.02
OCH_3 (**III**)	1.4±0.3	0.54±0.06
$CH_2CONHCH_2$—⟨⟩$\overset{+}{N}CH_3$ (**IV**)	1.5±0.3	0.84±0.06
$CH_2CONHCH_2CH_2\overset{+}{N}$⟨⟩—⟨⟩N (**V**)	0.4±0.1	0.84±0.02
$CH_2CONHCH_2CH_2\overset{+}{N}$⟨⟩—⟨⟩$\overset{+}{N}CH_3$ (**VI**)	1.0±0.2	0.93±0.03

Figure 7.7: Differential pulse voltammograms recorded in PBS of 2 x 10^{-4} M FcOH in the absence (a) and the presence (b) of 4 g L^{-1} BSA at A) unmodified and B – D) modified GC. B) *p*-phenyl substituent **I**, C) substituent **III** and D) substituent **VI**

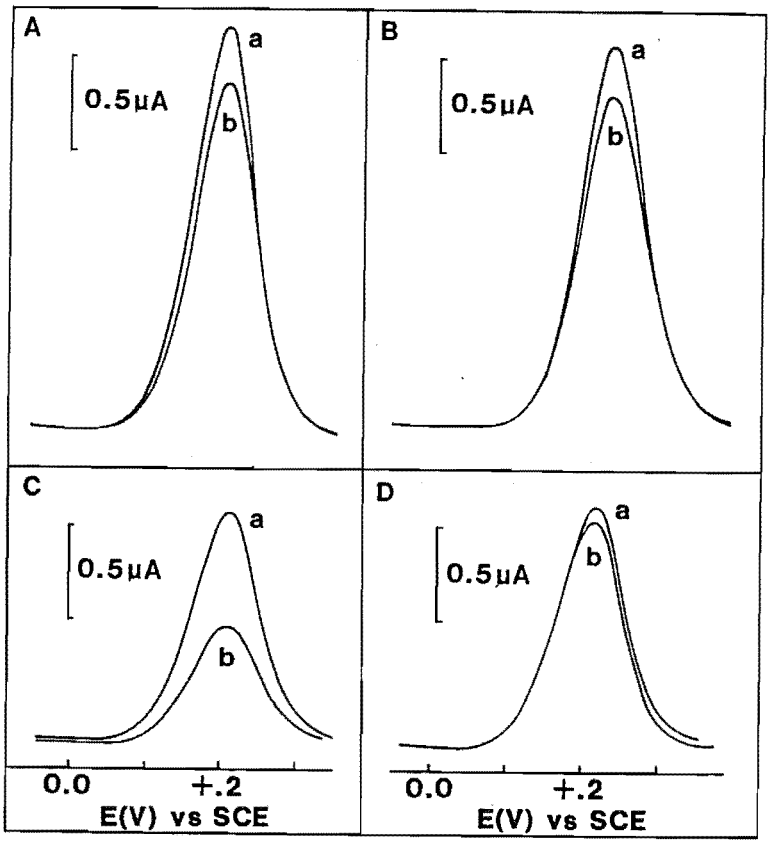

The peak potential for oxidation of FcOH was unchanged at modified electrodes relative to unmodified surfaces. The $i_{p,a}{}^{o}$ values for FcOH at the unmodified and modified electrodes show trends which are qualitatively similar to those described in previous Chapters. Modifiers which are hydrophilic and close to the electrode surface (i.e. CMEs **I** and **II**) have little effect on $i_{p,a}{}^{o}$ for FcOH. The uncharged hydrophobic *p*-methoxybenzene modifier **III**, substantially decreased $i_{p,a}{}^{o}$ of the probe analyte. A similar effect on the behaviour of FcOH peak currents was observed for DPV experiments with *p*-methylbenzene modified electrodes (see Chapter Five). The $i_{p,a}{}^{o}$ for FcOH in the presence of long modifiers (**IV**, **V** and **VI**) was decreased to varying degrees indicating that FcOH response was not merely a function of modifier length. It is assumed that the sensitivity for FcOH oxidation reflects the density, steric bulk and length of modifying groups. The yields of the coupling reactions between surface phenylacetates and amines is undoubtedly influenced by the charge densities of the resulting layers. Hence **VI** may form a less compact layer than **IV** and **V** because **VI** is doubly-charged. Comparing **IV** and **V**, both steric bulk and extension into solution are greater for **V** resulting in less FcOH reaching the surface at electrodes modified with **V**.

Second and more importantly, is the effect of modification on protein adsorption. According to the $i_{p,a}{}^{BSA}/i_{p,a}{}^{o}$ ratio the amount of BSA adsorption, relative to unmodified GC, increases at *p*-methoxybenzene **III** modified electrodes, is unchanged for modifiers **I**, **IV** and **V** and decreases for **II** and **VI**.

Considering modifiers **I** and **II**, *p*-phenylacetate **I** significantly decreased protein adsorption whereas modification with *p*-benzoate **II** groups did not change the peak current ratio in the presence and absence of BSA (relative to unmodified GC). Both CMEs have been shown in previous chapters to have comparable surface coverage of modifying groups. Thus, the increased peak current ratio observed at the *p*-phenylacetate CME relative to **II** may be due to the increased distance that this modifier extends from the electrode surface which would decrease the likelihood of protein interaction with the underlying electrode surface and hence protein adsorption.

The results for *p*-methoxybenzene **III** suggest that hydrophobic groups which are close to the surface make the electrode more prone to protein adsorption. This is consistent with the accepted model for BSA adsorption. In this model BSA adsorption is believed to be entropically driven by loss of associated water groups as the hydrophobic interior of the BSA molecule is brought into contact with a hydrophobic substrate[152]. Thus, increasing the hydrophobicity of the electrode surface is expected to facilitate protein adsorption.

The different behaviours of surfaces prepared from modifiers (**IV**, **V** and **VI**) in the presence of BSA suggest that two factors are operative: (i) interactions of the protein with the head groups via electrostatic attractions and, for modifier **V**, hydrogen bonding with the pyridine nitrogen, and (ii) blocking of protein access to the surface via size-exclusion. The first effect decreases access of FcOH to the electrode in the presence of protein and the second decreases the amount of protein adsorption. The most favourable situation (in terms of preventing protein adsorption) arises for CME **VI**. In this case it is thought that BSA interaction with the head groups of the modifier is disfavoured (and consequently the passage of FcOH to the electrode surface is not blocked) whilst the protein itself is blocked by a sufficiently dense modifying layer.

Analytical utility of the p-phenylacetate CME. Of the CMEs examined above, the *p*-phenylacetate modified electrode showed the most promising behaviour in the presence of BSA i.e. the peak current of FcOH was unaffected by modification and the protein adsorption was decreased. In the following experiments the *p*-phenylacetate electrode is applied to the measurement of biological analytes, acetaminophen and 4-MC in the presence of BSA. The acetaminophen-BSA interaction in solution was examined using a cellulose acetate coated GC detector to eliminate complications which arise from protein adsorption at the unmodified GC detector.

Preparation of the hydrolysed CA coating is described in Chapter Two. Application of the cellulose acetate coating successfully prevented protein adsorption and gave HD voltammograms for FCA which were almost identical in the presence and absence of BSA (see Figure 7.8).

An increasing current was observed for the FCA/BSA solution at potentials greater than 0.3 V and injections of BSA/PBS confirmed that this signal arose from the BSA solution. This response was attributed to sodium azide, which is electroactive over the same potential range and is used as a preservative for the BSA solution. The contribution from this other electroactive source only became important when analyte currents were low i.e. at coated detectors and the response of the BSA/PBS solution was subtracted from subsequent HD voltammograms of solutions containing BSA. The HD voltammogram of 2 x 10^{-5} M acetaminophen and 2 x 10^{-5} M acetaminophen plus 4 g L^{-1} BSA at the cellulose acetate (CA) coated detector are shown in Figure 7.9.

Figure 7.8: Hydrodynamic voltammograms of 2 x 10^{-5} M FCA/PBS in the presence and absence of 4 g L^{-1} BSA at a cellulose acetate coated GC detector

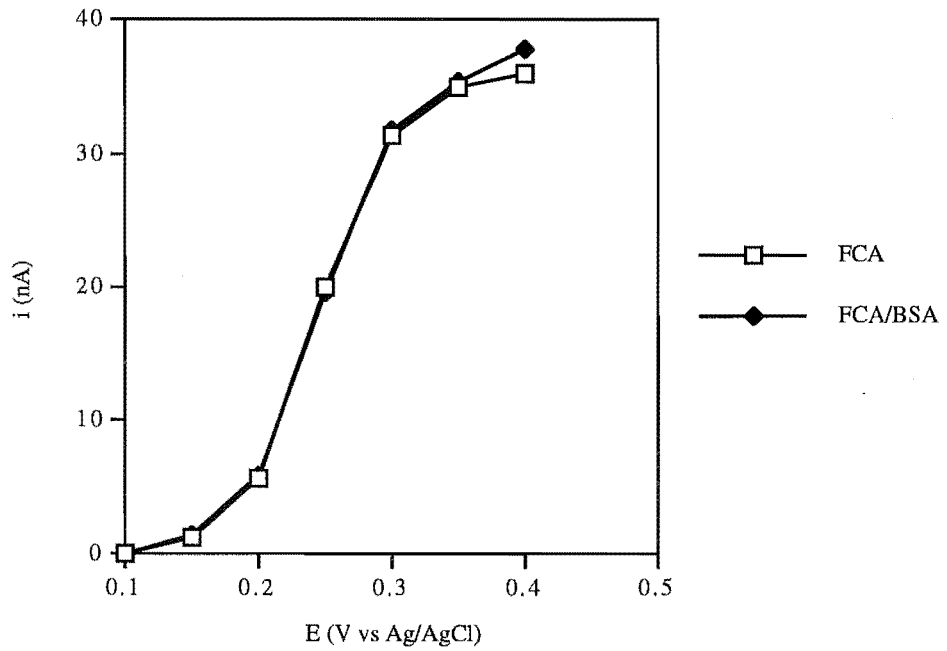

Figure 7.9: Hydrodynamic voltammograms of 2 x 10^{-5} M acetaminophen/PBS in the presence and absence of 4 g L^{-1} BSA at a cellulose acetate coated GC detector

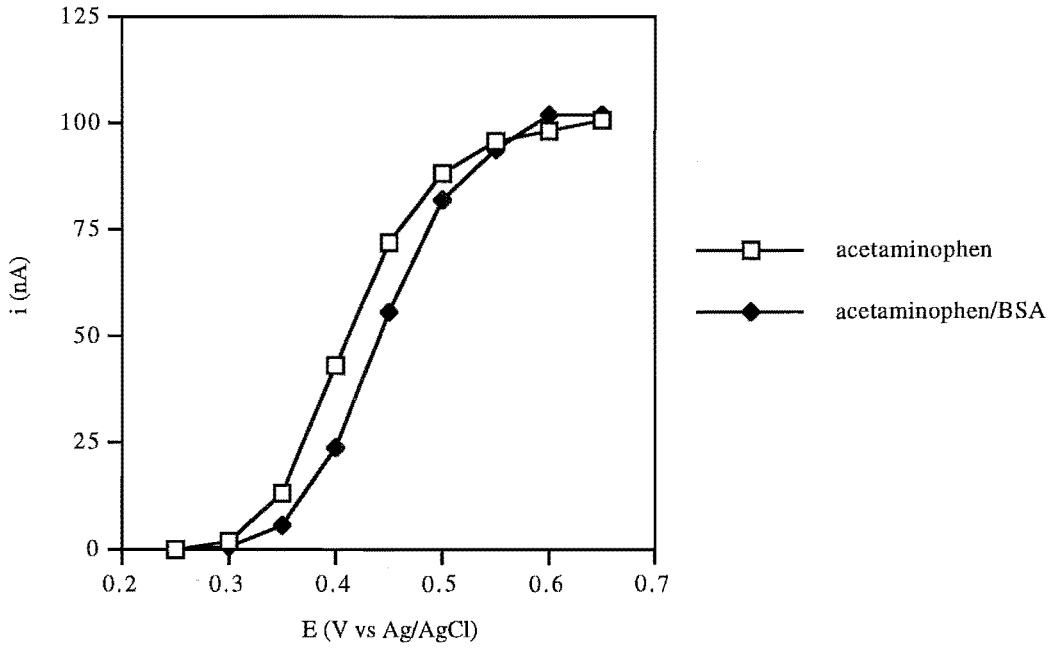

In the presence of BSA, the plateau current is unchanged, and $E_{1/2}$ is shifted to a more positive potential. This response is consistent with a CE (chemical step-electrochemical step) mechanism in which dissociation of an acetaminophen-BSA complex is fast on the electrochemical timescale[165]. A similar result is expected for DPV measurements i.e. peak currents for acetaminophen oxidation should be unperturbed by solution-based interactions of acetaminophen with BSA.

DPV of acetaminophen and 4-MC at the p-phenylacetate electrode. To investigate the analytical usefulness of this CME the DP voltammetric response of acetaminophen and 4-MC in the presence and absence of BSA was examined. Table 7.2 summarises the response of acetaminophen and 4-MC in BSA adsorption studies at unmodified GC and the *p*-phenylacetate CME.

Table 7.2: Electrochemical data for DP of acetaminophen and 4-MC (2×10^{-5} M/PBS) at unmodified and *p*-phenylacetate modified electrodes in the presence and absence of BSA[a]

analyte electrode type	$i_{p,a}^{o}$ (ave) (μA)	$E_{p,a}^{o}$ (V)	$i_{p,a}^{BSA}$ (μA)	$E_{p,a}^{BSA}$ (V)	$i_{p,a}^{BSA}/i_{p,a}^{o}$
acetaminophen unmodified GC	0.75	0.45	0.375	0.50	0.50
acetaminophen *p*-phenylacetate	0.40	0.45	0.30	0.455	0.76
4-MC unmodified GC	0.50	0.24	0.275	0.25	0.55
4-MC *p*-phenylacetate	0.32	0.25	0.25	0.25	0.78

[a] 4 g L^{-1} BSA, scan rate = 2 mV s^{-1}, data shown are the average results for n = 4 electrodes

The $i_{p,a}^{o}$ of both acetaminophen and 4-MC are decreased at the *p*-phenylacetate CME, relative to the unmodified electrode, possibly due to a decrease in adsorption of these species at the CME compared to GC. At the unmodified electrode, $i_{p,a}^{BSA}/i_{p,a}^{o}$ is significantly smaller than observed for probe analytes FcOH and FCA. For acetaminophen, the peak current in DPV experiments is not expected to be affected by interaction with BSA and hence the decrease in $i_{p,a}^{BSA}/i_{p,a}^{o}$ must be due to an increased effect of protein adsorption on this analyte with less reversible electrode kinetics. The interaction of BSA with 4-MC was not examined and hence the lower ratio for 4-MC may arise from the former effect and BSA-interactions. Acetaminophen shows a relatively large (50 mV) positive shift in $E_{p,a}$ with the addition of BSA at the unmodified electrode whilst 4-MC changes by only 10 mV in the presence of 4 g L^{-1} BSA.

Importantly, $i_{p,a}^{BSA}/i_{p,a}^{o}$ increased at the *p*-phenylacetate electrode and $E_{p,a}^{o} \approx E_{p,a}^{BSA}$ for both acetaminophen and 4-MC indicating BSA adsorption was decreased. Although the reproducibility of $i_{p,a}^{BSA}/i_{p,a}^{o}$ for repeat polishing or CME preparation was poor, the *p*-phenylacetate electrode gave improved results relative to unmodified GC i.e. the RSD for $i_{p,a}^{BSA}/i_{p,a}^{o}$ of acetaminophen went from 28% (n = 4) to 21% (n = 4) and that of 4-MC decreased from 28% (n = 4) to 7% (n = 4) after modification of the electrode.

Hence, the *p*-phenylacetate CME has desirable properties for use in media containing albumin.

7.3.4 Attempted preparation of poly(ethylene glycol) derivatised GC electrodes

In these experiments, GC electrodes were modified with *p*-carboxylate moieties in the usual way, following which they were converted to the acid chloride by a reported procedure[164]. Batches of four electrodes were simultaneously refluxed in a 50/50 (v/v) benzene/thionyl chloride solution and these electrodes were then exposed to PEG solutions. Scheme 7.3 illustrates the reactions attempted at the GC electrode surface.

Scheme 7.3: Proposed synthesis of the PEG modified electrode

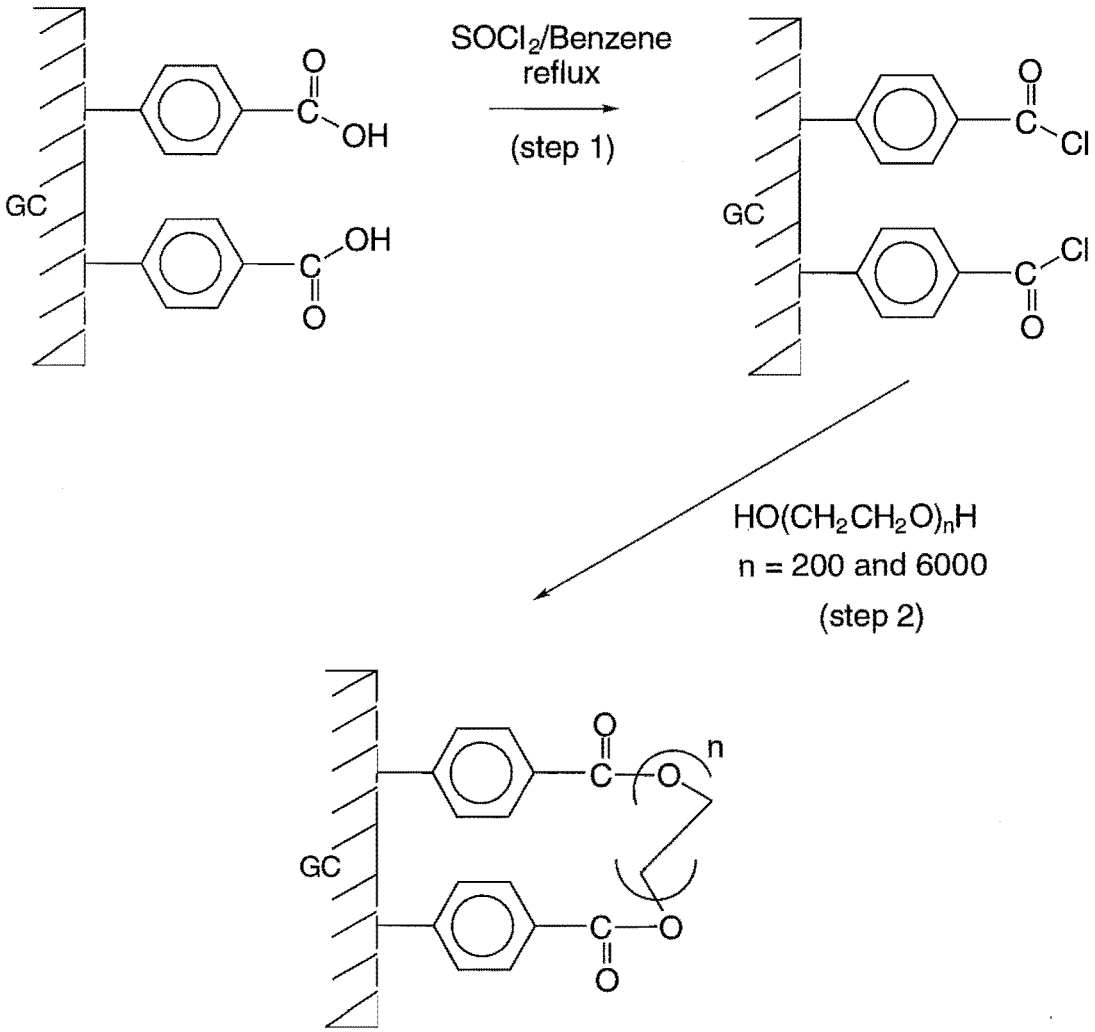

DPV was used to record the response of FCA (2 x 10^{-4} M/PBS) in the presence and absence of 4 g L^{-1} BSA at the modified electrode. The ratio of peak currents, $i_{p,a}{}^{BSA}/i_{p,a}{}^{o}$, was significantly decreased after the modification procedure described above. Control experiments in which *p*-benzoate CMEs were refluxed in the benzene/$SOCl_2$ mixture but not exposed to PEG also gave very low $i_{p,a}{}^{o}$ values and $i_{p,a}{}^{BSA}/i_{p,a}{}^{o}$ decreased (relative to

polished unreacted GC) indicating that protein adsorption was increased. The results for a typical set of PEG (n = 6000) "modified" electrodes are shown in Table 7.3.

Table 7.3: DPV of 2 x 10^{-4} M FCA/PBS in the presence and absence of 4 g L^{-1} BSA at treated and unmodified GC[a]

Treatment	$i_{p,a}^{BSA}/i_{p,a}^{o}$	$i_{p,a}^{o}$
polished, unreacted	0.83	1.69
control	0.37	0.345
"modified"[b]	0.38	0.266

[a] scan rate = 2 mV s^{-1}

[b] average results for triplicate electrode preparations, RSD of $i_{p,a}^{BSA}/i_{p,a}^{o}$ was 32% (n = 3)

There is no significant difference between the result at the control and "modified" electrodes and hence it is assumed that coupling of the PEG was not successful. It is most likely that reaction of the acid chloride activated electrode with water (rather than PEG) accounts for this result. Clearly, coupling reactions which proceed via the acid chloride activated CME give poor electrode response. Similar reactions with aqueous CMCT might prove more successful but were not attempted.

7.4 Conclusions

The amount of protein adsorption at a GC electrode may be controlled by monolayer modification of the surface. An increase in hydrophobicity increases protein adsorption whereas anionic/hydrophilic groups very close to the surface have no effect on protein adsorption. Hydrophilic groups which extend further into solution can decrease protein adsorption at the GC surface. When long modifiers are present, sensitivity to the analyte decreases, thus, relatively short hydrophilic monolayers were found to be the most suitable surface for measurements in the presence of protein.

Chapter Eight: Protein adsorption at electrochemically pretreated and chemically modified carbon electrodes

8.1 Introduction

In the previous chapter, it was shown that covalent modification of GC with charged groups which extend out into solution decreases protein adsorption whilst adsorption of BSA is increased by hydrophobic groups close to the surface. In this chapter, experiments aimed at modifying the nature of carbon electrode surfaces by electrochemical pretreatments (ECPs), aggregation of charged surfactants and modification with polymer coatings are described. The performance of these surfaces in the presence of protein is assessed.

Electrochemical pretreatment of carbon electrodes is routinely used to enhance the electrochemical response of analytes. Such treatments are particularly useful for biological species which often show poor kinetics at unpretreated carbon electrodes. Further, ECPs may enhance sensitivity of some analytes by inducing adsorption onto the electrode surface. Oxidative pretreatment in acid generates a porous layer rich in surface oxides, which has been described as electrochemical graphite-oxide (EGO)[51]. The same type of surface results from severe pretreatment (≥ ca. 1.5 V vs SCE) in neutral solutions. Pretreatments in base and by square-wave in NaCl solution increase the density of surface oxides (relative to the untreated electrode) without formation of EGO. These ECPs may also clean the surface, removing hydrophobic adsorbents and exposing pristine carbon sites. Both changes are expected to enhance the hydrophilicity of the surface, while oxide formation has the additional effect of conferring a negative charge on the surface at sufficiently high pH.

Electrochemical pretreatment of GC detectors by anodisation for 30 min at 1.5 V vs Ag/AgCl in neutral media, has been shown to decrease electrode deactivation caused by NADH, CPZ and dinitrophenol reaction products and to inhibit adsorption of BSA and plasma proteins in FIA conditions[87]. The pretreatment, however, did not confer the same properties for voltammetric measurements in quiescent solutions. The difference in electrode behaviour was attributed to dissimilarities in the electrochemical experiments, particularly exposure time of the electrode to the passivating species[87].

Amphiphilic surfactants have been used in electrochemical studies to investigate interactions between micelles and electroactive species[166] and to promote the electron transfer of some redox couples with slow kinetics at carbon surfaces[60-62]. At solution concentrations above the critical micelle concentration (cmc) it has been proposed that charged surfactants form hemimicelle layers at GC and rough pyrolytic graphite (RPG) electrodes[61]. In this case surface-head-tail-tail-head interactions produce a charged modifying layer.

An alternative method that has been used to enhance the electrochemical response of an otherwise slow redox couple is modification of basal plane graphite (BPG) with the anionic surfactant sodium dodecyl sulfate (SDS)[60]. Basal plane graphite is a very hydrophobic electrode material thus favourable hydrophobic interactions between the hydrocarbon tail of the surfactant molecule and the BPG are thought to occur leaving the charged head extending into solution.

Cellulose acetate (CA) films when applied to detectors in flowing streams can confer desirable antifouling properties to the electrode surface[26,27]. In an early study, Pt detectors were modified with CA films and the response of hydrogen peroxide was measured before and after exposure of the detector to BSA or serum. Peak currents of peroxide were unaffected by prior injection of organic foulants[26]. Base-hydrolysis of CA films has been used to increase the permeability of these coatings allowing measurement of larger analytes whilst retaining selectivity against high molecular weight organic adsorbents in flowing systems[27]. An alternative phase-inversion strategy has been applied to produce anisotropic CA coatings[37]; the preparation of these films is described in Chapter One.

In this Chapter, work aimed at preparing electrode surfaces which showed decreased susceptibility to electrode fouling is described. Initial experiments involved a systematic study of BSA adsorption at various types of carbon electrode surfaces. Electrode fouling was monitored by measuring perturbation of probe analyte response in the presence of BSA, as described in Chapter Seven. Electrochemical pretreatments commonly used to change the surface morphology of carbon electrodes (and hence the response of analytes) were applied to GC and graphite epoxy (GE) electrodes and BSA adsorption at these surfaces was examined. Protein adsorption was also investigated at CMEs which were assumed to have charged groups extending out from the electrode surface. These were prepared by immobilisation of charged surfactants into graphite epoxy and onto basal plane graphite (BPG) carbon surfaces. Attempts to prepare CA coatings which exclude BSA and give satisfactory response to the probe analytes in CV experiments are also described.

8.2 Experimental

8.2.1 Electrochemical pretreatment procedures

Electrochemical pretreatment in acid. The procedure of Cabaniss and coworkers was followed[86]. An activation cycle consisted of 30 s at 1.8 V, followed by 15 s at -0.2 V in 0.1 M H_2SO_4.

Electrochemical pretreatment in base. The procedures were based on those of Beilby and Carlsson[93]. In a solution of 1 M NaOH, the potential was scanned at 100 mV s^{-1} from 0 V to the upper potential limit and held at that potential for the required time. In some experiments, the potential was then scanned to a lower value and held at that potential before returning to 0 V.

Electrochemical pretreatment by square-wave. Modifications of the method of Wang and Hutchins[91] were used. Square waveforms of amplitudes ± 6 V, ± 7.5 V and ± 10 V were applied at frequencies of 35 or 20 Hz for the required time. Degassed saturated, or 1 M NaCl solutions were used.

8.2.2 CME preparation and experimental procedures

All analyte solutions were prepared in PBS pH 7.4. Temporary GC and graphite electodes were used for studies involving ECP and the fabrication of these are described in Chapter Two. The preparation of carbon paste, graphite epoxy and surfactant-graphite epoxy electrodes are also described in Chapter Two. The surfactants used in this study were; sodium dodecyl sulfate (SDS = $CH_3(CH_2)_{11}OSO_3Na$) which is a monoanion at pH 7.4 and hexadecyltrimethylammonium bromide (CTAB = $CH_3(CH_2)_{15}N(CH_3)_3Br$) which is a monocation at pH 7.4.

Polishing procedures and DPV experiments with GE electrodes. Prior to each set of DP voltammograms, electrodes were polished for 2 min on wet 600 grit sand paper, rinsed in DDW and further polished on 4/0 emery paper for 4 min. Electrodes were thoroughly rinsed with DDW between use in each analyte solution. Measurements were made in the order: analyte only followed by analyte-BSA. For each solution, 4 repeat voltammograms were recorded with stirring for ca. 5 s before each measurement. The peak current for the third DP scan in each solution was used as it was found to be a good approximation of the average response for 4 repeat scans. A scan rate of 5 mV s^{-1} and pulse amplitude of 25 mV were used.

Basal plane graphite procedures A new basal plane surface was prepared by cleaving the electrode parallel to its base with a razor blade, followed by sonication in DDW for ca. 5 min. For DPV measurements at unmodified BPG, the electrode was then placed in 2 x 10^{-4} M FCA solution and two scans were recorded with stirring for ca. 3 s between. Following this the electrode was removed, rinsed with DDW and placed in the FCA/BSA solution and scanned twice as above.

Prior to surfactant modification a fresh BPG surface was prepared and two DP voltammograms were recorded in the FCA solution. The electrode was then rinsed with DDW and modified by a reported procedure[60] which involved submerging the electrode in a stirred or quiescent solution of 1 g L^{-1} surfactant/ethanol. Ionic surfactants SDS and CTAB were used. After soaking in the modifying solution, the electrode was rinsed in DDW and DP voltammograms were recorded in the presence and absence of BSA as described above. Two types of BPG were used in these experiments: a coarse type, National AG KSP with geometrical area = 0.196 cm^2 and a finer material, POCO FX1 with geometrical area = 0.126 cm^2.

Preparation of cellulose acetate coatings. Base-hydrolysed and phase-inversion cellulose acetate coatings are described in Chapter Two.

8.3 Results

8.3.1 Protein adsorption at untreated carbon surfaces

BSA adsorption at untreated GC, graphite, carbon paste, graphite epoxy and basal plane graphite electrodes. Protein adsorption at electrodes composed of different carbon materials was investigated using DPV of the probe analyte FCA. As described in Chapter Seven, the change in sensitivity on addition of BSA is indicated by the ratio $i_{p,a}{}^{BSA}/i_{p,a}{}^{o}$ where $i_{p,a}{}^{BSA}$ and $i_{p,a}{}^{o}$ correspond to anodic peak currents in the presence and absence of BSA, respectively. Figure 8.1 shows the effect of increasing BSA concentration on the relative response ratios at various carbon electrodes.

Figure 8.1: Differential pulse voltammetric peak current ratios for 2 x 10^{-4} M FCA in the presence and absence of BSA at different carbon materials and with varying concentrations of BSA

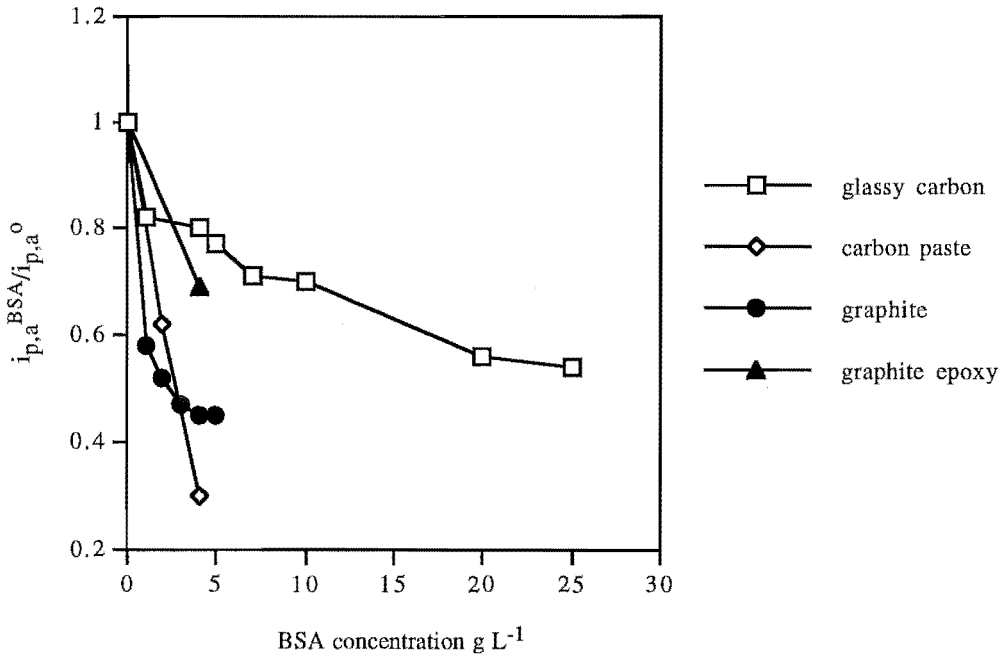

Glassy carbon gave consistently higher values of $i_{p,a}^{BSA}/i_{p,a}^{o}$ compared to graphite epoxy (GE), graphite and carbon paste (CP) surfaces. The response of FCA at GC showed a regular decrease as BSA content of the analyte solution was increased. Comparison of the different carbon surfaces with a constant amount of BSA present (4 g L^{-1}) showed that CP was affected the most by adsorption followed by graphite, basal plane graphite (BPG), GE and finally GC. These results are summarised in Table 8.1.

Table 8.1: Relative DPV peak currents for 2 x 10^{-4} M FCA in the presence and absence of BSA (4 g L^{-1}) at carbon electrodes[a]

	glassy carbon	**graphite**	**carbon paste**	**basal plane graphite[b]**	**graphite epoxy**
$i_{p,a}^{BSA}/i_{p,a}^{o}$	0.80±0.02 (n = 8)	0.46±0.02 (n = 3)	0.3±0.05 (n = 3)	0.71±0.03 (n = 12)	0.69±0.02 (n = 8)

[a]scan range = -0.2 to 0.55 V, scan rate = 5 mV s^{-1}, third scan in each solution reported [b]scan rate = 2 mV s^{-1}

Experimental results described in Chapter Seven indicated that hydrophobic groups close to the electrode surface increase BSA adsorption. The greater amount of protein adsorption at CP and GE (relative to GC) is attributed to the hydrophobic nature of the binder in these electrodes. The high-density graphite may have more basal plane character than GC and hence a more hydrophobic surface. The basal plane graphite results were obtained using the POCO FX 1 type BPG. These surfaces were less prone to BSA adsorption than might be expected considering their supposed large basal plane content and anticipated high hydrophobicity. The reason for this is not known although the method of resurfacing may be important if it produces a mixture of basal and edge plane graphite. For repeat experiments, the RSD for $i_{p,a}^{BSA}/i_{p,a}^{o}$ at GC was 2.5% (n = 8); the poorest reproducibility was observed at CP which gave an RSD of 15% (n = 3).

8.3.2 Protein adsorption at electrochemically pretreated GC

Electrochemical pretreatments are routinely applied to carbon electrodes to increase the sensitivity and electrode kinetics of biological analytes. Further, these pretreatments have been reported to yield electrode surfaces with greater wettability, as evidenced by decreased contact angles for water, compared to unpretreated electrodes. Hence, protein adsorption at ECP GC electrodes is of interest for two reasons: to examine the effect of creating a more hydrophilic surface and to ascertain how routinely applied ECPs are likely to affect electrode performance in biological matrices. Three types of ECP were investigated: dc pretreatment in acid[86], dc pretreatment in base[93] and square-wave pretreatment in chloride solution[91]. The probe analyte FCA was used for these studies and Tables 8.2, 8.3 and 8.4 show the effects of BSA adsorption on GC electrodes following these pretreatments.

Differential pulse voltammetry of 2 x 10^{-4} M FCA in the presence and absence of 4 g L^{-1} BSA was used to assess the effect of severe pretreatment in acid. As shown in Table 8.2, pretreatment in acid leads to a progressive loss of sensitivity in the presence of BSA i.e. $i_{p,a}^{BSA}/i_{p,a}^{o}$ was decreased, indicating BSA adsorption increased with increasing electrode "activation". When the oxidative step was not followed by reduction $i_{p,a}^{o}$ for FCA, and sensitivity in the presence of BSA decreased dramatically.

Table 8.2: Relative DPV peak currents for 2 x 10^{-4} M FCA in the presence and absence of 4 g L^{-1} BSA at acid pretreated electrodes[a]

No. of activation cycles	$i_{p,a}^{o}$ (μA)	$i_{p,a}^{BSA}$ (μA)	$i_{p,a}^{BSA}/i_{p,a}^{o}$
0	2.12	1.70	0.80
1	2.02	1.50[b]	0.74
2	2.00	1.22[b]	0.61
3	1.92	1.10[b]	0.57
90 s at 1.8 V	0.94	0.20[b]	0.21

[a]scan range = -0.2 to 0.55 V, scan rate=5 mV s^{-1}, [b]$i_{p,a}^{BSA}$ decreased on repeat scans

Table 8.3 shows CV and DPV results following base pretreatment. Pretreatment in base involving oxidative and reductive steps increased sensitivity in the presence of BSA (compared to untreated GC); however, for repeat DPV measurements there was an ~1% decrease in peak current sensitivity per scan. For CV measurements, the first scan gave erratic results, but the peak currents for subsequent voltammograms were constant. There was a small increase in ΔE_p (75 to 80 mV) in the presence of BSA after base pretreatment with oxidative and reductive steps.

Table 8.3: Relative peak currents for FCA in the presence and absence of BSA at base-pretreated GC electrodes

electrochemical pretreatment	DPV[a] $i_{p,a}^{BSA}/i_{p,a}^{o}$	CV[b] $i_{p,a}^{BSA}/i_{p,a}^{o}$
none	0.80	0.82
1.0 V, 5 min	0.69	0.84
1.4 V, 5 min	0.73	0.81
1.5 V, 1 min and -1.0 V, 1 min	0.83	0.87

[a] conditions as for Table 8.2; $i_{p,a}^{o}$ = 2.1 μA with and without pretreatment
[b] scan range = -0.2 to 0.55 V; ν = 100 mV s^{-1}; ~ 0.7 x10^{-3} M FCA; 4 g L^{-1} BSA; $i_{p,a}^{o}$ = 12 μA with and without pretreatment

The effect of square-wave pretreatment on GC electrodes was investigated using CV and the resulting electrochemical data are shown in Table 8.4. Square-wave pretreatment in aqueous NaCl also improved the response in the presence of BSA. The loss of sensitivity is reduced, and the response is stable on repeat scans. For 20 consecutive CV scans in the presence of BSA on an electrode pretreated with a square-wave of ±7.5 V at 20 Hz for 7 min, the RSD was 2%. The change in ΔE_p on addition of BSA varied randomly between 0 and 5 mV. Thus pretreatments in base and by square-wave reduced albumin adsorption.

Table 8.4: Relative CV peak currents for FCA in the presence and absence of BSA at square-wave pretreated GC electrodes[a]

potential limits (V)	**frequency (Hz)**	**duration (min)**	**NaCl concentration**	$i_{p,a}^{BSA}/i_{p,a}^{o}$
no pretreatment	—	—	—	0.82
±6	35	2	1 M	0.85
±6	35	5	1 M	0.88
±6	35	7	saturated	0.86
±10	35	1	saturated	0.88
±7.5	20	7	saturated	0.88

[a] conditions as for CV results in Table 8.3; $i_{p,a}^{o}$ = 12 μA with and without pretreatment

Acetaminophen response in the presence and absence of BSA at electrochemically pretreated GC. Having established that pretreatments under the appropriate conditions in base or by square-wave decrease BSA adsorption, these treatments were applied to GC electrodes for measurement of acetaminophen. Differential pulse voltammetry was used to measure the response of acetaminophen (2×10^{-5} M/PBS) in the absence and presence of BSA (4 g L^{-1}) and the results are shown in Table 8.5.

Table 8.5: Relative DPV peak currents for acetaminophen in the presence and absence of BSA at pretreated GC electrodes[a]

pretreatment	$E_{p,a}^{o}$ (V)	$E_{p,a}^{BSA}$ (V)	$i_{p,a}^{o}$ (nA)	$i_{p,a}^{BSA}$ (nA)	$i_{p,a}^{BSA}/i_{p,a}^{o}$
none	0.45	0.48	71	37	0.52
base[b,c]	0.32	0.33	800	490	0.61
square-wave[c,d]	0.37	0.39	137	100	0.73

[a] 2 x 10^{-5} M acetaminophen; scan rate = 2 mV s^{-1}, [b] 1.5 V (1 min), -1.0 V (1 min), [c] $i_{p,a}^{o}$ and $i_{p,a}^{BSA}$ decreased on repeat scans, first scan reported, [d] ± 6 V, 35 Hz, 5 min, saturated NaCl

Both pretreatments improved the ratio $i_{p,a}^{BSA}/i_{p,a}^{o}$; the loss in sensitivity in the presence of BSA was least after square-wave pretreatment. However, the reproducibility of response was better at the base-treated electrode. For the ratio $i_{p,a}^{BSA}/i_{p,a}^{o}$, the RSD was 1% (n = 4) after base ECP and 10% (n = 4) after square-wave ECP. At the polished electrode, the RSD was 10% (n = 12).

Peak currents were strongly enhanced after base pretreatment, while there was less than a twofold enhancement following square-wave ECP. Peak current enhancement after pretreatment can be ascribed to accumulation of analyte at the electrode surface and/or to improved electrode kinetics.

Experiments with FCA showed that BSA adsorption was less after base pretreatment than after the square-wave pretreatment used here. In contrast, for acetaminophen the more favourable ratio is obtained using square-wave ECP, indicating that the effects of accumulation of analyte must be considered. Partial blocking of the electrode surface by adsorbed BSA may prevent accumulation of analyte, while permitting oxidation of solution species. Thus, when BSA is present the electrochemical response that originates from accumulated analyte is decreased more than that which originates from solution species. It is therefore possible that an ECP which results in a very strong accumulation of analyte could give rise to a response that is more sensitive to protein adsorption than that at a polished electrode.

Similar experiments were attempted with UA. For this analyte however, the DPV response in the absence of BSA at unpretreated electrodes was very variable. Base ECP had a qualitiatively similar effect on UA response to that observed for acetaminophen i.e. a large enhancement of both i_p^o and i_p^{BSA} following activation and an improved peak current ratio in the presence of BSA. Square-wave pretreatment had a smaller effect on peak currents though the large variation in response after this ECP together with the irreproducible peak currents for UA at unpretreated electrodes prevents any further interpretation of results. The great sensitivity of this analyte to the condition of the electrode surface presumably arises from slow electrode kinetics and adsorption of oxidation products. Thus, DPV would not be the method of choice for UA measurement in clinical samples, even with ECP of the GC electrode.

8.3.3 Protein adsorption at graphite epoxy electrodes

Incorporation of charged surfactants into graphite epoxy electrodes. As shown in Table 8.1, graphite epoxy electrode materials gave decreased sensitivity in the presence of BSA relative to GC. Incorporation of surfactants, ion-exchange resins and redox mediators into the carbon-epoxy mixture during preparation can produce CMEs which are robust and have reproducible surface properties[69]. Hence, BSA adsorption was examined at unmodified GE electrodes and GE electrodes modified with charged surfactants in order to investigate the effect of conferring a charge on the electrode surface. Further, these electrodes were pretreated using the square-wave procedure.

Evidence for charge generation at the modified GE electrode. The peak currents of FCA and ruthenium(III) hexaammine were recorded using DPV at unmodified GE electrodes and GE electrodes into which 10% w/w surfactant had been incorporated. Surfactants used in this study were sodium dodecyl sulfate (SDS) which is a monoanion at pH 7.4 and hexadecyltrimethylammonium bromide (CTAB) which is a monocation at pH 7.4. Table 8.6 shows the differential pulse peak currents arising from probe analytes present at 2×10^{-4} M (ruthenium(III) hexaammine) and ~1.7×10^{-4} M (FCA) in PBS at unmodified GE and electrodes with 10% w/w surfactant.

Table 8.6: Differential pulse voltammetric peak currents of analytes at unmodified and surfactant modified GE electrodes[a]

electrode type	$Ru(NH_3)_6^{3+}$ $i_{p,c}^{o}$ (μA)	FCA $i_{p,a}^{o}$ (μA)
unmodified GE	0.44	0.38
GE-SDS	1.01	0.56
GE-CTAB	0.60	0.96

[a] 5 mV s^{-1}, scan range = -0.2 to 0.55 V FCA , 0.0 to -0.5 V $Ru(NH_3)_6^{3+}$

Both analytes gave greatest peak currents at the electrode incorporating the surfactant of opposite charge, consistent with the generation of the expected charged surfaces at the GE electrodes. Interestingly, incorporation of surfactant with the same charge as the analytes, still resulted in i_p^o values which were increased relative to the unmodified electrode. This may arise from an increase in the effective driving force for electron transfer at the charged surface (as discussed in Chapter One). Thus a negative charge at the surface of the electrode will increase the effective potential difference ($\phi_M - \phi_2$) driving the oxidation of FCA and similarly the positive charge will decrease the effective potential difference and increase the apparent reduction rate of ruthenium hexaammine[75].

Effect of incorporating different amounts of surfactant into GE electrodes. Cyclic voltammetry of FCA was used to investigate the response of GE-SDS electrodes prepared from different weight% of surfactant. As the weight% of surfactant increased (for compositions of 5, 10 and 36%), the peak current for FCA oxidation decreased and ΔE_p increased due to increasing electroinactive area. However, the peak current ratio in the presence and absence of BSA was optimised at the 10% w/w GE-SDS electrode ($i_{p,a}^{BSA}/i_{p,a}^{o} = 0.79$) and this composition was used in subsequent experiments.

BSA adsorption at unmodified, surfactant modified and square-wave pretreated GE electrodes. Protein adsorption was investigated at GE electrodes using DPV with FCA as the probe analyte. The resulting electrochemical data are shown in Table 8.7. The response of 2 x 10^{-4} M acetaminophen/PBS at unpretreated and square-wave pretreated GE and GE-SDS electrodes is also included in Table 8.7.

Table 8.7: Differential pulse voltammetric response of 2 x10^{-4} M acetaminophen and 2 x10^{-4} M FCA in the presence and absence of 4 g L^{-1} BSA at GE electrodes[a]

electrode type	FCA i_p^o (μA)	FCA i_p^{BSA} (μA)	FCA $i_{p,a}^{BSA}/i_{p,a}^o$	Acetaminophen $i_{p,a}^o$ (μA)
unpretreated				
unmodified GE	0.375	0.26	0.69	0.385
GE-SDS	0.58	0.46	0.79	0.105
GE-CTAB	0.81	0.58	0.72	—
square-wave pretreated				
unmodified GE	0.34	0.26	0.76	0.385
GE-SDS	0.49	0.41	0.84	0.190
GE-CTAB	0.81	0.59	0.73	—

[a] pretreatment was ± 6 V, 35 Hz, 5 min in saturated NaCl, DPV scan rate = 5 mV s^{-1}

The GE-SDS electrode is more resistant to BSA adsorption than the unmodified GE electrode. The incorporation of cationic surfactant results in a smaller increase in relative peak currents in the presence and absence of BSA. Square-wave pretreatment further increases $i_{p,a}^{BSA}/i_{p,a}^o$ at all GE electrodes although the peak current for FCA oxidation is relatively unaffected at unmodified and GE-CTAB electrodes and decreases at GE-SDS. The reasons for this were not investigated further. To be useful for analysis, the CME must respond satisfactorily to biological analytes and thus the response of acetaminophen at the GE and GE-SDS electrodes was also examined. Increasing the amount of inactive electrode area (by incorporating surfactant) has a much greater effect on the $i_{p,a}^o$ of acetaminophen (compared to results for FCA) due to its slower electrode kinetics. This is improved to some extent by square-wave pretreatment. Hence, although this CME is resistant to BSA the overall sensitivity to acetaminophen is decreased which makes it less desirable than GC as an electrode material for acetaminophen determination.

8.3.4 Protein adsorption at surfactant modified basal plane graphite

Aggregation of surfactants on BPG may be used to generate a charged electrode surface[60]. Hence, protein adsorption at BPG surfaces exposed to charged (SDS and CTAB) surfactants was examined.

Surfactant accumulation at the BPG surface is indicated by a decrease in background currents in CV experiments[60]. Two types of BPG were soaked in a 1 g L^{-1} SDS/ethanol solution and their CV background currents were recorded in PBS after 0, 1 and 60 min with a scan from 0.8 to -0.8 V at ν = 200 mV s^{-1}. Over a 1 h interval the background current of the National AG KSP BPG, measured at 0.6 V, was unchanged whilst that of POCO FX 1 decreased by 27%, as shown in Figure 8.2. All subsequent attempts to produce a modifying surfactant layer at the former BPG electrode were unsuccessful. This sample of BPG consistently gave a higher peak current ratio in the presence and absence of BSA (compared to POCO FX 1) and the surface was visibly uneven. Hence increased edge plane character and surface roughness of this type of BPG may be responsible for poor surfactant assembly. All results described below for BPG apply to POCO FX 1.

Figure 8.2: CV background currents of POCO FX 1 basal plane graphite after (A) 1 and (B) 60 min soaking in 1 g L^{-1} SDS/ethanol

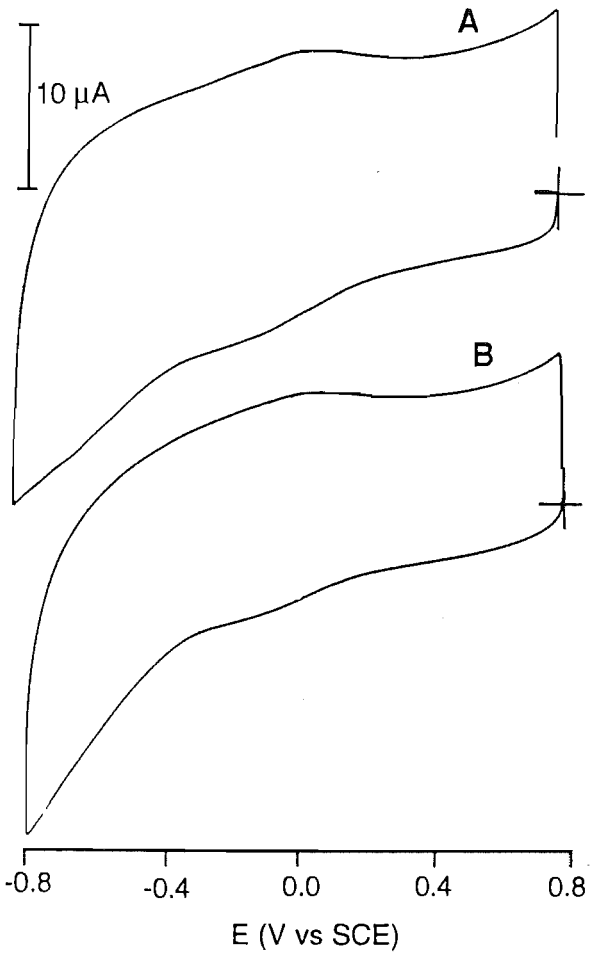

Small oxidation and reduction peaks occur at ca. 0.0 V in the cyclic voltammograms. Similar peaks have been observed at lauric acid (SDS) and laurylamine surfactant-modified BPG electrodes by other workers and were attributed to adsorbed impurities and/or C–O groups present on the electrode surface[60].

BSA adsorption at surfactant treated BPG. Differential pulse voltammetry of FCA was used to investigate BSA adsorption at BPG electrodes modified for varying lengths of time in surfactant/ethanol solutions. The anionic surfactant SDS was used because in previous (GE) studies it gave the best results (in terms of decreasing protein adsorption). The results for SDS modification are presented in Table 8.8.

Table 8.8: Differential pulse voltammetric response of 2 x10^{-4} M FCA in the presence and absence of 4 g L^{-1} BSA at unmodified and SDS treated BPG electrodes[a]

modifying treatment	$i_{p,surf}{}^{o}/i_{p}{}^{o}$	$i_{p,a}{}^{BSA}/i_{p,a}{}^{o}$
none	—	0.71
(1) 5 min, SDS/ethanol	0.96	0.71
(2) 40 min, SDS/ethanol	0.95	0.70
(3) 45 min, SDS/ethanol	0.83	0.75
(4) 50 min, SDS/ethanol	0.76	0.97
(5) 50 min, SDS/ethanol	0.97	0.66
(6) 60 min, SDS/ethanol	0.91	0.69

[a] At bare BPG; $i_{p,a}{}^{o}$ = 5.2 μA, $E_{p,a}{}^{o}$ = $E_{p,a(surf)}{}^{o}$ = 0.27 V and $E_{p,a}{}^{BSA}$ = $E_{p,a(surf)}{}^{BSA}$ = 0.28 V.

A decrease in $i_{p,surf}{}^{o}/i_{p}{}^{o}$ for FCA oxidation indicated that a blocking layer of surfactant was present at the electrode surface. As shown in Table 8.8 most of the electrode treatments failed to produce a successfully modified surface, however, when $i_{p,surf}{}^{o}/i_{p}{}^{o}$ was substantially decreased (electrode modifications (3) and (4)), increased $i_{p,a}{}^{BSA}/i_{p,a}{}^{o}$ values were observed. It is assumed that the hydrocarbon tails of SDS are adsorbed onto the hydrophobic carbon surface and that a charged surface is presented to solution[60]. Improved protein resistance may arise from an increase in hydrophilicity or

could be due to the physical blocking of BSA preventing its access to the electrode. The fact that the peak current of FCA is decreased after successful modification supports the presence of a more organised blocking film at these CMEs.

The possibility that the increased peak current ratio at the successfully modified BPG electrodes arises from the loss of integrity of this coating upon exposure to BSA (and hence the greater response of FCA is due to its increased access to the surface) was considered. Repeat (n = 15) cyclic voltammograms of FCA in the presence of 4 g L^{-1} BSA at a successfully modified electrode showed no change in background current indicating the coating was stable under these conditions.

The poor success rate of modification (i.e. 33%) probably reflects the dependence on the morphology of the underlying carbon surface. Uneven areas and regions of high edge plane content would be expected to disrupt assembly and cause defects in the coatings. It is anticipated that a sample of BPG superior to the one used in this study, would give an increased success rate for modification.

8.3.5 Protein adsorption at cellulose acetate coated GC electrodes

The aim of this work was to prepare CA coated GC electrodes which prevented BSA from fouling the surface but were permeable to the probe analyte, had fast response times and gave undistorted cyclic voltammograms. Coatings were prepared both by drop coating a CA solution (typically 2% w/v) onto the GC electrode followed by base-hydrolysis and by the phase-inversion method.

Base hydrolysed cellulose acetate coated electrodes. This method of preparing modified electrodes gave very irreproducible results (based on the CV response of FCA at the CME) despite stringent attempts to exactly reproduce film preparation procedures. A large number of coatings were prepared in order to establish conditions which gave high permeability to FCA, stable response and cyclic voltammograms which were undistorted. Thus the % w/v of CA in the casting solution was varied from 1, 2 or 5%, the volume applied to the electrode ranged from 1 to 5 µL and hydrolysis times in 0.06 M KOH varied from 15 to 60 min. Protein adsorption studies were not performed at coatings made from 1 or 5% solutions of CA as the responses of FCA at these CMEs were often distorted. Due to the irreproducibility of electrode coatings, which effectively meant identical film preparations performed very differently, it is impossible to give optimum film preparation conditions for preventing protein adsorption. However, relative film thicknesses can be deduced based on the volume of solution used for film preparation. The response of FCA gives a measure of the film permeability and hence the effect of film properties on protein adsorption can be assessed. Table 8.9 summarises CA coating characteristics and the observed protein adsorption at these CMEs.

Table 8.9: Summary of cellulose acetate film thickness, permeability to FCA and response in the presence and absence of BSA

relative coating thickness	**permeability to FCA**	$i_{p,a}^{BSA}/i_{p,a}^{o}$
unmodified	1.0	0.82
thick (5 μL, 2%)	high (0.7)[a]	0.82
thick (5 μL, 2%)	low (0.4)	0.94
moderate (2 μL, 2%)	low (0.2)	0.92
thin (1 μL, 2%)	intermediate (0.6)	0.80
thin (1 μL, 2%)	low (0.4)	0.82

[a] typical value for $i_{p,a}^{o}{}_{mod}/i_{p,a}^{o}{}_{unmod}$

An improvement in the peak current ratio in the presence and absence of BSA, $i_{p,a}^{BSA}/i_{p,a}^{o}$, relative to GC was only observed at coatings at which the response to FCA was decreased at least 50% relative to unmodified GC. Thin coatings e.g. 1 μL polymer solution with hydrolysis times greater than 20 min, were not observed to decrease BSA adsorption even when they gave a low response to FCA. Thicker films (2 or 5 μL polymer solution) typically required hydrolysis times between 40 to 60 min and were more likely to give an increased $i_{p,a}^{BSA}/i_{p,a}^{o}$ ratio when $i_{p,a}^{o}$ for FCA was low. In addition to protection from protein fouling, our interest is to produce a coating which equilibrates rapidly with solution species. To investigate the time required for film-analyte solution equilibration, a coated electrode (2% polymer, 2 μL, 40 min hydrolysis in 0.06 M KOH) was stirred in FCA (~0.8 mM/PBS) and cyclic voltammograms (ν = 100 mV s^{-1}) were recorded at various time intervals. The resulting peak currents for two separate coating preparations are shown in Figure 8.3. At polished GC $i_{p,a}^{o}$ of FCA was 12 μA.

Figure 8.3: Plot of cyclic voltammetric peak currents for FCA (~0.7 mM/PBS) oxidation at CA coated GC electrodes versus stirring time[a]

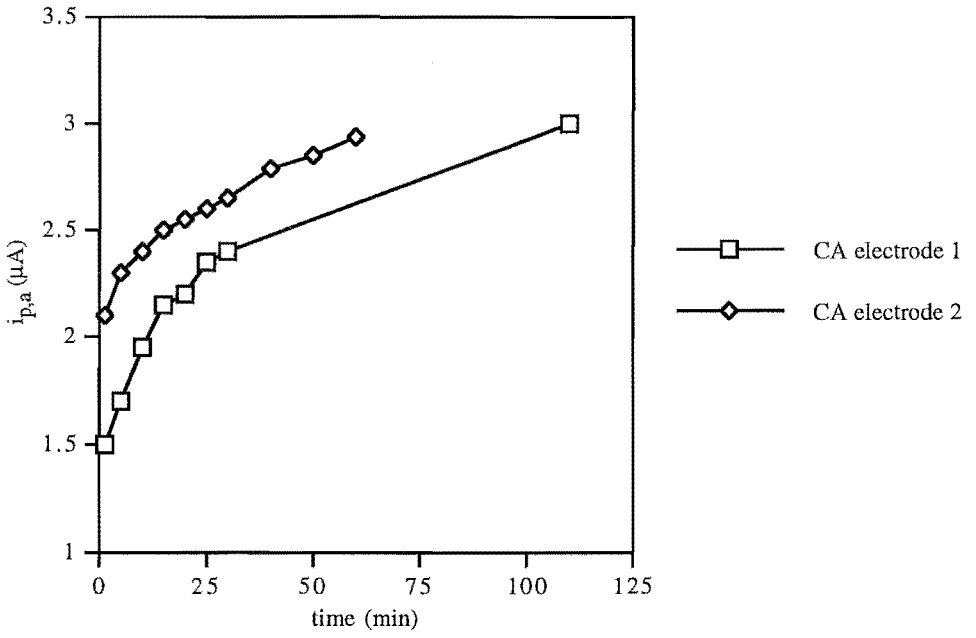

[a] cyclic voltammograms recorded at ν = 100 mV s^{-1}, one scan only

Both coated electrodes showed a strong dependence of peak current on stirring time in probe analyte solution. Clearly the variation in sensitivity is more pronounced at short times (i.e < 20 min) but an equilibrium response was not reached after coating-analyte contact times of more than 1 h. Thus, these coatings are not suited to analyses performed in short time frames.

Phase-inversion cellulose acetate membranes. The conditions chosen to prepare phase-inversion CA membranes in this study were those reported to produce thin films with fast response times[37] i.e. low amounts of CA (1.3%) and $Mg(ClO_4)_2$ (1.9%) were used. Increasing the proportions of these components gives rise to films that are thicker and show decreased diffusion coefficients for analytes. As observed for the base-hydrolysed cellulose coatings above, repeat electrode film preparations showed poor reproducibility. However, increased $i_{p,a}{}^{BSA}/i_{p,a}{}^{o}$ ratios were observed for some CMEs with a best result of 0.93 when 2 μL of CA solution was applied and a drying time of 25 s used. Further, this method of film fabrication produced coatings which were relatively permeable to FCA, typically decreasing $i_{p,a}{}^{o}$ 20–30% from that at uncoated GC and increasing ΔE_p by only 5–15 mV. These membranes also equilibrated with FCA solution more quickly, typically giving reproducible cyclic voltammograms after 10–15 min.

This method of preparing CA coatings was superior to the base-hydrolysis procedure for voltammetric measurements in which contact time in solution was relatively short. However, CME preparation was very irreproducible (for example, an improved ratio for $i_{p,a}{}^{BSA}/i_{p,a}{}^{o}$ compared to the unmodified surface was observed in only 50% of electrode preparations).

8.4 Discussion

8.4.1 Protein adsorption at electrochemically pretreated GC

Electrochemical pretreatments have been reported to increase the hydrophilicity of carbon electrodes[51]. Thus protein adsorption at these pretreated surfaces is of fundamental interest (to investigate the effect of hydrophilicity on protein adsorption), as well as practical interest (to assess how routinely applied ECPs are likely to affect electrode performance in biological matrices). Three different ECP protocols were applied to GC in this study: severe dc pretreatment in acid, which is reported to produce EGO; pretreatment in base and square-wave pretreatment in NaCl. The latter two ECPs are assumed to increase the amount of surface oxides (relative to unpretreated electodes) without the formation of EGO and all ECPs may clean the electrode surface by removing hydrophobic adsorbents.

Electrochemical pretreatments which lead to the formation of a graphite-oxide surface increased BSA adsorption in batch conditions i.e. CV and DPV. Similarly, these ECPs have been applied to enhance the sensitivity of carbon electrodes used as probes for catecholamines and the concomitant increase in response time occurring after pretreatment was attributed to adsorption of high molecular weight organic species[34]. The application of comparable ECPs to glassy carbon detectors in FIA systems, however, significantly improved electrode performance in the presence of foulants[87]. The strength of protein adsorption may be important when rationalising the difference in observed behaviour of these pretreated carbon surfaces in batch and FIA conditions. Increasing the surface roughness of carbon surfaces, for example, has been shown to enhance the rate of BSA adsorption but decrease the strength of the surface-protein interactions[167]. Hence, in FIA conditions the roughness effect (or other properties of the surface which increase the rate but produce weak BSA adsorption) are not important whereas in static conditions adsorbed species are more likely to remain at the electrode surface.

A decrease in protein adsorption occurred after base pretreatment which involved both oxidative and reductive steps whereas longer pretreatment in base increased protein adsorption in DPV experiments. These pretreatment procedures are reported to initially generate graphite-oxide layers which then dissolve, to a large extent, in the basic solution

leaving a surface rich in oxide functionalities (compared to an unpretreated surface)[51]. Hence, the increased protein adsorption observed after long treatments in base (5 min) is consistent with this pretreated surface having more EGO character (due to prolonged anodisation). The shorter anodisation times coupled to a reductive step in base therefore produces a surface that is not EGO and is resistant to BSA adsorption. Square-wave pretreatments consistently gave decreased protein adsorption. Scanning electron micrographs of GC electrodes following severe square-wave pretreatment have been reported to show pits which were assumed to arise from reaction of chlorine with the carbon surface[91]. Additionally, carbon debris was removed revealing scratches made during the polishing process.

Experiments in Chapter Seven, indicated that hydrophobic groups close to the electrode surface increased BSA adsorption whilst anionic moieties close to the electrode surface (i.e. *p*-benzoate groups) did not significantly change the amount of BSA adsorption. This implies that improvements in protein resistance after square-wave and base ECPs, results from surface cleaning (i.e. removal of hydrophobic adsorbents) rather than the generation of anionic charge at the electrode surface.

8.4.2 Surfactant modified carbon electrodes

Chemically modified GE electrodes prepared by physical incorporation of SDS and CTAB showed improved response in the presence of BSA relative to unmodified GE. The modified surface is poorly defined and it is likely that charged groups extend out at various angles and distances from the electrode surface. Incorporation of anionic surfactant produced a better ratio in the presence and absence of BSA than that observed for the cationic modified electrode. Square-wave pretreatment further enhanced the protein resistance of the SDS-GE electrode. This pretreatment however, had little effect on the CTAB-GE electrode but decreased protein adsorption at the GE electrode. Assuming that square-wave pretreatment exposes both charged surfactant head groups and some hydrocarbon backbone of the modifier, this suggests that generation of more negative charges effectively blocks BSA from reaching the surface (which is now more hydrophobic) whereas increasing the positive charge of the electrode does not prevent BSA approaching the surface. Thus in this instance, anionic groups are useful for preventing BSA adsorption but GE electrodes modified with cationic surfactants are less protein resistant than pretreated (clean) surfaces. It was shown in Chapter Seven, that positively charged groups can decrease BSA adsorption if they extend out from the electrode surface and are sufficiently dense that they block the access of protein whilst not impairing the approach of analyte to the electrode. Therefore, the disorganised nature of CTAB assembly in GE may be responsible for its decreased protein resistance. Studies described in Chapter Seven also indicated that anionic groups do not have to extend very far into

solution to decrease protein adsorption and hence the disorganised assembly of SDS in GE is relatively unimportant.

Assembly of SDS on BPG electrodes improved the sensitivity ratio in the presence and absence of BSA when a highly organised surface layer appeared to be present. Further, this layer was shown to be stable to repeat CV measurements in the presence of BSA and while reproducibility of coatings was poor in these experiments it is anticipated that a superior sample of BPG would increase the success rate of modification. Hence, this is a very good method for further development. As the length of the surfactant hydrocarbon backbone is increased the density of modifiers is also expected to increase (analogous to self-assembled monolayers on Au) reducing the sensitivity to analytes. Thus, development of a CME with an optimised compromise between protein resistance, and sensitivity to analytes should be achievable.

8.4.3 Cellulose acetate coated electrodes

Results shown in this study indicate that cellulose acetate CMEs can effectively decrease protein adsorption during CV measurements. However, base-hydrolysed CA coated electrodes gave a time-dependent response for the probe analyte even after contact times in excess of 1 h making them unsuitable for rapid measurement of biological samples under batch conditions. Cellulose acetate membranes which decreased BSA adsorption were also prepared using the phase-inversion procedure and these CMEs were more permeable to the probe analyte and equilibrated with solution species on a shorter timescale (ca. 10–15 min). Hence this method of coating preparation appears superior. Both methods of casting CA films on GC electrodes have severe disadvantages however, being time-consuming (typically taking 1.5 to 2 h) and showing poor reproducibility.

8.5 Conclusions

Glassy carbon was the untreated carbon electrode material of choice for measurements in the presence of BSA as it gave the best reproducibility and least perturbation of electrochemical response. Electrochemical pretreatments can be applied to further increase the protein resistance of GC although for measurements in batch conditions pretreatments that produce EGO should be avoided. It is assumed that decreased protein adsorption occurs as a result of removal of hydrophobic adsorbents from the electrode surface. Analytes that accumulate as a result of pretreatment will be more affected by protein adsorption as accumulation is hindered by protein at the electrode surface. However, the analyte response may still be enhanced relative to that at the unpretreated surface and under these conditions, the responses at the polished and pretreated electrodes must be compared to assess the analytical utility of the ECP.

Chemically modified electrodes made by incorporating charged surfactants into the (GE) matrix or assembly of SDS at BPG showed protein adsorption responses which are consistent with results for CMEs prepared by diazonium modification described in Chapter Seven. For modified GE electrodes, anionic groups decreased protein adsorption even when they were randomly distributed at the electrode surface. Cationic groups were less successful at preventing the access of BSA to the electrode surface as a blocking layer which is remote from the electrode surface is required. An organised layer of SDS on BPG was very effective at excluding BSA.

Cellulose acetate coatings can be used to decrease BSA adsorption when making CV measurements although long equilibration times, poor reproduciblilty and long preparation times make this method less desirable than monolayer modifications.

Chapter Nine: Conclusions

The work described in this thesis was aimed at investigating methods which extend the application of electroanalytical techniques to direct measurements in biological fluids. In particular, two problems which arise when performing electrochemical analyses in biological matrices were addressed, namely, interference from "non-target" electroactive components and adsorption of high molecular weight organic species onto the electrode surface.

Chemically modified electrodes prepared by the diazonium salt procedure were used in a large part of this study. At pH 7.4, electrostatic interactions controlled selectivity of response at both the *p*-phenylacetate and *p*-benzoate modified electrodes. Consequently, these CMEs could be used to selectively measure cationic analytes in the presence of anionic species. Importantly, when GC electrodes, which had different initial activities (with respect to oxidation of biological analytes), were modified with *p*-phenylacetate or *p*-benzoate monolayers, the activities of CMEs were very similar. Therefore, this modification procedure may be useful as an alternative to routine polishing (which often fails to improve the kinetics of some analytes at the carbon surface).

The suitability of the CMEs as probes for DA was investigated. The main advantage of the CMEs over Nafion coated electrodes, was the fast response time to DA. This trait, together with the good sensitivity to DA over AA, suggests that both the *p*-phenylacetate and *p*-benzoate modified electrodes are well-suited to application as DA probes for fast timescale measurements. Although experiments with carbon fibre microelectrodes utilised the *p*-phenylacetate modification, results at conventional-size GC suggest that *p*-benzoate may be superior. This CME formed a denser surface coating (compared to *p*-phenylacetate) and gave increased selectivity to DA over AA in chronoamperometric experiments. *In vivo* experiments are required to confirm the suitability of these CMEs for application as DA probes.

The *p*-phenylacetate modified electrode also showed favourable anti-fouling properties which make it an extremely useful electrode surface for analytical purposes. Superior resistance to fouling by reaction products of many biological analytes (compared to unmodified GC) was repeatedly observed at the *p*-phenylacetate modified detector in FIA experiments. Further, this CME was shown to be resistant to protein adsorption in DPV experiments.

When GC electrodes were covalently modified with *p*-alkylbenzene moieties, the main factor controlling selectivity was the simplicity of the electron transfer reaction.

Analyte hydrophobicity/hydrophilicity was also important. Selectivity at *p*-alkybenzene CMEs was controlled by varying the coating density. Fast measurement of some hydrophobic analytes i.e. without the need for preconcentration protocols, was possible. An analytically significant example was the selective response of CPZ over AA and UA in CV experiments. Further studies investigating the range of analytes which may be measured at this CME would be useful.

The analytical utility of covalently modified GC detectors was investigated in FIA conditions. In particular, the measurement of acetaminophen or CPZ in the presence of UA and AA was examined. Increased selectivity for acetaminophen and CPZ (relative to unmodified GC) was observed at *p*-phenylacetate and *p*-alkylbenzene modified detectors. Using a retention-time based technique, the response of CPZ was measurable at *p*-phenylacetate/*p*-alkylbenzene modified detectors because the sample zone was dispersed by favourable interactions with the electrode coating. It was shown that the oxidation of CPZ could be measured in the presence of a four-fold greater concentration of UA. Further optimisation of the technique is needed to extend the application to biologically relevant analyte/interferent levels. To achieve this, the area of modified surface to which the sample is exposed could be increased and the flow rate of the FIA system decreased. Both of these adaptations are expected to increase sample dispersion and hence increase selectivity for CPZ. Acetaminophen showed less tendency to be dispersed in retention-time based experiments. The partial selectivity for this acetaminophen was exploited using a multi-electrode detector array. The simultaneous measurement of acetaminophen, AA and UA from multi-component solutions and diluted urine was achieved using a relatively simple analytical protocol. In particular, the *p*-phenylacetate modified detector was shown to be well suited to measurement in diluted urine. To optimise the use of covalently modified electrodes in multi-electrode detector arrays for analysis of biological samples, modified detectors which are resistant to adsorption of high molecular weight organic species should be used, for example, *p*-phenylacetate or doubly quaternised bipyridinium CMEs.

A study of BSA adsorption at covalently modified electrodes was undertaken using CV and DPV techniques. A novel approach was employed to monitor the amount of protein in contact with the electrode surface. This involved observing perturbation of the electrochemical response of probe analytes FCA and FcOH. The extent of protein adsorption could be controlled by covalent attachment of a monolayer to the GC electrode surface. Protein adsorption increased when hydrophobic moieties (*p*-methoxybenzene) were attached close to the surface and was unaffected by modification with anionic groups (*p*-benzoate) which did not extend very far from the underlying GC substrate. Modifiers which extended further into solution (*p*-phenylacetate) and (doubly quaternised bipyridinium) were successful at decreasing BSA adsorption. Short modifiers are more desirable because they are less likely to impede the approach of the analyte to the electrode

surface (and hence will give greater sensitivity). Future work examining protein adsorption at electrodes modified with short cationic groups would be useful. Increased protein adsorption at such surfaces would indicate that the physical blocking of protein from the electrode surface was responsible for the improved response in the presence of protein for the doubly quaternised bipyridinium CMEs.

Alternative procedures were applied to generate electrode surfaces for further protein adsorption studies. Electrochemical pretreatment of GC electrodes increased protein adsorption in conditions where electrochemical graphite oxide was formed. Other ECPs (dc treatment in basic solutions and square-wave in chloride solutions) decreased protein adsorption. When ECPs caused analyte adsorption, the relative sensitivity in the presence of protein was decreased, although the absolute senstitivity to analyte may still be increased (relative to an unpretreated electrode) by ECP. It is recommended that these considerations be taken into account when designing pretreatment protocols for analytes which adsorb on carbon electrodes.

Anionic surfactants incorporated into graphite epoxy were effective at decreasing BSA adsorption whereas cationic modifiers were less successful. This implies that a more organised blocking layer is needed to prevent protein approach when cationic modifying groups are used. Modification of basal plane graphite with anionic surfactant produced a surface which gave superior performance, compared with unmodified carbon electrodes, in the presence of protein. This CME seems useful for future development and it is recommended that the highest quality BPG available be used to increase the success rate of modification. Glassy carbon electrodes coated with cellulose acetate gave decreased BSA adsorption in CV measurements. However, prolonged equilibration times, long preparation time and poor reproducibility make this method less desirable than monolayer modifications.

In conclusion, covalently modified GC electrodes were shown to be selective for some analytes of biological interest relative to interferents. The appropriate choice of *para*-substituent allowed modified surfaces to be generated which gave superior resistance to BSA adsorption than unmodified surfaces without inducing problematic time-dependent behaviour.

REFERENCES

1. J. Wang, *Electroanalytical techniques in clinical chemistry and laboratory medicine,* VCH, NY, Germany, 1988.

2. G. J. Patriarche and H. Zhang, *Electroanalysis,* 2 (1990) 573.

3. J. P. Hart, *Electroanalysis of biologically important compounds*, Ellis Horwood, NY, London, 1990.

4. J. A. Stamford, F. Crespi and C. A Marsden In *Monitoring neuronal activity; A practical approach*, J. A. Stamford Ed., IRL Press, Oxford, NY, Tokyo, 1992 pp 113 – 145.

5. J. Millar, M. Armstrong-James and Z. L. Kruk, *Brain Research*, 205 (1981) 419.

6. A. C. Michael, M. Ikeda and J. B. Justice Jr, *Brain Research*, 421 (1987) 325.

7. W. G. Kuhr and R. M. Wightman, *Brain Research*, 381 (1986) 168.

8. J. E. Baur, E. W. Kristensen, L. J. May, D. J. Wiedemann and R. M. Wightman, *Anal. Chem.*, 60 (1988) 1268.

9. R. M. Wightman, C. Amatore, R. C. Engstrom, P. D. Hale, E. W. Kristensen, W. G. Kuhr and L. J. May, *Neuroscience*, 25 (1988) 513.

10. L. J. May and R. M. Wightman, *Brain Research*, 487 (1989) 311.

11. J. B. Zimmerman and R. M. Wightman, *Anal. Chem.*, 63 (1991) 24.

12. K. T. Kawagoe, P.A. Garris, D. J. Wiedemann and R. M. Wightman, *Neuroscience*, 51 (1992) 55.

13. R. T. Kennedy, S. R. Jones and R. M. Wightman, *Neuroscience*, 47 (1992) 603.

14. S. D. Young and A. C. Michael, *Brain Research*, 600 (1993) 305.

15. R. D. O'Neill, *Analyst*, 119 (1994) 767.

16. D. C. Johnson, S. G. Weber, A. M. Bond, R. M. Wightman, R. E. Shoup and I. S. Krull, *Anal. Chim. Acta,* 180 (1986) 187.

17. A. Fallon, R. F. G. Booth and L. D. Bell, *Laboratory techniques in biochemistry and molecular biology: Applications of HPLC in biochemistry,* R. H Burdon and P. H. van Knippenberg Eds., Elsevier, Amsterdam, 1987.

18. R. W. Murray, *Anal. Chem.,* 66 (1994) 505 A.

19. R. M. Murray, *Electroanal. Chem.*, 13 (1984) 191.

20. R. W. Murray, A. G. Ewing and R. A. Durst, *Anal. Chem.*, 59 (1987) 379 A.

21. G. J. Moody and J. D. R.Thomas, *Selected Electrode. Rev.,* 13 (1991) 113.

22. R. J. Geise, J. M. Adams, N. J. Barone, A. M. Yacynych, *Biosensors and Bioelectronics*, 6 (1991) 151.

23. C. Hsueth and A. Brajter-Toth, *Anal. Chem.*, 66 (1994) 2458.

24. J. Wang, S-P. Chen and M. S. Lin, *J. Electroanal. Chem.*, 273 (1989) 231.

25. J. Wang and J. Liu, *Anal. Chim. Acta*, 294 (1994) 201.

26. G. Sittampalam and G. S. Wilson, *Anal. Chem.*, 55 (1983) 1608.

27. J. Wang and L. D. Hutchins, *Anal. Chem.*, 57 (1985) 1536.

28. P. J. Peerce and A. J. Bard, *J. Electroanal. Chem.*, 112 (1980) 97.

29. G. Nagy, G. A. Gerhardt, A. F. Oke, M. E. Rice, R. N. Adams, R. B. Moore, M. N. Szentirmay and C. R. Martin, *J. Electroanal. Chem.,* 188 (1985) 85.

30. B. Hoyer and T. M. Florence, *Anal. Chem.*, 59 (1987) 2839.

31. B. Hoyer, T. M. Florence and G. E. Batley, *Anal. Chem.*, 59 (1987) 1608.

32. M. P. Brazell. R. J. Kasser, K. J. Renner, J. Feng, B. Moghaddam and R. N. Adams, *J. Neurosci. Methods*, 22 (1987) 167.

33. G. A. Gerhardt, A. F. Oke, G. Nagy, B. Moghaddam and R. N. Adams, *Brain Research*, 290 (1984) 390.

34. P. Capella, B. Ghasemzadeh, K. Mitchell and R. N. Adams, *Electroanalysis*, 2 (1990) 175.

35. J. Wang and P. Tuzhi, *Anal. Chem.*, 58 (1986) 3257.

36. A. R. Guadalupe and H. D. Abruña, *Anal. Chem.,* 57 (1985) 142.

37. L. S. Kuhn, S. G. Weber and K. Z. Ismail, *Anal. Chem.*, 61 (1989) 303.

38. I. Christie, S. Leeds, M. Baker, F. Keedy and P. Vadgama, *Anal. Chim. Acta*, 272 (1993) 145.

39. J. Wang, T. Golden and P. Tuzhi, *Anal. Chem.*, 59 (1987) 740.

40. Y. Zhang, Y. Hu, G. S. Wilson, D. Moatti-Sirat, V. Poitout and G. Reach, *Anal. Chem.*, 66 (1994) 1183.

41. D. S. Bindra and G. S. Wilson, *Anal. Chem.*, 61 (1989) 2566.

42. M. Delamar, R. Hitmi, J. Pinson and J-M. Saveánt, *J. Am. Chem. Soc.*, 114 (1992) 5883.

43. C. Bourdillon, M. Delamar, C. Demaille, R. Hitmi, J. Moiroux and J. Pinson, *J. Electroan. Chem.*, 336 (1992) 113.

44. R. S. Deinhammer, M. Ho, J. W. Anderegg and M. D. Porter, *Langmuir,* 10 (1994) 1306.

45. F. Malem and D Mandler, *Anal. Chem.*, 65 (1993) 37.

46. A. M. Becka and C. J. Miller, *J. Phys. Chem.*, 96 (1992) 2657.

47. C. Miller, P. Cuendet and M. Grätzel, *J. Phys. Chem.*, 95 (1991) 877.

48. H. O. Finklea and D. D. Hanshew, *J. Am. Chem. Soc.*, 114 (1992) 3173.

49. Q. Cheng and A. Brajter-Toth, *Anal. Chem.*, 67 (1995) 2767.

50. A. J. Bard, H. D. Abruña, C. E. Chidsey, L. R. Faulkner, S. W Feldberg, K. Itaya, M. Majda, O. Melroy, R. M. Murray, M. D. Porter, M. P. Soriaga and H. S. White, *J. Phys. Chem.*, 97 (1993) 7147.

51. R. L. McCreery In *Electroanalytical Chemistry,* A. J. Bard Ed., Marcel Dekker, NY, 1991, Vol 17 pp 221-374.

52. D. Tse and T. Kuwana, *Anal. Chem.,* 50 (1978) 1315.

53. H. Jaegfeldt, T. Kuwana and G. Johansson, *J. Am. Chem. Soc.*, 105 (1983) 1805.

54. J. Wang and T. Golden, *Anal. Chim. Acta*, 217 (1989) 343.

55. J. H. Zagal, S. Lira and S. Ureta-Zañartu, *J. Electroanal. Chem.,* 210 (1986) 95 and references therein.

56. O. Chastel, J. M. Kauffmann and G. J. Patriarche, *Anal. Chem.*, 61 (1989) 170.

57. J. Wang and M. Ozsoz, *Electroanalysis*, 2 (1990) 595.

58. J. Wang and Z. Lu, *Anal. Chem.*, 62 (1990) 826.

59. O. J. Garcia, P. A. Quintela and A. E. Kaifer, *Anal. Chem.*, 61 (1989) 979.

60. A. Guerrieri, T. R. I. Cataldi and H. A. O. Hill, *J. Electroanal. Chem.*, 297 (1991) 541.

61. A. Marino and A. Brajter-Toth, *Anal. Chem.*, 65 (1993) 370.

62. A. Jaramillo, A. Marino and A. Brajter-Toth, *Anal. Chem.*, 65 (1993) 3441.

63. R. N. Adams, *Anal. Chem.,* 30 (1958) 1576.

64. K. Kalcher, J. M. Kauffmann, J. Wang, I. Svancara, K. Vytras, C. Neuhold and Z. Yang, *Electroanalysis*, 7, (1995) 5.

65. M. Khodari, J. M. Kauffmann, G. J. Patriarche and M. A. Ghandour, *Electroanalysis*, 1 (1989) 501.

66. L. Hernandez, P. Hernandez and E. Lorenzo, *Electroanalysis,* 2 (1990) 643.

67. C. D. Blaha and R. F. Lane, *Brain Res. Bull.*, 10 (1983) 861.

68. P. D. Lyne and R. D. O'Neill, *Anal. Chem.*, 62 (1990) 2347.

69. J. Wang, T. Golden, K. Varughese and I. El-Rays, *Anal. Chem.*, 61 (1989) 508.

70. F. Cespedes, E. Fabregas, J. Bartoli and S. Algeret, *Anal. Chim. Acta*, 273 (1993) 409.

71. S. A. Wring and J. P. Hart, *Analyst*, 17 (1992) 1215.

72. H. Li, R. Ge and E. Wang, *Anal. Chim. Acta,* 292 (1994) 107.

73. W. W. Kubiak and J. Wang, *Anal. Chim. Acta,* 221 (1989) 43.

74. A. J. Bard and L. R. Faulkner, *Electrochemical methods: Fundamentals and applications*, Wiley & sons, NY, 1980 pp 540-546.

75. K. Takehara and H. Takehara, *Bull. Chem. Soc. Jpn.*, 68 (1995) 1289.

76. J. M. Savéant, *J. Electroanal. Chem.*, 302 (1991) 91.

77. C. Amatore, J-M. Savéant and D. Tessier, *J. Electroanal. Chem.*, 147 (1983) 39.

78. Reference 74, pp 538-540.

79. P. Chen, M. A. Fryling and R. L. McCreery, *Anal. Chem.*, 67 (1995) 3115.

80. G. N. Kumau, W. S. Willis and J. F. Rusling, *Anal. Chem.*, 57 (1985) 545.

81. R. J. Bowling, R. T. Packard and R. L. McCreery, *J. Am. Chem. Soc.*, 111 (1989) 1217.

82. J. C. Hoogvliet, C. M. B.Van Den Beld, C. J. Van Der Poel and W. P. Van Bennekom, *J. Electroanal. Chem.*, 201 (1986) 11.

83. M. L. Bowers, J. Hefter, D. L. Dugger and R. Wilson, *Anal. Chim. Acta*, 248 (1991) 127.

84. L. J. Kepley and A. J. Bard, *Anal. Chem.*, 60 (1988) 1459.

85. R. M. Wightman, M. R. Deakin, P. M. Kovach, W. G. Kuhr and J. Stutts, *J. Electrochem. Soc.*, 131 (1984) 1578.

86. G. E. Cabaniss, A. A. Diamantis, W. R. Murphy Jr., R. W. Linton and T. J. Meyer, *J. Am. Chem. Soc.*, 107 (1985) 1845.

87. J. Wang and P. Tuzhi, *Anal. Chem.*, 58 (1986) 1787.

88. A. L. Beilby, T. A. Sasaki and H. M. Stern, *Anal. Chem.*, 67 (1995) 976.

89. R. C. Engstrom, *Anal. Chem.*, 54 (1982) 2310.

90. R. C. Engstrom and V. A. Strasser, *Anal. Chem.*, 56 (1984) 136.

91. J. Wang and L. D. Hutchins, *Anal. Chim. Acta*, 167 (1985) 325.

92. L. Falat and H. Y. Cheng, *Anal. Chem.*, 54 (1982) 2108.

93. A. L. Beilby and A. Carlsson, *J. Electroanal. Chem.*, 248 (1988) 283.

94. D. M. Anjo, M. Kahr, M. M. Khodabakhsh, S. Nowinski and M. Wanger, *Anal. Chem.*, 61 (1989) 2603.

95. S. S. Lord and L. B. Rogers, *Anal. Chem.*, 26 (1954) 284.

96. Southampton electrochemistry group, *Instrumental methods in electrochemistry,* Ellis Horwood Ltd., Chichester, 1985.

97. M. R. Deakin, P. M. Kovach, K. J. Stutts and R. M. Wightman, *Anal. Chem.,* 58 (1986) 1474.

98. M. G. Simic and S. V. Jovanovic, *J. Am. Chem. Soc.*, 111 (1989) 5778.

99. J. J. Van Benschoten, J. Y. Lewis, W. R. Heineman, D. A. Roston and P. T. Kissinger, *J. Chem. Ed.*, 60 (1983) 772.

100. K. Takamura, S. Inoue, F. Kusu, M. Otagiri and K. Uekama, *Chem. Pharm. Bull.*, 32 (1983) 839.

101. E. L. Ciolkowski, K. M. Maness, P. S. Cahill, R. M. Wightman, D. H. Evans, B. Fosset and C. Amatore, *Anal. Chem.*, 66 (1994) 3611.

102. M. Koppenol, J. B. Cooper and A. M. Bond, *Am. Lab.*, 26 (1994) 25.

103. K. H. Saunders and R. L. M. Allen, *Aromatic diazo compounds,* Third edn., Edward Arnold, London, 1985.

104. H. Kamogawa, H. Mizuno, Y. Todo and M. Nanasawa, *J. Pol. Sc. PC,* 17 (1979) 3149.

105. A. J. Downard and M. J. Ratcliffe, unpublished results.

106. L. D. Pettit and H. K. J. Powell, SC-Database, Stability Constants Database, (IUPAC/Academic Software) 1993.

107. J. Wang, L. M. Frostman and M. D. Ward, *J. Phys. Chem.*, 96 (1992) 5224.

108. J. J. Betts and B. A. Pethica, *Trans. Farady Soc.,* 52 (1956) 1581.

109. M. Mille, *J. Colloid Interface Sci.*, 81 (1981) 169.

110. F. C. Anson, *Anal. Chem.*, 38 (1966) 54.

111. R. F. Lane and A. T. Hubbard, *J. Phys. Chem.,* 77 (1973) 1411.

112. C. D. Allred and R. L. McCreery, *Anal. Chem.,* 64 (1992) 444.

113. D. E. Weisshaar, M. M. Walczak and M. D. Porter, *Langmuir,* 9 (1993) 323.

114. M. A. T. Gilmartin, J. P. Hart and B. Birch, *Analyst,* 117 (1992) 1299.

115. J. Wang and R. Li, *Anal. Chem.,* 61 (1989) 2809.

116. P. T. Kissinger, J. B. Hart and R. N. Adams, *Brain Res.*, 55 (1973) 209.

117. H. Curtis, *Biology,* Worth Publ. Inc., NY, Fourth Ed. (1985) p 825.

118. O. Niwa, M. Morita and H. Tabei, *Electroanalysis*, 6 (1994) 237.

119. M. B. Gelbert, D. J. Curran, *Anal. Chem.*, 58 (1986) 1028.

120. P. D. Lyne and R. D. O'Neill, *Anal. Chem.*, 61 (1989) 2323.

121. M. S. Freund and A. Brajter-Toth, *J. Phys. Chem.*, 96 (1992) 9400.

122. A. G. Ewing, M. A. Dayton and R. M. Wightman, *Anal. Chem.*, 53 (1981) 1842.

123. R. M. Wightman, *Anal. Chem.,* 53 (1981) 1125 A.

124. K. B. Oldham, *J. Electroanal. Chem.*, 122 (1981) 1.

125. P. Bianco and J. Haladjian, *Electroanalysis*, 7 (1995) 442.

126. M. D. Porter, T. B. Bright, D. L. Allara and C. E. D. Chidsey, *J. Am. Chem. Soc.,* 109 (1987) 3559.

127. K. R. Kneten and R. L. McCreery, *Anal. Chem.,* 64 (1992) 2518.

128. K. K. Cline, M. T. McDermott and R. L. McCreery, *J. Phys. Chem.,* 98 (1994) 5314.

129. J. Wang, H. Wu and L. Angnes, *Anal. Chem.,* 65 (1993) 1893.

130. J. Wang, L. Chen and H. Wu, *Anal. Chim. Acta*, 300 (1995) 127.

131. W. P. Carey, K. R. Beebe and B. R. Kowalski, *Anal. Chem.*, 59 (1987) 1529.

132. W. P. Carey, K. R. Beebe, B. R. Kowalski, D. L. Illman and T. Hirschfeld, *Anal. Chem.*, 58 (1986) 149.

133. W. P. Carey and B. R. Kowalski, *Anal. Chem.*, 60 (1988) 541.

134. J. R. Stetter, P. C. Jurs and S. L. Rose, *Anal. Chem.*, 58 (1986) 860.

135. M. Otto and J. D. R. Thomas, *Anal. Chem.*, 57 (1985) 2647.

136. K. Beebe, D. Uerz, J. Sandifer and B. R. Kowalski, *Anal. Chem.*, 60 (1988) 66.

137. J. Wang, G. D. Rayson, Z. Lu and H. Wu, *Anal. Chem.*, 62 (1990) 1924.

138. J. Simons, M. Bos and W. E. van der linden, *Analyst*, 120 (1995) 1009.

139. W. Peng, T. Li, H. Li and E. Wang, *Anal. Chim. Acta,* 298 (1994) 415.

140. P. A Vaughan, L. D. L. Scott and J. F. McAleer, *Anal. Chim. Acta,* 248 (1991) 361.

141. A. M. Almuaibed and A. Townsend, *Talanta,* 39, (1992) 1459.

142. M. A. Ross, *J. Chromatogr. B,* 657 (1994) 197.

143. S. V. Sasso, R. J. Pierce, R. Walla and A. M. Yacynych, *Anal. Chem.,* 62 (1990) 1111.

144. H. A. Harper, *Review of physiological chemistry,* Lange Medical Publications, Canada, edn. 10 (1965) pp 343-344.

145. J. Ruzicka and E. H. Hansen, *Flow injection analysis,* J. D. Winefordner and I. M. Kolthoff Eds., Wiley & Sons, New York, 1988 pp 47 – 48.

146. V. V. Cosofret, M. Erdösy, T. A. Johnson, R. P. Buck, R. B. Ash and M. R. Neuman, *Anal. Chem.,* 67 (1995) 1647.

147. J. M. Elbiki and S. G. Weber, *Biosensors,* 4 (1989) 251.

148. J. Cassidy and C. Lowney, *Anal. Chim. Acta,* 234 (1990) 479.

149. J. Wang and Z. Taha, *Electroanalysis,* 2 (1990) 383.

150. J. Wang and L. D. Hutchins-Kumar, *Anal. Chem.,* 58 (1988) 402.

151. J. Wang, M. Bonakdar and M. M. Pack, *Anal. Chim. Acta,* 192 (1987) 215.

152. W. Norde, *Advances Coll. Interface Sci.,* 25 (1986) 267.

153. B. Raspor, *J. Electroanal. Chem.,* 316 (1991) 223.

154. H. A. Sober (Ed.), *Handbook of biochemistry:Selected data for molecular biology,* CRC, Cleveland, 1968, p C-36.

155. T. Peters In *Advances in protein chemistry,* C. B. Anfinsen, J. T. Edsall and F. M. Richards, Eds., Academic Press, NY, 1985 pp 161-243.

156. W. Norde, *Croat. Chem. Acta,* 56 (1983) 705.

157. P. Bernabeu and A. Caprani, *Biomaterials,* 11 (1990) 258.

158. A. Caprani and F. Lacour, *Bioelectrochem. Bioenergetics,* 25 (1991) 241.

159. S. H. Lee and E. Ruckenstein, *Coll. Interface Sci.,* 125 (1988) 365.

160. K. L. Prime and G. M. Whitesides, *J. Am. Chem. Soc.,* 115 (1993) 10714.

161. S. I. Joen, J. H. Lee, J. D. Andrade and P. G. De Gennes, *Coll. Interface Sci.,* 142 (1991) 149.

162. S. I. Joen and J. D. Andrade, *Coll. Interface Sci.,* 142 (1991) 159.

163. K. L. Prime and G. M. Whitesides, *Science,* 252 (1991) 1164.

164. B. F. Watkins, J. R. Behling, E. Kariv and C. C. Miller, *J. Am. Chem. Soc.,* 97 (1975) 3549.

165. Reference 74, Ch 11.

166. A. E. Kaifer and A. J. Bard, *J. Phys. Chem.,* 89 (1985) 4876.

167. F. Lacour, J. P. Frayret and A. Caprani, *J. Electrochem. Soc.,* 139 (1992) 153.